UNIVERSITAT ROVIRA I VIRGIL

BIOANALYTICAL APPLICATIONS OF POLYOXOMETALATES USING MOLECULAR TOOLS FOR DETECTION OF DNA AND SNPS IN PRIMER EXTENSION

Ahmed Mehdi Debela

Dipòsit Legal: T 1223-2014

DOCTORAL THESIS

AHMED MEHDI DEBELA

Bioanalytical applications of polyoxometalates using molecular tools for detection of DNA and SNPs in primer extension

Universitat Rovira i Virgili

Department of Chemical Engineering

AHMED MEHDI DEBELA

Bioanalytical applications of polyoxometalates using molecular tools for detection of DNA and SNPs in primer extension

DOCTORAL THESIS

Supervised by

Dr. Ciara K. O'Sullivan and Dr. Mayreli Ortiz

Department of Chemical Engineering

Universitat Rovira i Virgili

Tarragona

2014

People inspire you, or they drain you-pick them wisely

Hans F.Hansen

UNIVERSITAT ROVIRA I VIRGILI

Department of Chemical Engineering

Universitat Rovira i Virgili

Avinguda Països Catalans, 26

43007, Tarragona Spain

Tel: +34-977-558740/8722

Fax:+34-977-559621/8205

Dr. Ciara K. O' Sullivan and Dr. Mayreli Ortiz

Certify that:

The present study, entitled "**Bioanalytical applications of polyoxometalates using molecular tools for detection of DNA and SNPs in primer extension**", presented by Ahmed Mehdi Debela for the award of the degree of Doctor, has been carried out under our supervision at the Department of Chemical Engineering of this university, and that it fulfils all the requirements to be eligible for the International Doctorate Award.

Tarragona, June 12, 2014

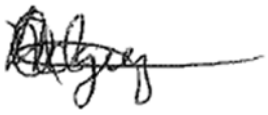

Doctoral Thesis Supervisors

Dr. Ciara K. O' Sullivan

Dr. Mayreli Ortiz

Acknowledgement

Above all I am grateful to the almighty Allah. It's a privilege to convey my deep sense of gratitude and immense reverence to my supervisor Prof. Ciara O'Sullivan, for her subtle supervision and constructive criticism, throughout the research and for her painstaking efforts in preparation of this thesis. She has indeed been very patient in inculcating the required research attitude and writing capabilities in me, which shall go a long way in the coming years. Thanks to the digression she made during her teaching discourse that gave me the insight to view life and how to face troubles and competitions while maintaining my equanimity. I also convey my reverence to Dr. Mayreli Ortiz for her idealistic personality, inspiring intellectual and for her encouragement, motivation and assistance in improving my work etiquettes. The teaching that she has bestowed upon me will help me in my future endeavors. I fail to gather words to pay the deepest heartfelt regards to my former supervisor Dr. Valerio Beni for his advice, who taught me the art of research through continuous encouragement. It would be insincere on my part if I don't acknowledge the help, encouragement, timely advice and ideas rendered by Prof. Serge Thorimbert and Prof. Bernold Hasenknopf in my short stay in Paris.

It is an honor to pay my respect and heartfelt thanks to department of chemical engineering, URV (Tarragona) and Institut Parisien de Chimie Moléculaire (IPCM), UPMC (Paris) for providing exceptional facilities in an extremely stimulating research ambience in their premises.

I would like to acknowledge my lab mates for their sincere efforts, support and co-operation and for maintaining the cordial atmosphere during the research work. The brotherly sanctity, love and care laid upon me had made my days in Tarragona the most memorable and unforgettable. Last, but not the least, I would like to express my heartfelt appreciation to my loving wife, Shemsia Mohammed for her love, blessings, persistent motivation and soothing words, I could not have accomplished this arduous task, Mere words cannot suffice or acknowledge the enormous confidence, endless affection, untiring help and the mental support rendered.

Table of contents

Summary

This thesis aimed to develop an electrochemical platform for genotyping of single nucleotide polymorphisms (SNPs) using arrayed primer extension (APEX). APEX is a template dependent genotyping method that makes use of dideoxy nucleotides for scanning unknown mutations in a DNA sequence. In order to achieve the overall objective of developing an electrochemical APEX genotyping platform, various stages of the final platform were developed in parallel. One critical element was the need for a robust surface functionalisation technique which can withstand the elevated temperature used during enzymatic incorporation of labels, whilst another critical element was the functionalisation of DNA (primers, dNTPs, ddNTPs) with electrochemically distinguish able redox labels. These subobjectives define the outline of the thesis, with each subobjective being individually addressed in each chapter, as delineated below.

Chapter 1. Introduction, state of the art and scope of the project

Chapter 2. A two-step process for the electrochemical hydrogenation of glassy carbon followed by either chemical or electrochemical chlorination to provide a highly reactive surface for further functionalisation is reported. The carbon surface at each stage of the process was characterised using AFM, SEM, Raman, ATR FT-IR, XPS and electroanalytical techniques. Electrochemical chlorination of hydrogen-terminated surfaces was achieved in just 5 minutes at room temperature using hydrochloric acid whilst chemical chlorination required the use of phosphorous pentachloride at 50^{o}C over a three-hour period. A more controlled and uniform surface was obtained using the electrochemical approach as chemical chlorination was observed to damage the glassy carbon surface. As a model system to demonstrate the genericity and potential application of the formed highly reactive chlorinated surface a ferrocene labelled alkylthiol was used and the methodology optimised. This process was then applied to thiolated DNA and the functionality of the immobilised DNA probe was demonstrated. XPS revealed the covalent bond formed to be a C-S bond and the thermal stability of the glassy carbon anchored thiolated molecules was evaluated and a far superior performance to stability on gold surfaces was observed. This is the first report of the electrochemical hydrogenation and electrochemical chlorination of a glassy carbon

surface and this facile process can be applied to the highly stable functionalisation of carbon surfaces with a plethora of diverse molecules, finding widespread application.

Chapter 3. In this work the functionalisation of monolacunary Keggin POM to obtain stable organotin hybrids and investigation of their properties using various characterisation techniques reported. The hybrid compounds are also observed to have tunable solubility and redox properties; while switching the solubility of the synthesised compounds (from organic to aqueous) have been shown to shift the redox potentials closer to zero. As revealed in the electrochemical properties all compounds show a reversible one electron process. The electrochemical properties in aqueous solution further indicate their structural stability for redox labeling of biomolecules to utilise POMs for electroanalytical applications. The various tetrabutyl ammonium (TBA) salts of organotin derivatives synthesised include: $(TBA)_4SiW_{11}O_{39}SnC_2H_4COOH$ (**1**), $(TBA)_4SiW_{11}O_{39}SnC_2H_4CO$ (**2**), $(TBA)_5SiW_{11}O_{39}SnC_2H_4CONHC_3H_6N_3$ (**3**), $TBA_7[(SiW11O_{39})\{Sn(CH_2)_2CONH(CH_2)_3(N_3CH_2)C_{10}H_9Fe\}]$(**4**) and an ammonium salt $(NH_4)_5[SiW_{11}O_{39}\{SnCH_2CH_2C(=O)\ NH(CH_2)_3N_3\}]$(**6**)**.** These have been synthesised for the first time by utilising the various organic functionalisation strategies from the lacunary Keggin. The products were characterised using elemental analysis, FTIR, NMR, ESI MS, and electrochemical techniques.

Chapter 4. In this work the synthesis, characterisation and application of polyoxometalate biofunctionalised oligonucleotides (DNA-POMs) are described. Copper mediated Husgen 1, 3 cycloaddition click chemistry was compared with generic amidino coupling for both Keggin and Dawson POMs, in either acetonitrile or DMSO. The POM-primer conjugates were characterised using ESI-MS, Raman spectroscopies, gel electrophoresis and AFM, and successful coupling of the DNA primer to each of the POMs was observed. The functionality of the primer-POM was demonstrated via electrochemical detection of hybridisation to a surface immobilised probe. The POM-labelled forward primer was then used in combination with a biotinylated reverse primer for the PCR amplification of a *Francisella tularensis* related sequence. The amplicon was evaluated using gel electrophoresis and efficient DNA amplification was obtained. Streptavidin coated beads were used to generate single stranded DNA from the duplex PCR product and the POM-labelled strand was liberated for subsequent detection. Gold electrodes were functionalised with 3'-thiol or 5'-thiol terminated probes and

electrochemical detection of the POM-5'-labelled single stranded DNA demonstrated that a slightly better limit of detection and a markedly improved sensitivity was achieved with the 3'thiol probe that resulted in the POM-label being in closer proximity to the electrode surface. The report details the first use of POMs as primer labels, not only showing that they do not interfere in the polymerase chain reaction, but also demonstrating their use for the sensitive, direct and substrate-free electrochemical detection of DNA.

Chapter 5. In this work the design, synthesis, characterisation and use of polyoxometalate (POM) modified deoxynucleotides in PCR is described. POMs were linked at position 7 of 7 deaza modified purines and position 5 of modified pyrimidines by adopting a method developed for linking activated carboxy POMs with amine terminated molecules (Chapter 3). The synthesised POM – nucleotide conjugates were characterised using high resolution ESI MS and subsequently used in PCR along with unmodified dNTPs. The gel electrophoresis analysis showed successful amplification until 60% substitution of the natural dNTP for Keggin (SiW_{11}) POM modified dNTPs. The hindrance of amplification is very pronounced for Dawson POM (P_2W_{17}) modified dNTPs, with amplification only observed for substitution less than 20% of the modified dNTPs. The labelled dNTPs will be used for the direct detection of PCR products.

Chapter 6. In this report four different organic molecules were used to covalently label ddNTPs for use in electrochemical APEX. The labels were chosen based on their distinguishable redox potentials. Two strategies were developed to test solid phase nucleotide incorporation and detect SNPs known to occur in the cardiomyopathy related MYH7 gene. As a proof of concept labelled ddNTPs were incorporated close to the electrode surface at the 3'OH terminal and once demonstrated, the more realistic situation of having the ddNTP incorporated at the 3'OH terminal further from the electrode surface . The results obtained confirm the possibility of SNP detection, demonstrating a huge stride in the development of electrochemical APEX.

List of publications and conferences attended

I. Research Papers

1. Ahmed M. Debela, Mayreli Ortiz, Ciara K. O´Sullivan, Serge Thorimbert, Bernold Hasenknopf, Postfunctionalisation of Keggin silicotungstates by general coupling procedures (2014) Polyhedron, 68,131-137 (IF= 1.946)
2. Ahmed M. Debela, Mayreli Ortiz, Valerio Beni, Ciara K. O´Sullivan, Facile electrochemical hydrogenation and chlorination of glassy carbon to produce highly reactive and uniform surfaces for stable anchoring of thiolated molecules (2014) Chem. A Eur. J. (in press) (IF= 5.931) DOI: 10.1002/chem.201402051 (HOT PAPER).
3. Ahmed M. Debela, Mayreli Ortiz, Valerio Beni, Ciara K. O´Sullivan, Surface functionalisation of carbon materials for highly stable and low cost fabrication of electrochemical genosensors, *(under preparation for submission to Electrochemical Communications)*
4. Ahmed M. Debela, Mayreli Ortiz, Valerio Beni, Serge Thorimbert, Denis Lesage, Cole Richaed, Bernold Hasenknopf, Ciara K. O´Sullivan, Polyoxometalate biofunctionalised primers: Use in polymerase chain reaction and electrochemical detection of PCR product *(under preparation for submission to Chemical Sciences)*
5. Ahmed M. Debela, Mayreli Ortiz, Marketa Svobodova, Serge Thorimbert, Denis Lesage, Cole Richaed, Bernold Hasenknopf, Ciara K. O´Sullivan Synthesis characterisation and PCR incorporation polyoxometalate labeled d(d)NTPs as novel class of redox labels for electrochemical SNP typing *(under preparation)*
6. Ahmed M. Debela, Mayreli Ortiz, Serge Thorimbert, Bernold Hasenknopf, Ciara K. O´Sullivan, Electrochemical APEX for genotyping MYH7 gene; a low cost strategy for detection of disease causing mutations *(under preparation)*

II. Papers from master thesis

1. Olivier Y. F. Henry, Ahmed M. Debela, Sinead Kirwan, Josep L. Acero, Ciara K.O'Sullivan, Three-dimensional Arrangement of Short DNA Oligonucleotides at Surfaces via the Synthesis of DNA-branched Polyacrylamide Brushes by SI-ATRP (2011), Macromol Rapid Commun. 32(18), 1405–1410.
2. Olivier Y. F. Henry, Sinead Kirwan, Ahmed M. Debela, Ciara K. O'Sullivan, Electrochemical genosensor based on three-dimensional DNA polymer brushes monolayers(2011), Electrochem Com.,13, (11), 1155-1158.

III. Conferences

1. poster presentations

a. Transfronterera Meeting on Sensors and Biosensors ' XV, september (2010) which is held at la Rapita , Spain
b. XVI^{èmes} Rencontres Transfrontalieres « Capteurs Et Biocapteurs » September (2011), Toulouse France.
c. 7th annual conference recombinant systems biology and regulatory genomics from October (2011) Barcelona.
d. III International Workshop on Analytical Miniaturisation and NANOtechnologies". (WAM – NANO) (2012), Barcelona, June 11-12,2012
e. Poster presentation at 9th and 11th doctoral day at Department of chemical Engineering ,University Rovira I Virgili,Tarragona , Spain

2. Oral presentation

Transfronterera Meeting on Sensors and Biosensors, XVII September (2012), Tarragona, Spain, Covalent immobilisation of thiolated oligonucleotide onto glassy carbon: a highly stable surface chemistry.

List of Figures

Chapter 1

Chapter 2

Chapter 3

Chapter 4

Chapter 5

Chapter 6

List of tables

Chapter 2

Chapter 3

Chapter 4

Chapter 5

Chapter 6

List of abbreviations

dsDNA= double stranded deoxy ribonucleic acid

ssDNA= single stranded deoxy ribonucleic acid

dNTP = deoxy nucleotide triphosphates

ddNTPs = dideoxy nucleotide triphosphates

HGP= Human Genome Project

SNPs = Single nucleotide polymorphisms

HapMap =Haplotype Mapping

CRT = cyclic reversible termination

SBS = sequencing by synthesis

PME = Pulsed Multi-line Excitation

SBH = Sequencing by Hybridisation

AS-PE = allele specific primer extension

APEX = arrayed primer extension,

CPE = common primer extension

ASPEX = allele specific primer extension

SBE = single base extension

S/N = signal-to-noise

FENs = Flap endonucleases

SPR = surface plasmon resonance

SERS = surface-enhanced Raman scattering

SAM = self assembled monolayer

PCR = polymerase chain reaction

PEX = primer extention

RP = Reporter probe

Fc =ferrocene

POM = polyoxometalates

AFM = atomic force microscopy

SEM = scanning electron microscopy

ATR FT-IR = attenuated total internal reflection furrier transform infrared spectroscopy

XPS= X ray photoelectron spectroscopy

GCE = glassy carbon electrode

HOPG = highly pyrolitic ordered graphite

TCEP = tris (2-carboxyethyl) phosphine

RuHex = hexa-amine ruthenium (III) chloride ($[Ru(NH_3)_6]Cl_3$)

TMB = 3, 3', 5, 5'- tetramethyl benzidine

ELISA = enzyme linked immunosorbent assay

PGSTAT = potentiostat/galvanostat

GPES = General Purpose Electrochemical System

KPFM = Kelvin probe force microscopy

UHV = ultra high vacuum

HRP = horse radish peroxidase

DPV = pulse voltammetry

O/C = oxygen/carbon atomic ratio

NHE = Normal hydrogen electrode

CuAAC = copper catalysed azide alkyne cyclo addition

TMS = Tetramethylsilane

DMSO-d6 = duetrated dimethyl sulfoxide

The LMCO = low-mass cutoff

MCH = mercaptohexanol

PBS = phosphate-buffered saline

TAE = triethyl ammonium

TBA = tetra butyl ammonium

EDTA= tert-butanol, ethylenediaminetetraacetic acid disodium salt dehydrate

TBTA = tris[(1-benzyl-1H-1,2,3-triazol-4-yl)methyl]amine

FWHM = full width at half maximum

M/Z = mass to charge

SSC= saline-sodium citrate

LOD= limit of detection

Introduction

1.1 Deoxy ribonucleic acids (DNA)

DNA is a double-stranded molecule inside the nucleus of a cell and carries the genetic information enabling the construction and function of every living cell. The year 2013 marked the 60th anniversary of the elucidation of the structure of the DNA double helix by Watson and Crick[1]. Its' molecular structure comprises a backbone of repetitive units of sugar (2′-deoxyribose) phosphate, with each sugar bearing one of the four nucleobases adenine (A), thymine (T), guanine (G), and cytosine (C)) through glycosidic linkages at the 1' carbon of the sugar, and the phosphate is esterified to the 5' oxygen. The phosphate group acts as a "bridge" linking successive nucleotides in a phosphodiester backbone (see Figure 1). The information is carried in the form of a genetic code and is determined by the sequence of these four bases. The information of DNA is also converted into information used by each cell to build proteins in processes called transcription and translation. Genetic information in DNA is precisely copied into RNA, ribonucleic acid, which is then translated into proteins.

The noncovalent interaction between the nucleosides is responsible for holding the double strand together. Hydrogen bonding interactions between complementary base pairs, and base stacking interactions are the two major forces that keep the duplex intact.

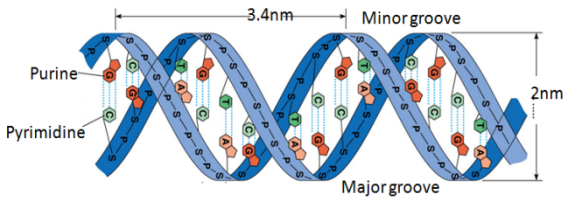

Figure 1. 1 Double stranded DNA illustrating the the purine and and pyrimidine bases and the hydrogen bonds formed between the bases GC(3) and AT(2*). (from © 1999 Addison wesley longman Inc.)*

1.2 DNA sequencing

In 1977 two methods of DNA sequencing were reported, the dideoxy chain terminating method of Sanger and coworkers [Sanger's method] and Maxim and Gilbert's chemical degradation method [2,3]. Sanger and Gilbert shared the Nobel Prize [1980] in chemistry for their development of an analytical method for DNA sequencing. Sanger DNA sequencing is based on extending a DNA primer hybridised to the targeted single stranded DNA template. In this approach a small proportion of the dNTPs used in the amplification are replaced by ddNTPs (dideoxyribonuclotide phosphates); the polymerase will extend the primer with dNTPs until it incorporates a ddNTP, thus terminating the extension, generating in this way, fragments of all possible lengths. The original detection method involved the use of radiolabeled primers and amplification using four parallel reactions, each with only one terminating ddNTP. The amplification products obtained were then electrophoretically separated according to size in four lanes of a polyacrylamide gel and the sequence then simply "read" from the sizes of the fragments in each lane.

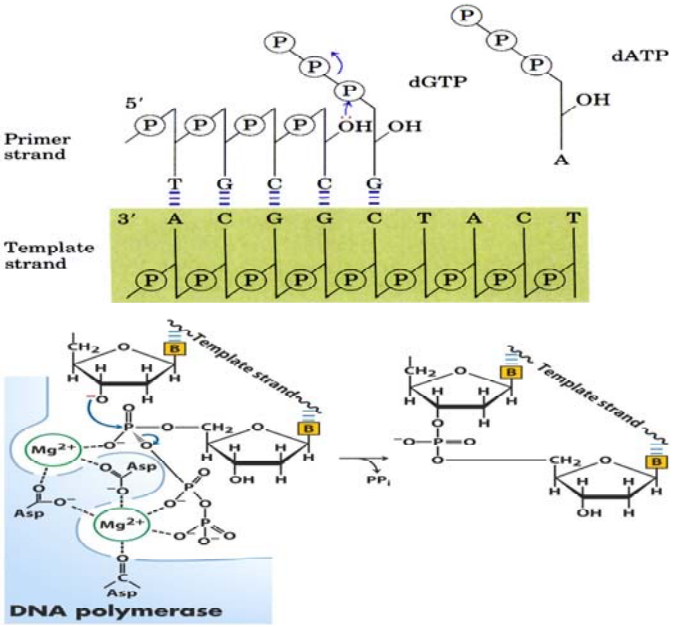

Figure 1. 2. Mechanism of nucleotide triphosphate (dNTP) incorporation by a polymerase. (*adapted from: Nature Reviews Molecular Cell Biology 2000, 1(2), 101-109.)*

Considerable improvements of the Sanger´s method have been achieved by the introduction of thermostable DNA polymerases[4], of fluorescent labeling of the ddNTPs[5, 6], capillary electrophoresis separation and parallelisation of amplification reactions. There

is currently a huge amount of research focused on the reduction of costs of DNA sequence in order to meet the target of whole genome sequencing for less than $1000, via arrayed/multiplexed techniques.

1.3 The Human Genome Project (HGP)

A decade has since after the completion of HGP, one of the most important scientific achievements in history, where the sequence of the human genome is reported to contain 3.2-gigabase[7]. The completion of the draft of the human genome has paved the way for mapping diversity in the overall genome sequence which helps to understand the genetic causes of inherited diseases as well as susceptibility to drugs, metabolites and environmental toxins. Identifying genetic variations between individuals will increase our understanding of genetically related diseases and disorders and lead to molecular-level treatment specific to each individual. Consequently, a great deal of effort is being put into the development of robust, cost-effective, and high-throughput technologies for genetic-variation analysis.

1.4 Single nucleotide polymorphism

From the genome sequence there are individual variations which include: single nucleotide polymorphisms (SNPs), insertions and deletions (indels), microsatellites (MSs), and differences in the methylation status of important regions (e.g. CpG islands). However the majority of the variations attributable to SNPs. SNPs are -point mutations which are DNA sequence variations that occur when a single base pair in a genome is altered where the less common variant occurs in at least 1% of the total population[8]. SNPs are attributable to 90% of the genetic variations[9] and the reainder is attributable to insertions or deletions of one or more bases, repeat length polymorphisms and rearrangements[10]. The decoding of the human genome has revealed the presence of around 10 million SNPs (roughly 1 every 300-1000 bases)[9], opening up exciting new capabilities for associating individual SNPs, haplotypes, and linkage disequilibrium with disease states and pharmacological responses[11-13].

Almost all SNPs are diallelic and fall into four classes, one transition (C↔T/G↔A) and three transversions (C↔A/G↔T, C↔G/G↔C andT↔A/A↔T) [14]. Depending on their

location in the genome, SNPs may have different consequences at the phenotypic level. SNPs present in regulatory sites of a gene will perturb the transcriptional rate, affecting the expression level of encoded protein. In the coding region, SNPs may alter the structure and, hence, function of encoded protein. These SNPs are often recognised as molecular markers of genetic disorders and disease predisposition. Among the genetic diseases known many are associated with genetic variations including Tay Sachs[15], cystic fibrosis[16], thalassaemia[17], sickle cell anaemia[18], Bardet–Biedl syndrome[19], retinitis pigmentosa[20].

1.5 Genotyping and sequencing technologies

The need for sequencing or mapping is increasing for applications spanning diverse research sectors including comparative genomics and evolution, forensics, epidemiology, and applied medicine for diagnostics and therapeutics. Arguably, the strongest rationale for ongoing sequencing is the quest for identification and interpretation of human sequence variation as it relates to health and disease.According to M. L. Metzker[21], the current sequencing techniques are grouped in two: Group 1. DNA polymerase-dependent strategies which encompases three major categories: Sanger sequencing, single nucleotide addition (SNA), and cyclic reversible termination (CRT), the other group includes all polymerase dependent sequencing techniques under the heading sequencing by synthesis (SBS).

1.5.1 Single nucleotide addition (SNA): this involves detection of the identity of each nucleotide immediately after its incorporation into a growing strand of DNA in a polymerase reaction. One example is "fluorescent in situ sequencing" (FISSEQ)[22]. A different fluorophore is linked to each of the four bases through a photocleavable linker. DNA polymerase incorporates a complementary single-nucleotide analogue. The unique fluorescence emission detected depends upon which dNTP is incorporated, and the Fluorophore is subsequently photochemically removed. The 3-OH group is chemically regenerated and the cycle proceeds. This method allows parallel sequencing and the photocleaving is easy and rapid.

1.5.2 Pyrosequencing^{tm} (Biotage, Sweden): employs chemiluminescence based detection for sequencing and uses a cascade of enzyme reactions. It involves the

sequencing-by-synthesis approach in which nucleotides (dATP, dCTP, dGTP, or dTTP) are added one at a time to a primer extension reaction mixture. When the added nucleotide is complementary to the nucleotide being extended, polymerase enzyme utilises it for primer extension, releasing inorganic pyrophosphate (PPi). In a series of enzymatic reactions, the released PPi is used to generate light [(Figure 1. 3 b). No light signal is produced for an unincorporated nucleotide and it is removed from the reaction mixture before adding a new nucleotide. Therefore, by monitoring the light signal from the primer extension reaction, one can verify the incorporation of a specific nucleotide[23].

1.5.3 Pulsed Multi-line Excitation (PME): is a method for multifluorescence discrimination of nucleotides separated by capillary electrophoresis. Four laser dye systems excites near absorption maximum to achieve a uniformly intense emission signal. This technique is preferred as it avoids cross-talk between dye channels has higher sensitivity, quicker analysis, and a lower cost as well as shortened preparation time, reduced sample and reagent volumes and less data data processing[24].

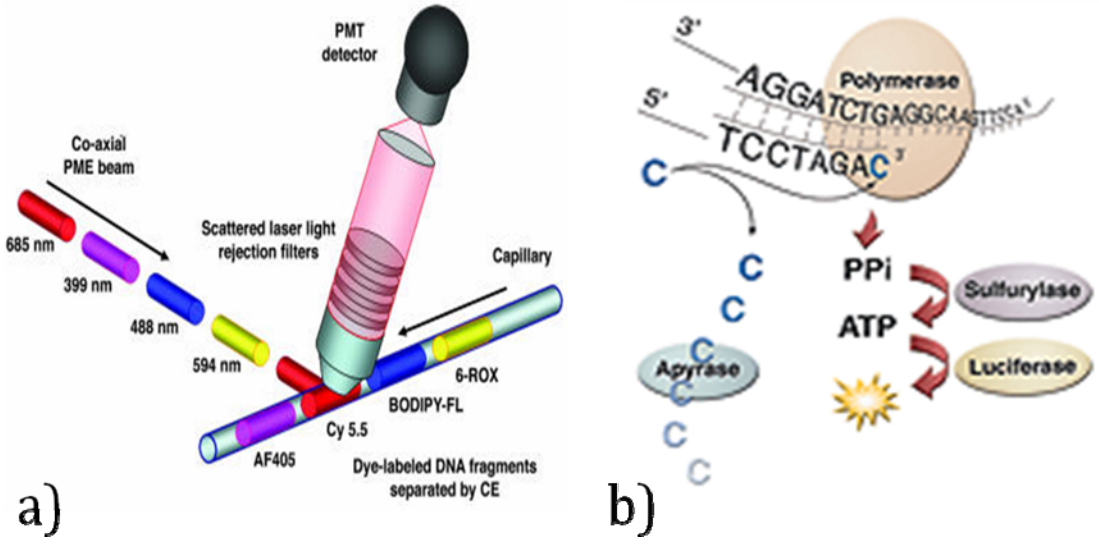

Figure 1. 3. Drawings showing the PME technology in a)[24] and pyrosequencing b). *(from J Comput Sci Syst Biol ,2009, 2, 074-092)*

1.5.4 Sequencing by hybridisation (SBH): Sequencing by hybridisation is a novel DNA sequencing technique in which an array (SBH chip) of short sequences of nucleotides (probes) is brought in contact with a solution of target DNA sequence. A biochemical method determines the subset of probes that bind to the target sequence (the spectrum of the sequence), and a combinatorial method is used to reconstruct the DNA sequence from the spectrum. SBH is reported not to be competitive with standard gel based methods due to the lack of tools to handle the levels of hybridisation errors and its limitation on the length of reconstructible sequences by standard universal arrays as well as the requirement of large libraries of oligonucleotides[25] .

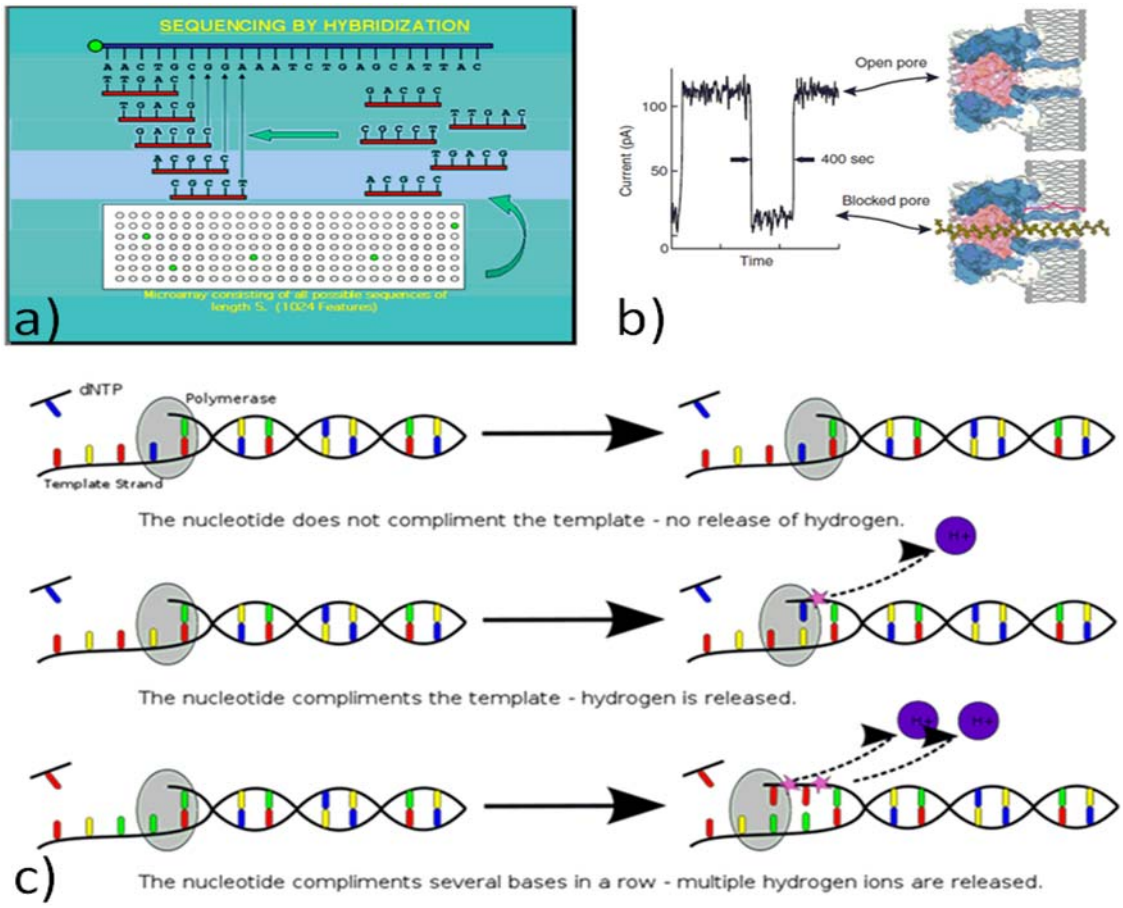

Figure 1.4. Illustration of the sequencing by hybridisation (a) and nanopore sequencing (b) and semiconductor sequencing (c). *(J. Comput. Biol. 2004, 11(4): 753-765.)*

1.5.5 Nanopore sequencing: utilises a nanoscale device that translocates polymer molecules in asequential monomer order through a very small volume of space. This technique includes a detector that directly converts characteristic features of the

translocating polymer into an electrical signal. Transduction and recognition occur in real time, on a molecule-by-molecule basis. It can probe thousands of different molecules in a few minutes. And one of the major advantages is that it can probe very long lengths of DNA[26].

1.5.6 Semiconductor sequencing: developed by Life Technology and Ion Torrent, the Ion Personal Genome [IPG] Machine, which represents an affordable and rapid bench top system and capable of sequencing the human genome in a day. The IPG system harbours an array of semiconductor chips capable of sensing minor changes in pH and detecting nucleotide incorporation events by the release of a hydrogen ion from natural nucleotides. The Ion Torrent system does not require any special enzymes or labelled nucleotides and takes advantage of the advances made in the semiconductor technology and component miniaturisation[27].

1.6. SNP genotyping strategies

SNP genotyping is of fundamental importance for the early identification and diagnosis of genetic disorders and disease predisposition which will potentially facilitate for a more personalised approach to medicine. SNP genotyping strategies typically involve two steps: allele-discrimination and allele-detection[14, 28], Allele-discrimination can be achieved by primer extension[29-36], allele specific hybridisation[37, 38], ligation[39-41], or enzymatic cleavage[42, 43], and most allele-detection methods are based on mass spectroscopy[31], fluorescence/optical[44], or electro/chemiluminescence[45, 46], electrochemical[47,48], gravimetric[49] and electrophoretic[50] techniques.

1.6.1 Single nucleotide Primer extension

This technique is known by variety of acronyms such as primer guided nucleotide incorporations, primer extension technique, solid phase minisequencing, allele specific primer extention (AS-PE), genetic bit analysis (GBA), arrayed primer extension (APEX), first nucleotide change (FNC), template directed dye terminator incorporation (TDI), probe oligobase extension (PROBE) and pin point assay (PP assay)[51]. This method is derived from Sanger DNA sequencing and uses labelled dideoxynucleotides for termination of a growing DNA strand from a primer with its 3′-end designed

immediately upstream of a polymorphic site[52]. Primer extensions involve allele-specific incorporation of nucleotides in a primer extension reaction with a DNA template, utilising enzyme specificity to achieve allelic discrimination. Primer extention assays either use: A common primer for detecting both alleles (APEX, SBE) (more common method) or a specific primer for detecting each allele (ASPEX). The former is commonly termed as common primer extention (CPE). In a typical CPE reaction, a primer is designed to anneal with its 3′end adjacent to a SNP site and extend with nucleotides using a polymerase enzyme [30].

Arrayed primer extension (APEX): This is a template dependent single base extension technique with an array of primers attached to a solid support through their 5′end[53, 54]. Complementary DNA strands are hybridised to the primers and fluorescence is used for genotype determination after polymerase incorporation of a flourophore labeled ddNTP. The advantage of solid-phase reaction approaches is the reduction in primer-primer interaction leading to improved specificity as compared with hybridisation-based DNA chip analysis. Furthermore, APEX offers a high signal-to-noise (S/N) ratio and consequent high fidelity. Typically SBE is considered to offer about an order of magnitude better SNP discrimination than allele-specific hybridisation[53]. Generally accepted in vitro error rates for polymerase base insertion vary between 10^{-3} and 10^{-6} suggesting that even low fidelity enzymes such as reverse transcriptase should be suitable for highly quantitative SBE genotyping[55]. In practice, however, the power of discriminating between genotypes and the sensitivity of detecting a minority sequence.
variant by the minisequencing reaction are at least one or two orders of magnitude lower than the theoretical values predicted. The reasons for this discrepancy between theory and practice, are probably, due to the fact that the labelled nucleotide analogues may contain other nucleotides as impurities, and that the labelled moieties of the nucleotide analogue affect the specificity of the nucleotide incorporation by the DNA polymerase[51].

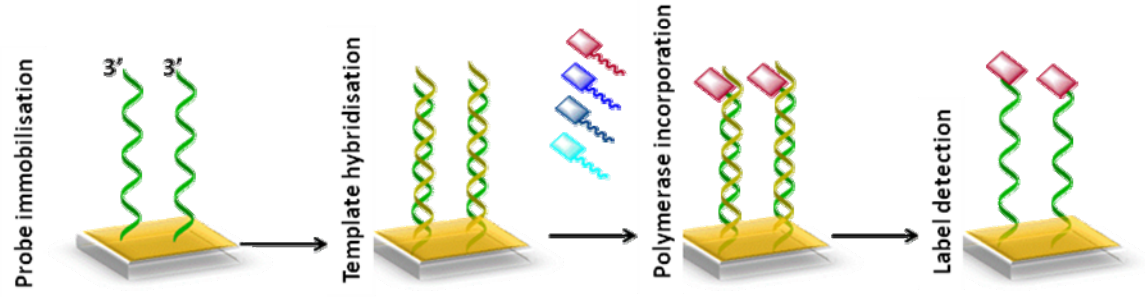

Figure 1.5. Illustrating the APEX reaction and the steps involved

1.6.2 Oligonucleotide Ligation reaction: Ligation approaches employ specificity of ligase enzymes to achieve allelic discrimination. When two oligonucleotides hybridise to single-stranded template DNA with perfect complementarity, adjacent to each other, ligase enzymes join them to form a single oligonucleotide. Three oligonucleotide probes are used in traditional ligation assays, two of which are allele specific and bind to the template at the SNP site[39-41]. The third probe is common and binds to the template adjacent to the SNP immediately next to the allele-specific probe. If the allele-specific probe binds at the SNP site with perfect complementarity, DNA ligase joins it with the common probe. The ligation products are then detected by various means to reveal base identity at the SNP position. Most ligation methods employ allele-specific probes with their 3′ ends at the SNP sites because ligases are more sensitive to mismatches at the 3′end.

1.6.3 Invasive cleavage: This method employs allele-specific probes containing a "tag" sequence at the 5′-end unrelated to the target. An invader probe hybridises to the "tag" 5′ of the polymorphic site, and if there is a perfect match, a specific enzyme recognises the overlapping structure formed and cleaves the 5′-segment of the allele-specific probe[42,43].

1.6.4 Differential Hybridisation: Hybridisation approaches use differences in thermal stability of double-stranded DNA to distinguish between perfectly matched and mismatched target-probe pairs for achieving allelic discrimination. Generally, the effectiveness in allele differentiation depends on the length and sequence of the probe, location of SNP in the probe, as well as hybridisation conditions[38]. The different assays

utilising this approach include TaqMan® assay, Dynamic allele-specific hybridisation (DASH[tm]; DynaMetrix, UK) [37], Qbead[tm] approach (Quantum Dot, CA) [38].

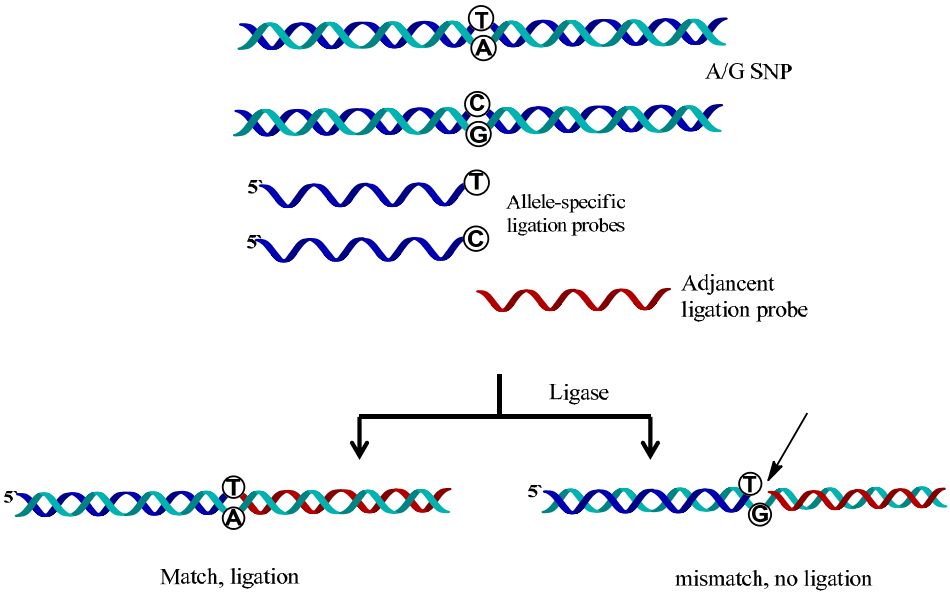

Figure 1.6. Schematic depiction of allele discrimination by ligation method. *(adapted from Nature Reviews Genetics2001 2: 930-942)*

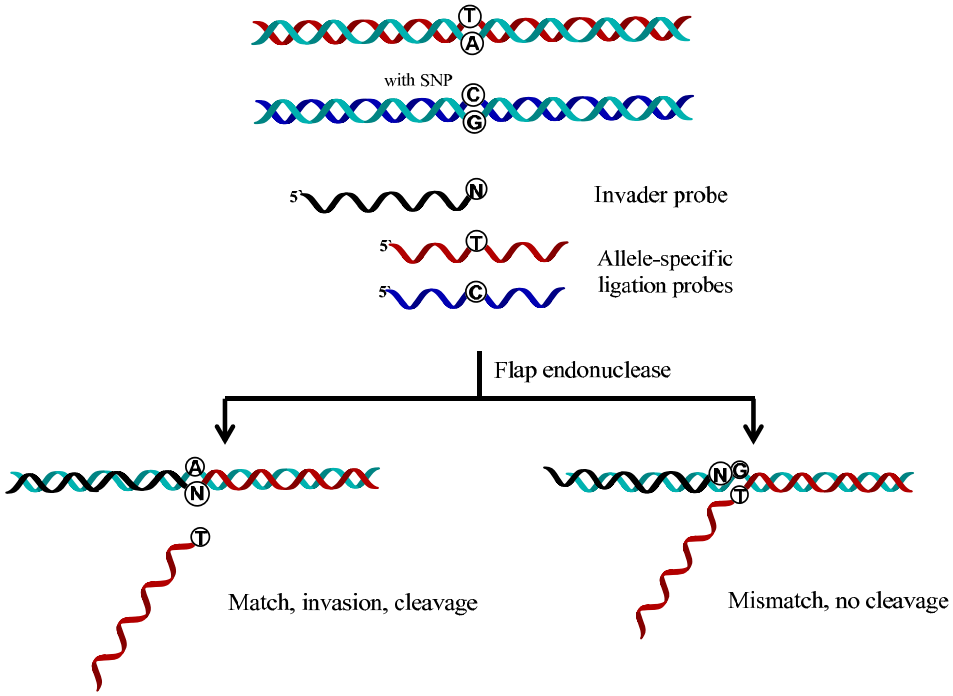

Figure 1.7. Allele-specific cleavage in an Invader® reaction by flap endonucleases (FENs). *(adapted from Nature Reviews Genetics2001 2: 930-942)*

1.7 SNP detection methods

The various allele discrimination steps described above have been coupled to signal transduction and amplification schemes for the development of sensitive assays for SNP genotyping. To date, assays based on mass spectrometry, optical, fluorescence, and electrochemical methods have been described. A variety of reporters such as enzymatic probes[56, 57], binary probes[58], nanoparticles[59, 60], redox molecules[61-63], and fluorescent dyes[64] have been used. Until now there has been no consensus for the best SNP detection method in terms of SNP throughput, sample throughput, simplicity, robustness, and cost. Although they are sensitive and specific, many of these systems have features that limit their practical use, such as tedious assay processes, the need for expensive instruments (e.g., mass spectrometer), and the need for tight control over the experimental conditions (e.g., temperature). Here in some of the methods are briefly described.

1.7.1 Mass spectrometry–based detection: this approach involves the use of a primer that anneals one base upstream of the SNP site followed by its extension with ddNTPs. Extension products are detected by mass spectrometry and the difference between the mass of the extension product and the primer facilitates the identification of the incorporated nucleotide(s) and hence the SNP genotype. Various high throughput technologies employ this detection method, e.g. MassARRAYtm (Sequenom, CA)[31]

1.7.2 Optical methods are the commonest methods of DNA sequencing and genotyping. Optical SNP typing comprises fluorescence, surface plasmon resonance (SPR)[65], chemiluminescence[45,46], colorimetry[66-68], interferometry[69], or surface-enhanced Raman scattering (SERS) spectroscopy[70] techniques. Optical DNA schemes suffer drawbacks due to a high background noise, photo- bleaching of dye labels and the need for sophisticated instrumentation for readout and analysis of data. These drawbacks limit the development of portable, rapid and robust platforms for gene analysis.

1.7.3 Fluorescence detection: With progress in automated DNA synthesis and phosphoroamidite chemistry as well as organic synthesis, it has become possible to attach fluorophores covalently to oligonucleotides and modified nucleotides. Different fluorescent dyes have been used to engineer oligonucleotide probes, for example fluorescein, TAMRA, Cy dyes, Texas red, HEX, JOE, Oregon green, rhodamine 6 G,

coumarin, pyrene, and others. Additionally, in fluorescence quenching approaches, quencher molecules have also been covalently attached to the fluorescent oligonucleotides. Dimethylaminophenylazobenzoic acid (DABCYL) has been widely used as a universal quencher for many fluorophores[64].

1.7.4 Electrochemical methods

Electrochemical devices have attracted much attention for the transduction of biomolecular interactions. Electrochemistry has the potential to be a leading molecular detection strategy for genotyping as it can be performed with miniaturised, relatively compact, simple to operate, and low cost instrumentation. Moreover, electrochemical measurements are rapid and very low limits of detections can be achieved. These properties make electrochemical transduction very versatile and suitable for on-site analysis[71].

A large number of electrochemical DNA detection platforms for SNP analysis have been reported[72-80]. For instance, Barton et al. described a system that detects changes in long-range charge transport though the π-stack of duplex DNA by combining redox-active intercalators with exogenous electrocatalytic species[73]. In this approach, targets that alter base-pair stacking, such as a mismatched base within the DNA duplex, are identified via reduced charge transfer relative to perfectly matched targets. Other groups have employed electrochemically active DNA probes in a variety of SNP analysis strategies, including the post-hybridisation application of exogenous redox-active reporters with preferential affinity for duplex DNA[75] or sandwich assays based on redox-labeled DNA probes that bind to a target DNA sequence[76].

1.8 Challenges with electrochemical SNP detection

A major concern with most electrochemical genotyping approaches is the implementation of multistep enzymatic discrimination reactions on the surface, which possibly leads to steric hindrance and thus influences enzymatic efficiency and reproducibility. Additionally for those strategies using redox labels, current assay configurations fail to render electroactive reporters in close proximity to the electrode interface, limiting the sensitivity of the detection strategies[48]. These approaches offer accurate room temperature SNP detection but are often susceptible to false positives

arising from non-specific binding of redox reporters and require exogenous reagents and posthybridisation washing steps[81]. Some further technology challenges and limitations with electrochemical SNP detection, include the expensive cost of a DNA labeling instrument, time-consuming and complicated surface modification, difficulty in quantification of the amount of DNA immobilised on the substrate, stability of the DNA probes (both to temperature and atmospheric conditions) as well as the limited number of truly selective probes. Thus there still exists a huge challenge for the simple, low-cost, rapid and highly selective detection of SNPs. [80]

1.8. 1 Surface chemistry

The most widely used protocol for attaching DNA to an electrode surface is through thiol-based self assembled monolayer (SAM) formation. However, this has been reported to suffer from instabilities to elevated temperature and extreme redox potential. To improve the thermal stability, different approaches have been tested destined to enhance both lateral stability with SAMs and their coupling to substrates. Examples include lateral polymerisation[82], hydrogen bonding[83], multiple sulfur substrate coupling[84, 85], and the utilisation of more rigid aromatic SAMs[85]. The electrodes can be grafted through various other strategies such as through diazonium salts or similar tethering[86] for subsequent DNA attachment of amine/carboxy grafted electrodes through the generic carbodiimide coupling. The increased stability of surface tethered DNA helps to improve reproducibility, provide physical insight into processing steps such as post-hybridisation washing, and to mitigate noisy signals that otherwise can render large fractions of measured information unusable[87].

1.8. 2 DNA Labelling

A variety of redox active species have been used to conjugate with DNA to increase sensitivity of detection. These species are selected for use in DNA sensing based on their redox potential (with in -0.9V to 0.9V vs Ag/AgCl potential window) in such a way that no damage occurs to the probe on the surface as a result of the redox reaction. There are three groups of labels used for DNA labelling, the first group of labels are the so called groove binders which preferentially bind to the DNA duplex, (they simply intercalate preferentially to dsDNA, but this class of labels is reported to have insufficient

discriminating ability for dsDNA). The second class of labels exploits the electrostatic interaction with DNA sugar phosphate back bone, The two most commonly used from this class are $[Ru(NH_3)_6]^{3+}$. However, ruthenium hexamine suffers from a high background current due to the negative charge of the DNA. This can be circumvented by the use of peptide nucleic acids [PNA] probes due to their pseudopeptide backbone with no electric charge. In this way, the redox active cationic species would not interact electrostatically with the PNA probe, and thus the signal could be attributed to hybridisation with negatively charged DNA[88]. The third class of labels are electroactive labels covalently attached to either target nucleotides or to the reporter probe (e.g. in a sandwich assay). Examples in this class include osmium/osmium tetra oxide, ruthenium, ferrocene, anthraquinone, aminophenyl and nitrophenyl groups, polyhedral boron clusters, enzyme tags, nanoparticles, as well as quantum dots and carbon nanotubes[89].

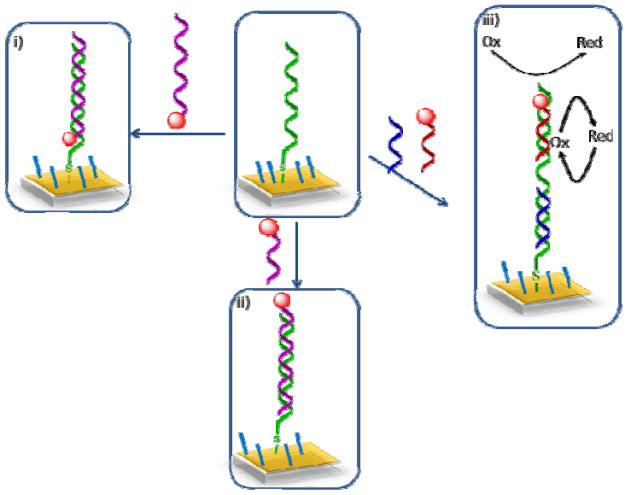

Figure 1. 8. The various strategies of electrochemical detection of DNA hybridisation using redox active labels.

1.8.3 Polymerase incorporation

Great strides have been made in the enzymatic synthesis and replication of nucleic acids comprising of unnatural chemical modifications through elegant chemistry, judicious use of polymerases and optimisation of the reaction conditions and additives[90]. In general, B-family thermo-stable polymerases (Vent (exo-), Pwo, KOD) are the best enzymes tolerating the presence of most modifications. Improved polymerases with a high tolerance to modifications have been engineered by in vitro selection[91]. The thermo-

stable polymerases are not only used for PCR but also for primer extensions, although here the Klenow fragment can be efficiently used in some cases[92]. The ability of DNA polymerases to incorporate these nucleotides linked to detectable reporter or functional groups has been important in monitoring gene expression, in situ hybridisation and four colour sequencing[93].

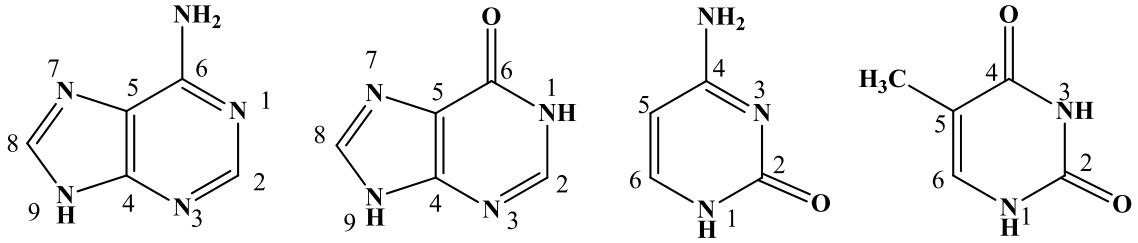

Figure 1. 9. Nucleobases with their numbering R indicates the position of the sugar in the corresponding nucleotide.

Studies have revealed that modifications to the major groove of the nucleobase allow for the best incorporation efficiency with the 5-position of pyrimidines and the 7-position of purines being the optimal site[94]. The flexibility of the linker arm attaching the modification can also influence nucleotide utilisation, with rigid, linear linkers providing the strongest dNTP substrate properties. Linker arm length also plays a role in modified dNTP incorporation. Modified dNTPs with shorter linker arms (i.e., biotin-4-dUTP) are better substrates than nucleotides with longer linker arms (i.e., biotin-11-dUTP or biotin-14-dUTP). In most cases it is reported that complete substitution of a modified dNTP for its natural counterpart causes inhibition of PCR, resulting in low and often undetectable product formation. This is due to the compounding effect of a lower efficiency of nucleotide incorporation over multiple cycles[95]. Most natural DNA polymerases have been found to be capable to incorporate bulky fluorescent nucleotide analogues, but with slower kinetics than their unlabeled counterparts. This is probably due to a charge difference and a steric interference when compared to the natural substrates[96]. The steric interaction is particularly problematic when several labeled nucleotides are to be inserted sequentially[97]. Hence the knowledge of linker position and length, functional groups, the size of the label as well as the optimised concentration of the unnatural dNTPs is crucial to achieve successful incorporation.

The polymerase incorporation of modified dNTPs has been used for a variety of functional groups. Fluorescent markers have been incorporated via TAMRA-labelled dUTPs[91]. Whilst others have constructed modified DNA bearing amino, cyano, guanidine, amino acids, acridone, fluoroalkyls, nitroxide spin labels, alkynes, diols, steroids, as well as sugars[89]. Several types of redox active labels such as ferrocene and Ru(bpy)2-containing dNTPs were also prepared, incorporated and used for bioanalytical applications. Hocek and co-workers have recently investigated properties of both pyrimidine and purine analogs with conjugated bipyridine, terpyridine, and phenanthroline moieties. The nonmetalated nucleoside analogs were prepared via cross-coupling reactions of the ethynyl/phenyl-modified polypyridyl arm with the unprotected halo-nucleosides[92]. The organic labelling of dNTPs with various electroactive functional groups and their subsequent enzymatic incorporation into DNA by polymerases has been extensively reported independently by different groups for the successful incorporation of Fc, anthraquinone and others [36, 98, 99].

1.9 Multipotential SNP detection approaches

The past decade has seen some glimpse of advances to replicate the results obtained for the multicolor optical labeling employed in the DNA sequencing techniques[100] as well as in gene "chips" (arrays)[101], by utilising several electrochemical approaches with electroactive labels differing in their redox potentials. There are some notable examples, including that of Kuhr and co-workers who utilised four different ferrocene derivatives as DNA tags in a DNA sequencing technique using capillary electrophoresis coupled to a sinusoidal-voltammetric detector[102]. Three ferrocene labels complemented with anthraquinone (representing a tag for the fourth DNA base) were used by Di Giusto et al. who reported the detection of primer extension reactions on self-assembled monolayer-modified gold electrodes[36,103].

More than a decade ago Weizman and Tor introduced[103] a set of "tunable" electroactive DNA tags based on Ru or Os complexes involving negatively charged ligands (L^-) such as acetylacetonate or hydroxamate. The $[Me(bipy)_2L^-]^{2+}$ complexes (bipy) 2,2'-bipyridine) exhibited substantially lower oxidation potentials than those of analogous $[Me(bipy)_3]^{2+}$ complexes. The authors proposed the utilisation of the redox-tunable complexes as

potential DNA labels for the "multicolor" electrochemical DNA detection allowing parallel analysis of multiple target DNAs. This was followed by a related work by Fojta and coworkers[104], who reported related compounds by replacing bipy with other nitrogenous ligands (L) and obtained considerable shifts in peak potentials (at a carbon electrode) for DNA-Os, L. The authors suggested the potential of reporter probe [RP] labeling with the Os, L for electrochemical "multicolor "(multipotential) DNA coding. Another approach has been introduced by Wang et al [105] who proposed a electrochemical DNA coding technology based on sulfide nanoparticles of metals (quantum dots) differing in their redox potentials for simultaneous electrochemical measurements of multiple DNA targets. The products yielded well-defined and resolved stripping peaks at –1.12 V (Zn), –0.68 V (Cd), and –0.53 V (Pb) at the mercury-coated glassy-carbon electrode (vs Ag/AgCl reference). Husken et al[106] reported ferrocene –peptide nucleic acid (Fc-PNA) conjugates the redox potential of which was separated by 60mV vs $FcH^{0/+}$ which could have a potential application for PNA based electrochemical multipotential mapping of SNPs.

Various reports[107] have reported the enzymatic incorporation of labelled dNTPs to achieve multipotential redox coding with potential future application for diagnostics. However, all are far from their intended purpose due to problems with stability (both in moisture and air), poor substrates for polymerase failing to incorporate to adjacent positions due to their size and some of the labels have a redox potential beyond the potential window required for diagnostic applications.

1.10 Polyoxometalates

Polyoxometalates (POMs) are nanometer sized inorganic polyanions usually based on oxides of molybdenum or tungsten, and less frequently vanadium niobium and tantalum or mixture of these elements, in their highest (d^0, d^1) oxidation state. According to Pope[108] POMs can generally represented by the formula:

$[M_mO_y]^{p-}$ Isopolyanions

$[X_xM_mO_y]^{q-}$ $(x \leq m)$ Heteropolyanions

Each metal, also called *addenda* atoms M, is located at the center of polyhedra, MO_x, and the polyhedra are all bonded together through their corners or their edges and rarely faces. For heteropolyanions, the polyhedra are assembled around a heteroatom, X,

typically PO_4^{3-} or SiO_4^{4-} their symmetry follows that of the central heteroatom. This is the case for example of the polyoxometalate Keggin which has tetrahedral symmetry of the phosphate [PO_4^{3-}] ion or the silicate SiO_4^{4-} .

In 1826, Berzelius was the first to report the so called molybdenum blue for ammonium salt of $PMo_{12}O_{40}$. Keggin[109] reported the structural elucidation of the compound $H_3PW_{12}O_{40}.5H_2O$ by X-ray diffraction. Since then, a range of different types of POMs have been synthesized. Many different oxide clusters have been prepared including Lindqvist ($[M_6O_{19}]^{n-}$), Anderson ($[XM_6O_{24}]^{n-}$.), Dawson ($[X_2M_{18}O_{62}]^{n-}$), Preyssler ($X_5W_{30}O_{110}]^{n-}$) structures. However, Keggin and Dawson structures are the most widely used anion clusters (see Figure 1.10). And in this thesis we will only focuse on Dawson and Keggin type POMs and try to review details of their structure and physicochemical properties.

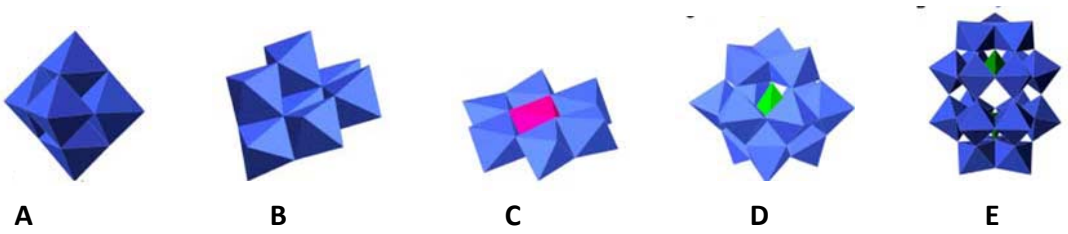

Figure 1.10. Polyhedral representations of the common polyoxometalate structures110; Lindqvist ($[M_6O_{19}]^{n-}$), A ,Waugh, $X^{n+}M_9O_{32}$(10-n)-, B, Anderson ($[XM_6O_{24}]^{n-}$),C, Keggin($X_5W_{30}O_{110}]^{n-}$), D, Dawson ($[X_2M_{18}O_{62}]^{n-}$), E, structures. ***Chem. Commun.,** 2008, 1837–1852 (ref 110)*

1.10.1 Structure of Keggin and Dawson POMs

Structure of Keggin anions: Keggin anions are spherical in shape (with a diameter of ~1.2 nm), and a general formula, α-$[XM_{12}O_{40}]^{n-}$ (M = Mo^{VI}, W^{VI}; heteroatom X = P^V, Si^{IV}, Ge^{IV}, Fe^{III}, Co^{II}, etc.), assembled by four $\{M_3O_{13}\}$ groups at the corners of a tetrahedron XO_4, comprising a large group of molecules in shape and composition. Each group is formed by three octahedra sharing edges and having a common oxygen atom, which is also shared with a central tetrahedron XO_4. Lacunary Keggin molecules can be formed by the removal of one or more MO groups[108].

Structure of Dawson Anion: Kehrmann first reported[111] the synthesis of phosphotungstic Wells Dawson type compounds in 1892 for the first time but the X ray crystal structure was only published[112] by Dawson in 1953.The general formula of the Dawson anion is $[(X^{n+})_2M_{18}O_{62}]^{(16-2n)-}$, where X^{n+} represents the central heteroatom such as phosphorous (V), arsenic(V), sulfur (VI) surrounded by *addenda* atoms each composed of MO_6 octahedral units. The Wells Dawson anion can be chemically manipulated to generate a lacunary anion by removing a metal oxo (MO_6) group eith from the cap (α2) or from the belt (α1). Lacunary α_1-$[P_2W_{17}O_{61}]^{10-}$ isomerises easily to the α_2 form or decomposes and reconstitutes the parent $[P_2W_{18}O_{62}]^{6-}$ [113]. The lacunary species of both Keggin and Dawson anions can be filled with a variety of elements, Sn, Ti, Mo, V, lanthanides etc. Lacunary POMs have several unique properties distinct from their parent structures, such as reduced symmetry, higher charge density, and increased reactivity[108].

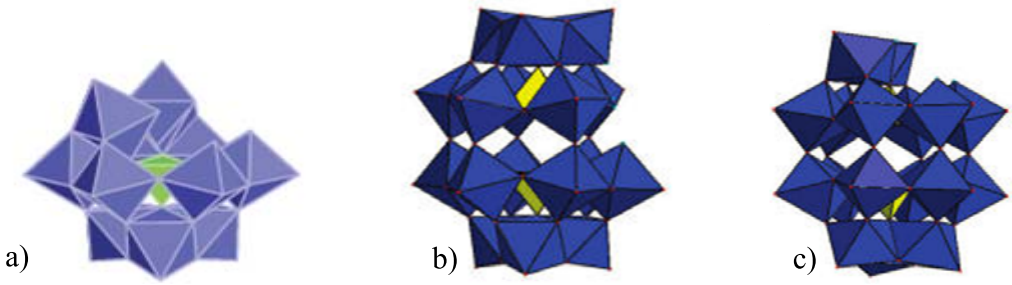

Figure 1,11. Polyhedral representation of lacunary Keggin $(XM_{11}O_{39})^{n-}$ (a) and and lacunary Dawson (α1-P2$W_{17}O_{61}$)10–isomer. (b) (α_2-$P_2W_{17}O_{61}$)10– isomer. (c)[111]

1.10.2 Organic functionalisations of POMs

Organic POM derivatives are of particular interest, as they combine the features of both, the inorganic polyanion and the covalently bound organic units in one discrete molecular assembly. Hybrid organic–inorganic POMs may also combine several interesting features, such as chirality[114, 115] magnetic and electrical properties[116, 117] as well as catalytic properties. The interesting features of POMs can be exploited by functionalising and utilising the various covalent fuctionalisation strategies which not only broaden their applications but also improve long-term stability, solubility, lipophilicity, size, shape, redox behavior, acid base properties, spectroscopic response and biological activities of the clusters, as well as facilitating the construction of novel

POM based functional materials[118-120]. In nonlacunary heteropolyoxometalates the negative charge is delocalised over the entire structure. In lacunary heteropolyoxometalates, the nucleophilic properties of the oxygen atoms localised at the surface of the lacuna are increased and therefore make these oxygen atoms more reactive toward electrophilic groups such as organophosponates, organoarsonates, organotin, etc. The variety of electrophilic groups available combined with the various topologies observed in lacunary heteropolyoxometalates has facilitated the recent development of such organic/inorganic hybrids. The structure of the lacuna and the structural organisation of the functionalising agents are key parameters that need to be considered for the synthesis of functionalised heteropolyoxometalates. Hence replacement of oxo ligands with different organic groups such as imido[121, 122] or diazenido [123,124] or the coupling of lacunary POMs with organosilyl/germyl [125-128] organo-phosphoryl/phosphonates[129-132] and organotin derivatives[133-138] are the most common routes for functionalisation of POMs.

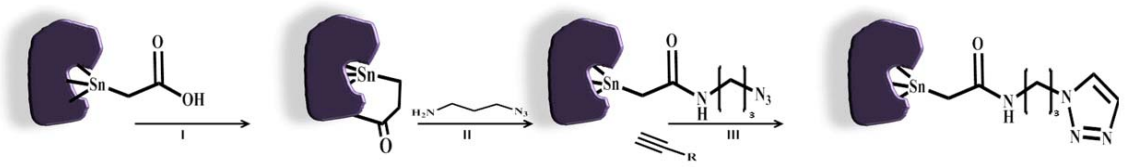

Figure 1.12. Organic functionalisation strategies employed to introduce organic arm bearing carboxylic group for further functionalisation. {I= triethyl amine, in the presence of isobutyl trichloroformate, in acetonitrile, II= azido propyl amine I acetonitril and triethyl amine and III= 1,3 cyclo addition in aquous solution with copper sulfate and sodium ascorbate}

Among the various reported strategies for organic fuctionalisation the organotin route is the most widely studied and reported to provide robust and hydrolytically stable oxide clusters which will be functional under physiological conditions[136-138]. Furthermore the similarity in the size of Sn^{IV} and W^{VI} and therefore the facile inclusion of organotin fragments in lacunary polyoxotungstates to 'simply' fill the lacuna. In 1979 Pope reported[144] on the hydrolytic stability of organotin derivatised Keggin and Dawson structures over a wide pH range. According to this report tin derivatised Dawson POMs [P2W17SnR] are stable in the pH range from 2-8 while the range for Keggin type POMs is

narrower over pH 4 to 6. Pope in his recent paper, however, studied the stability of organotin functionalised Keggin POMs anda slightly wider pH range[136].

Organotin: Organotin derivatives were first reported by W.H. Knoth and M.T. Pope for Keggin and Dawson polyanions, $[XM_{11}O_{39}(SnR)]^{n-}$ and $[P_2W_{17}O_{61}(SnR)]^{7-}$ Over the past few years various reports from different groups have contributed to the chemistry of organotin derivatives. For instance the Kortz group[133, 134] used monophenyltin $\{SnPh\}^{3+}$ and dimethyltin $\{Sn(CH_3)_2\}^{2}$ fragments to generate various POM hybrids. Hasenknopf and coworkers mainly focused on the reactivity of lacunary polyoxometalates with monoorganotin trichloride[139-141] with the objective of attaching a pendant reactive group such as carboxylic acid, alkyne, or azide and further react these pendant groups through amide bond formation or click chemistry in order to graft a large variety of organic functions onto polyoxometalates. Proust and coworkers reported organotin POM hybrid bearing an iodo-aryl moiety which were further used for palladium cross coupling and used to study electro and photochromic properties of the clusters[142,143].

1.10.3 Physicochemical properties of Polyoxometalates

The applications of POMs are centered primarily on their redox properties, photochemical response, ionic charge, conductivity, and ionic weights[144]. Among the interesting properties POMs possess are their rich redox properties, with long stable redox states, and multiple electron-transfer steps[145] Furthermore these properties can be controlled and fine tuned through the heteroions, and addenda ions that are incorporated into the structural framework and are, therefore, attractive candidates for selective, long-lived, and tunable redox-active devices[146-150]. Tunability can also be achieved through organic functionalisation.

POMs also known for their stability at elevated temperatures (up to 300-350 °C), aqueous, air and acidic conditions. Their stability in solutions centered to their redox property and be controlled using the *addenda* atoms. Various reports indicated that the order of acidity and stability in solution to be influenced by substitution of addenda and metal atoms. For instance, the order of basicity in the following POMs ($PW_{12} > SiW_{12} > P_2W_{18} > P_2W_{17}Mo > P_2W_{16}Mo_2 > P_2W_{15}Mo_3$) Basicity increases with Mo in the Dawson

series. The order of oxidizing power and order of acidity can be translated into stability to higher pH[150-153] .

1.10.4 Electrochemistry of POMs

The heteropolyanions undergo several rapid one- and two-electron reversible reductions to produce the so-called "heteropoly blue", and further irreversible multielectron reductions with concomitant decomposition. The occurrence of reversible reductions can be found for type I polyoxotungstates where the WO_6 octahedra have only one terminal oxygen atom and are associated with the fact that the electrons added to M enter an orbital that is predominantly non-bonding, with minimal subsequent bond length alteration. On the other hand, in the type II polyoxotungstates, the WO_6 octahedra have two terminal oxygen atoms and the added electrons enter an anti-bonding orbital, resulting in large structural changes[108, 154] Both Keggin ($XM_{12}O_{40}$), Dawson ($X_2M_{18}O_{62}$) related structures belong to this type I category and form heteropoly blues, and have been historically employed in analytical applications[155] . Type II compounds such as the Anderson structure (XMo_6O_{24}), do not form heteropoly blues.

In the type I form, which is more electrochemically active with reproducible redox features, the oxidation ability of *addenda* atoms can be adjusted according to $V^{(+5)} > Mo^{(+6)} > W^{(+6)}$. In the case of one electron transfer to a mixed addenda polyoxometalate species, the electron is localised at the more reducible atom at room temperature[150]. The electrons are accepted by the *addenda* ions of the heteropolyanions ($XM_{12}O_{40}^{n-}$ and $X_2M_{18}O_{62}^{n-}$). If the *addenda* ions are all identical, the electrons are delocalised on the addenda ion oxide framework at room temperature by rapid electron hopping (intramolecular electron transfer). The reduction increases the negative charge density at the heteropolyanions and thus their basicity. And as a consequence, the reduction can be accompanied by protonation depending on the pK_a of the produced oxometalates. The electrochemical behavior of each of the heteropolyanions exhibits a different feature, because they differ in their redox potentials, their pK_a and their stabilities.

The formal redox potential depends on a lot of factors, of which the nature of the *addenda* and hetero-ions have the highest influence/ importance. For example, the redox potential of incorporated metal increases as a function of formal charge on the hetero-

ion, A. For a given oxidation state, the redox potential increases with the size and decreasing electronegativity of X. The redox potential of Mn (III/II) increases with X, where X= B < Zn < Si < Ge < P {$XM_{11}O_{39}M'^{n-}$ and $X_2M_{18}O_{61}M'^{n-}$)} [150] and other extrinsic factors that influence the redox potentials of POMs include the electrolysis conditions (pH, countercation, additives, and solvents). Pope reported that in aqueous solution where no protonation accompanies the reduction for α-$XW_{12}O_{40}^{n-}$ (X = $P^{(V)}$, $Si^{(IV)}$, $Ge^{(IV)}$, $Fe^{(III)}$, $B^{(III)}$, $Co^{(II)}$, H_2, $Cu^{(I)}$) two one-electron reductions are observed. Their potentials are linearly dependent on the ionic charge by –0.18 V per unit charge[155, 156]. A similar trend is also reported in organic solvents[157].

Israel and Xavier in their paper[158] generalised for Keggin type $XW_{12}O_{40}^{q-}$ anions, the following main parameters appear to govern their voltammetric behaviors: (i) the basicity of the first reduced species and, occasionally, of the fully oxidised species; (ii) the overall negative charge of the POM, which is a function of the central heteroatom charge; (iii) the size of this central heteroatom,X; (iv) in the vast majority of the most studied Keggin-type POMs, the central heteroatom, X, is not electroactive, and the voltametric behavior is mostly concerned with the redox behavior s of the addenda atoms.

1.10.5 Organic functionalisation and redox property of POMs

As described in the previous section, the formal potentials determined by electrochemical methods are strongly affected by a number of experimental conditions including pH, electrolyte, and electrode. Nevertheless, most of the electrochemical measurements reported have been carried out under different conditions[159, 160]. In majority of the organic fuctionalisations the formal potential was not changed due to minimal electronic communication between the cluster and the organic group. The ease of reduction of the POM shows a clear dependence on the nature of the linkage or more specifically on the type of anchoring group used for the attachment. Groups which donate electrons make the formal potential and cathodic as a result difficult to reduce (the converse is true for electron withdrawing groups). This is clearly evident with the trioxifunctionalisation of Dawson POMs reported by Hasenknopf and coworkers where reversal of reduction potentials is observed as a result of the organic substituent[162], furthermore POMs substituted with the silyl anchoring group display a more cathodic

first-reduction step than those with the phosphoryl contact[163, 164], and the organosilyl POMs derivatives are easier to reduce than the organotin ones, due to the one-charge difference[142]. As supported by some theoretical[165] and experimental evidences the Keggin-type POMs are easier to reduce since they bear lower negative charges than the corresponding Dawson hybrids.

1.11 Scope and objective of the project

Over the past decade the development of new strategies for genotyping has attracted increasing interest, driven by the need for cost effective and efficient strategies to take advantage of the knowledge acquired during the Human Genome Project (HGP) and of the large variety of molecular methods developed to assess a broad range of biological phenomena (e.g., genetic variation, RNA expression, protein-DNA interactions and chromosome conformation).

Whilst there are diverse reports of the enzymatic incorporation of fluorescently labeled dNTPs and ddNTPs, there are a limited number of groups working on enzymatic incorporation of electrochemical redox labeled nucleotides, which could be attributed to the challenges related with the synthesis, stability and enzymatic incorporation of electrochemically labeled nucleotides.

The overall objective of this PhD thesis is the realisation of an electrochemical platform for the detection of single nucleotide polymorphisms via primer extension. In order to achieve this overall goal, several subobjectives were achieved. Primarily, polyoxometalates were exploited as novel electrochemical labels and a generic strategy for coupling of polyoxometalates with amine containing compounds was established and applied to conjugation with DNA primers, dNTPs and ddNTPs. Each of these labelled DNA moieties were exploited in different assay formats for the detection of DNA as well as in electrochemical primer extension (éPEX). In parallel, work was carried out to develop a robust surface chemistry to ensure the stable immobilisation of DNA probes to be used in éPEX and a novel route to achieve facile, environmentally friendly and cost-effective means of producing a halogenated carbon surface for anchoring of DNA.

Specific objectives of the project

1. The development of robust surface functionalisation strategies
2. The design, synthesis and characterisation of redox active labels
3. Evaluation of the enzymatic incorporation and electrochemical properties of the electrochemical labels
4. The development of four "colour type " multi potential éPEX

References

1. J. D. Watson; F. H. C. Crick, Molecular structure of nucleic acids; a structure for deoxyribose nucleic acid. *Nature,* **1953**, 171, 737– 739.
2. F.Sanger, S.Nicklen, R. A. Coulson, DNA sequencing with chain-terminating inhibitors*, Proc. Nat. Acc. Sci.*, **1977**, 74, 5463-5467.
3. M. A. Maxam, W. Gilbert, A new method for sequencing DNA, *Proc. Nat. Acc. Sci.* **1977**, 74, 560-564.
4. L. M. Smith, J. Z. Sanders, R.J. Kaiser, P. Hughes, C. Dodd, C. R. Connell, C. Heiner, S.B. Kent, L.E. Hood. Fluorescence detection in automated DNA sequence analysis. *Nature.* **1986**; 321, 607, 1674-9.
5. J.M. Prober, G.L. Trainor, R.J. Dam, F.W. Hobbs, C.W. Robertson, R.J. Zagursky, A.J. Cocuzza, M.A. Jensen, K.A. Baumeister, system for rapid DNA sequencing with fluorescent chain termmating dideoxynucleotldes, *Science*, **1987**, 238,336–341.
6. W. Ansorge, S. B. Sproat, J. Stegemann, C. Schwager, A non-radioactive automated method for DNA sequence determination, *J biochem biophys methods* **1986,** 13, 315-317.
7. Consortium, I.H.G.S., Initial sequencing and analysis of the human genome, *Nature,* **2001**, 409, 860-921.
8. J. Brookes, The essence of SNPs. *Gene* 1999, 234, 177–86.
9. J.C. Venter, M.D. Adams, E.W. Myers, *et al.* The sequence of the human genome. *Science*, **2001**, 291, 1304–1351.
10. R. Sachidanandam, D. Weissman, S. C. Schmidt, et al. A map of human genome sequence variation containing 1.42 million single nucleotide polymorphisms. *Nature,* **2001**, 409:928–33
11. The International HapMap Consortium. *Nature,* **2007,** 449, 851-861,
12. Scuteri, S. Sanna, W. M. Chen,M. Uda, G. Albai, J. Strait, Genome-Wide Association Scan Shows Genetic Variants in the FTO Gene Are Associated with Obesity-Related Traits, *PLoS Genet.* **2007**, 3, e115.
13. Shabo, Integrating genomics into clinical practice: Standards and regulatory challenges. *Curr. Opin. Mol. Ther*. **2008**, 10, 267–272.

14. S. Kim, A. Misra, SNP genotyping: technologies and biomedical applications, *Annu Rev Biomed Eng.* **2007;** 9,289-320.
15. F. A. Gravel, J. T. R. Clarke, M. M. Kaback, D. Mahuran, K. Sandhoff, K. Suzuki In The metabolic and molecular basis of inherited disease; C.R. Scriver, A.L. Beauder, W.S. Sly, D. Valle, Eds.; McGraw-Hill: New York, **1995**; 2,2839-2879.
16. H. Levy, A. Murphy, F. Zou, C. Gerard, B. Klanderman, B. Schuemann, R. Lazarus, C. K. García, C. J. Celedón, M. Drumm, M. Dahmer, M. Quasney, K. Schneck, M. Reske, R. M. Knowles, B. G. Pier, C. Lange, T.S. Weiss, IL1B polymorphisms modulate cysticfibrosis lung disease, *Pediatr. Pulmonol.*, **2009**, 44, 580–593.
17. Muniz, G. Martinez, J. Lavinha, P. Pacheco, β-Thalassaemia in Cubans: Novel Allele Increases the Genetic Diversity at the HBB Locus in the Caribean, Am. J. Hemathology, 2000, 64, 7-14.
18. Y. D. Wu, L. Ugozzoli, K. B. Bal, B. R. Wallace, Allele-specific enzymatic amplification of beta-globin genomic DNA for diagnosis of sickle cell anemia, *Proc. Natl Acad. Sci.* USA, **1989**, 86, 2757–2760.
19. P. A. Chiang, S. J. Beck, J. H. Yen, K. M. Tayeh, E. T. Scheetz, et al., Homozygosity mapping with SNP arrays identifies TRIM32, an E3 ubiquitin ligase, as a Bardet– Biedl syndrome gene (BBS11), *Proc. Natl Acad. Sci.* **2006**,103, 6287–6292.
20. K. Neveling, R.W. Collin, C. Gilissen, R.A. van Huet, L. Visser, M.P. Kwint, S.J. Gijsen, M.N. Zonneveld, N. Wieskamp, J. de Ligt, A.M. Siemiatkowska, L.H. Hoefsloot, M.F. Buckley, U. Kellner, K.E. Branham, A.I. den Hollander, A. Hoischen, C. Hoyng, B.J. Klevering, L.I. van den Born, J.A. Veltman, F.P. Cremers, H. Scheffer, Next-Generation Genetic Testing for Retinitis Pigmentosa, *Human Mutation*, **2012**, 33, 963–972.
21. L. M. Metzker, Emerging technologies in DNA sequencing, *Genome Res.* **2005** 15: 1767-1776
22. T.S. Seo, X. Bai, D.H. Kim, Q. Meng, S. Shi, H. Ruparel, Z. Li, N.J. Turro, J. Ju, Four-color DNA sequencing by synthesis on a chip using photocleavable fluorescent nucleotides, *Proc. Natl. Acc. Sci*. **2005,** 102, 5926-5931
23. H. Fakhrai-Rad, N. Pourmand, M. Ronaghi, **P**yrosequencing™, An accurate detection platform for single nucleotide polymorphisms, Hum Mutat. **2002**,19, 479–485

24. E. K. Lewis, W.C. Haaland, F. Nguyen, D,A. Heller, M.J. Allen, R.R. MacGregor, CS Berger, B Willingham, LA Burns, GB Scott, l CKittrel, BR Johnson, RF Curl, M.L. Metzker, Color-blind fluorescence detection for four-color DNA sequencing. *Proc. Natl. Acc.Sci*. **2005,** 102,5346-51
25. Z. Strezoska, T. Paunesku, D. Radosavlievic, I. Labat, R. Drmanac, R. Crvenjakov, DNA sequencing by hybridization: 100 bases read by a non-gel-based method, *Proc. Nati. Acad. Sci. USA*, **1991,** 88, 10089-10093
26. , D. Branton et al. The potential and challenges of nanopore sequencing. *Nature Biotech*. **2008**, 26, 1146–1153
27. E. Pennisi,Semiconductors inspire new sequencing technologies*, Science*, **2010** 327, 1190
28. V. E. Bichenkova, Z. Lang, X. Yu, C. Rogert, T. K. Douglas, DNA-mounted self-assembly: New approaches for genomic analysis and SNP detection *Biochim. et. Biophys.* **2011**,1809, 1-23
29. D. Di Giusto, C. G. King, Single base extension (SBE) with proofreading polymerases and phosphorothioate primers: improved fidelity in single-substrate assays, *Nuc. Ac. Res.* **2003**, 31, e7
30. P. Sokolov Primer extension technique for the detection of single nucleotide in genomic DNA. Nucleic Acids Res. **1990,**18,671
31. K. Meyer, M. P. Ueland, Use of Matrix assisted laser desorption ionization time of flight mass spectrometry for multiplex genotyping*, Advances in Clinical Chemistry*, **2011,** 53,1-29
32. J. N. Hirschhorn, P. Sklar, K. Lindblad-Toh, Y.M. Lim, M. Ruiz-Gutierrez, et al. SBE-TAGS: an array-based method for efficient single-nucleotide polymorphism genotyping. *Proc. Natl. Acad. Sci.* **2000.**97:12164–69
33. M. H. Shapero, K. K. Leuther, A. Nguyen, M. Scott, K.W. Jones, SNP genotyping by multiplexed solid-phase amplification and fluorescent minisequencing., *Genome Res.* **2001**11:1926–34.
34. R. A. Gibbs, P. N. Nguyen, C. T. Caskey, Detection of single DNA base differences by competitive oligonucleotide priming. *Nucleic Acids Res*. **1989.**17:2437–48.
35. Latorra, K. Campbell, A. Wolter, J. M. Hurley. Enhanced allele-specific PCR discrimination in SNP genotyping using 3′locked nucleic acid (LNA) primers. *Hum. Mutat*. **2003**, 22:79–85.

36. D. A. Di Giusto;, W. A. Wlassoff;, S. Giesebrecht;, J. J. Gooding;,G. C. King, Multipotential Electrochemical Detection of Primer Extension Reactions on DNA Self-Assembled Monolayers, *J. Am. Chem. Soc.* **2004**, 126, 4120–4121.
37. W. M. Howell, M. Jobs, U. Gyllensten, A. J. Brookes, Dynamic allele-specific hybridization. A new method for scoring single nucleotide polymorphisms. *Nat. Biotechnol.* **1999**.17:87–88.
38. Whitcombe, J. Theaker, S. P. Guy, et al. Detection of PCR products using self probing amplicons and fluorescence. *Nat Biotechnol* **1999**; 17, 804–7.
39. Y. S. Huh;A. J. Lowe; A. D. Strickland;, C. A. Batt;, D. Erickson, Surface-Enhanced Raman Scattering Based Ligase Detection Reaction, *J. Am. Chem. Soc.* ***2009***, 131, 2208.
40. K. Toubanaki, T. K. Christopoulos, P. C. Ioannou, C. S. Flordellis, Identification of Single-Nucleotide Polymorphisms by the Oligonucleotide Ligation Reaction: A DNA Biosensor for Simultaneous Visual Detection of Both Alleles, *Anal.Chem*. **2009,** 81, 218–224
41. Y. Li, A. W. Wark, H. J. Lee, R.M. Corn , a nanoparticle-enhanced surface plasmon resonance imaging measurements of surface enzymatic ligation reaction for the detection of SNP in DNA, *Anal Chem*., **2006**,78,3158
42. V. Lyamichev;, A. L. Mast;, J. G. Hall;, J. R. Prudent;, M. W. Kaiser Polymorphism identification and quantitative detection of genomic DNA by invasive cleavage of oligonucleotide probes., *Nat. Biotechnol.,* **1999,** 17, 292–296.
43. M. Olivier, The Invader® assay for SNP genotyping, *Mutat Res.* **2005** , 573, 103–110
44. X. Duan;, L. Liu;, S. Wang Homogeneous and one-step fluorescent allele-specific PCR for SNP genotyping assays using conjugated polyelectrolytes, *Biosens. Bioelectro* 2009, 24, 2095–2099.
45. C. Ding, Z. Wang, H. Zhong, S. Zhang, Ultrasensitive chemiluminescence quantification of single-nucleotide polymorphisms by using monobase-modified Au and CuS nanoparticles, *Biosensors and Bioelectronics,* **2010**, 25,1082-1087
46. H-Q. Wang, W-Y. Liu, Z. Wu, L-J. Tang, X.-M. Xu, R.-Q. Yu, J.-H. Jiang, *Anal. Chem*. **2011**, 83, 1883–1889, Homogeneous Label-Free Genotyping of Single Nucleotide Polymorphism Using Ligation
47. Y. Wang,;, J. Zhang;, G. Liu;, D. Pan;, L. Wang;, S. Song;, C. Fan Ligase-based multiple DNA analysis by using an electrochemical sensor array, *Biosens. Bioelectron.* **2009,** 24, 1209

48. Y. Huang;, Y. Zhang;, X. Xu;, J. Jiang;, G. Shen;, R. Yu, Highly Specific and Sensitive Electrochemical Genotyping via Gap Ligation Reaction and Surface Hybridization Detection, *J. Am. Chem. Soc*. **2009,** 131, 2478-2480
49. D. Wang, W. Tang, X. Wu, X. Wang, G. Chen, Q. Chen, N. Li, F. Liu, Highly Selective Detection of Single-Nucleotide Polymorphisms Using a Quartz Crystal Microbalance Biosensor Based on the Toehold-Mediated Strand Displacement Reaction, *Anal Chem.* **2012,** 84, 7008–7014
50. T. R. Gaunt, L. J. Hinks, H. Rassoulian, I. N. Day, Manual 768 or 384 well microplate gel 'dry' electrophoresis for PCR checking and SNP genotyping *Nucleic Acids Res.***2003**, 31, E48.
51. A.C., Syvanen, from gels to chips: ''minisequencing" primerextension for analysis of point mutations and single nucleotide polymorphisms,*Human mutation* **1999**,13,1-10
52. A.C. Syvanen, K. Aalto-Setala, L.Harju, K. Kontula, H.A. Soderlund, primer-guided nucleotide incorporation assay in the genotyping of apolipoprotein E. *Genomics,* **1990,** 8, 684-692
53. T.Pastinen, A. Kurg, A. Metspalu, L. Peltonen, A.-C. Syvanen, Minisequencing: a speci®c tool for DNA analysis and diagnostics on oligonucleotide arrays. *Genome Res*., **1997**, 7, 606-614.
54. J.M. Shumaker, A. Metspalu, C.T. Caskey, Mutation detection by solid phase primer extension. *Hum Mutat.* **1996**, 7, 346–354.
55. T.A. Kunkel, K. Bebenek, DNA replication fidelity. *Annu. Rev.Biochem.,* **2000**, 69, 497-529
56. K. J. Livak, J. Marmaro, J. A. Todd, Towards fully automated genome-wide polymorphism screening. *Nat. Genet*. **1995,** 9, 341–342.
57. Patolsky, A. Lichtenstein, I. Willner, Detection of single-base DNA mutations by enzyme-amplified electronic transduction, *Nat. Biotechnol.* **2001**, *19*, 253–257
58. M. D. Kolpashchikov, Binary Probes for Nucleic Acid Analysis*, Chem. Rev.* **2010,** *110,* 4709–4723
59. D. Liu, T. M. H. Lee; J. Wang,Nanocrystal-based bioelectronic coding of single nucleotide polymorphisms, *J. Am. Chem. Soc.* **2005**, *127*, 38–39
60. Liu, Y. Lin, *J. Am. Chem. Soc.* **2007**, *129*, 10394–10401. Electrochemical quantification of single-nucleotide polymorphisms using nanoparticle probes, *J. Am. Chem. Soc.* **2007**, *129*, 10394–10401.

61. Y. L Zhang, Y. Huang, J.-H. Jiang, G. L Shen, R. Q. Yu, electrochemical aptasensor based on proximity-dependent surface hybridization assay for single-step, reusable, sensitive protein detection. *J. Am. Chem. Soc.* **2007,** *129*, 15448–15449
62. C. H. Fan, K. W. Plaxco, A. L. Heeger, Electrochemical interrogation of conformational changes as a reagentless method for the sequence-specific detection of DNA. *Proc. Natl. Acad. Sci. U.S.A.* **2003**, *100*, 9134–9137.
63. Abi, E.E. Ferapontova, electroanalysis of single nucleotide polymorphism by hair pin DNA architechtures, *Anal Bioanal Chem,* **2013**, 405, 3693-3703
64. Rosler, L. Bailey, S. Jones, J. Briggs, S. Cuss, I. Horsey, M. Kenrick, S. Kingsmore, L. Kent, J. Pickering, et al., Rolling circle amplification for scoring single nucleotide polymorphisms, *Nucleosides Nucleotides Nucleic Acids*, **2001**, 20, 893–894
65. Y. Li, W. A. Wark, J. H. Lee, M. R. Corn, Single Nucleotide Polymorphism Genotyping by Nanoparticle-Enhanced SPR Imaging Measurements of Surface Ligation Reactions, *Anal Chem.* **2006** 78, 3158–3164.
66. L. Y. Jung, C. Jung, H. Parab, Y. D. Cho-, G., H. Park, Colorimetric SNP genotyping based on allele-specific PCR by using a thiol-labeled primer, *ChemBioChem,* **2011**, 12, 1387 – 1390
67. X. Chena, A. Yinga, Z. Gao, Highly sensitive and selective colorimetric genotyping of single-nucleotide polymorphisms based on enzyme-amplified ligation on magnetic beads, *Biosensors and Bioelectronics* **2012**, 36, 89–94
68. Y. Kitamura, T. Ihara, Y. Tsujimura, Y. Osawa, D. Sasahara, M. Yamamoto, K. Okada, M. Tazaki, A. Jyo, Template-directed formation of luminescent lanthanide complexes: Versatile tools for colorimetric identification of single nucleotide polymorphism, *Inorg. Biochem.***2008**, 102, 1921-1931
69. E. Özkumura, S. Ahn, A. Yalcin¸ A. C. Lopez, E. Cevik, , J. R.C. Irani, M. D Chiarid, S. M. Ünlü, label-free microarray imaging for direct detection of DNA hybridization and single-nucleotide mismatches. *Biosensors and Bioelectronics,* **2010** 25, 1789–1795
70. Hu, C. Zhang, Sensitive Detection of Nucleic Acids with Rolling Circle Amplification and Surface-Enhanced RamanScattering Spectroscop *Anal. Chem*. **2010**, 82, 8991–8997
71. Wang, Electrochemical biosensors: towards point-of-care cancer diagnostics. *Biosensor Bioelectronics* **2006**, 21, 1887-1892.

72. Abbaspour, A. Noori, Electrochemical detection of individual single nucleotide polymorphisms using monobase-modified apoferritin-encapsulated nanoparticles., *Biosensors and Bioelectronics* **2012**, 36, 11-18
73. Boon, E. M.; Ceres, D. M.; Drummond, T. G.; Hill, M. G.; Barton, J. K. Mutation detection by electrocatalysis at DNA-modified electrodes. *Nat. Biotechnol.* **2000**, 18, 1096–1100.
74. E. L. S. Wong, J. J Gooding. Charge transfer through DNA: A selective electrochemical DNA biosensor.*Anal. Chem*. **2006,** 78, 2138–2144.
75. M. Inouye, R. Ikeda,M. Takase,T. Tsuri, J. Chiba, Single-nucleotide polymorphism detection with "wire-like" DNA probes that display quasi "on-off" digital action, *Proc. Natl. Acad. Sci. U.S.A.* **2005**, *102*, 11606–11610.
76. Y. Xiao, A. A. Lubin, B. R Baker, K. W. Plaxco, A. J. Heeger, Single-step electronic detection of femtomolar DNA by target-induced strand displacement in an electrode-bound duplex, *Proc. Natl. Acad. Sci. U.S.A.* **2006**, *103*,16677–16680.
77. A. Lubin, R. Y. Lai, B. R. Baker, A. J. Heeger, K. W. Plaxco, Sequence-specific, electronic detection of oligonucleotides in blood, soil, and foodstuffs with the reagentless, reusable E-DNA sensor. *Anal. Chem.* **2006**, *78*, 5671–5677
78. Y. Xiao, X. G. Qu, K. W. Plaxco, A. J. Heeger, Label-free electrochemical detection of DNA in blood serum via target-induced resolution of an electrode-bound DNA pseudoknot, *J. Am. Chem.Soc*. **2007**, 129, 11896–11897
79. J. Cash, A. J. Heeger, K. W. Plaxco, Y. Xiao, Optimization of a reusable, DNA pseudoknot-based electrochemical sensor for sequence-specific DNA detection in blood serum, *Anal. Chem.* **2009**, *81*, 656–661
80. H. He, J. Xia, G. Chang, X. Peng, Z. Lou, K. Nakatani, X. Zhou, S. Wang, Selective recognition of G-G mismatch using the double functional probe with electrochemical active ferrocenyl, *Biosensors and Bioelectronics* **2013**, 42 36–40
81. Y. Xiao, X. Lou, T. Uzawa, I J. K. Plakos, W. K. Plaxco, T. H. Soh, An Electrochemical Sensor for Single Nucleotide Polymorphism Detection in Serum Based on a Triple-Stem DNA Probe, *J. Am. Chem. Soc.* **2009**, 131, 15311–15316
82. R. S. Clegg, S. M. Reed, and J. E Hutchison,Self-Assembled Monolayers Stabilized by Three-Dimensional Networks of Hydrogen Bonds,.*J. Am. Chem. Soc.*, **1998,** *120* 2486–2487
83. H. J. Lee, A.C. Jamison, Y. Yuan, C.-H Li, S. Rittikulsittichai, I. Rusakova, T. R. Lee, L*angmuir*, **2013**, *29* , 10432–10439

84. Y.-S. Shon, T. R. Lee , Desorption and Exchange of Self-Assembled Monolayers (SAMs) on Gold Generated from Chelating Alkanedithiols, *J. Phys. Chem. B*, **2000**, 104 , 8192–8200,

85. E. Sabatani , J. Cohen-Boulakia, M. Bruening , I. Rubinstein, Thioaromatic monolayers on gold: a new family of self-assembling monolayers, *Langmuir*, **1993**, *9* , 2974–2981

86. N. M. Hansen, E. Farjami, M. Kristiansen, L. Clima, U. S. Pedersen ; K. Daasbjerg, E. E. Ferapontova, K.V. Gothelf, Synthesis and Application of a Triazene–Ferrocene Modifier for Immobilization and Characterization of Oligonucleotides at Electrodes, *J. Org. Chem.*, **2010,** 75:2474–2481

87. D. Ge X., Wang, K. Williams, R. Levicky, Thermostable DNA Immobilization and Temperature Effects on Surface Hybridization, *Langmuir*. **2012**, 28, 8446–8455.

88. Steichen, Y. Decrem, E. Godfroid,C. Buess-Herman, Electrochemical DNA hybridization detection using peptide nucleic acids and $[Ru(NH_3)_6]^{3+}$ on gold electrodes, *Biosens. Bioelectron.* **2007**, 22, 2237

89. E. Paleček and M. Bartošík, Electrochemistry of Nucleic Acids,*Chem. Rev.,* **2012**, 112, pp 3427–3481

90. D. Loakes, P. Holiger, Polymerase engineering: towards the encoded synthesis of unnatural biopolymers. *Chem. Commun* **2009,**4619-4631

91. Staiger, A. Marx, A DNA polymerase with increased reactivity for ribonucleotides and C5-modified deoxyribonucleotides. ChemBioChem, **2010,** 11, 1963–1966

92. M. Hocek, M. Fojta, Nucleobase modification as redox DNA labelling for electrochemical detection. *Chem. Soc. Rev*., **2011,** 40, 5802–5814

93. J.P. Anderson, B. Angerer, L.A. Loeb, Incorporation of reporter-labeled nucleotides by DNA polymerases, *Biotechniques*. **2005** 38, 257-64

94. G. H. McGall, Nucleoside triphosphate analogs for nonradioactive labeling of nucleic acids. In M.M. Vaghefi (Ed.) Nucleoside Triphosphates and Analogs: Their Chemistry, Biotechnology, and Biological Applications. Marcel Dekker, New York.). **2005**

95. Paul, J. Yee, PCR incorporation of modified dNTPs: the substrate properties of biotinylated dNTPs, *BioTechniques,* **2010,** 48, , 333–334

96. Z. Zhu, A. S. Waggoner. Molecular mechanism controlling the incorporation of fluorescent nucleotides into DNA by PCR. *Cytometry* **1997** 28, 206-211

97. Braslavsky, B. Hebert., E. Kartalov, S. R Quake, Sequence information can be obtained from single DNA molecules. *Proc. Natl. Acad. Sci. USA,* **2003,** 100, 3960-3964.

98. S. S. W. Yeung, T. M. H. Lee, I. M. Hsing. Electrochemical real-time polymerase chain reaction, *J. Am.* Chem. Soc. **2006**, 128, 13374,

99. D. A. Di Giusto, W. A. Wlassoff, S. Giesebrecht, J. J. Gooding, G. C King. Enzymatic synthesis of redox-labeled RNA and dual-potential detection at DNA-modified electrodes. *Angew. Chem., Int. Ed.* **2004**, 43, 2809

100. . Zhang, Y. Fang, J.Y. Hou, H.J. Ren, R. Jiang, P Roos, N.J. Dovichi, Use of non-cross-linked polyacrylamide for four-color DNA sequencing by capillary electrophoresis separation of fragments up to 640 bases in length in two hours. *Anal. Chem.*, **1995,** 67 ,589–4593

101. V. Trevino, F. Falciani, H. A. Barrera-Saldaña, DNA Microarrays: a Powerful Genomic Tool for Biomedical and Clinical Research, *Mol Med* , **2007**, 13, 527-541

102. S.A. Brazill, P.H. Kim, W.G. Kuhr, Capillary gel electrophoresis with sinusoidal voltammetric detection: a strategy to allow four-"color" DNA sequencing, *Anal. Chem.*, **2001**, *73* , 4882–4890,

103. H. Weizman, Y. Tor, Redox-active metal-containing nucleotides: synthesis, tunability, and enzymatic incorporation into DNA. *J. Am. Chem. Soc.*, **2002**, 124 , 1568–1569

104. M. Fojta, P. Kostecka, M. Trefulka, L. Havran, E. Palecek, "Multicolor" electrochemical labeling of DNA hybridization probes with osmium tetroxide complexes. *Anal. Chem.*, **2007**, 79, 1022–1029,

105. J. Wang, G. Liu, A. Merkoçi, Electrochemical coding technology for simultaneous detection of multiple DNA targets. *J. Am. Chem. Soc.*, **2003**, *125*, 3214–3215

106. Husken, G. Gasser, S. D. Koster, N. M.- Nolte, "Four-Potential" Ferrocene Labeling of PNA Oligomers via Click Chemistry, *Bioconjugate Chem*. **2009,** 20, 1578–1586

107. J. Balintov, M. Plucnara, P. Vidlkov, R. Pohl, L. Havran, M. Fojta, M. Hocek, Benzofurazane as a new redox label for electrochemical detection of DNA: towards multipotential redox coding of DNA bases. *Chem. Eur. J.* **2013,** 19, 12720 – 12731

108. M. T. Pope, Heteropoly and Isopoly Oxometalates, Springer-Verlag, Berlin **1983**.

109. J. Keggin, *Nature* **1933,** *131*, 908

110. A. Proust, R. Thouvenot, P. Gouzerh, Functionalization of polyoxometalates: towards advanced applications in catalysis and materials science., *Chem. Commun., **2008**, 1837–1852*

111. F. Kehrmann, z. *Anorg. Chem*.1,(1892),432

112. B, Dawson, *Acta Cryst* **1953**. 6, 113

113. J. Bartis, M. Dankova, J.J. Lessmann, Q.H. Luo, W. deW.Horrocks Jr, L.C. Francesconi, Lanthanide Complexes of the alpha-1 Isomer of the $[P_{(2)}W_{(17)}O_{(61)}]^{(10-)}$ Heteropolytungstate: Preparation, Stoichiometry, and Structural Characterization by $^{(183)}W$ and $^{(31)}P$ NMR Spectroscopy and Europium(III) Luminescence Spectroscopy. *Inorg. Chem*. **1999**, 38, 1042.

114. E. Coronado, S. Curreli, C. Giménez-Saiz, C. J. Gómez-García, J. , Roth, A new BEDT-TTF salt and polypyrrole films containing the chiral polyoxometalate $[H_4Co_2Mo_{10}O_{38}]^{6-}$, *Synth. Met.* **2005,** 154, 241– 244

115. Hasenknopf, K Micoine, E. Lacote, S. Thorimbert, M. Malacria, R. Thouvenot, Chirality in Polyoxometalate *Chemistry Eur. J. Inorg. Chem.* **2008,** 5001– 5013

116. E. Coronado, P. Day, Magnetic Molecular Conductors, *Chem. Rev.* **2004,** 104,5419– 5448

117. E. Coronado, C. Giménez-Saiz, C. J. Gómez-García; Recent advances in polyoxometalate-containing molecular conductors, *Coord. Chem. Rev*. **2005**, 249, 1776– 1796

118. Proust, B. Matt, R. Villanneau, G. Guillemot, P. Gouzerh, G. Izzet, Functionalization and post-functionalization: a step towards polyoxometalate-based materials.*Chem. Soc. Rev,* **2012**. 41, 7605

119. Li, P. Yin, T. Liu, Supramolecular architectures assembled from amphiphilic hybrid polyoxometalates. Dalton Trans. **2012**, 41, 2853-2861

120. S. Thorimbert, B. Hasenknopf, E. Lacôte, Cross-Linking Organic and Polyoxometalate Chemistries *Isr. J. Chem*. 51, **2011**, 275-280.,

121. Y. Zhu, L. S. Wang, J. Hao, Z. C. Xiao, Y. G. Wei, Y. Wang, Synthetic, Structural, Spectroscopic, Electrochemical Studies and Self-assembly of Nanoscale Polyoxometalate–Organic Hybrid Molecular Dumbbells, *Cryst. Growth Des.* **2009**, 9 , 3509-3518.

122. J. Zhang, F. Xiao, J. Hao, Y. Wei, The chemistry of organoimido derivatives of polyoxometalates, *Dalton Trans*. **2012**, 41, 3599-3615

123. Bustos, D. M-L. Carey, K. Boubekeur, R. Thouvenot, A. Proust, P. Gouzerh, Aryldiazenido derivatives: A new entry to the functionalization of Keggin polyoxometalates, *Inorg. Chim. Acta* **2010,** 363, 4262-4268

124. C. Bustos, B. Hasenknopf, R. Thouvenot, J. Vaissermann, A. Proust, P. Gouzerh, Lindqvist-Type (Aryldiazenido)polyoxomolybdates – Synthesis, and Structural and Spectroscopic Characterization of Compounds of the Type $(n\mathrm{Bu_4N})_3[\mathrm{Mo_6O_{18}(N_2Ar)}]$, *Eur. J. Inorg. Chem*. **2003** 2757-2766

125. K. Nomiya, Y. Togashi, Y. Kasahara, S. Aoki, H. Seki, M. Noguchi, S. Yoshida Synthesis and Structure of Dawson Polyoxometalate-Based,Multifunctional, InorganicOrganic Hybrid Compounds: Organogermyl Complexes with One Terminal Functional Group andOrganosilyl Analogues with Two Terminal Functional Groups, *Inorg. Chem*. **2011**, 50, 9606-9619

126. N. Joo, S. Renaudineau, G. Delapierre, G. Bidan, L.-M. Chamoreau, R. Thouvenot, P. Gouzerh, A. Proust, Organosilyl/germyl polyoxotungstate hybrids for covalent grafting onto silicon surfaces: towards molecular memories, *Chem. Eur. J*. **2010,** 16, 5043-5051.

127. B. Matt, S. Renaudineau, LM, Chamoreau, C. Afonso, G. Izzet, A. Proust Hybrid Polyoxometalates : Keggin and Dawson Silyl Derivatives as Versatile Platforms *J. Org. Chem.*, 76, **2011,** 3107-3112.

128. B. Matt, X. Xiang, L.A. Kaledin, N. Han, J. Moussa, H. Amouri, S. Alves, C.L. Hill, T. Lian, D. G. Musaev, G. Izzet, A. Proust, Long lived charge separation in iridium(III)-photosensitized polyoxometalates: synthesis, photophysical and computational studies of organometallic–redox tunable oxide assemblies, *Chemical Science,* **2013,** 4, 1737

129. G. S. Kim, K. S. Hagen, C. L. Hill, Synthesis, structure, spectroscopic properties, and hydrolytic chemistry of organophosphonoyl polyoxotungstates of formula $[\mathrm{C_6H_5P(O)}]_2\,\mathrm{X^{n+}W_{11}O_{39}^{(8-n)-}}$ ($\mathrm{X^{n+}} = \mathrm{P^{5+}}$, $\mathrm{Si^{4+}}$) *Inorg. Chem* **1992**. 31, 5316-5324.

130. U. Kortz, M.T. Pope, Synthesis, structure, spectroscopic properties, and hydrolytic chemistry of organophosphonoyl polyoxotungstates of formula $[\mathrm{C6H5P(O)}]^2\,\mathrm{Xn^{+}W_{11}O_{39}^{(8-n)-}}$ ($\mathrm{X^{n+}} = \mathrm{P^{5+,}}$ $\mathrm{Si^{4+}}$) *Inorg. Chem* **1995**. 34 3848-3850

131. C. R. Mayer, M. Hervé, H. Lavanant, J.-C. Blais, F. Sécheresse, Hybrid Cyclic Dimers of Divacant heteropolyanions: Synthesis, Mass Spectrometry (MALDI-

TOF and ESI-MS) and NMR Multinuclear Characterisation, *Eur. J. Inorg. Chem*. **2004,** 5, 973-977.

132. R. Villanneau, D. Racimor, E. Messner-Henning, H. Rousselière, S. Picart, R. Thouvenot, A. Proust, Insights into the Coordination Chemistry of Phosphonate Derivatives of Heteropolyoxotungstates, *Inorg. Chem***. 2011**,50 1164-1166
133. S. Reinoso, H. M. Dickman, A., Praetorius, F L Piedra-Garza, U. Kortz, Phenyltin-Substituted 9-Tungstogermanate and Comparison with Its Tungstosilicate Analogue, *Inorg. Chem* **2008**., 47 , 8798-8806
134. L. F. Piedra-Garza, M. Barsukova-Stuckart, B. S. Bassil, R. Al-Oweini, U. Kortz, Diethyltin-Containing Tungstoarsenate(V), $[\{Sn(C_2H_5)_2\}_3(H_2O)_6(A\text{–}\alpha\text{–}As^{V}W_9O_{34})]^{3-}$, *J. Cluster Sci.* **2012**, 23 () 939-951.
135. Bar-Nahum, J. Ettedgui, L. Konstantinovski, V. Kogan, R. Neumann, A New Method for the Synthesis of Organopolyoxometalate HybridCompounds, *Inorg. Chem,* **2007**, 46,5798-5804
136. G. Sazani, M. T. Pope,Organotin and organogermanium linkers for simple, direct functionalization of polyoxotungstates , *Dalton Trans*. **2004**, 1989-1994
137. N. Belai, M. T. Pope, Synthesis and structural characterization of new organotin derivatives of polyoxotungstates via transmetallation and coupling reactions, *Polyhedron* **2006**, 25 2015–2020
138. Zonnevijlle, M. T. Pope, Attachment of Organic Groups to Heteropoly Oxometalate Anions, *J. Am. Chem. Soc.* **1979**, 101, 2731– 2732
139. Micoine, B. Hasenknopf, S. Thorimbert, E. Lacote; M. Malacria, A General Strategy for Ligation of Organic and Biological Molecules to Dawson and Keggin Polyoxotungstates, Org. *Lett*. **2007**, 9, 3981.
140. C. Boglio, K. Micoine, E Derat, R. Thouvenot; B. Hasenknopf, S. Thorimbert, E. Lacote, M. Malacria, Regioselective Activation of Oxo Ligands in Functionalized Dawson Polyoxotungstates, *J. Am. Chem. Soc***. 2008,** 130, 4553
141. S. Bareyt, S. Piligkos;, B. Hasenknopf, P. Gouzerh, E. Lacote, S. Thorimbert, , M. Malacria, Efficient preparation of functionalized hybrid organic/inorganic Wells-Dawson-type polyoxotungstates, *J. Am. Chem. Soc*. **2005,** 127, 6788
142. Parrot, G. Izzet, L.-M. Chamoreau, A. Proust, O. Oms, A. Dolbecq, K. Hakouk, H. El Bekkachi, P. Deniard, R. Dessapt, P. Mialane, Photochromic Properties of Polyoxotungstates with Grafted Spiropyran Molecules *Inorg. Chem.* **2013**, 52, 11156–11163

143. Matt, J. Moussa, L.-M. Chamoreau, C. Afonso, A. Proust, H. Amouri, G. Izzet, Elegant Approach to the Synthesis of a Unique Heteroleptic Cyclometalated Iridium(III)-Polyoxometalate Conjugate, *Organometallics* **2012**, 31, 35–38

144. L. Hill. Chem. Rev**., 1998,** 98, cluster issue ,1-390

145. D.L. Long, E Burkholder, L. Cronin, Polyoxometalate clusters, nanostructures and materials: From selfassembly to designer materials and devices*, Chem. Soc. Rev.* **2007,***36,* 105–121

146. R. Neumann, Activation of Molecular Oxygen, Polyoxometalates, and Liquid-Phase Catalytic Oxidation, *Inorg. Chem.,* **2010**, 49, 3594–3601

147. M. T. Pope. In Mixed Valence Compounds; Brown, D. B., Ed.; D.Reidel: Dordrecht, **1980**; p 365.

148. M. T. Pope, Molybdenum oxygen chemistry: Oxides, oxocomplexes, and polyoxoanions. *Prog. Inorg. Chem* **1991**,39, 181-257

149. M. Sadakane, E. Steckhan, Electrochemical Properties of Polyoxometalates as Electrocatalysts , *Chem. Rev*. **1998,** 98,219-238

150. B. Tommasino, R. Contant, J. P. Michaut and J. Roncin Electrochemical characterization of a series of substituted Dawson type tungstophosphates ,α- $[P_2W_{18-x}Mo_zV_yO_{62}]^{n-}$ (x= y+z; n = 6+y) **,** *Polyhedron,* **1998,** 17,357-366

151. Contant R., Abbessi M., Thouvenot R., and Herve G., Dawson Type Heteropolyanions. 3. Syntheses and ^{31}P, ^{51}V, and ^{183}W NMR Structural Investigation of Octadeca (molybdo–tungsto–vanado) diphosphates Related to the $[H_2P_2W_{12}O_{48}]^{12-}$ Anion, *Inorg. Chem***. 2004**, 43, 3597–3604.

152. C. Li, Y. Zhang, K. P. O'Halloran, J. Zhang, H. Ma, electrochemcial behaviour of vanadium substituted Keggin-type polyoxometalates in aqueous solution, *J Appl Electrochem* **2009** 39:421–427

153. T. Pope, A. Muller, Polyoxometalate Chemistry: An Old Field with New Dimensions in Several Disciplines, *Angew. Chem., Int. Engl*., **1991** , 30, 34-48

154. J.J. Borrás-Almenar, E. Coronado.; A. Müller, M.T. Pope, Ed. "Polyoxometalate Molecular Science". NATO Science Series: II: Mathematics, Physics and Chemistry, vol. 98, Kluwer Academic Publishers, Dordrecht, **2003.**

155. J. J. Altenau, M. T. Pope, R. A. Prados, H. So, Models for heteropoly blues. Degrees of valence trapping in vanadium (IV)- and molybdenum(V)-substituted Keggin anions *Inorg. Chem.* **1975**, 14, 417-421.

156. T. Okuhara, N. Misuno, M. Misono, Catalytic chemistry of heteropoly compounds, *Adv. Catal*. **1996**, 41, 113.

157. K. Maeda., H. Katano, T. Osakai, S. Himeno; A. Saito, Charge dependence of one-electron redox potentials of Keggin-type heteropolyoxometalate anions, *J. Electroanal. Chem*, **1995**, 389, 167,

158. I.-M. Mbomekallé, X. López, J. M. Poblet, F. Sécheresse, B. Keita, L. Nadjo, Influence of the Heteroatom Size on the Redox Potentials of Selected Polyoxoanions, *Inorg. Chem.* **2010,** 49, 7001–7006

159. J.A.F. Gamelas, M.S. Balula, H.M. Carapuça, A.M.V. Cavaleiro, Unusual electrochemical reduction of copper (II) to copper (I) in polyoxotungstates, *Electrochem. Commun*., **2003**,5 378–382

160. B. Keita, F. Girard, L. Nadjo, R. Contant, J. Canny, M. Richet, Metal ion complexes derived from the α_1 isomer of $(P_2W_{17}O_{61})^{10-}$: comparison with the corresponding α_2 species, *J. Electroanal. Chem.* **1999**, 478, 76-82.

161. B. Keita, E. Abdeljalil, L. Nadjo, B. Avisse, R. Contant, J. Canny, M. Richet, Ligand and electrolyte effects in the electroreduction of copper-substituted heteropolyanions, *Electrochemistry Communications* , **2000**, 2 , 145-149

162. J. Li, I. Huth, L.-M. Chamoreau, B. Hasenknopf, E. Lacote, S. Thorimbert, M. Malacria, Insertion of amides into a polyoxometalate, Angew. Chem., Int. Ed. **2009**, 48, 2035-

163. Boujtita, J. Boixel, E. Blart; C. R. Mayer, F Odobel, Redox properties of hybrid Dawson type polyoxometalates disubstituted with organo-silyl or organo-phosphoryl moieties *Polyhedron* **2008**, *27*, 688-.

164. Harriman, J. K. Elliott, H. A. M. Alamiry, L. Le Pleux, M. Séverac, Y. Pellegrin, E. Blart, C. Fosse, C. Cannizzo, R. C. Mayer, F. Odobel, Intramolecular Electron Transfer Reactions Observed for Dawson-Type Polyoxometalates Covalently Linked to Porphyrin Residues *J. Phys. Chem. C*, **2009**, 113 ,5834–5842

165. X. López., J. J. Carbó, C. Bo. M. J Poblet , Structure, properties and reactivity of polyoxometalates: a theoretical perspective, *Chem. Soc. Rev.* **, 2012**, 41, 7537-7571

Chapter 2.

Facile electrochemical hydrogenation and chlorination of glassy carbon to produce highly reactive and uniform surfaces for stable anchoring of thiolated molecules

Ahmed M. Debela[a], Mayreli Ortiz[a]*, Valerio Beni[a], and Ciara K. O´Sullivan[a,b]*

[a] *Departament d'Enginyería Química, Universitat Rovira i Virgili, Avinguda Països Catalans, 26, 43007 Tarragona, Spain*

[b] *ICREA, Passeig Lluis Companys 23, 08010 Barcelona, Spain*

Chem. A Eur. J. 2014(in press), *DOI: 10.1002/chem.201402051*

Facile electrochemical hydrogenation and chlorination of glassy carbon to produce highly reactive and uniform surfaces for stable anchoring of thiolated molecules

Ahmed M. Debela[a], Mayreli Ortiz[a]*, Valerio Beni [a] †, and Ciara K. O´Sullivan[a,b]*

[a] *Departament d'Enginyería Química, Universitat Rovira i Virgili, Avinguda Països Catalans, 26, 43007 Tarragona, Spain*

[b]*ICREA, Passeig Lluis Companys 23, 08010 Barcelona, Spain*

Abstract:

Carbon is a highly adaptable family of materials and as one of the most chemically stable materials known, this can provide a remarkable platform for the development of tunable molecular interfaces. Here we report a two-step process for the electrochemical hydrogenation of glassy carbon followed by chlorination to provide a highly reactive surface for further functionalization. The carbon surface at each stage of the process was characterised using AFM, SEM, Raman, ATR- FT-IR, XPS and electroanalytical techniques. Electrochemical chlorination of hydrogen-terminated surfaces was achieved in just 5 minutes at room temperature using hydrochloric acid and compared to the use of chemical chlorination using phosphorous pentachloride at 50°C over a three-hour period. A much more controlled and uniform surface was obtained using the electrochemical approach as chemical chlorination was observed to damage the glassy carbon surface. As a model system to demonstrate the genericity of potential application of the formed highly reactive chlorinated surface a ferrocene labelled alkylthiol was used. The optimised process was applied to thiolated DNA probes on the glassy carbon substrate and the functionality of the immobilised DNA probe was demonstrated. XPS revealed the covalent bond formed to be a C-S bond and the thermal stability of the glassy carbon anchored thiolated molecules was evaluated and a far superior performance to stability on gold surfaces was observed, This is the first report of the electrochemical hydrogenation and electrochemical chlorination of a glassy carbon surface and this facile process can be applied to the functionalisation of carbon surfaces with a plethora of diverse molecules, finding widespread application.

Introduction

Carbon is a highly adaptable family of materials and as one of the most chemically stable materials known, this can provide a remarkable platform for the development of tunable molecular interfaces[1]. Carbon materials can be used for a wide range of applications and the surface chemistry of these materials are critical for their performances, and the ability to functionalise carbon-based materials facilitates tailoring their chemical properties and reactivities. Carbon-based surfaces including diamond, glassy carbon, and other diamond-like carbons, are attractive substrates for biological interfaces due to their biocompatibility, mechanical hardness and chemical robustness[1,2].

Chemisorption of aryldiazonium salts is one approach for the functionalisation of carbon surfaces[3]. This is a very versatile approach that can be applied to materials of different composition ranging from pure sp_2 material including graphite[4] and carbon nanotubes[5], to 100% sp_3 materials such as diamond[6,7]. Chemisorption is mediated by the electrochemical[8-10] or spontaneous reduction of the aryldiazonium cation[8,9] with this reduction process resulting in the dediazonation of the aryl group and the subsequent formation of a robust aryl–substrate linkage. However, the high reactivity of aryldiazonium cations can lead to the formation of multilayers and poorly defined organic films[8]. Various[9,10] studies have suggested that multilayer formation is regulated by, the potential and the charge consumed during the electrografting process as well as the composition of the grafting solution and the duration of the grafting step. However, control of all these parameters is not facile, thus hindering a good management of the surface properties[11]. these modified carbon surfaces have been demonstrated to have excellent stability, as for example, compared to thiol-based self-assembled monolayers (SAMs) on gold, even at elevated temperatures[12-14], which can be attributed to the strength of the C-C (348 kJ/mol) and C-S bonds (272 kJ/mol) as compared to those of the Au-S bond (167 kJ/mol).

Alternatively, one of the most powerful and extensively explored ways of activating carbon materials is H-termination, a process which is commonly performed using hydrogen plasma[15] resulting in the formation of C-H dipoles in which the

electropositive H is slightly susceptible to nucleophilic attack[16] . Hydrogen terminated substrates have found application in the highly stable photofunctionalisation of surfaces with alkenes[1,17,18] azides[19,20] and alkyl thiols[21].

To increase the reactivity of the H-terminated surfaces, halogenation with thionyl chloride ($SOCl_2$) or phosphorous tri/penta chloride ($PCl_{3/5}$) in organic solvents have recently been reported. These brominated or chlorinated surfaces have then been modified via the formation of carbon-carbon bonds between the surface and different types of alkyl-Grignard reagents[22,23] or alklythiols[13] and the so formed monolayers have been demonstrated to be extremely stable even at temperatures > 200^{o}C [13]. This chemical halogenation presents a straightforward approach as compared to previously used methods e.g. atomic beams[24] and a new approach based on the use of carbon tetrachloride cold plasma has been reported for the extensive chlorination of carbon nanotubes[25]. However, these chlorination process suffers from an inherent requirement to use toxic materials as well as difficulty in controlling the reaction, which can result in etching and damaging the substrates[26]. An alternative approach exploits the photochemical grafting of organic alkenes to link functional organic molecules to surfaces of carbon, including diamond[1], amorphous carbon[22] glassy carbon(GC)[27] highly pyrolitic ordered graphite (HOPG)[19,21] and carbon nanofibers[28].

Electrochemical methods for either chlorination or hydrogenation of surfaces have been demonstrated to be valuable methods due to their simplicity and ability to control the modification process and the resulting reduced surface damage. Electrochemical hydrogenation of boron doped diamond[29] and germanium[30] has been reported there are several reports of the electrochemical conversion of C-H to C-X (X= F or Cl) for organic molecule functionalisation[31,32] but to the best of our knowledge, there are no reports to date on the electrochemical halogenation of hydrogen terminated carbon substrates.

In the work reported herein, we describe a two-step process for the electrochemical hydrogenation and subsequent chemical/electrochemical chlorination to form a highly reactive surface with huge potential application. As an example of the potential use of this activated carbon surface for linking thiolated molecules, a ferrocene labelled alkylthiol was used as a model to optimise the immobilisation process. The developed methodology was then applied to a thiolated DNA probe and the functionality of the DNA probe following immobilisation demonstrated. The modified surfaces were characterised using AFM, Raman, ATR-FTIR, XPS and SEM. The thermal stability and functionality of the immobilised DNA was evaluated and compared to the stability of self-assembled monolayers on gold. The developed methodology is extremely robust, cost-effective and applicable to scale-up with a simple two-step process to produce a highly reactive carbon surface that can subsequently be functionalised with a plethora of different molecules.

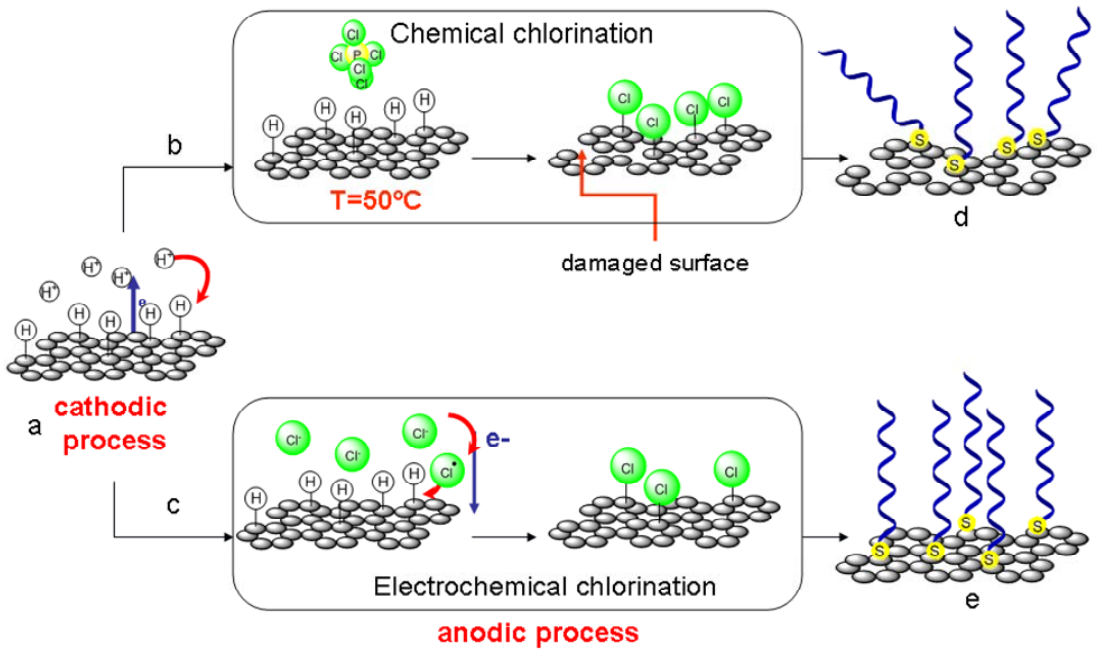

Figure 2.1. Schematic representation of surface preparation. a) electrochemical hydrogenation b) chemical chlorination of hydrogen-terminated surface c) electrochemical chlorination of hydrogen-terminated surface. d) Immobilisation of thiol molecules on chlorinated GC surface produced by b) and e) Immobilisation of thiol molecules on chlorinated GC surface produced by c).

Materials & Methods

Reagents

Hydrochloric acid, sulfuric acid, potassium dihydrogen phosphate, sodium chloride, and potassium chloride were purchased from Scharlau (Barcelona Spain); methylene blue, potassium hexacyanoferrate (II) and (III) ($K_4[Fe(CN_6)]$ /$K_3[Fe(CN_6)]$) were obtained from Fluka (Barcelona Spain). Trizma base, tris (2-carboxyethyl) phosphine (TCEP), 6-(ferrocenyl) hexane thiol, hexa-amine ruthenium (III) chloride ($[Ru(NH_3)_6]Cl_3$), phosphorous pentachloride (PCl_5), benzoyl peroxide, sodium perchlorate, sodium carbonate and 3,3',5,5'- tetramethyl benzidine (TMB) for ELISA were supplied by Sigma Aldrich. Sodium hydroxide pellets were from Panreac and benzene from Acros Organics. Highly Ordered Pyrolytic Graphite (HOPG) was supplied by SPI, Japan. Thioctic acid-DNA was purchased from Biomers as lyophilised powder and reconstituted in PBS pH 7.4.

DQA1*0301 probe for immobilisation on glassy carbon surface:
Thiotic acid-5'CAAATCTAAGTCTGTGGA-3'
DQA1*0301 target:
5' GAG AGG AAG GAG ACT GTC TGG AAG TTG CCT CTG T TC CAC AGA CTT AGA TTT G AC CCG CAA TTT GCA CTG ACA AAC ATC GCT GTG CTA AAA CATA 3'
Reporting sequence:
HRP-5'CCCCAGTGTTTCAGAAGA3´

chemicals and reagents were of analytical grade and used without further purification. All solutions were prepared in ultra-pure water (18 MΩ.cm) obtained using a Simplicity Water Purification System (Millipore, France).

All electrochemical measurements were carried out using an Autolab model PGSTAT 12 potentiostat/galvanostat controlled with the General Purpose Electrochemical System (GPES) software (Eco Chemie B.V., The Netherlands). A classical three electrode configuration was used: Ag/AgCl reference electrode, Pt wire counter electrode and as working electrode: glassy carbon electrodes, diameter 3 mm (ALS Japan) and gold electrodes, diameter 2 mm (CHI Instruments, Inc,). All the potentials were recorded with respect to the reference electrode.

Surface characterisation Glassy carbon sheets of 1.0 x10 x10 mm (ALS, Japan) were used to characterise the surface of the GCE during the different steps of the functionalisation process. Kelvin probe force microscopy (KPFM) images were acquired in non-contact mode where the chromium platinum coated conductive silicon microcantilever tip was set at 5 nm above the surface. A resonant frequency of 75 kHz and a constant force of 3 N/m were applied to the tip using a 5420 Atomic Force Microscope (AFM) from Agilent Technologies (USA). Scans were executed by applying a potential of 1 V to the tip, at a scan speed of 1.5 lines/s. The images were processed using WSxM 5.0 Develop 3.2 and Pico View 1.8. AFM was recorded using the same microscope in tapping-mode with a tip of a resonant frequency of 75 kHz.

Acquisition of the Raman spectra was achieved using a Renishaw 2003 Spectrometer operating at wavelength of 514 nm. The spectra were analysed using Wire 3.2 version software (Renishaw plc, United Kingdom).

The ATR-FTIR spectra were recorded using a Jasco FT/IR-600 Plus spectrometer. Typically, 128 scans at 2 cm^{-1} resolution were recorded. During measurement the cell compartment was flushed with dry nitrogen gas.

The X-ray Photoelectron spectroscopy (XPS) measurements were recorded using a PHI ESCA-5500 spectrometer Aluminum X-ray source. Samples were analysed in an ultra high vacuum (UHV) chamber pressure between $5x10^{-9}$ and $2x10^{-8}$ torr.

Static contact angles of DI water on the various glassy carbon substrates were measured using an OCA15EC instrument equipped with DropImage Standard software. Measurements were made by delivering a 3 µL drop of Milli-Q water from a microsyringe onto the surface of the sample mounted on an illuminated horizontal stage. The reported contact angle results are the average of four measurements, taken at different positions on each GC surface.

Electrode preparation The glassy carbon electrodes (GCE) were sequentially polished with 1.0, 0.3 and 0.05 µm alumina for ca. 5 minutes and were sonicated in water in between each polishing step. The activation of the GCEs was performed in saturated

sodium carbonate solution for 5 min at a potential of 1.2 V vs Ag/AgCl to eliminate any hydrocarbon adsorbed from the environment, followed by sweeping the potential for 40 cycles between 0 and 1.0 V vs Ag/AgCl at 250 mV/s in 0.1 M sodium perchlorate.

Hydrogenation of GCE: H-termination of the GCEs was performed electrochemically as described previously for boron doped diamond substrates[29] with some minor modifications. Briefly, the GCE was immersed in 2 M HCl and used as the cathode, and a platinum wire, immersed in a 2 M H_2SO_4 solution was used as the anode. The solutions were separated via a glass tube with a porous membrane and a potential of -5 V and 20 mA current were applied for 15 min. During the electrolytic process the solutions were stirred to avoid the accumulation of bubbles at the electrode surface.

Chemical chlorination of hydrogenated GCE: H-termination was followed by chemical chlorination of the GCE[13,22]. The H-terminated electrodes were immersed in a vial containing anhydrous benzene with a catalytic amount of benzoyl peroxide and 100 mM phosphorous pentachloride for 3 h at 50 ^{o}C. Following the chlorination reaction the electrodes were rinsed with ethanol and water, dried under nitrogen and immediately used for analysis or modification with the thiolated molecules.

Electrochemical chlorination of hydrogenated GCE: In this process, hydrogen-terminated GCE was used as an anode and immersed in 3:1 ratio of 2 M HCl: 2 M HNO_3. A platinum wire was used as the cathode and immersed in 2 M H_2SO_4. Both solutions were separated via a glass tube with a porous membrane. A potential of + 2 V and 20 mA of current were applied for 5 min.

6-(ferrocenyl) hexane thiol immobilisation on modified GCE: In order to functionalise the surface with thiolated molecules, the electrochemically hydrogenated and chlorinated GC electrodes were incubated in an ethanolic solution of 6-(ferrocenyl) hexane thiol overnight at room temperature, followed by extensive washing and sonication in ethanol and iso-propanol, to remove any non-specifically adsorbed molecules.

DNA probe immobilisation on GCE: A thioctic acid - DNA probe (50 µL, 5 µM) in the presence of 0.5 mM TCEP in Trizma base (pH = 8) was pipetted onto the surface of a chlorinated GCE and left to incubate for 24 hours at room temperature. The electrodes

were then rinsed with Tris-HCl buffer, pH 7.4 and dried under a stream of nitrogen. To test functionality of the immobilised probe, specific and non-specific synthetic oligonucleotide targets (in Tris-HCl, pH 7.4 containing 1 M NaCl) were hybridised with the on-surface immobilised DNA probes for 1 hour. Following the target capture a secondary reporting probe modified with an enzymatic label (HRP) was introduced. Electrochemical detection of the presence of captured target oligonucleotides was performed by monitoring the reduction of the product enzymatically produced from the TMB substrate using fast amperometric detection at -0.2 V vs Ag/AgCl.

DNA Probe immobilisation on gold: A clean gold electrode was immersed in a thioctic acid-DNA probe (50 µL, 5 µM) in 1.0 M KH_2PO_4 for 24 hours. After chemisorption, the electrodes were rinsed with water, dried under nitrogen and immediately used.

Thermal stability studies of the oligonucleotide monolayers: The DNA modified glassy carbon and gold electrodes were washed for 10 min, under gentle shaking, with an aliquot of 10 mM Tris-HCl buffer, pH=7.4, and thermostatted to the desired temperature using a thermomixer (Eppendorf Iberica, Spain), in the range of 25 ^{o}C to 85 ^{o}C in steps of 10^{o}C. Following the thermal incubation and subsequent thorough washing, the electrode was immersed in 10 mM Tris-HCl, pH=7.4 containing 20 µM methylene blue, at 25 ^{o}C for 5 min. Finally, the electrodes were transferred to 10 mM Tris-HCl pH=7.4, with 1 M NaCl and differential pulse voltammetry (DPV) measurements were performed. The experimental conditions for the DPV measurements were: potential between 0.1 and -0.6 V, amplitude of 0.1 V at a scan rate of 100 mV/s.

Results and discussion

We developed a facile methodology for the electrochemical hydrogenation and chlorination of glassy carbon surfaces, yielding a highly reactive surface for the anchoring of a plethora of diverse molecules (Figure 2. 1). To demonstrate the generic applicability of the produced reactive surface we applied it to the immobilisation of thiolated molecules.

In the first step, hydrogenation was achieved using glassy carbon substrate as a cathode, where H^+ protons from aqueous acidic solution were reduced at a negative potential

forming C-H bonds, producing a hydrogen terminated surface in far milder and less damaging conditions than previously reported[33].

In the second step, electrochemical chlorination of the H-terminated carbon surface was completed in just 5 minutes at room temperature, with the glassy carbon electrode now acting as the anode where Cl- anions from HCl were oxidised at a positive potential, producing highly reactive Cl. radicals in close proximity to the hydrogenated surface to form C-Cl bonds. This was compared to a previously reported chemical chlorination approach13,22 based on refluxing the carbon surface in dichloromethane at 50 oC in presence of a chemical chlorination agent (PCl5), the highly reactive chlorinated surface was subsequently used for the anchoring of thiolated molecules and analysed. All the modified surfaces were examined using a variety of characterisation techniques.

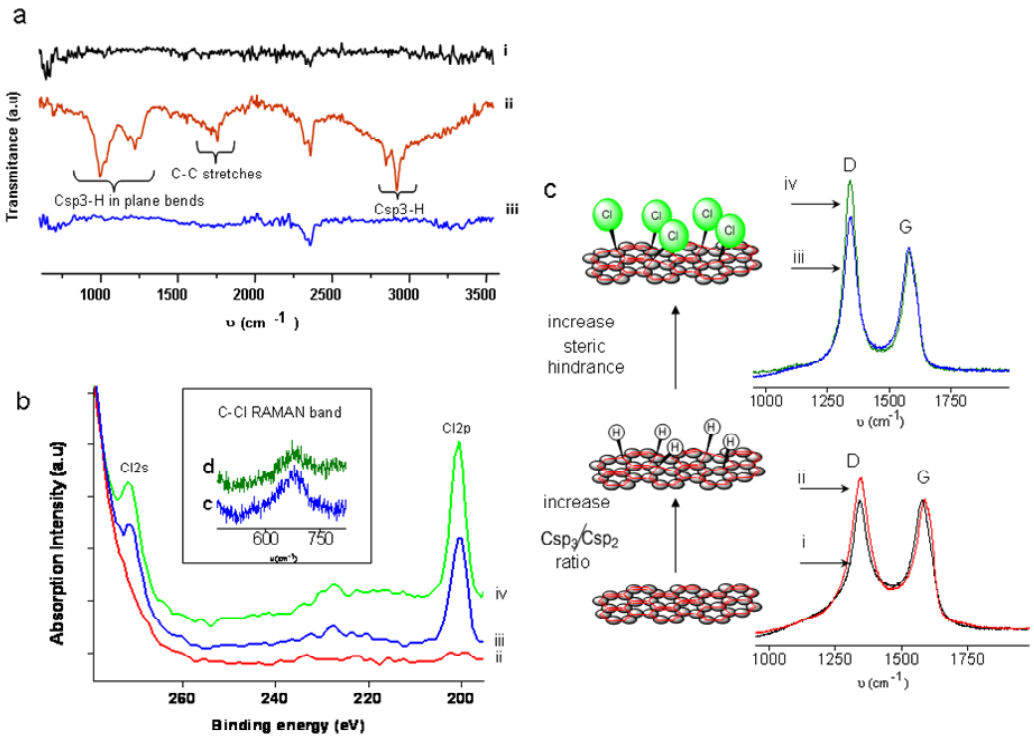

Figure 2.2 FTIR (a), XPS (b) and Raman spectra (c) of GC surfaces (i), hydrogen-terminated GC surface (ii), electrochemically chlorinated GC (iii) and chemically chlorinated GC (iv).

Characterisation of modified surfaces using FTIR, Raman and X- Ray photoelectron spectroscopies

The different steps of the glassy carbon (GC) surface preparation were followed using XPS, ATR-FTIR and Raman spectrocopies. The combination of these techniques is commonly used for a better understanding of surface processes.[22,33,34]

X-Ray Photoelectron Spectroscopy (XPS) is probably the more appropriate tool for determining the chemical composition of organic thin layers[13,35] because it analyses just the first 10 nm of the surface. For the same reason is widely used for evaluating the percent of atoms covalently bonded to the surfaces.[25,36]

Since neither the hydrogen or helium can be detected by XPS,[25] a low value of oxygen/carbon (O/C) atomic ratio[37], is indicative of successful hydrogenation of a carbon surface. After electrochemical hydrogenation, the O/C atomic ratio was found to be around 4.4 %, which is comparable with the 1 to 4 % reported for plasma hydrogenated glassy carbon surfaces and considerable lower than that obtained for polished glassy carbon (8-15%).[33]

In more direct way, the presence of hydrogen atoms linked to the carbon in the hydrogen terminated GC surface is demonstrated by the FTIR bands corresponding to the asymmetric and symmetric vibration modes of a Csp_3-H bond at 2913 and 2843 cm^{-1}, respectively. In the chlorinated GC generated using both the chemical and electrochemical approaches, these bands are not present, indicative of the successful conversion of the C-H bond into a C-Cl bond (Figure 2A). Finally, the presence of signals at 201.0 and 272.0 eV corresponding to Cl2p and Cl2s in the XPS[22,25] spectra and the band at 673 cm^{-1}, corresponding to a C-Cl vibration in the Raman spectra of the chlorinated GC substrates, (Figure 2.2B) further confirmed the presence of chlorine atoms bound to the carbon.

In addition to FTIR, Raman spectroscopy is also a useful tool for studying the structural differences on carbon surfaces according to the behavior of the G and D bands[33,38]. The G band appears in the region of 1560 cm^{-1} due to the C-C bond vibration, whilst the origin of the D band (at 1360 cm^{-1}) is related with structural disorders produced by mechanical

treatments including polishing[33] or chemical reactions due to changes on the hybridisation of carbon from sp_2 to sp_3.[38,39] Thus, the D/G ratio will increase in direct proportion with the physical and/or chemical disorder. GC substrates at each of three different steps of the functionalisation process were studied by recording 15 Raman spectra, and calculating the average D/G ratio (Figure 2.2C, Table 2. 1). A fresh and unpolished GC surface was found to have a D/G ratio of 1.16, whilst after electrochemical hydrogenation this ratio increased to 1.36, due to the formation of C-H bonds that changed the hybridisation of the carbon from sp_2 to sp_3. D/G ratios for the chlorinated surfaces were increased with respect to the hydrogen-terminated surface as the chlorine increases the steric hindrance due to the larger atomic ratio and thus magnifies the structural disorder. The significantly higher value obtained for GC modified by chemical chlorination (1.81) than for the corresponding electrochemical procedure (1.54) indicated differences in the degree of disorder on the glassy carbon. This increased disorder of the chemically chlorinated surfaces may be due to damage caused to the substrate surface to the strength of the aggressive chemical agents used. To see if the electrochemically chlorinated surface was more uniform and less damaged SEM imaging was carried out.

Characterisation of surfaces using by SEM

Figure 2. 3 shows scanning electron microscopy images of the GC surface before and after both chlorination procedures. As can be seen, electrochemical hydrogenation slightly increases the roughness of the surface as compared with the bare electrode, in agreement with the increase in D/G ratio observed by Raman (Figure 2. 3B), where "islands" of chlorine are distributed across the surface. The chemically chlorinated surface is, as anticipated, more damaged, which, as mentioned above, can be attributed to the aggressive chlorination treatment. The relative percentage of chlorine bound is higher in the case of the chemically prepared surfaces (0.62 %) as compared with the electrochemically prepared surfaces (0.55 %) with both values being comparable to the value of 0.75 % previously reported for diamond.[40] It is generally accepted that electron-transfer reactions such as the reduction of H^+ from acid media, are more probable to occur in the “defects” on the planar structure, where the charge concentration is higher. It is thus expected that the anodic oxidation of chlorine anions has a greater probability to occur at these points, where the highest concentration of C-H is present, because with

removal of hydrogen by the produced chlorine radicals and concomitant formation of the the C-Cl bond.

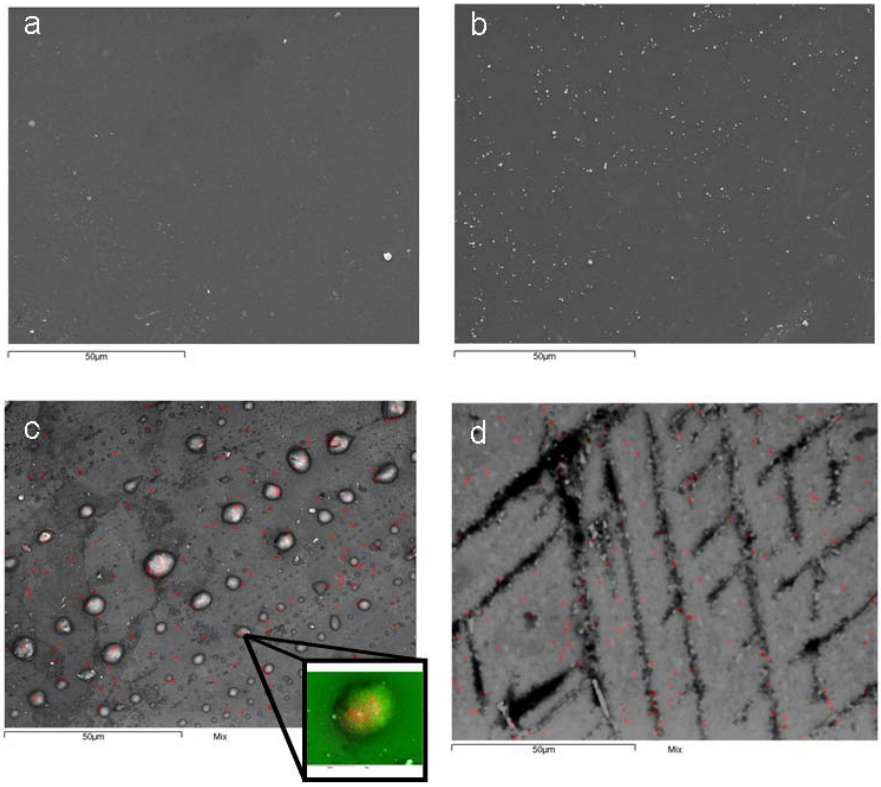

Figure 2. 3. SEM images of: A) Bare GC surface, B) hydrogen terminated GC surface and after C) electrochemical chlorination (Inset c1: magnified image, scale bar 4 µm showing chlorine in red and carbon in green, and D) chemical chlorination Scale bar = 50 µm, (overlapped with the chlorine distribution (red points in false color).

Characterisation of modified surfaces using contact angle measurements

The contact angle obtained for the bare GC surface was 47º, due to the presence of polar carbon oxides on the surface.[33] The cathodic hydrogenation decreased the hydrophilic character of the surface by forming less polar C-H bonds and the contact angle increased up to 72º. The subsequent electrochemical chlorination of the surface slightly decreased the contact angle to 70º due to the formation of the more polar C-Cl bonds that confer a more hydrophilic character. In agreement with the results obtained in Raman and SEM,

the physical damage of the surface when chemical chlorination was carried out resulted in an increased roughness, which gave rise to a more hydrophobic surface (formation of air cavities at the surface), which was reflected in an increase of the contact angle to 77°. (Table 2. 1, see also Fig S1, supplementary information).

Table 2. 1. D/G ratio values from Raman spectra and static contact angle for the GC substrate at different steps of reactions.

Substrate	**D/G area ratio**	**Static contact angle (deg) (n=4)**
Glassy carbon electrode	1.16	47.0 ± 2.0
Hydrogenated GCE	1.36	72.1 ± 4.8
Electrochemically chlorinated GCE	1.54	70.0 ± 3.5
Chemically chlorinated GCE	1.81	77.4 ± 5.5

Functionalisation of modified glassy carbon with (6-(ferrocenyl)-hexanethiol): Both the chemical and electrochemical chlorination methods were then compared as supports for the immobilisation of thiolated molecules. For this purpose, a model thiol molecule bearing an electroactive ferrocene moiety (6-(ferrocenyl)-hexanethiol) was selected. The presence of S2p1 and S2p3 XPS signals at 162 and 163 eV indicates the chemical binding of the alkylthiol to the carbon surface, via the formation of C-S covalent bond (Figure 2. 4A), according to previously reported for arythiol immobilised on previously chlorinated surface by chemical method[13] and by self assembly on gold.[35] Different situation was observed when alkyl thiol was photochemically tethered on HOPG. As no XPS sulfur peak was found on surface after immobilisation process, the author suggested a mechanism where a grafting of alkyl chains on the HOPG involved the formation of alkyl radicals and surphydryls acted as sacrificial species.[21] In addition the signals at 712 eV and 727 eV corresponding to the ferrocene moiety further supports the linking of the ferrocenylated alkylthiol molecule[35] (Figure 2. 4B).

Observing the cyclic voltammetry behaviour of the modified surfaces revealed well-defined oxidation and reduction waves with a ΔE_p around 20 mV, (Figure 2.4C), with a higher current obtained for the GC modified using electrochemical chlorination, again

highlighting the damage to the surface caused by the chemical chlorination. The confinement of the 6-(ferrocenyl)-hexanethiol to the surface was confirmed by the linearity of the plot of anodic peak current vs scan rate (Figure 2. 4D). As a control, an unmodified GC electrode was exposed to the ferrocene linked alkanethiol and negligible redox waves were observed.

Optimisation of electrochemical surface preparation: Based on the mechanism proposed by Hoffman[27] hydrogen radicals are generated at negative potentials and react with the carbon surface. Very negative potentials (-35 V vs NHE) were reported for an efficient hydrogenation of boron-doped diamond, but the optimum potential and duration of hydrogenation step should be optimised according to the carbon substrate used. This was achieved by varying the potential from 0 to -12.5 V vs NHE, and increasing the hydrogenation time from 10 to 40 min. Evaluation of the process was performed using cyclic voltammetry to calculate the surface coverage of the Fc-alkanethiol. (Supporting Information, Figure S2 A and B). Surface coverage was calculated by integrating the peak area of the CV.

Since the energy level of the hydrogen radical electron is 3.68 eV, the applied potential for the generation of hydrogen radicals should be more negative than -3.68 V (vs NHE),[27] (Supporting Information, Figure S2). The applied potential was optimised to be -5V vs NHE with a hydrogenation duration of 15 minutes and an electrochemical chlorination time of just 5 minutes. Longer time and higher voltages gave lower surface coverage, which can be attributed to the damages to the surface resulting from the etching involved in the hydrogenation and chlorination processes.[15,33]

Using the optimum conditions for hydrogenation (-5.0 V for 15 min) in combination with chemical chlorination, a maximum surface coverage of the Fc-alkane thiol was found to be 2.3 x 10^{14} molecules/cm^2 (average value measured for six electrodes). The surface coverage for surfaces modified following the optimised electrochemical hydrogenation and electrochemical chlorination was found to be 2.51×10^{14} molecules/cm^2. The results obtained were in the same order as those reported for the theoretical density of a monolayer of the ferrocenyl-alkylthiol on gold (2.7 x 10^{14} molecules/cm^2)[41,42]

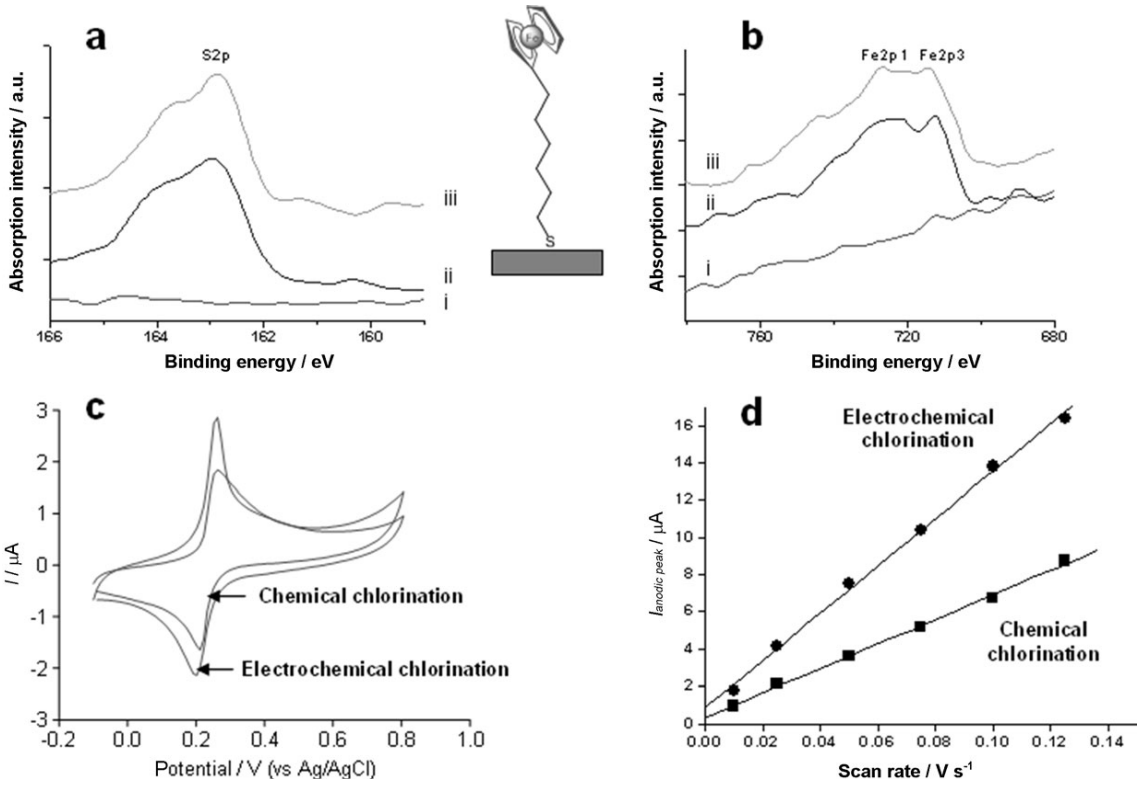

Figure 2.4. a, b) XPS of i) hydrogen-terminated GC surface, ii) electrochemically chlorinated GC, and iii) chemically chlorinated GC. c) Cyclic voltammograms of 6-(ferrocenyl)-hexanethiol immobilised on both chlorinated GC surfaces recorded in 0.1m $NaClO_4$ (scan rate=20 mVs^{-1}, reference Ag/AgCl). d) Dependence of anodic current on scan rate of 6-(ferrocenyl)-hexanethiol immobilised on both chlorinated GC surfaces.

The duration of the step for immobilisation of the alkylthiol on each of the chlorinated surfaces was evaluated [Supporting Information, Figure S3]. The result reveals faster monolayer formation for chemically chlorinated substrates but as incubation time increases a higher surface coverage and better reproducibility is obtained for electrochemically chlorinated electrodes, which is attributable to the lower degree of surface damage by the latter process.

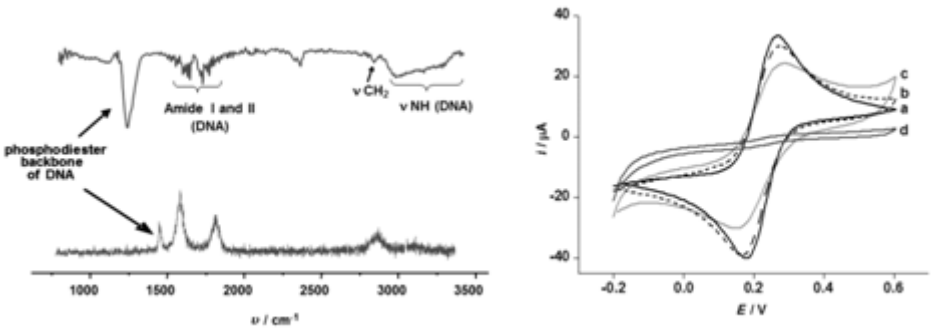

Figure 2. 5. Left) FTIR and Raman spectra of DNA immobilised on GC surfaces using electrochemical hydrogenation and chlorination. Right) Cyclic voltammetry recorded in 1 mM of $K_4[Fe(CN_6)]/K_3[Fe(CN_6)]$ in PBS of: a) GC electrode, b) hydrogen-terminated GC electrode c) electrochemically chlorinated GC electrode and d) DNA immobilized on GC surface.

Functionalisation of modified glassy carbon with thiolated DNA

Immobilisation of thioctic acid DNA was accomplished in the presence of TCEP at basic pH, where the TCEP has the function of breaking the disulfide bond to form a dipodal terminated thiolated oligonucleotide for interaction with the chlorinated surface. In addition, this alkaline solution impedes the protonation of the sulfur moiety and counteracts the HCl formed as a result of the final C-S bond formation on the surface.
The Raman analysis of the DNA modified surface confirmed the successful modification of the GC substrate, and a band of medium intensity, not present in the chlorinated and hydrogenated surface, was observed at 1220 cm^{-1} (Figure 2. 5) and can be assigned to the C-O-P-O-C phosphodiester network of DNA[43]. Other bands representing the DNA bases (A, T, C) expected to appear in the region 800 to 1600 cm^{-1}were suppressed by the D and E_{2g} (G) modes of carbon.

In the ATR-FTIR (Figure 2. 5a) of the DNA modified GC, characteristic bands for DNA at 1650 cm^{-1} (exocyclic NH_2), 1450 cm^{-1} (purine and pyrimidine rings) and 1110 cm^{-1} (DNA phosphodiester backbone), in addition to the Amide I and II stretch and bends (3350, 3200, 1660 and 1625 cm^{-1}), were observed[44]. Finally, the contact angle of DNA functionalised GC substrates decreased to 64±2 (n=4), in agreement with previous reports[45].

For better visualisation of the surface at nanoscale, Highly Ordered Pyrolytic Graphite HOPG) was selected as flatter substrate than GC. (HOPG) was modified in the same way as the GC surface and used to visualise the modified surface using AFM in tapping mode. The topography image of the Fc-alkyl-thiol modified HOPG (Supporting Information, Figure S4) shows the homogeneous formation of islands, indicative of thiolated molecules linking to the carbon at nucleation points formed during the electrochemical hydrogenation and/or chlorination process. The immobilised DNA is also observed to link at these nucleation points. Imaging of the surfaces modified using chemical chlorination was not possible due to the high surface roughness. In addition, the surface charge of around -150 mV, recorded by KPFM when single stranded DNA molecules were immobilised is consistent with values previously reported[46].

The different steps of DNA immobilisation were followed by cyclic voltammetry (Figure 2. 5B) and the detection of a complementary DNA target in a sandwich format using a secondary HRP-labeled probe was tested on both surfaces, resulting in a markedly higher signal for the electrochemically activated surface, which can be assumed to be due to the higher degree of order of the immobilised layer (Figure 2.6a).

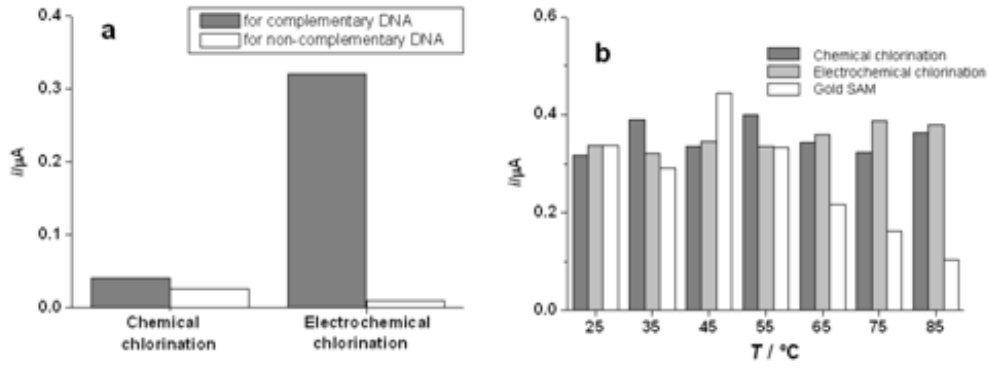

Figure 2. 6. Amperometric responses obtained for the detection of of 10 nM complementary and non-complementary DNA targets using chemical or electrochemically chlorinated surfaces. b) Temperature stability of DNA immobilized via chemical/electrochemical chlorination and thiolated on gold.

Evaluation of thermal stability of immobilised DNA probe. The thermal stability of the thiolated oligonucleotide modified GC was evaluated using an electrochemically hydrogenated and chlorinated electrode functionalised with the DNA probe (Figure 2.6B). A self-assembled monolayer of DNA on a gold electrode was used for comparison. The presence of immobilised DNA on the electrode surface was detected by DPV measurements of methylene blue (MB). Similar responses, after area normalisation, for both gold and GC electrodes indicated a very similar DNA surface coverage before being exposed to elevated temperatures.

In the case of the gold electrode, (Figure 2. 6) the current peak value decreased significantly with an almost 70% reduction in signal at 85 °C, due to breakage of the gold-sulfur bond and the removal of immobilised DNA.[47] On the other hand, almost no loss in signal was recorded in the case of the probes immobilised on the GCEs, in agreement with previous reports detailing thermal stability of alkylthiols[13] and carbon[48]. This improved stability of the DNA immobilised on carbon is due to the high stability of the C-S bond (bond energy 272 kJ/mol) when compared to that of the Au-S bond (bond energy 167 kJ/mol)[49] . The functionality of the thiolated DNA probe immobilised on the GCE following exposure to elevated temperatures (85 °C) was evaluated. Following the above experiment, the functionalised electrode was exposed to complementary and non-complementary DNA, followed by HRP labeled reporter probe. As can be seen in the inset in Figure 6A, the immobilised probe successfully hybridised its complementary sequence, whilst negligible response was observed when exposed to a non-complementary sequence, thus demonstrating that the DNA probe maintains its function following immobilisation and exposure to high temperatures.

Conclusions

We have described a two-step process for the electrochemical hydrogenation and subsequent electrochemical chlorination to form a highly reactive surface with wide potential application. Electrochemical chlorination was extremely rapid and does not require elevated temperatures or noxious reagents, making it very attractive for industrial application. Furthermore, the surface obtained following electrochemical chlorination was compared to that obtained after chemical chlorination and observed to be markedly less damaged and probably consequently, notably more organised. The highly reactive surface obtained could be used for anchoring of a plethora of moecules

ranging from olefins to thiols), but due to the huge range of easily available diverse thiolated molecules, we decided to use this as a model system. In the first instance, a ferrocene labelled alkylthiol was used as a model to optimise the immobilisation process in terms of hydrogenation and chlorination times, applied potential and duration of immobilisation. The developed methodology was then used in an example of an "application" of the formed reactive surface for anchoring of a thiolated DNA probe and the functionality of the DNA probe following immobilisation was demonstrated. The thermal stability and functionality of the immobilised DNA was evaluated and compared to the stability of self-assembled monolayers on gold. The modified surfaces were characterised using AFM, Raman, ATR-FTIR, XPS and SEM. all of which concurred on the superior surface obtained using electrochemical chlorination as well as confirming the presence of a C-S bond. The developed methodology is extremely robust, cost-effective and applicable to scale-up with a simple two-step electrochemical process to produce a highly reactive carbon surface that can subsequently be functionalised with a plethora of different molecules.

References

1. C. Stavis, T. L. Clare, J. E. Butler, A. D. Radadia, R. Carre, H. Zeng,W. P. King, J. A. Carlisle, A. Aksimentiev, R. Bashir, R. J. Hamers, Surface functionalization of thin-film diamond for highly stable and selective biological interfaces, *Proc. Nat. Acc. Scien.(USA)* **2011** 108, 983.
2. B. Sun, E. P. Colavita, H. Kim, M. Lockett, S. M. Marcus, L. Smith, J. R. Hamers, Covalent Photochemical Functionalization of Amorphous Carbon Thin Films for Integrated Real-Time Biosensing, *Langmuir* **2006** *22*, 9598.
3. S. Mahouche-Chergui, S. Gam-Derouich, C. Mangeney, M. M. Chehimi Aryl diazonium salts: a new class of coupling agents for bonding polymers, biomacromolecules and nanoparticles to surfaces *Chem. Soc. Rev.* **2011** *40*, 4143.
4. D. M. Murphy, R. J. Cullen, D. R. Jayasundara, E. M., Scanlan, P. E Colavita. Study of the spontaneous attachment of polycyclic aryldiazonium salts onto amorphous carbon substrates *RSC Adv.* **2012** *2* 6527.
5. C. D. Doyle, J.D. Rocha, R. B. Weisman, J. M Tour, Structure-Dependent Reactivity of Semiconducting Single-Walled Carbon Nanotubes with Benzenediazonium Salts, *J. Am. Chem. Soc.* **2008** *130*, 6795.
6. M. Delamar, R. H., J. Pinson Covalent modification of carbon surfaces by grafting of functionalized aryl radicals produced from electrochemical reduction of diazonium salts ,*J. Am. Chem. Soc.* **1992**, *114* 5883.
7. H. Uetsuka,D. Shin, N. Tokuda, K. Saeki, C. E. Nebel, Electrochemical Grafting of Boron-Doped Single-Crystalline Chemical Vapor Deposition Diamond with Nitrophenyl Molecules , *Langmuir* **2007**, *23*, 3466–3472.
8. J. K. Kariuki, M. T. McDermott, Formation of Multilayers on Glassy Carbon Electrodes via the Reduction of Diazonium Salts, *Langmuir* **2001** *17*, 5947.
9. P. Allongue, C. Henry de Villeneuve, G. Cherouvrier, R. *J.* Cortes, Phenyl layers on H/Si (111) by electrochemical reduction of diazonium salts: monolayer versus multilayer formation, *Electroanal. Chem.* **2003** 550, 161–174.
10. A. Ricci, C. Bonazzola, E.J. Calvo, An FT-IRRAS study of nitrophenyl mono- and multilayers electro-deposited on gold by reduction of the diazonium salt *Phys. Chem. Chem.Phys.* **2006** *8*, 4297.

11. J. J. Gooding, Advances in Interfacial Design for Electrochemical Biosensors and Sensors: Aryl Diazonium Salts for Modifying Carbon and Metal Electrodes *Electroanalysis* **2008**, *20* 573
12. L. Civit, A. Fragoso,K. C. O'Sullivan, Thermal stability of diazonium derived and thiol-derived layers on gold for application in genosensors, *Electrochem. Commun.* **2010** *12*, 1045.
13. R. M. Lockett, M. L. Smith, Formation and Stability of Alkylthiol Monolayers on Carbon Substrates, J. *Phys. Chem. C* **2010**, *114*, 12635.
14. L. Y. Zhong, P. K. Loh, The Chemistry of C-H Bond Activation on Diamond , *Chem. Asian J.* **2010** *5* 1532
15. R. DeClements, G. M. Swain, T. Dallas, M. W. Holtz, II, R. D. Herrick, J. L. Stickney, Electrochemical and Surface Structural Characterization of Hydrogen Plasma Treated Glassy Carbon Electrodes , *Langmuir* **1996** *12* 6578.
16. C. E. Nebel, H. Kato, B. Rezek, D. Shin,D. Takeuchi, H. Watanabe, T. Yamamoto, Electrochemical properties of undoped hydrogen terminated CVD diamond , *Diamond & Related Materials* **2006** *15*, 264
17. L. T. Lasseter, W. Cai, J. R. Hamers, Frequency-dependent electrical detection of protein binding events, *Analyst* **2004** *129*, 3.
18. P. E. Colavita, B. Sun, K. Y. Tse, J. R. Hamers, Photochemical Grafting of n-Alkenes onto Carbon Surfaces: the Role of Photoelectron Ejection , *J. Am. Chem. Soc.* **2007** *129*, 13554.
19. M. Tanaka, T. Sawaguchi, Y. Sato, K. Yoshioka, O. Niwa, Surface Modification of GC and HOPG with Diazonium, Amine, Azide, and Olefin Derivatives ,*Langmuir* **2011** *27*, , 170.
20. N. Dontha,W. B. Nowall, W. G. Kuhr, Generation of Biotin/Avidin/Enzyme Nanostructures with Maskless Photolithography, *Anal. Chem.* **1997** *69,*, 2619.
21. L. Soldi, R. J. Cullen, D. R. Jayasundara,E. M. Scanlan,S. Giordani, P. E. Colavita, Photochemically Triggered Alkylthiol Reactions on Highly Ordered Pyrolytic Graphite, *J. Phys. Chem. C* **2011** *115*, 10196.
22. R. M. Lockett, M. L. Smith, Attaching Molecules to Chlorinated and Brominated Amorphous Carbon Substrates via Grignard Reactions, *Langmuir* **2009** *25*, 3340.
23. M. Wang, M. R. Das, V. G. Praig, F. LeNormand, M. Li, R. Boukherroub, S. Szunerits,Wet-chemical approach for the halogenation of hydrogenated boron-doped diamond electrodes *Chem. Commun.,* **2008,** 6294-.

24. A. Freedman, Halogenation of carbon surfaces by atomic beams: HOPG graphite, *Diamond Relat. Mater.* **1995**, *4*, 216-.
25. V. K. S. Abdelkader, C. Garcia-Gallarin, M. L. Godino-Salido, M. Domingo-Garcia; F. J Lopez-Garzon, M. *J.* Perez-Mendoza, , Carbon Tetrachloride Cold Plasma for Extensive Chlorination of Carbon Nanotubes, *Phys. Chem. C.* **2013** *117*, 16677.
26. A. Toshihiro, N.-G. Mikka, E. R. Robin,Y. Kazuo, K. Mutsukazu, S. Yoichiro, Chemical modification of diamond surfaces using a chlorinated surfaceas an intermediate state, *Diamond Rel. Mater.* **1996** 5, 1136.
27. S. C. S. Yu, J. A. Downard, Photochemical Grafting and Activation of Organic Layers on Glassy Carbon and Pyrolyzed Photoresist Films *Langmuir* **2007**, *23* 4662.
28. C. E. Landis, L. K. Klein, A. Liao, E. Pop,K. D. Hensley, V. A. Melechko, J. R. Hamers, Covalent Functionalization and Electron-Transfer Properties of Vertically Aligned Carbon Nanofibers: The Importance of Edge-Plane Sites, *Chem. Mater* **2010** *22*, 2357.
29. R. Hoffmann, A. Kriele, H. Obloh,J. Hees, M. Wolfer, W. Smirnov, N. Yang, E. C. Nebel, Electrochemical hydrogen termination of boron-doped diamond *Appl. Phys. Lett.* **2010**, *97*, 052101.
30. H. C. Choi, J. M. Buriak , Preparation and functionalization of hydride terminated porous germanium *Chem. Commun.* **2000**.
31. B. V. Lyalin, V. A. Petrosyan, Electrochemical Halogenation of Organic Compounds, *Russian Journal of Electrochemistry* **2013** *49* 497.
32. T. Fuchigami, S. Inagi, Selective electrochemical fluorination of organic molecules and macromolecules in ionic liquids, *Chem. Commun.* **2011**, *47*,, 10211.
33. T.-C.Kuo, L. R.McCreery, Surface Chemistry and Electron-Transfer Kinetics of Hydrogen-Modified Glassy Carbon Electrodes, Anal. *Chem.* **1999** *71*, 1553.
34. R. M.Lockett, M. L. Smith, Halogenation of Carbon Substrates for Increased Reactivity with Alkenes, *Langmuir* **2010** *26*, 16642.
35. T. Kitagawa,H. Matsubara, K. Komatsu, K. Hirai, T. Okazaki, T. Hase, Ideal Redox Behavior of the High-Density Self-Assembled Monolayer of a Molecular Tripod on a Au(111) Surface with a Terminal Ferrocene Group. *Langmuir,* **2013,***29* 4275.
36. E. Papirer, R. Lacroix, J-B. Donnet, G. Nansé, P. Fioux, XPS study of the halogenation of carbon black—Part 2. Chlorination. *Carbon* **1995**, *33,* 63.
37. A. Deslandes, J. G. Shapter, E. L. Lawrance, J. S. Quinton, Preparation of Carbon Surfaces for Sensing Applications via Plasma Hydrogenation *Nanoscience and*

Nanotechnology, 2006. ICONN '06. International Conference on. **E-ISBN :** 1-4244-0453-3, Brisbane, Qld.

38. A. Jorio, Raman Spectroscopy in Graphene-Based Systems: Prototypes for Nanoscience and Nanometrology, *International Scholarly Research Network ISRN Nanotechnology*, 2012 doi:10.5402/2012/234216
39. B. Li, L. Zhou., D. Wu, H. Peng, H. Yan, Y. Zhou, Z. Liu,, Photochemical Chlorination of Graphene, *ACS Nano* **2011** *5*, 5957.
40. T. I. Hukka, T. A. Pakkanen, M. P. D'Evelyn, Chemisorption of Fluorine, Chlorine, HF, and HCl on the Diamond (100)2x1 Surface: An ab Initio Study, *J. Phys. Chem.* **1995** *99*, 4710.
41. M. M. Walczak, D. D. Popenoe, S. R. Deinhammer, D. B. Lamp, C. Chung, D. M. Porter, Reductive Desorption of Alkanethiolate Monolayers at Gold A Measure of Surface Coverage, *Langmuir* **1991** *7*, 2687.
42. E. D. C. Chidsey, R. C. Bertozzi, M. T. Putvinski, M. A. Mujsce, Coadsorption of Ferrocene-Terminated and Unsubstituted Alkanethiols on Gold: Electroactive Self-Assembled Monolayers, *J. Am. Chem. Soc.* **1990** *112,* , 4301.
43. Y. Guan, C. J. Wurrey, G. J. Thomas, Vibrational Analysis of Nucleic Acids. 1. The Phosphodiester Group in Dimethyl Phosphate Model Compounds: $(CH_3O)_2PO_2^-$, $(CD_3O)_2PO_2^-$, and $(^{13}CH_3O)_2PO_2^-$, J. *Biophysical Journal* **1994** *66*, 225.
44. P. He, , L. He, Synthesis of Surface-Anchored DNA-Polymer Bioconjugates Using Reversible Addition-Fragmentation Chain Transfer Polymerization, *Biomacromolecules* **2009**, *10*, 1804.
45. T. Sakata, , A. Ueda, H. Otsuka, Y. Miyahara, stable Immobilization of an Oligonucleotide Probe on a Gold Substrate Using Tripodal Thiol Derivatives , *Langmuir* **2007** *23* 2269.
46. C. Leung, , H. Kinns, , W. B. Hoogenboom, , S. Howorka, P. Mesquida, Imaging Surface Charges of Individual Biomolecules, *Nano Lett.* **2009** *9*, 2769.
47. M. D. Shewchuk, T. M. McDermott, Comparison of Diazonium Salt Derived and Thiol Derived Nitrobenzene Layers on Gold, *Langmuir* **2009** *25,* 4556.
48. H. Sabbah,S. Ababou-Girard, A. Zebda, D. David, B. Fabre, S. Députier, A. Perrin, M. Guilloux-Viry, F. Solal, C. Gode,, Thermal grafting of organic monolayers on amorphous carbon and silicon (111) surfaces: A comparative study , *Diamond & Related Material* **2009** *18,* 1074.

49. E. de la Llave, A. Ricci, E. J. Calvo, D. A. Scherlis, Binding between Carbon and the Au(111) Surface and What Makes It Different from the S-Au(111) Bond, *J. Phys. Chem. C* **2008**, *112*,, 17611.

Supporting information

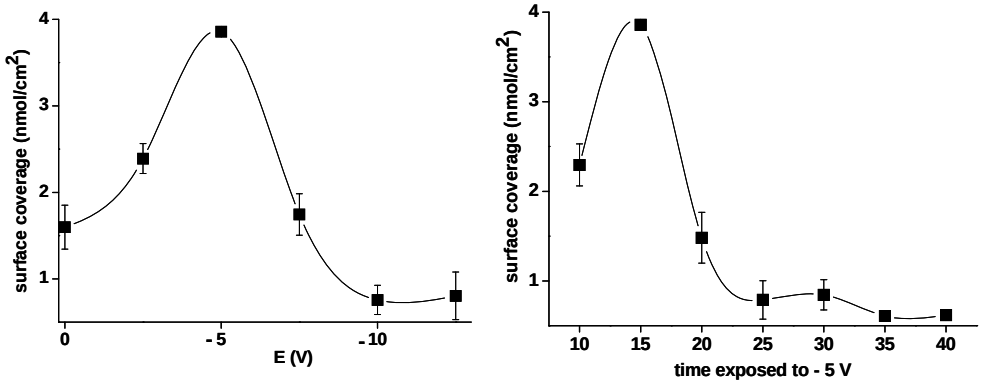

Figure S1. Optimisation of hydrogenation procedure by calculating the surface coverages of Fc-thiol obtained on surfaces prepared by electrochemical hydrogenation (followed by electrochemical chlorination) A) At different negative potentials and 15 minutes of H- termination and (B) at different times and potential of -5 V.

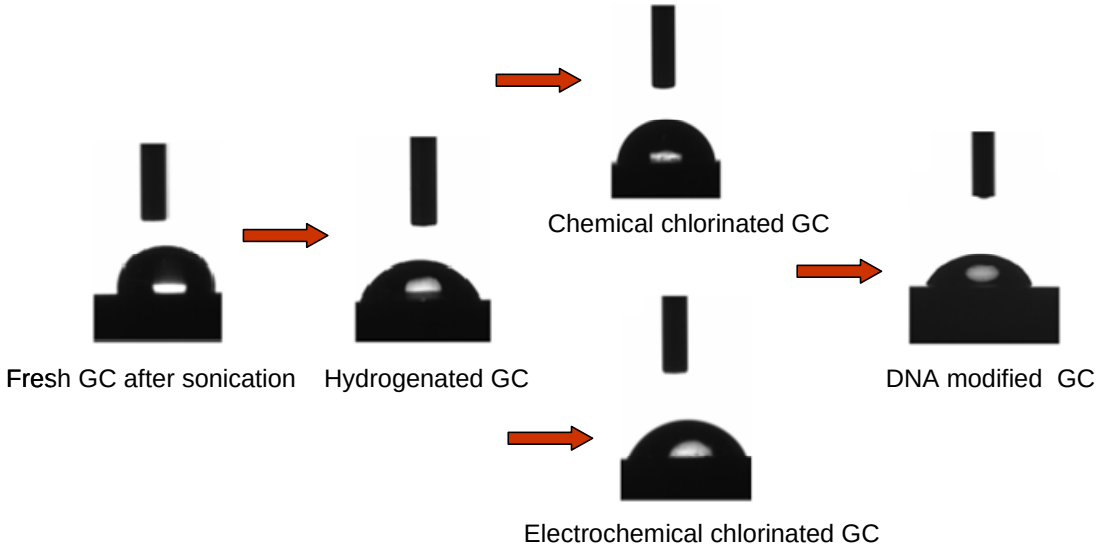

Figure S2. Contact angle measured for various glassy carbon substrates

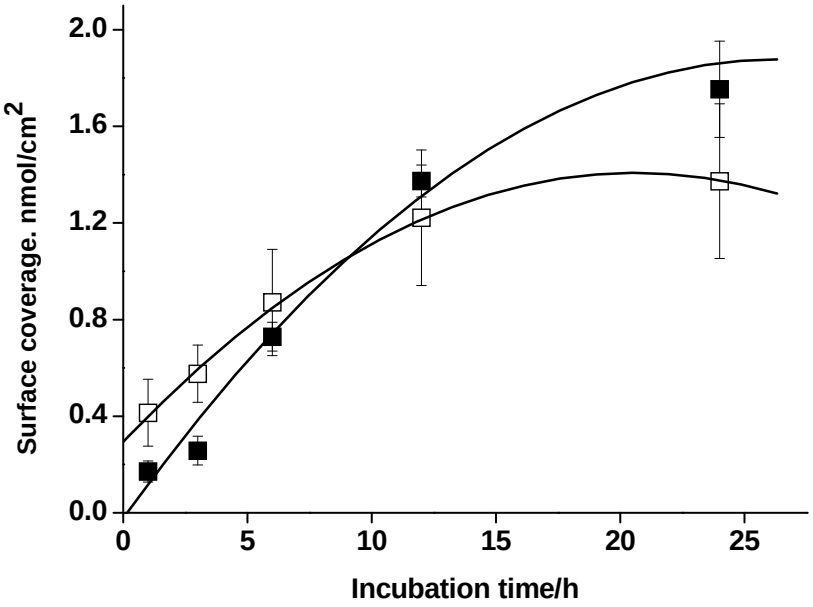

Figure S3. Surface coverage of ferrocene hexane thiol as a function of incubation time for the two routes of GC chlorination.

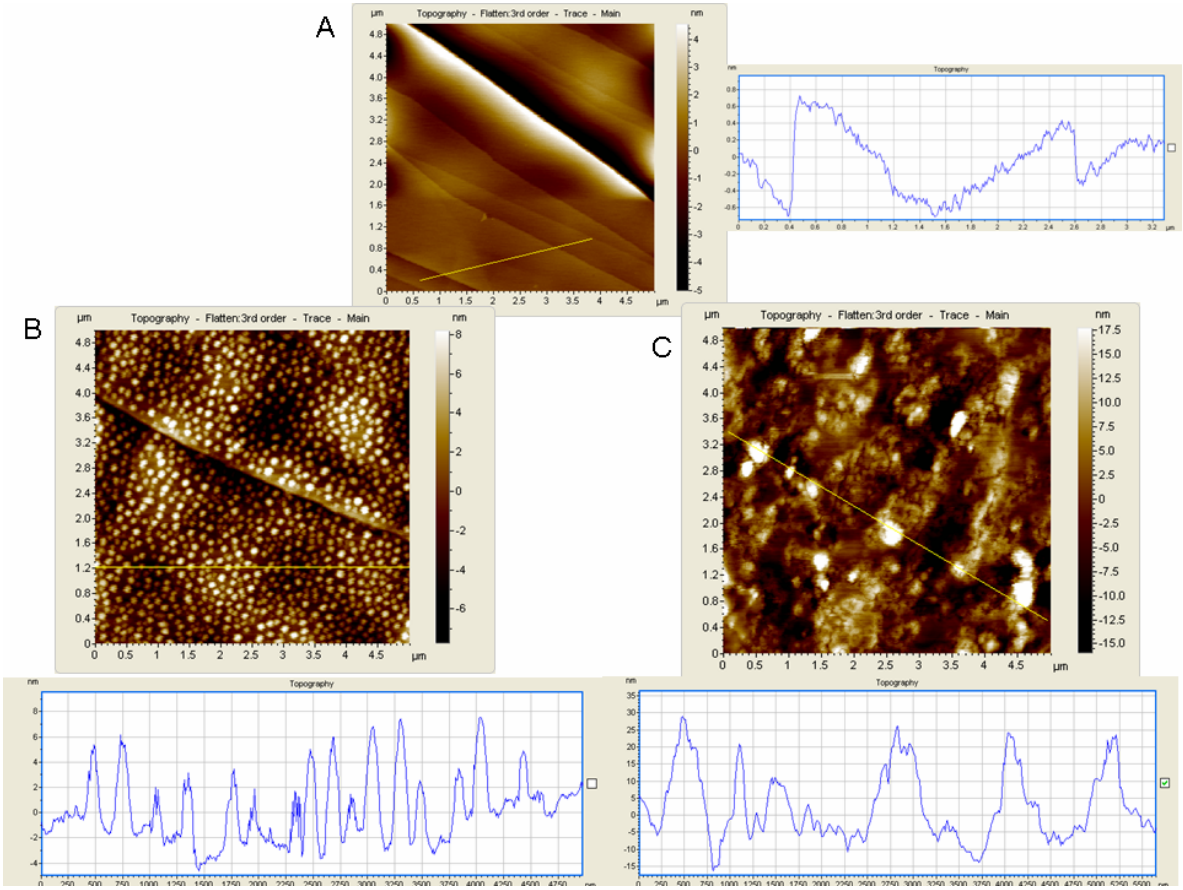

Figure S4. AFM images of A) HOPG, B) Fc-thiol on HOPG and c) DNA on HOPG

Chapter 3.

Postfunctionalisation of Keggin silicotungstates by general coupling procedures

Ahmed M. Debela, Mayreli Ortiz,Ciara K. O´Sullivan, Serge Thorimbert, Bernold Hasenknopf, Postfunctionalisation of Keggin silicotungstates by general coupling procedures *Polyhedron,* **2014,** 68,131-137

Postfunctionalisation of Keggin silicotungstates by general coupling procedures

Ahmed M. Debela,[a] Mayreli Ortiz,[a] Ciara K. O´Sullivan,[a,b] Serge Thorimbert,[c] Bernold Hasenknopf[c]

[a]Departament d'Enginyería Química, Universitat Rovira i Virgili, Avinguda Països Catalans, 26, 43007 Tarragona, Spain,

[b]ICREA, Passeig Lluis Companys 23, 08010 Barcelona, Spain, E-mail: ciara.osullivan@urv.cat

[c]UPMC Univ Paris 06, Institut Parisien de Chimie Moléculaire UMR CNRS 7071, 4 place Jussieu, 75252 Paris Cedex 05, France. E-mail: serge.thorimbert@upmc.fr, bernold.hasenknopf@upmc.fr

Abstract

Tetrabutyl ammonium (TBA) salts of organotin derivatives of polyoxometalates $(TBA)_5[SiW_{11}O_{39}\{Sn(CH_2)_2COOH\}]$ (**1**), $(TBA)_4[SiW_{11}O_{39}\{Sn(CH_2)_2CO\}]$ (**2**), $(TBA)_5[SiW_{11}O_{39}\{Sn(CH_2)_2CONH(CH_2)_3N_3\}]$ (**3**), $TBA_5[SiW_{11}O_{39}\{Sn(CH_2)_2CONH(CH_2)_3(N_3C_2H)C_{10}H_9Fe\}]$ (**4**) and an ammonium salt $(NH_4)_5[SiW_{11}O_{39}\{Sn(CH_2)_2CONH(CH_2)_3N_3\}]$(**3'**) have been synthesized for the first time by adapting the organic functionalisation strategies developed earlier for phosphotungstates. The products were characterised using FTIR, NMR, ESI MS, and electrochemical techniques. The Keggin silicotungstate is more nucleophilic than the Keggin phosphotungstate and displays reactivity previously known only for Dawson phosphotungstates. The methodology of CuAAC "click" reaction for silico- and phosphotungstates allows the coupling by a common protocol of diverse POMs with different redox properties, which is potentially useful for bioelectroanalytical applications with redox labels.

Introduction

Polyoxometalates (POM) are structurally well defined anionic metal oxygen clusters that exhibit great diversity in nuclearity, size, shape and electrochemical properties[1-6]. They are constructed from early transition metals M (mainly W, Mo or V) and oxygen, and often with a heteroatom (Si, P, Ge, etc). Although such compounds have been known for a very long time, their fascinating properties of high added value (tunable redox

properties, large size, high negative charges, photo and electrochromism[2], magnetism[3, 7, 8] and potential applications in various fields including catalysis[9] medicine [2, 4, 10-12] as well as material science [3,6] are the driving forces for the increasing attention they have garnered in the past decades.

Organic functionalisation of POMs occurs via either replacement of oxo ligands with different organic groups such as imido[13-16] or diazenido [17, 18] or the coupling of lacunary POMs with organosilyl/germyl[19-21] organo-phosphoryl/phosphonates [22-28] and organotin derivatives [29-37].
These covalent functionalisation strategies not only broaden the applications of POMs but also improve long-term stability, solubility, redox behavior, spectroscopic response and biological activities of the clusters as well as facilitating the construction of novel POM based functional materials[38-42].

About a decade ago, we started to systematically investigate the organic derivatisation of Keggin $[PW_{11}O_{39}\{SnR\}]^{4-}$ and Dawson $[P_2W_{17}O_{61}\{SnR\}]^{7-}$ phosphotungstates bearing organotin side chains R with reactive groups [43-48]. This approach corresponds to what is now called postfunctionalisation of POMs. In this context, it is highly desirable to have some standard reactions that can be applied to couple virtually any organic molecule to a POM. We have focused on amidation and CuAAC click chemistries that were applied to a broad range of organics. In order to diversify the inorganic moiety, we now investigated these reactions with $[SiW_{11}O_{39}\{SnR\}]^{5-}$ derivatives. This Keggin silicotungstate is smaller than our previous Dawson phosphotungstates, but with a higher charge than the $[PW_{11}O_{39}\{SnR\}]^{4-}$ analog. It would therefore be a valuable complementary compound for a number of applications; in particular those including POM based redox processes.

Pope prepared organotin derivatives of the monolacunary $[SiW_{11}O_{39}]^{8-}$, among those $Cs_5[SiW_{11}O_{39}\{Sn(CH_2)_2COOH\}]$ [36]. He also investigated some side chain reactivities (ester and nitrile hydrolysis), which demonstrated the hydrolytic stability of the POM-hybrid and he performed amide-coupling reactions on the organotin precursor. We show here the possibilities i) to prepare an intramolecularly activated mixed anhydride from $[SiW_{11}O_{39}\{Sn(CH_2)_2COOH\}]^{5-}$ that allows residue-free coupling with amines and ii) to perform CuAAC click chemistry on an azide derivative

$[SiW_{11}O_{39}\{Sn(CH_2)_2CONH(CH_2)_3N_3\}]^{5-}$. This type of reactions is important for introducing the silicotungstate as redox label in different applications.

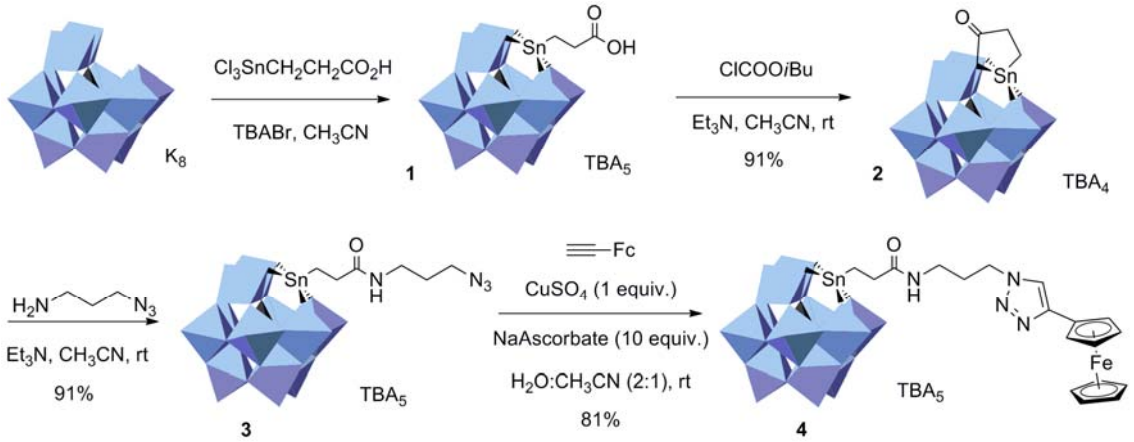

Scheme 3. 1. Schematic representation showing the stepwise functionalisation of $[\alpha\text{-}SiW_{11}O_{39}]^{8-}$

Experimental

Materials and instrumentations

All the chemical compounds and reagents were purchased from Sigma Aldrich and used without further purification. Acetonitrile was dried and distilled over CaH_2. All reactions were carried out under argon atmosphere with magnetic stirring. The monovacant Keggin POM $K_8[\alpha\text{-}SiW_{11}O_{39}]$ was prepared as previously described [49].

FT-IR spectra were recorded from a Bruker Tensor 27 ATR diamond PIKE spectrophotometer. The ^1H and ^{13}C NMR spectra were respectively recorded at 400 and 100 MHz with a Bruker AVANCE 400. Chemical shifts are reported in ppm from TMS using the residual ^1H and ^{13}C solvent peaks as internal reference (δ = 7.26 and 77.2 ppm, respectively, for $CDCl_3$, δ= 2.50 and 39.5 ppm for DMSO-d_6, δ = 1.94 and 118.26 ppm for CD_3CN).

Mass spectrometry was carried out using an ion trap type Bruker Esquire (R=3000) coupled to an electrospray source (ESI-MS) at the Paris Institute of Molecular Chemistry (IPCM). 50 µM POM solutions in CH_3CN were injected using a syringe pump with flow

rate 160 µL.min^{-1}. The detector was used in negative ion mode at a voltage of 3500V. The voltage difference between the orifice and the skimmer is set at 45 V to avoid decomposition of the POMs. The LMCO (low-mass cutoff) of the ion trap was set at 80-140 in order to preferentially trap ions of higher m/z ratio.

All electrochemical measurements were carried out using an Autolab model PGSTAT 12 potentiostat/galvanostat controlled with the General Purpose Electrochemical System (GPES) software (Eco Chemie B.V., The Netherlands). A classical three electrode set up was used with a Ag/AgCl reference electrode, Pt wire counter electrode and glassy carbon electrode (with inner diameter of 3 mm), which were purchased from CHI Instruments, Inc. All the potentials are recorded with respect to the reference electrode. the diffusion coefficient was calculated using Randeles –Sevcik equation[50] $Ip = 2.69 \times 10^5 AD^{1/2}Cn^{3/2}V^{1/2}$, where Ip is for the peak current of the voltammograms, A is the electrode surface area (cm2) D the diffusion coefficient, V is the scan rate (V s^{-1}), n the number of electrons.

Synthesis of $TBA_5[(SiW_{11}O_{39}\{SnCH_2CH_2CO_2H\}]$(**1**)*:* Trichloro propionic acid (0.587 mmol) was added to a solution of TBABr (4.06 mmol) in 30 mL of acetonitrile and the lacunary Keggin POM, $K_8SiW_{11}O_{39}$ (0.409 mmol) was subsequently added. The mixture was stirred for 1 h at room temperature under argon. After the reaction time was completed the remaining solid was filtered off. Evaporation of the solvent resulted in a pale yellow oily solid, which was precipitated with acetone/ethanol/diethyl ether (1/1/excess) to give the desired product as a white solid. (92% yield). IR: υ = 2962 (m), 2947 (w), 2885 (m), 1728 (w), 1481 (m), 1388 (w), 1010 (s), 964 (s), 902 (s), 771 (vs) cm^{-1}; ^{1}H NMR (400 MHz, CD_3CN): δ = 1.03 (t, *J* = 8 Hz, 60 H, $N(CH_2CH_2CH_2\mathit{CH_3})_4$), 1.26 (m, 2 H, $SnCH_2$), 1.39-1.51 (m, 40 H, $N(CH_2CH_2\mathit{CH_2}CH_3)_4$), 1.64-1.75 (m, 40 H, $N(CH_2\mathit{CH_2}CH_2CH_3)_4$), 2.69 (dd, *J* = 8.6, 7.1 Hz, 2 H, $CH_2C{=}O$), 3.12-3.30 (m, 40 H, $N(\mathit{CH_2}CH_2CH_2CH_3)_4$); ^{13}C NMR (100 MHz, CD_3CN): δ = 12.6 ($N(CH_2CH_2CH_2\mathit{CH_3})_4$), 17.5 ($SnCH_2$), 19.1 ($N(CH_2CH_2\mathit{CH_2}CH_3)_4$), 23.1 ($N(CH_2\mathit{CH_2}CH_2CH_3)_4$), 28.8 ($\mathit{CH_2}C{=}O$), 58.0 ($N(\mathit{CH_2}CH_2CH_2CH_3)_4$), 175.2 (C=O).

Synthesis of $TBA_4[SiW_{11}O_{39}\{Sn(CH_2)_2C(=O)\}]$(**2**)*:* To a solution of **1** in freshly distilled acetonitrile (25 mL) triethyl amine (2.2 equiv) and isobutyl chloroformate (1.2 equiv.) were added. The reaction mixture was stirred at room temperature overnight under

argon. A cation exchange resin (Amberlyst 15, 16-50 mesh, TBA^+ form) was then added followed by addition of 10 mL acetone and the mixture was stirred for 1 h under rotary. The resin was filtered off and the filtrate concentrated under vacuum. The oil obtained was dissolved in acetone (7 mL) and precipitated by addition of ethanol (7 mL) and diethyl ether (30 mL) and the white solid was centrifuged and dried using a vacuum pump. A white fluffy powder was obtained in 91% yield. IR: υ = 2962 (m), 2947 (w), 2877 (m), 1735 (w), 1473 (m), 1388(w), 1226 (w), 1010 (s), 964 (s), 902 (s), 771 (vs) cm^{-1}; ^{1}H NMR (400 MHz, CD_3CN): 1.01 (t, *J* = 8 Hz, 48 H, $N(CH_2CH_2CH_2\mathit{CH_3})_4$), 1.30-1.50 (m, 34 H, $N(CH_2CH_2\mathit{CH_2}CH_3)_4$ + $SnCH_2$), 1.60-1.77 (m, 32 H, $N(CH_2\mathit{CH_2}CH_2CH_3)_4$), 2.81 (m, 2H, $CH_2C{=}O$), 3.12-3.26 (m, 32 H, $N(\mathit{CH_2}CH_2CH_2CH_3)_4$); ^{13}C NMR (100 MHz, CD_3CN): δ = 12.6 ($N(CH_2CH_2CH_2\mathit{CH_3})_4$), 17.2 ($SnCH_2$), 19.1 ($N(CH_2CH_2\mathit{CH_2}CH_3)_4$), 23.1 ($N(CH_2\mathit{CH_2}CH_2CH_3)_4$), 30.8 ($\mathit{CH_2}C{=}O$), 57.8 ($N(\mathit{CH_2}CH_2CH_2CH_3)_4$), 168.7 (C=O).

Synthesis of $TBA_5[SiW_{11}O_{39}\{SnCH_2CH_2CONH(CH_2)_3N_3\}]$(**3**)*:* The product **2** was dissolved in 30 mL acetonitrile to which triethyl amine (1.2 equiv) and azidopropylamine (2 equiv) were added. The mixture was stirred at room temperature overnight. Cation exchange resin (Amberlyst 15, 16-50 mesh, TBA^+ form) was added followed by addition of 10 mL acetone and the mixture was stirred for 1 h under rotary. The resin was filtered off and the filtrate concentrated under vacuum. The oil obtained was dissolved in acetone (7 mL) and precipitated by addition of ethanol (7 mL) and diethyl ether (30 mL). The white solid was centrifuged and dried under vacuum (91% yield). IR: ν = 2962 (m), 2942 (w), 2877 (m), 2098 (m), 1658 (w), 1482 (m), 1380 (w), 1002 (s), 956 (s), 894 (s), 771 (vs) cm-1; ^{1}H NMR (400 MHz, CD_3CN): 0.98 (t, *J* = 8 Hz, 60 H, $N(CH_2CH_2CH_2\mathit{CH_3})_4$), 1.37-1.47 (m, 42 H, $N(CH_2CH_2\mathit{CH_2}CH_3)_4$ + $SnCH_2$), 1.61-1.69 (m, 40 H, $N(CH_2\mathit{CH_2}CH_2CH_3)_4$), 1.74-1.85 (m, 2 H, $CH_2\mathit{CH_2}CH_2$), 2.49 (t, *J* = 8 Hz, 2 H, $CH_2C{=}O$), 3.12-3.29 (m, 42 H, $N(\mathit{CH_2}CH_2CH_2CH_3)_4$ +$NH\mathit{CH_2}$), 3.39-3.42 (m, 2 H CH_2N_3), 7.01 (t, 1 H, *J* = 8 Hz, NH); ^{13}C NMR (50 MHz, CD_3CN + 5% D_2O; repurified on cation exchange resin): 12.7 ($N(CH_2CH_2CH_2\mathit{CH_3})_4$), 19.1 ($N(CH_2CH_2\mathit{CH_2}CH_3)_4$), 19.2 ($SnCH_2$), 23.2 ($N(CH_2\mathit{CH_2}CH_2CH_3)_4$), 28.3 ($CH_2\mathit{CH_2}CH_2$), 31.9 ($CH_2C{=}O$), 36.1 ($NHCH_2$), 48.8 ($CH_2N_3$), 57.8 ($\mathit{CH_2}CH_2CH_2CH_3)_4$), 174.0 (C=O).

Synthesis of $TBA_5[(SiW_{11}O_{39})\{Sn(CH_2)_2CONH(CH_2)_3(N_3C_2H)C_{10}H_9Fe\}]$(**4**)*:* To a solution of **3** (0.04 mmol) in acetonitrile (1 mL) was added ethynyl ferrocene (0.08 mmol, 2 equiv.). This was followed by subsequent addition of a solution of $CuSO_4{\cdot}5H_2O$ (0.04 mmol, 1

equiv) in water (1 mL) and a solution of sodium ascorbate (1.6 mmol, 40 equiv) in water (1 mL). The mixture was stirred at RT for 24 hours. A cation-exchange resin (Amberlyst 15, 16-50 mesh, TBA^+ form) was added, followed by acetone (10 mL) and the mixture was stirred for 1 hour or until the disappearance of the precipitate (if any appeared). The resin was filtered off and the filtrate was concentrated *in vacuo*. White powder residue was washed twice with water (10 mL) and isolated by centrifugation. After drying *in vacuo*, the residue was dissolved in acetone (2 mL) and precipitated by adding CH_2Cl_2/Et_2O (2 mL/30 mL). The new solid was isolated by centrifugation, washed with Et_2O and dried *in vacuo* and the desired POM was obtained as a white powder (81 % yield). IR: υ = 2968 (m), 2958 (w), 2879 (m), 1664 (w), 1485 (m), 1388 (w), 1108 (s), 1002, 952 (s), 902 (s), 887 (s), 781 (vs) cm-1; ^{1}H NMR (400 MHz, CD_3CN + 5% D_2O): δ = 1.00 (t, *J* = 8Hz, 60 H, $N(CH_2CH_2CH_2\mathit{CH_3})_4$), 1.07-1.17 (m, $SnCH_2$), 1.40-1.49 (m, 40 H, $N(CH_2CH_2\mathit{CH_2}CH_3)_4$), 1.64-1.72 (m, 40 H, $N(CH_2\mathit{CH_2}CH_2CH_3)_4$), 2.30 (m, 2 H, $CH_2\mathit{CH_2}CH_2$), 2.57 (m, 2 H, $\mathit{CH_2}C{=}O$), 3.15-3.28 (m, 42 H, $N(\mathit{CH_2}CH_2CH_2CH_3)_4$ + $NH\mathit{CH_2}$), 4.09 (s, 5H, C_5H_5Fe), 4.28 (s, 2H, C_2H_2Fe), 4.57 (m, 2H, CH_2N), 4.77 (s, 2 H, C_2H_2Fe), 7.56 (t, *J* = 4 Hz, 1H, NH), 8.30 (s, 1 H, C=CHN); ^{13}C NMR (50 MHz, CD_3CN + 5% D_2O): δ= 12.7 ($N(CH_2CH_2CH_2\mathit{CH_3})_4$), 19.1 ($N(CH_2CH_2\mathit{CH_2}CH_3)_4$), 19.2 ($SnCH_2$), 23.2 ($N(CH_2\mathit{CH_2}CH_2CH_3)_4$), 28.8 ($CH_2\mathit{CH_2}CH_2$), 32.0 ($CH_2CO$), 35.5 ($NH\mathit{CH_2}$), 47.3 ($CH_2\mathit{CH_2}N$), 58.0 ($N(\mathit{CH_2}CH_2CH_2CH_3)_4$), 66.3 ($C_2H_3Fe$), 67.8 ($C_2H_2Fe$), 69.2 ($C_5H_5Fe$), 76.5 ($\mathit{C}{=}CCFe$), 121.6 ($C{=}\mathit{CH}N$), 144.9 ($\mathit{C}{=}CHN$), 174.1 (C=O).

*Synthesis of $(NH_4)_5[SiW_{11}O_{39}\{SnCH_2CH_2CONH(CH_2)_3N_3\}]$(**3'**):* To a solution of **3** (0.025 mmol) in 1 mL of CH_3CN, a filtered solution of 51 mg (13 equiv.) of NH_4PF_6 in 0.5 mL of CH_3CN was added. A precipitate was formed instantly. The solid was then centrifuged, washed 3 times with 0.5-1 mL of acetonitrile and then once with 15 mL of diethyl ether and the solid was then dried under vacuum for several hours. (112 mg, 95 %). IR: υ = 2067 (m), 1641 (m), 1436 (m), 970 (s), 852 (s), 781 (vs) cm-1; ^{1}H NMR (400 MHz, D_2O): δ= 1.44 (t, *J* = 8 Hz, 2 H, $SnCH_2$), 1.80 (q, *J* = 8 Hz, 2 H, $CH_2\mathit{CH_2}CH_2$), 2.67 (t, *J* = 8 Hz, 2 H, $\mathit{CH_2}C{=}O$), 3.28 (t, *J* = 8 Hz, 2H, $NH\mathit{CH_2}CH_2$), 3.38 (t, *J* = 8 Hz,, 2H, CH_2N_3), 7.07 (s, very large, 1H, NH), ^{13}C NMR (50 MHz, D_2O): 18.9 ($SnCH_2$), 27.5 ($CH_2\mathit{CH_2}CH_2$), 31.0 ($\mathit{CH_2}C{=}O$) 36.9 ($NH\mathit{CH_2}$), 48.7 ($CH_2\mathit{CH_2}N$), 174.6 (C=O).

Results and dicussion

Synthesis of hybrids: We adapted our published procedure for the preparation of $[P_2W_{17}O_{61}\{Sn(CH_2)_2COOH\}]^{7-}$ [45] to obtain the tetrabutylammonium (TBA) salt $(TBA)_5[SiW_{11}O_{39}\{Sn(CH_2)_2COOH\}]$ (**1**) by reacting $K_8[SiW_{11}O_{39}]$ with $Cl_3Sn(CH_2)_2COOH$ in acetonitrile in the presence of TBABr. The carboxylic function of organically soluble POM **1,** was then activated in the presence of isobutyl chloroformate and triethylamine in CH_3CN. It results in the clean formation of the mono-oxo acylated silico polyoxotungstate $[SiW_{11}O_{39}\{Sn(CH_2)_2CO)\}]^{8-}$ (**2**) which was isolated by precipitation in 91% yield (Scheme 1).

Such intramolecular cyclization was performed earlier with Dawson phosphotungstates, but not with the Keggin phosphotungstate[45]. The possible cyclization of the hybrid SiW_{11} Keggin POM compared to the inertness of the corresponding PW_{11} may be attributed to the higher overall negative charge of the former, which globally leads to an increase of the nucleophilicity of the oxygen atoms. The oxo ligands bound to the Sn atom are the most nucleophilic[45, 47] and presumably are involved in the formation of this intramolecular mixed anhydride between the carboxylic acid and the heteropolyacid.

The subsequent coupling of **2** with a slight excess of aminopropyl azide delivered in good yield, after precipitation and cation exchange, the expected azido derivative $TBA_5[SiW_{11}O_{39}\{Sn(CH_2)_2CONH(CH_2)_3N_3\}]$ (**3**) required for further Huisgen 1,3 cycloaddition. Following our recent report on the utilisation of this cycloaddition reaction for POM functionalisations[46] compound **3** was coupled with ethynyl ferrocene, in the presence of $CuSO_4$ (1 equiv.) and sodium ascorbate (10 equiv.) in aqueous-acetonitrile (2:1) solution, giving the POM-ferrocenyl hybrid **4** $(TBA_5[(SiW_{11}O_{39})\{Sn(CH_2)_2CONH(CH_2)_3(N_3C_2H)Fc\}])$ in 81% yield**.**

NMR Analysis of hybrids **1** and **2:** The success of the organic modifications of the Keggin POM have been followed by NMR analysis. Indeed, the ^1H and ^{13}C NMR spectra exhibit signals from the organic part and tetrabutylammonium (TBA) (see Supplementary Information). A detailed analysis of the ^1H spectra of **1** and **2** supports the internal cyclization upon activation of the carboxyl group. Indeed the signal attributed to methylene protons next to the carbonyl group significantly differed in their multiplicity (Figure 1). In acyclic **1**, both protons of $COCH_2$ are chemically equivalent and appear as a

triplet, centered at 2.69 ppm, by coupling with the vicinal CH_2 (Figure 3. 1, left). After activation, the rigidity of the cyclic structure breaks the chemical equivalence of the geminal protons and the signal attributed to the $COCH_2$ appears as a multiplet centered at 2.81 ppm (Figure 3. 1, right).

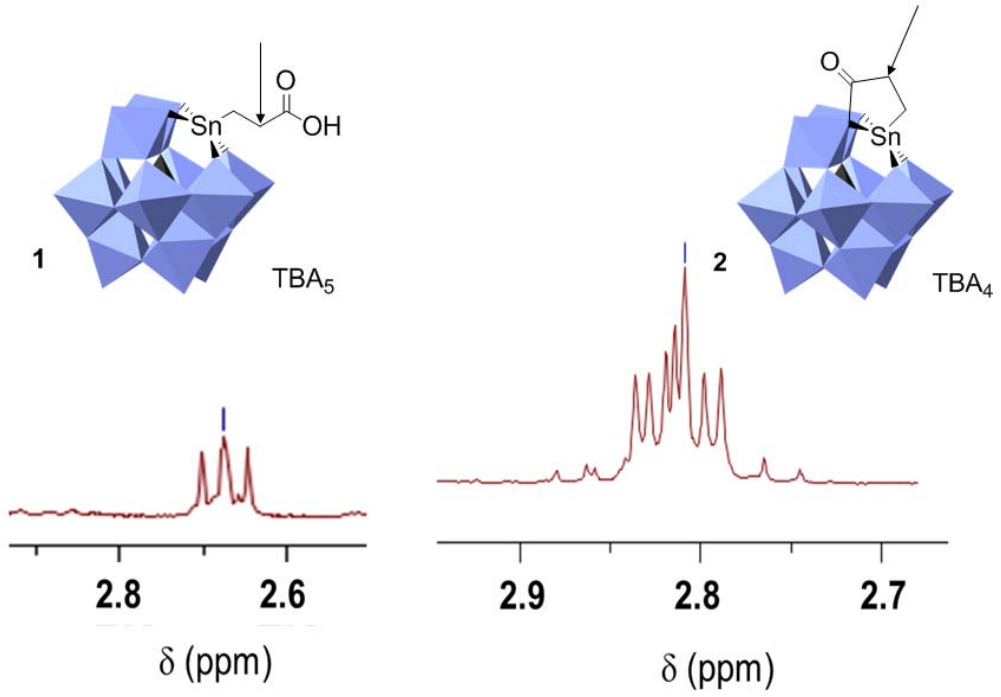

Figure 3. 1. Comparison of the α carbonyl protons signals in compound 1 (left) and 2 (right).

NMR Analysis $TBA_5[SiW_{11}O_{39}\{Sn(CH_2)_2CONH(CH_2)_3N_3\}]$ *(3):* The ^{1}H NMR spectrum of 3 (Figure 2) shows the characteristic signal that confirms amide formation through the signals at 7.05 ppm attributed to the s-*cis* and s-*trans* amide proton (NH). In addition to this, four of the six protons of the aminopropyl group appear at 3.45 ppm (a triplet for the methylene group adjacent to the azide) and a multiplet at 1.7 ppm respectively. However, the third methylene group appears at 3.1 ppm masked by the signal of the TBA protons. While after amide coupling the organic arm of the hybrid POM finds again free rotation, the signal for the methylene group adjacent to the carbonyl group ($\delta = 2.5$ ppm) becomes a triplet with again the presence of the signals attributed to the s-*cis* and s-*trans* conformations. The ^{13}C NMR spectrum (see SI) shows six signals corresponding to the organic moiety in addition to the intense signals for tetrabutyl ammonium.

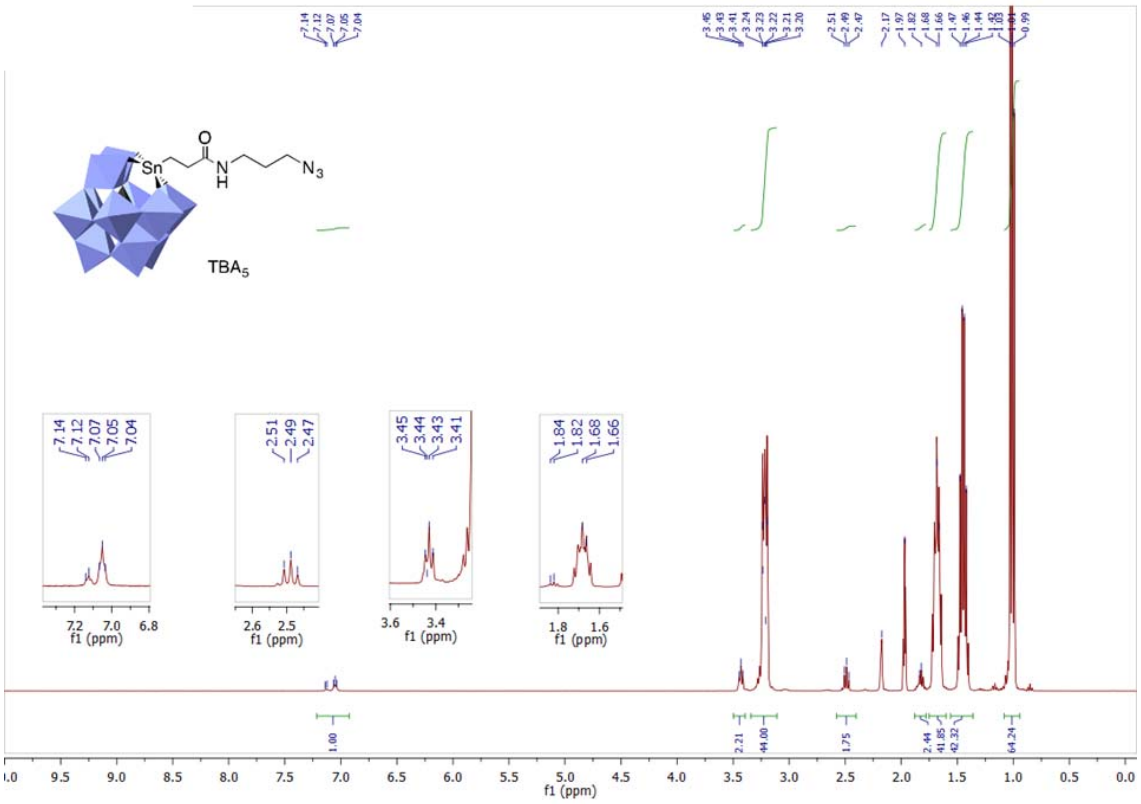

Figure 3.2. The ^{1}H NMR spectra of *$TBA_5[SiW_{11}O_{39}\{Sn(CH_2)_2CONH(CH_2)_3N_3\}]$(3)* in CD_3CN.

NMR Analysis of $TBA_5[SiW_{11}O_{39}\{Sn(CH_2)_2CONH(CH_2)_3(N_3C_2H)Fc\}]$(4): The ^{1}H NMR spectrum of **4** confirmed the success of the 1,3-dipolar cycloaddition reaction. The presence of the olefinic proton of the triazole ring (δ = 8.30 ppm) was a good indicator. In addition to this, the protons of the ferrocenyl group are also present as a singlet at δ = 4.09 ppm integrating for 5H (C_5H_5Fe) and two symmetric triplets at δ = 4.28 and δ = 4.77 for 2 × 2H (C_5H_4Fe), (see SI). Moreover, the ^{13}C NMR shows 11 signals corresponding to the ferrocenyl functionalised POM in addition to the four intense signals for the tetrabutyl ammonium counter ion (see SI).

Electrospray mass spectrometry

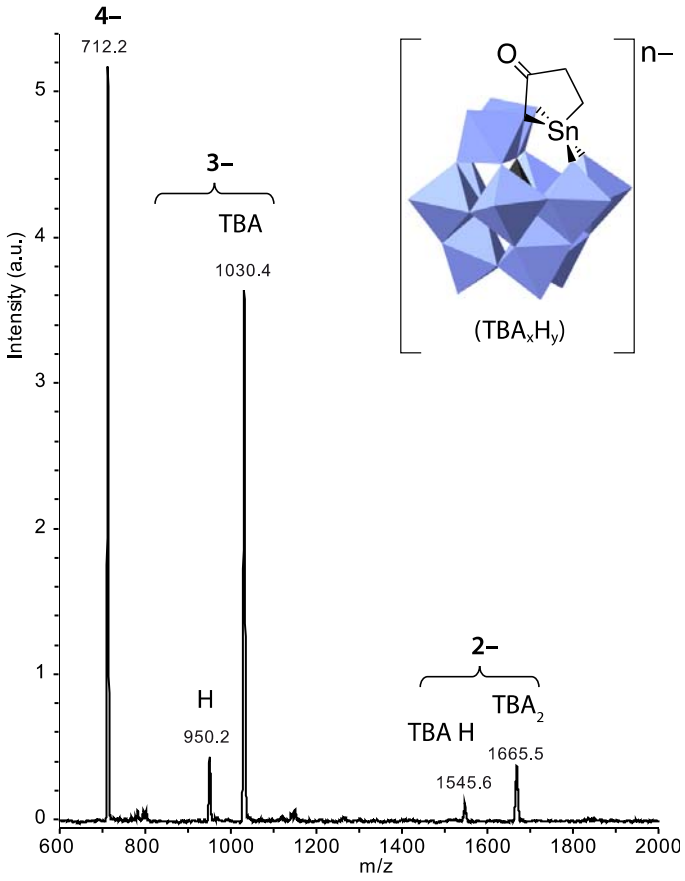

Figure 3.3 Negative mode ESI MS spectrum of compound 2 at concentration of 50 μM in acetonitrile. The m/z, cation composition and total charge are given above each signal.

Only peaks corresponding to the expected POMs were observed by electrospray ionization mass spectrometry (ESI MS), proving the successful functionalization. As an example, Figure 3.3 displays the spectrum of the activated complex 2 (see SI for other compounds). The signals can be assigned to the POM 2 associated with different numbers of TBA or H^+ cations and charge-states 2–, 3– and 4–. One must note that no other species is present, in particular no POM carboxylic acid 1 (which has strong signals at m/z 716.3 and m/z 1036.2). This is again clear evidence that the intramolecular activation is successful and the mixed anhydride is isolated.

IR Analysis: The characteristic IR bands of the Keggin silicotungstate[51-53] **1** in the region 700-1100 cm^{-1} were also observed for POMs **2**, **3**, and **4** (Figure 3. 4). This similarity proves

the intact POM framework. One could observe additional peaks corresponding to the TBA cations (around 1480 and 1380 cm^{-1}) as well some belonging to the covalently linked organic part. Of particular interest are the band at 2050 cm^{-1} specific to the azide group in the spectrum of **3**, and the bands at 1728 cm^{-1} (**1**), 1735 cm^{-1} (**2**), 1658 cm^{-1} (**3**), and 1664 cm^{-1} (**4**) attributed to the carbonyl groups.

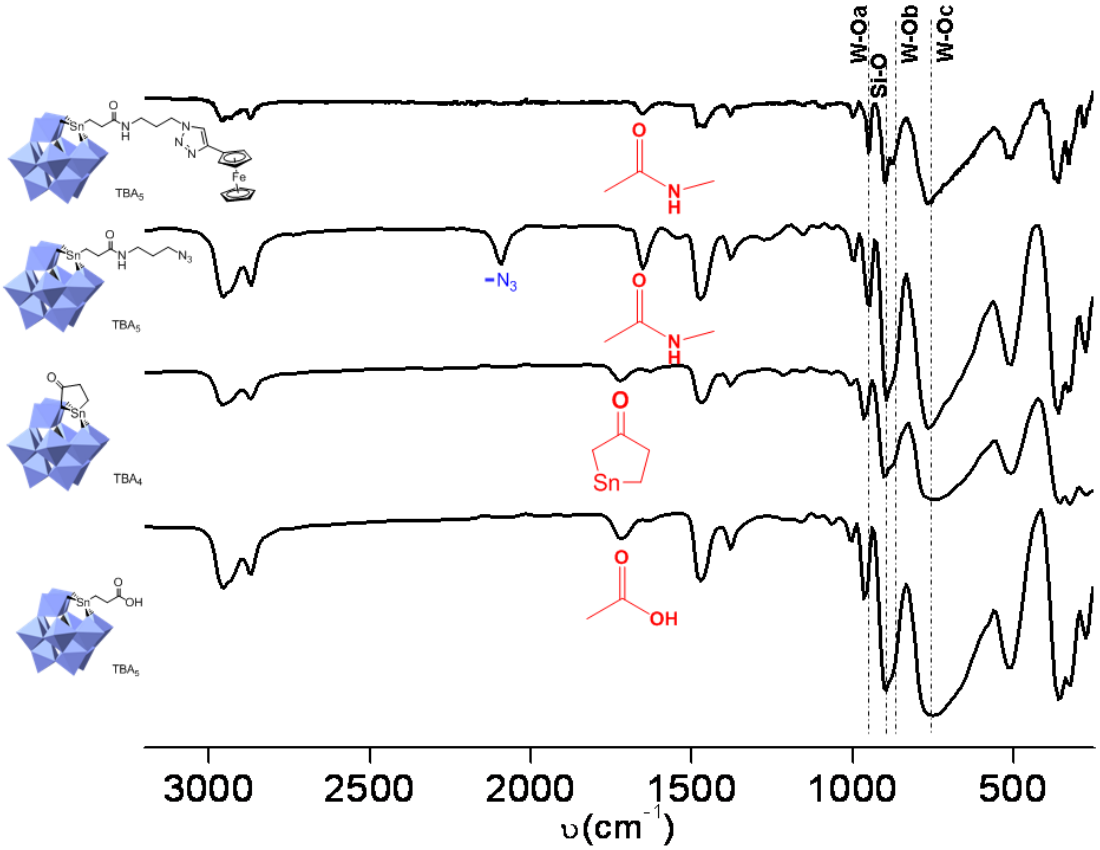

Figure 3. 4. FT-IR spectra of functionalised Keggin silicotungstates 1-4.

Electrochemical characterisation: One of our ultimate goals is to use functionalised POMs in bioelectroanalytical applications. It is therefore important to have compounds with multiple well separated and reversible redox processes.

Figure 3. 5. shows the cyclic voltammogram of the POM-Fc complex **4** in acetonitrile, where four redox processes between +1 and –2.5 V vs. Ag/AgCl, can be observed (Table 1). The signal at +0.32 V corresponds to the ferrocene moiety (+0.375 V for native ferrocene), the remaining signals are assigned to the tungsten (VI/V) redox processes. The equivalent peak current of the ferrocene based process and the tungsten processes in the differential pulse voltammogram (DPV, see SI) indicates that all processes are monoelectronic.

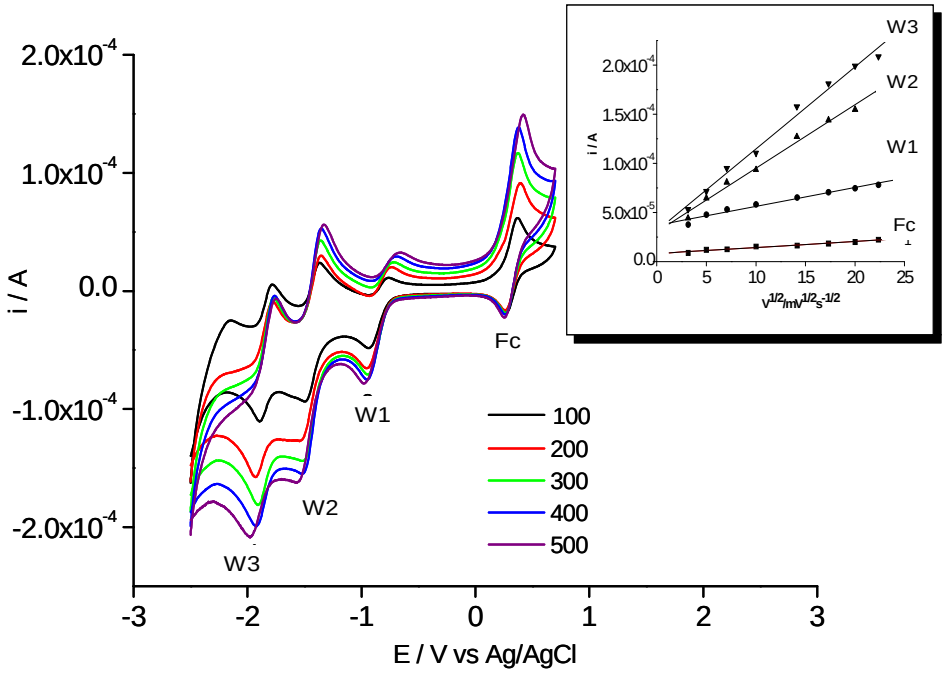

Figure 3. 5. CV of ferrocene functionalised Keggin silicotunstate (4) in acetonitrile and 0.1M $TBAPF_6$. The inset is a plot of I_{pc} versus square root of scan rate in mV/s.

Table 3. 1. The electrochemical data extracted from the cyclic voltammograms of the functionalised POMs[a]

Compound	Redox process	E_{pa}(V)	E_{pc}(V)	$E_{1/2}^{*}$(V)	ΔE_{p}^{*}(V)
1	W1	-0.78	-0.90	-0.84	0.12
	W2	-1.50	-1.55	-1.52	0.05
	W3	-1.90	-1.97	-1.93	0.07
2	W1	-0.77	-0.88	-0.83	0.11
	W2	-1.39	-1.47	-1.43	0.07
	W3	-1.81	-1.88	-1.85	0.07
3	W1	-0.78	-0.89	-0.83	0.11
	W2	-1.40	-1.47	-1.43	0.06
	W3	-1.82	-1.89	-1.85	0.07
4	Fe	0.36	0.29	0.30	0.06
	W1	-0.79	-0.90	-0.84	0.12
	W2	-1.41	-1.46	-1.44	0.04
	W3	-1.83	-1.88	-1.85	0.04

[a] 1 mM solution of the POMs in acetonitrile and $TBAPF_6$ as supporting electrolyte, scan rate 50 mV/s. * $E_{1/2}=(E_{pc}+E_{pa})/2$; $\Delta E=(E_{pa}-E_{pc})$; E_{pc} and E_{pa} are cathodic and anodic peak-potentials.

The analysis of peak current as a function of different scan rates also reveals the structural stability of the organic hybrid during all the electrochemical redox processes. The plots of the cathodic peak currents (I_{pc}) versus the square root of the scan rate gave a practically straight line (Figure 5 inset) indicating a diffusion-controlled process with a diffusion constant of 1.719×10^{-9} $cm^2\cdot s^{-1}$. This very low D value compared to unmodified ferrocene is due to the higher molecular weight of the hybrid molecules synthesised, [54] and proves again the covalent functionalisation.

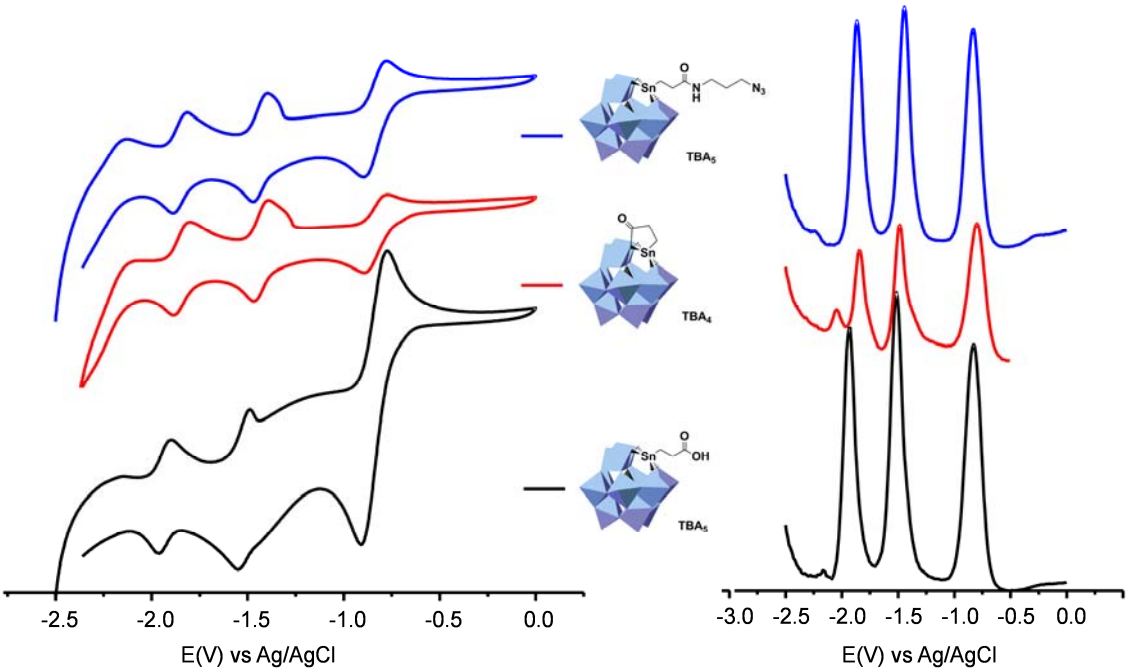

Figure 3. 6. Cyclic voltammograms (left) and differential pulse voltammograms (right) of the functionalised Keggin POMs in acetonitrile, at glassy carbon electrodes, 1 mM POM, 0.1 M $TBAPF_6$.

Similar results have been obtained for POMs 1-3. Figure 6 displays the CV together with the DPV measurements. The symmetric shape of the DPV signals confirms once more the reversibility of the electron transfer. Table 1 lists the peak potentials E_{pa}, E_{pc}, the half-way potential $E_{1/2}$ and the peak-to-peak separation ΔE_p for all these compounds. The three signals are assigned to the successive one-electron reductions of W^{VI} centers. As shown in Table 1, ΔE_p are close to the values expected for a reversible process (50-60 mV) except for the first process. The values (100-120 mV) are slightly higher indicating a slower electron transfer process.

POM-azido compound **3** appears as a useful redox label for biological molecules. For that purpose, it would be used in aqueous solution. As it is well known in POM chemistry that the redox processes depend strongly on the solvent and the protonation state, we converted the TBA salt **3** into the NH_4^+ salt **3'** by metathesis with NH_4PF_6. NMR (^1H, ^{13}C) and FT-IR analysis showed that the intact hybrid POM was maintained (see SI for details). This salt was studied in aqueous solution containing sodium perchlorate and perchloric acid at pH 3.2. Figure 3. 7 shows two equivalent waves for the reductions of tungsten at $E_{1/2}$ –0.64 and –0.85 V vs Ag/AgCl. A third peak at –0.53 V appears very small

and can be considered as an impurity. These results confirm those obtained by Pope et al. for $[SiW_{11}O_{39}Sn(CH_2)_2COOH]^{5-}$ (–0.647 and –0.830 V vs Ag/AgCl at pH 2.9).[36] They are also in line with other metal substituted silicotungstates $[SiW_{11}O_{39}M(H_2O)]^{n-}$ (M = $Co^{II/III}$, Ni^{II}, Fe^{III}, Cr^{III}) [55,56] and organotin substituted Keggin tungstates $[XSiW_{11}SnC_6H_5]^{n-}$ (X = Zn^{II}, Co^{II}) [57]. In accordance with Pope et al [36], and in contrast to Liu et al [57], we observed only the two W(VI/V) redox processes, and no tin based reduction. The reductions are accompanied by protonation, and therefore going to more negative values with increasing pH, as it is usual for POM based processes [58].

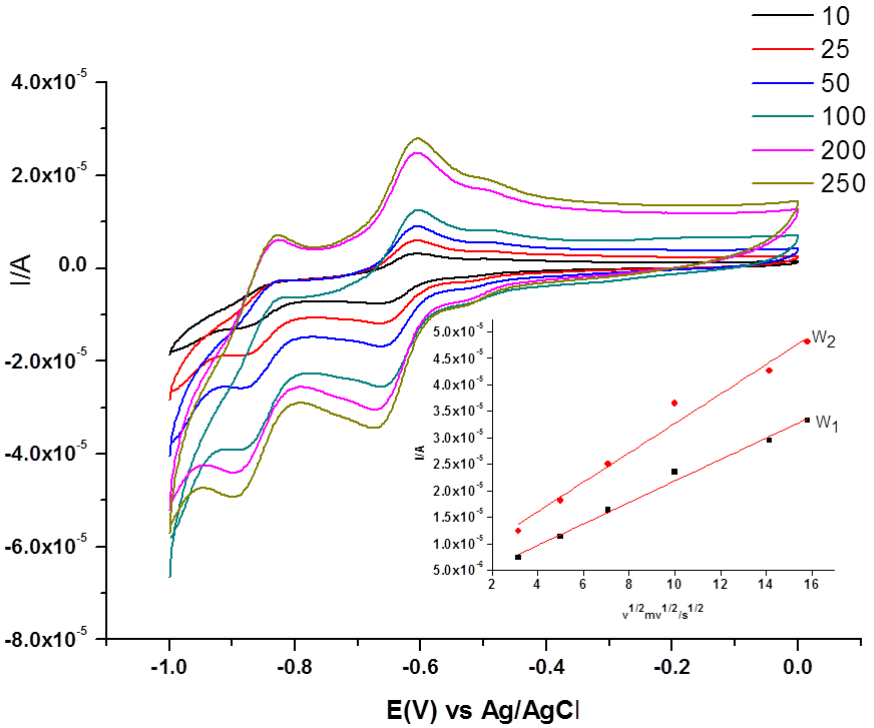

Figure 3. 7. Cyclic voltammograms with different scan rates of 0.8 mM (NH4)5[SiW11O39{SnCH2CH2C(=O) NH(CH2)3N3}] (3') obtained in 10 mM HClO4, 0.1 M NaClO4 at pH 3.2. The inset is a plot of Ipc versus square root of scan rate in mV/s.

Conclusions

In the work reported here, we have functionalised monolacunary Keggin silicotungstate $[SiW_{11}O_{39}]^{8-}$ to obtain stable organotin hybrids and characterised them using various analytical techniques. Organic coupling reactions were successfully adapted from previous work with phosphotungstates. As a result, silico- and phosphotungstates together represent now a family of POMs with different electrochemical properties, but a common coupling methodology. Thus, they are potentially suited for use as specific

redox labels in bioanalytical applications. Work along this line will be reported in due course.

Acknowledgement

All authors would like to acknowledge "Universitat Rovira i Virgili (Tarragona Spain), Université Pierre et Marie Curie (Paris, France) for research facilities. AMD acknowledges "Generalitat de Catalunya" for mobility grant awarded for the stay at IPCM, UPMC, Paris, France.

References

1. M.T. Pope, A. Müller, Polyoxometalate Chemistry: An Old Field with New Dimensions in Several Disciplines, *Angew. Chem. Int. Ed.* **1991**, 30, 34-48.
2. C. L. Hill, Special issue on polyoxometalates, *Chem. Rev.* **1998**, 98,1-390.
3. L. Cronin and A. Müller, Special issue on polyoxometalates, *Chem. Soc. Rev.*, **2012**, 41, 7325-7648.
4. K. Hindson, U. Kortz and T. Liu, Special issue on polyoxometalates, *Eur. J. Inorg. Chem*, **2013**,1556–1967.
5. A. Dolbecq, E. Dumas, C. R. Mayer, P. Mialane, Hybrid Organic–Inorganic Polyoxometalate Compounds: From Structural Diversity to Applications, *Chem. Rev.* **2010,**110, 6009-6048.
6. D.L. Long, E. Burkholder, L. Cronin, Polyoxometalate clusters, nanostructures and materials: From self assembly to designer materials and devices, *Chem. Soc. Rev.* **2007,** 36, 105-112.
7. P. Kögerler, B. Tsukerblat, A. Müller, Structure-related frustrated magnetism of nanosized polyoxometalates: aesthetics and properties in harmony, *Dalton Trans.*, 2010, 39, 21-36.
8. U. Kortz, A. Müller, J. van Slageren, J. Schnack, N. S. Dalal, M. Dressel, olyoxometalates: Fascinating Structures, Unique Magnetic Properties, *Coord. Chem. Rev.* **2009**, 253, 2315-2327.
9. R. Neumann, Activation of Molecular Oxygen, Polyoxometalates, and Liquid-Phase Catalytic Oxidation, *Inorg. Chem*. **2010**, 49, 3594-3601.

10. B. Hasenknopf, Polyoxometalates: introduction to a class of inorganic compounds and their biomedical applications, *Front. Biosci.,* 2005, 10, 275-287.
11. M. Aureliano, D. C. Crans, Decavanadate ($V_{10}O_6^{28-}$) and oxovanadates: Oxometalates with many biological activities, *J. Inorg. Biochem.* **2009**,103, 536-546.
12. L. Wang, B-B. Zhou, K. Yu, Z.-H. Su, S. Gao, L.-L. Chu, J.-R. Liu, G.-Y. Yang, Novel Antitumor Agent, Trilacunary Keggin-Type Tungstobismuthate, Inhibits Proliferation and Induces Apoptosis in Human Gastric Cancer SGC-7901 Cells, *Inorg. Chem.* **2013**, 52,5119-5127.
13. Z. Peng, Rational Synthesis of Covalently Bonded Organic–Inorganic Hybrids *Angew. Chem. Int. Ed.* **2004**, 43, 930-935.
14. J. L. Stark, A. L. Rheingold, E. A. Maatta, Polyoxometalate clusters as building blocks: preparation and structure of bis(hexamolybdate) complexes covalently bridged by organodiimido ligands, *J. Chem. Soc. Chem. Commun.* **1995**,1165-1166.
15. M. Lu, Y. Wei, B. Xu, C.F.C. Cheung, Z. Peng, D. R. Powell, Hybrid Molecular Dumbbells: Bridging Polyoxometalate Clusters with an Organic π-Conjugated Rod, *Angew. Chem. Int. Ed.* **2002**, 41,1566-1568.
16. J. Zhang, F. Xiao, J. Hao, Y. Wei, The chemistry of organoimido derivatives of polyoxometalates, *Dalton Trans.* **2012**, 41, 3599-3615.
17. C. Bustos, D. Mac-Leod Carey, K. Boubekeur, R. Thouvenot, A. Proust, P. Gouzerh, Aryldiazenido derivatives: A new entry to the functionalization of Keggin polyoxometalates, *Inorg. Chim. Acta* **2010**, 363, 4262-4268.
18. C. Bustos, B. Hasenknopf, R. Thouvenot, J. Vaissermann, A. Proust, P. Gouzerh, Lindqvist-Type (Aryldiazenido)polyoxomolybdates – Synthesis, and Structural and Spectroscopic Characterization of Compounds of the Type $(nBu_4N)_3[Mo_6O_{18}(N_2Ar)]$, *Eur. J. Inorg. Chem.* **2003,** 2757-2766.
19. K. Nomiya, Y. Togashi, Y. Kasahara, S. Aoki, H. Seki, M. Noguchi, S. Yoshida, Synthesis and Structure of Dawson Polyoxometalate-Based, Multifunctional, Inorganic–Organic Hybrid Compounds: Organogermyl Complexes with One Terminal Functional Group and Organosilyl Analogues with Two Terminal Functional Groups, *Inorg. Chem.* **2011**, 50, 9606-9619.
20. N. Joo, S. Renaudineau, G. Delapierre, G. Bidan, L.-M. Chamoreau, R. Thouvenot, P. Gouzerh, A. Proust, Organosilyl/germyl polyoxotungstate hybrids for covalent grafting onto silicon surfaces : towards molecular memories,*Chem. Eur. J.* **2010**,16, 5043-5051.

21. B. Matt; S. Renaudineau; LM. Chamoreau; C. Afonso; G. Izzet, A. Proust, Hybrid Polyoxometalates : Keggin and Dawson Silyl Derivatives as Versatile Platforms, *J. Org. Chem.* **2011**,76, 3107-3112.
22. C. R Mayer, C. Roch-Marchal, H. Lavanant, R. Thouvenot, N. Sellier, J.-C. Blais, F. Sécheresse, New Organosilyl Derivatives of the Dawson Polyoxometalate [α_2-$P_2W_{17}O_{61}(RSi)_2O]^{6-}$: Synthesis and Mass Spectrometric Investigation, *Chem. Eur. J.* **2004**,10, 5517-5523.
23. G. S. Kim, K. S. Hagen, C. L. Hill, Synthesis, structure, spectroscopic properties, and hydrolytic chemistry of organophosphonoyl polyoxotungstates of formula $[C_6H_5P(O)]_2X^{n+}W_{11}O_{39}^{(8-n)-}$ ($X^{n+} = P^{5+}, Si^{4+}$), *Inorg. Chem.* **1992,** 31, 5316-5324.
24. U. Kortz, M.T. Pope, Polyoxometalate-Diphosphate Complexes. 4. Structure of $Na_4[(O_3PCHN(CH_3)_2PO_3)W_2O_6]$.cntdot.11$H_2O$, *Inorg. Chem.* **1995**, 34, 3848-3850.
25. C. R. Mayer, M. Hervé, H. Lavanant, J.-C. Blais, F. Sécheresse, Hybrid Cyclic Dimers of Divacant Heteropolyanions: Synthesis, Mass Spectrometry (MALDI-TOF and ESI-MS) and NMR Multinuclear Characterisation, *Eur. J. Inorg. Chem.* **2004**,5, 973-977.
26. C. R. Mayer, P. Herson, R. Thouvenot, Organic–Inorganic Hybrids Based on Polyoxometalates. 5.1 Synthesis and Structural Characterization of Bis(organophosphoryl)decatungstosilicates $[\gamma\text{-}SiW_{10}O_{36}((RPO)_2]^{4-}$, *Inorg. Chem.* **1999,** 38, 6152-6158.
27. C. R. Mayer, R. Thouvenot, Organophosphoryl derivatives of trivacant tungstophosphates of general formula α-A-$[PW_9O_{34}(RPO)_2]^{5-}$: synthesis and structure determination by multinuclear magnetic resonance spectroscopy (^{31}P, ^{183}W) , *J. Chem. Soc. Dalton.Trans.* **1998,** 7-14.
28. R. Villanneau, D. Racimor, E. Messner-Henning, H. Rousselière, S. Picart, R. Thouvenot, A. Proust, Insights into the Coordination Chemistry of Phosphonate Derivatives of Heteropolyoxotungstates, *Inorg. Chem.* **2011**, 50,1164-1166.
29. S. Reinoso, M. H. Dickman, A. Praetorius, L. F. Piedra-Garza, U. Kortz, Phenyltin-Substituted 9-Tungstogermanate and Comparison with its Tungstosilicate Analogue *Inorg. Chem*. **2008**, 47, 8798-8806
30. L. F. Piedra-Garza, S. Reinoso, M. H. Dickman, M. M. Sanguineti, U. Kortz, The first 3-dimensional assemblies of organotin-functionalized polyanions *Dalton Trans.* **2009**, 38, 6231-6234.
31. H. Reuter, M. Izaaryene, Monoorganotin–polyoxometal-compounds. Part IV: Na2$[(iPrSn_3)(OV)_4O_{10}(OH)_3]\cdot 5H_2O\cdot 3$DMSO, a novel branched tetravanadate(V)

stabilized by a trimeric monoorganotin-oxo-hydroxo unit, *Inorg. Chim. Acta* **2010,** 363, 4277-4281.

32. L.-C. Zhang, S.-L. Zheng, H. Xue, Z.-M. Zhu, W.-S. You, Y.-G. Li, E. Wang, New tetra (organotin)-decorated boat-like polyoxometalate, *Dalton Trans.,* **2010**, 39, 3369-3371.
33. R. Cao, K. P. O'Halloran, D. A. Hillesheim, S. Lense, K. I. Hardcastle, C. L. Hill, Controlled synthesis of a functionalized polytungstate ligand and a $\{M_aM_bM_c(PW_9)2\}$ sandwich complex, *CrystEngComm* **2011,**13, 738-740.
34. L. F. Piedra-Garza, M. Barsukova-Stuckart, B. S. Bassil, R. Al-Oweini, U. Kortz, Diethyltin-Containing Tungstoarsenate (V), $[\{Sn(C_2H_5)_2\}_3(H_2O)_6(A\text{–}\alpha\text{–}As^VW_9O_{34})]^{3-}$, *J. Cluster Sci.* **2012**, 23, 939-951.
35. H. Liu, N. A. G. Bandeira, V. Felix, M. J. Calhorda, Tris(organotin)tungstogermanate, a Sandwich Organometallic Derivative of a Keggin-Type Polyoxometalate: Synthesis and DFT Study, *Eur. J. Inorg. Chem.* **2013**, 1713-1719.
36. G. Sazani, M. T. Pope, Organotin and organogermanium linkers for simple, direct functionalization of polyoxotungstates, *Dalton Trans.* **2004,**1989-1994.
37. I. Bar-Nahum, J. Ettedgui, L. Konstantinovski, V. Kogan, R. Neumann, A New Method for the Synthesis of Organopolyoxometalate Hybrid Compounds, *Inorg. Chem*. **2007**, 46, 5798-5804.
38. C. P. Pradeep, M. F. Misdrahi, F.-Y. Li, J. Zhang, L. Xu, D. L. Long, T. Liu, L. Cronin, Synthesis of Modular "Inorganic–Organic–Inorganic" Polyoxometalates and Their Assembly into Vesicles, *Angew. Chem. Int. Ed.* **2009**, 48, 8309-8313.
39. A. Proust, B. Matt, R. Villanneau, G. Guillemot, P. Gouzerh , G. Izzet, Functionalization and post-functionalization: a step towards polyoxometalate-based materials, Chem. Soc. Rev**. 2012**, 41, 7605-7622.
40. D. Li, P. Yin, T. Liu, Supramolecular architectures assembled from amphiphilic hybrid polyoxometalates, *Dalton Trans*. **2012**, 41, 2853-2861.
41. S. Thorimbert, B. Hasenknopf, E. Lacôte, Cross-Linking Organic and Polyoxometalate Chemistries, *Isr. J. Chem*. **2011**, 51, 275-280.
42. Y. Zhu, LS. Wang, J. Hao, ZC. Xiao, YG. Wei, Y. Wang, Synthetic, Structural, Spectroscopic, Electrochemical Studies and Self-assembly of Nanoscale Polyoxometalate–Organic Hybrid Molecular Dumbbells, *Cryst. Growth Des.*, **2009,** 9, 3509-3518.

43. S. Bareyt, S. Piligkos, B. Hasenknopf, P. Gouzerh, E. Lacôte, S. Thorimbert, M. Malacria, Highly Efficient Peptide Bond Formation to Functionalized Wells-Dawson-Type Polyoxotungstates, *Angew. Chem., Int. Ed.* **2003**, 42, 3404-3406.
44. S. Bareyt, S. Piligkos, B. Hasenknopf, P. Gouzerh, E. Lacôte, S. Thorimbert, M. Malacria, Efficient preparation of functionalized hybrid organic/inorganic Wells-Dawson-type polyoxotungstates, *J. Am. Chem. Soc.* **2005**, 127, 6788-6794.
45. C. Boglio, K. Micoine, E. Derat, R. Thouvenot, B. Hasenknopf, S. Thorimbert, E. Lacôte, M. Malacria, Regioselective Activation of Oxo Ligands in Functionalized Dawson Polyoxotungstates, *J. Am. Chem. Soc.* **2008**,130, 4553-4561.
46. K. Micoine, B. Hasenknopf, S. Thorimbert, E. Lacôte, M. Malacria, A General Strategy for Ligation of Organic and Biological Molecules to Dawson and Keggin Polyoxotungstates, *Org. Lett.* **2007**, 9, 3981-3984.
47. K. Micoine, M. Malacria, E. Lacôte, S. Thorimbert, B. Hasenknopf, Regioselective Double Organic Functionalization of Polyoxotungstates through Electrophilic Addition of Aromatic Isocyanates to $[P_2W_{17}O_{61}(SnR)]^{7-}$, *Eur. J. Inorg. Chem* **2013**, 1737-1741.
48. J. Rieger, T. Antoun, S. H. Lee, M. Chenal, G. Pembouong, J. Lesage de la Haye, I. Azcarate, B. Hasenknopf, E. Lacôte, Synthesis and Characterization of a Thermoresponsive Polyoxometalate–Polymer Hybrid, *Chem. Eur. J.* , **2012**,18,3355-3361.
49. A. Tézé, G. Hervé, R. G. Finke, D. K. Lyon, *Inorg. Synth*. **1990,** 27, 85-96.
50. J. Wang, Analytical Electrochemistry, Chapter 2, John Wiley & Sons **2000**
51. R. Thouvenot, M. Fournier, R. Franck, C. Rocchiccioli-Deltcheff, Vibrational investigations of polyoxometalates. 3. Isomerism in molybdenum (VI) and tungsten (VI) compounds related to the Keggin structure, *Inorg. Chem*. **1984,** 23, 598-605.
52. K. Wassermann, R. Palm, H.-J. Lunk, J. Fuchs, N. Steinfeldt, R. Stoesser, Condensation of Keggin Anions Containing Chromium(III) and Aluminum(III), Respectively. 1. Synthesis and X-ray Structural Determination of [{A-.alpha.-$SiO_4W_9O_{30}$ $(OH)_3Cr_3\}_2(OH)_3]^{11-}$, *Inorg. Chem.* **1995**, 34, 5029-5036.
53. R. G. Finke, M. W. Droege, P. J. Domaille, Trivacant heteropolytungstate derivatives. 3. Rational syntheses, characterization, two-dimensional tungsten-183 NMR, and properties of tungstometallophosphates $P_2W_{18}M_4(H_2O)_2O_{68}^{10-}$ and $P_4W_{30}M_4(H_2O)_2O_{112}^{16-}$ (M = cobalt, copper, zinc), *Inorg. Chem*. **1987**, 26, 3886-3896.

54. T. Morikita, T. Yamamoto, Electrochemical determination of diffusion coefficient of π-conjugated polymers containing ferrocene unit, *J. Organomet. Chem*. **2001**, 637–639, 809-812.
55. S. Gaspar, L. Muresan, A. Patrut, I. C. Popescu, PFeW11-doped polymer film modified electrodes and their electrocatalytic activity for H2O2 reduction, *Anal. Chim. Acta*, **1999**, 385,111-117.
56. F. A. R. S. Couto, A. M. V. Cavaleiro, J. D. P. de Jesus, J. E. J. Simao, Study of polyoxotungstates with the Keggin structure by cyclic voltammetry, *Inorg. Chim. Acta,* **1998,** 281, 225-228.
57. Q. H. Yang, H. C. Dai, J. F. Liu, Heteropolytungstates containing organotin and cobalt or zinc atoms,*Transition Met. Chem.* **1998**, 23, 93-95.
58. A. Müller, L. Dloczik, E. Diemann, M. T. Pope, A cyclic voltammetric study of mangano(II) undecatungstosilicate: an illustrative example of the reduction, protonation and disproportionation pathways of transition metal substituted heteropolytungstates in aqueous solution, *Inorg. Chim. Acta* **1997,** 257, 231-239.

Supporting information

Differential Pulse Voltammogram of compound 4

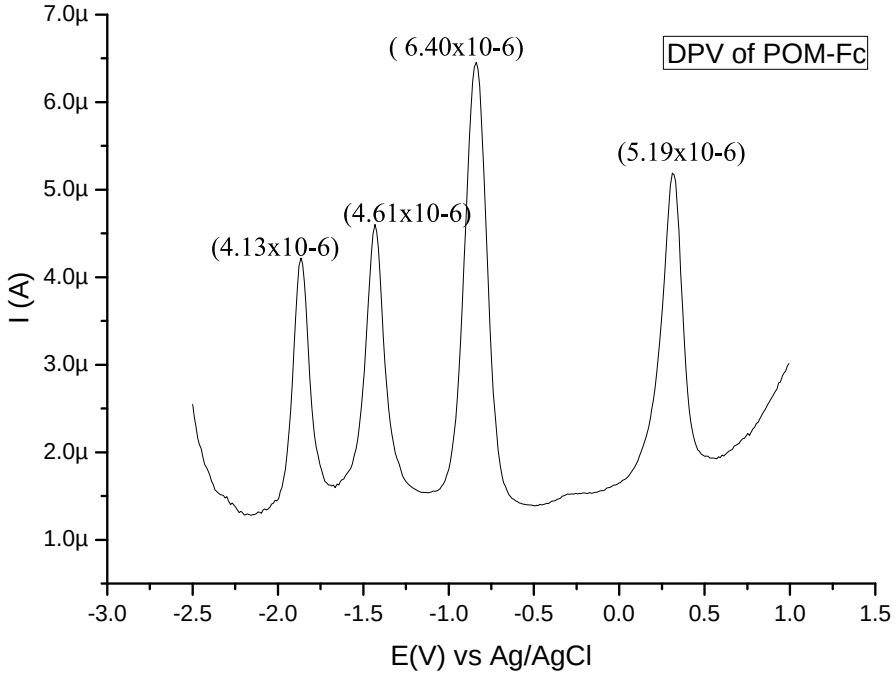

Figure S1. DPV taken in acetonitrile, 1 mM TBA5[SiW11O39{Sn(CH2)2CONH(CH2)3(N3C2H)Fc}], 0.1 M TBAPF6.

Differential Pulse Voltammogram of compound 3'

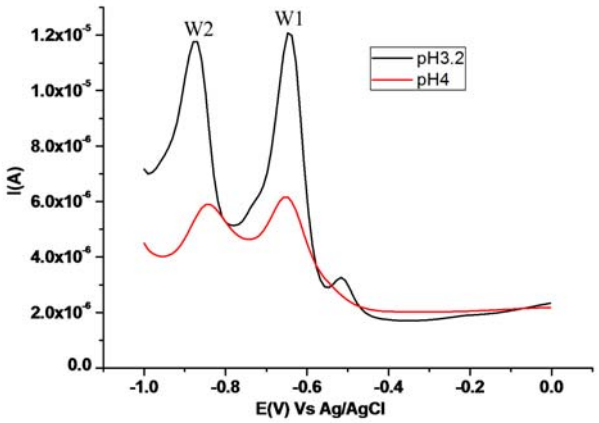

Figure S2. DPV taken in 10 mM HClO4, 0.1 M NaClO4 at pH 3.2 (black) and pH4 (red) for 0.8 mM solution of (NH4)5[SiW11O39SnC2H4CONHC3H6N3]

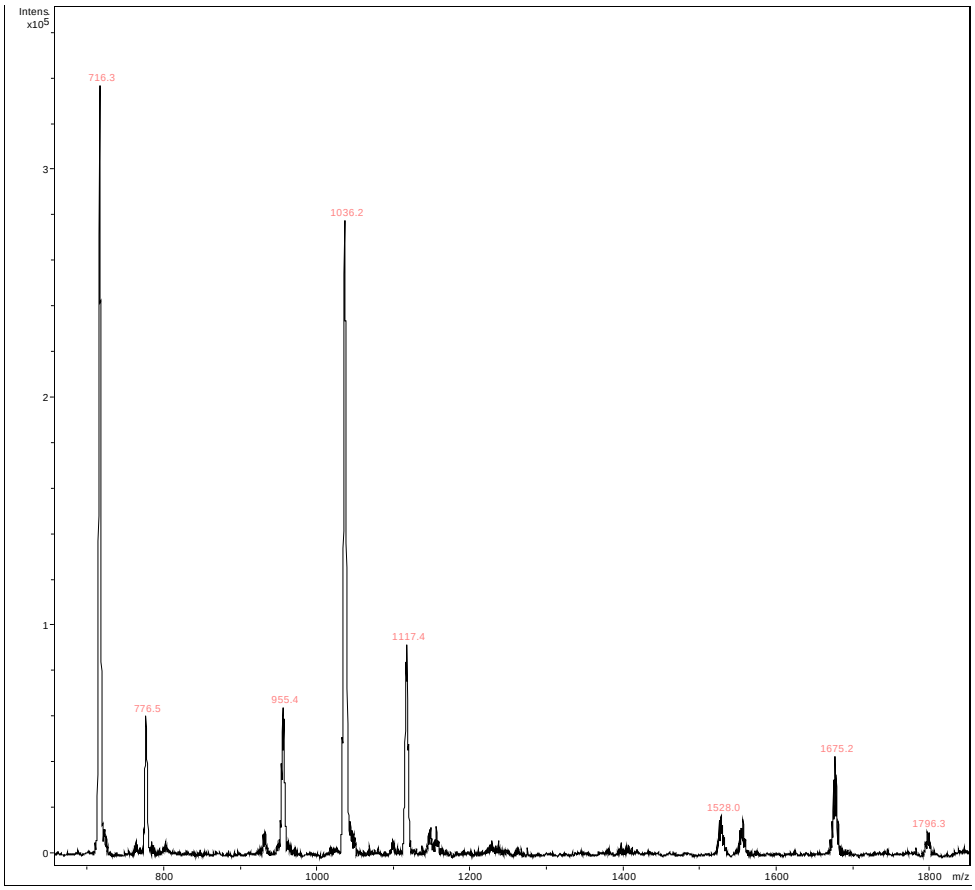

Figure S3. ESI MS data for compound 1

Table S1. ESI MS data for compound 1

Entry	Charge	Calcd. (m/z)	Exp. (m/z)	Composition
1	4–	777.14	776.5	TBA $[SiW_{11}O_{39}SnC_2H_4COOH]$
2	3–	1117.01	1117.4	TBA_2 $[SiW_{11}O_{39}SnC_2H_4COOH]$
3	2–	1797.51	1796.3	TBA_3 $[SiW_{11}O_{39}SnC_2H_4COOH]$
4	4–	716.78	716.3	H $[SiW_{11}O_{39}SnC_2H_4COOH]$
5	3–	1036.53	1036.2	TBA H $[SiW_{11}O_{39}SnC_2H_4COOH]$
6	2–	1676.02	1675.2	TBA_2 H $[SiW_{11}O_{39}SnC_2H_4COOH]$
7	4–	956.04	955.4	H_2 $[SiW_{11}O_{39}SnC_2H_4COOH]$
8	3–	1555.28	1555	TBA H_2 $[SiW_{11}O_{39}SnC_2H_4COOH]$

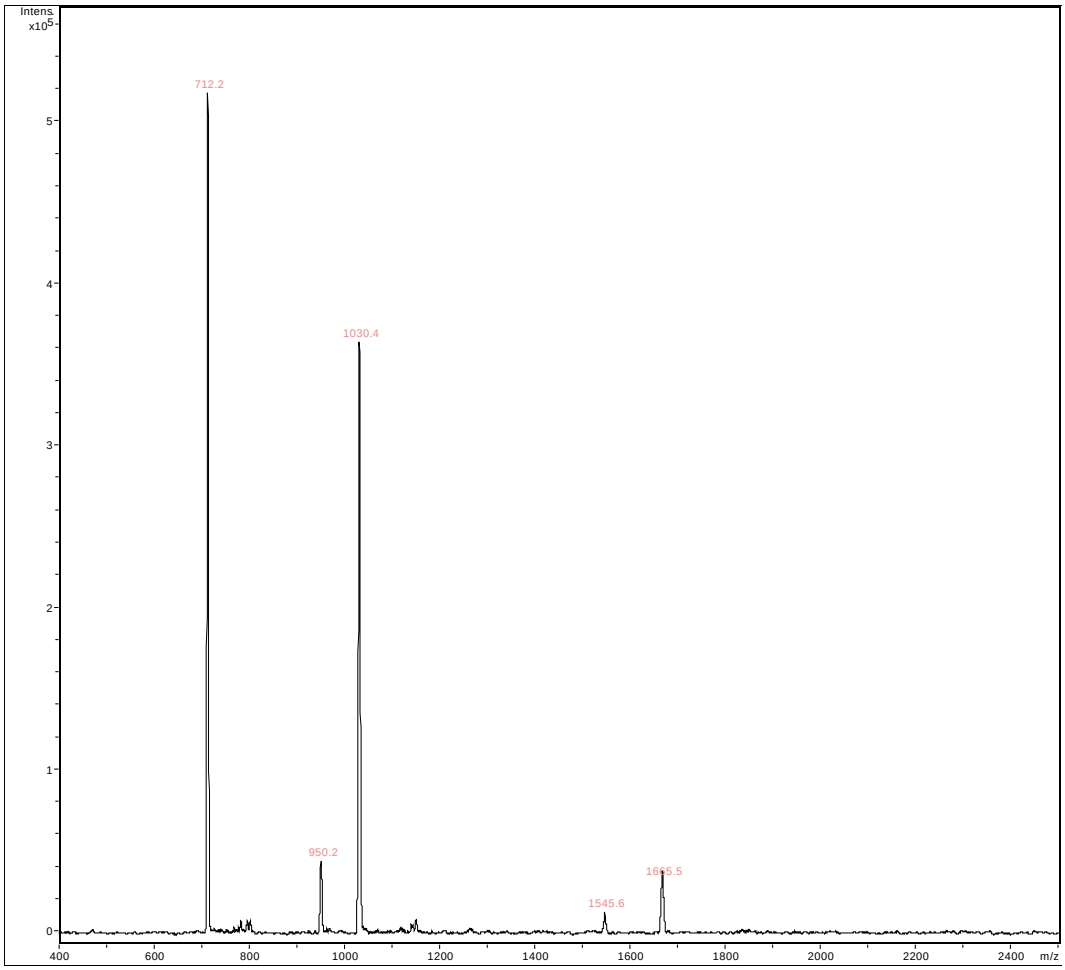

Figure S4. ESI MS data for compound 2

Table S2. ESI MS data for compound 2

Entry	Charge	Calcd. (m/z)	Exp. (m/z)	Composition
1	3–	950.03	950.2	H $[SiW_{11}O_{39}SnC_2H_4CO]$
2	2–	1546.28	1545.6	TBA H $[SiW_{11}O_{39}SnC_2H_4CO]$
3	4–	712.27	712.2	$[SiW_{11}O_{39}SnC_2H_4CO]$
4	3–	1030.52	1030.4	TBA $[SiW_{11}O_{39}SnC_2H_4CO]$
5	2–	1667.01	1665.5	TBA_2 $[SiW_{11}O_{39}SnC_2H_4CO]$

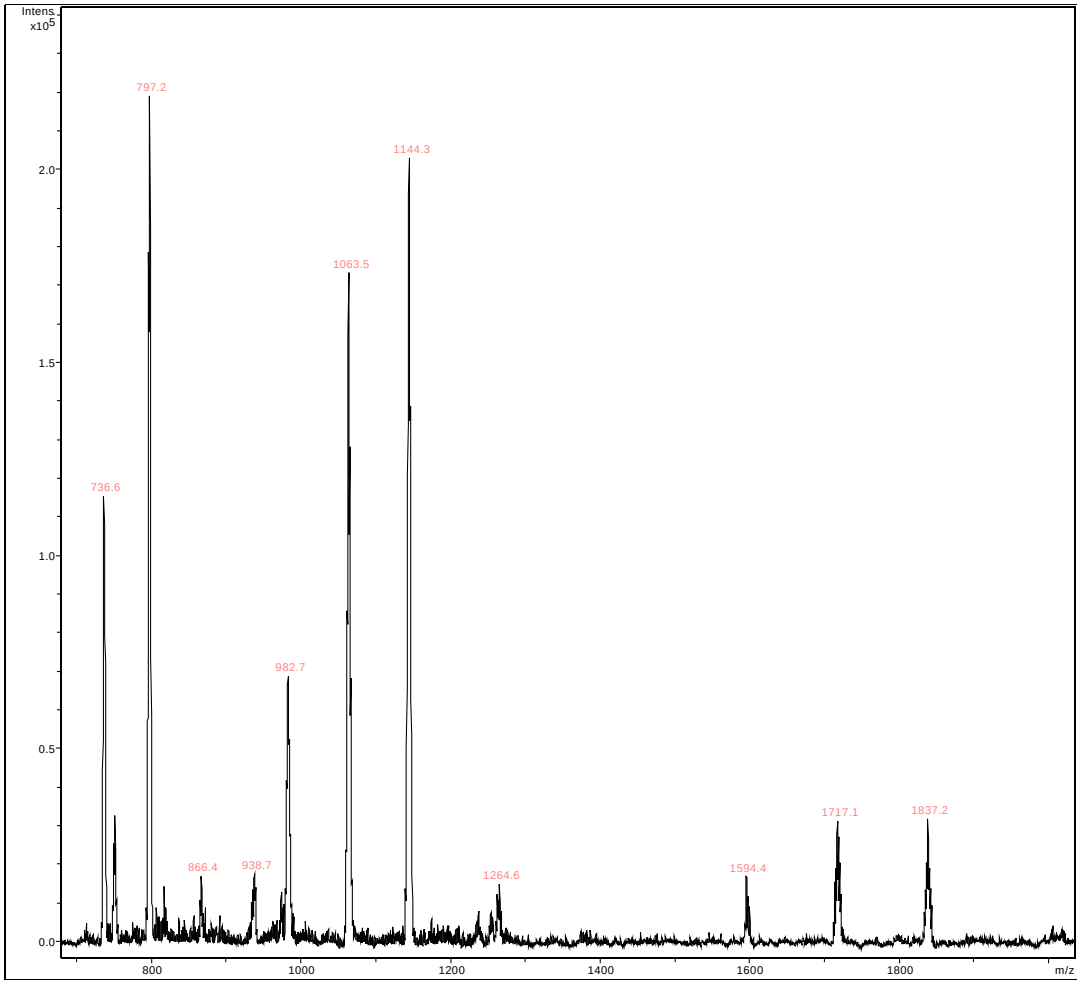

Figure S5. ESI MS data for compound 3

Table S3. ESI MS data for compound 3

Entry	Charge	Calcd. (m/z)	Exp. m/z)	Composition
1	3–	983.41	982.7	H_2 [$SiW_{11}O_{39}SnC_2H_4CONHC_3H_6N_3$]
2	2–	1596.35	1594.4	TBA H_2 [$SiW_{11}O_{39}SnC_2H_4CONHC_3H_6N_3$]
3	4–	737.31	736.6	H [$SiW_{11}O_{39}SnC_2H_4CONHC_3H_6N_3$]
4	3–	1063.89	1063.5	TBA H [$SiW_{11}O_{39}SnC_2H_4CONHC_3H_6N_3$]
5	2–	1717.07	1717.1	TBA_2 H [$SiW_{11}O_{39}SnC_2H_4CONHC_3H_6N_3$]
6	4–	797.67	797.2	TBA [$SiW_{11}O_{39}SnC_2H_4CONHC_3H_6N_3$]
7	3–	1144.38	1144.3	TBA_2 [$SiW_{11}O_{39}SnC_2H_4CONHC_3H_6N_3$]
8	2–	1837.81	1837.2	TBA_3 [$SiW_{11}O_{39}SnC_2H_4CONHC_3H_6N_3$]

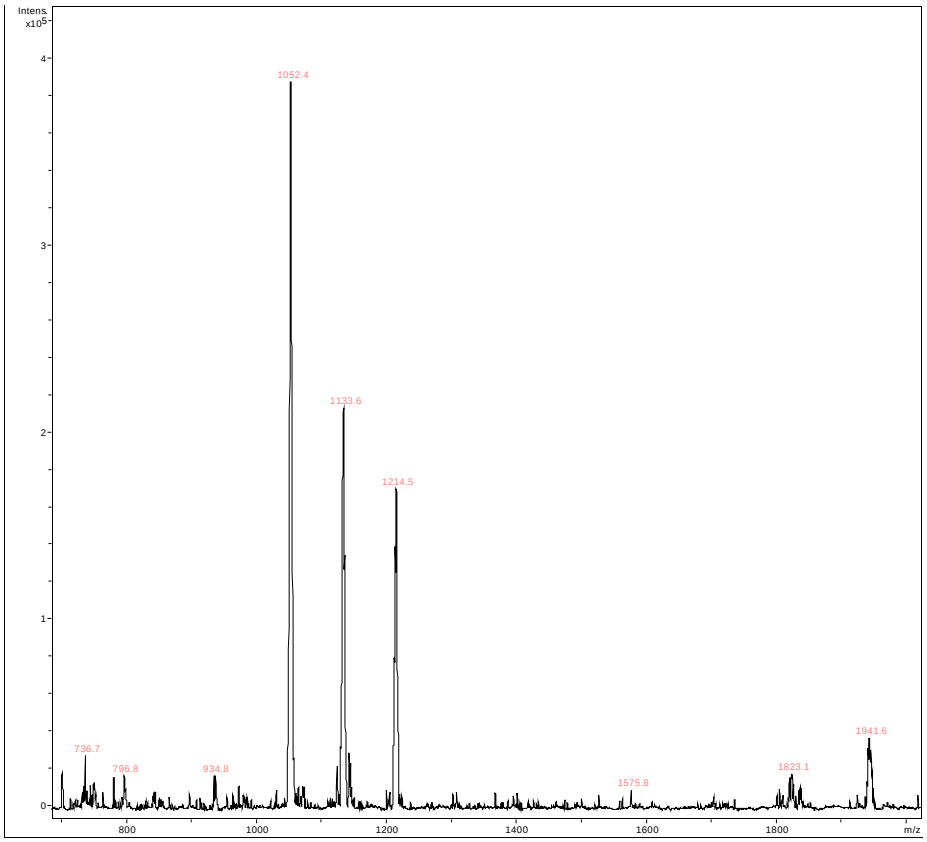

Figure S6. ESI MS data for compound 4

Table S4. ESI MS data for compound 4

Entry	Charge	Calcd. (m/z)	Exp. (m/z)	Composition
1	3–	1214.40	1214.5	TBA_2 $[SiW_{11}O_{39}SnC_2H_4CONHC_3H_6(C_2HN_3)C_{10}H_9Fe]$
2	2–	1942.82	1941.6	TBA_3 $[SiW_{11}O_{39}SnC_2H_4CONHC_3H_6(C_2HN_3)C_{10}H_9Fe]$
3	3–	1133.91	1133.6	TBA H $[SiW_{11}O_{39}SnC_2H_4CONHC_3H_6(C_2HN_3)C_{10}H_9Fe]$
4	2–	1822.10	1823.1	TBA_2 H $[SiW_{11}O_{39}SnC_2H_4CONHC_3H_6(C_2HN_3)C_{10}H_9Fe]$
5	3–	1053.43	1052.4	H_2 $[SiW_{11}O_{39}SnC_2H_4CONHC_3H_6(C_2HN_3)C_{10}H_9Fe]$

Chapter 4.

Polyoxometalate biofunctionalised DNA primers for use in polymerase chain reaction and electrochemical detection of PCR product

Ahmed M. Debela[a], Mayreli Ortiz[a], Valerio Beni[a], Serge Thorimbert [c], Denis Lesage[c], Cole Richaed [c], Bernold Hasenknopf [c] Ciara K. O´Sullivan,[a,b]

[a]Departament d'Enginyería Química, Universitat Rovira i Virgili, Avinguda Països Catalans, 26, 43007 Tarragona, Spain,

[b]ICREA, Passeig Lluis Companys 23, 08010 Barcelona, Spain

[c]UPMC Univ Paris 06, Institut de Chimie Moléculaire UMR CNRS 7071, 4 place Jussieu, 75252 Paris Cedex 05, France.

Polyoxometalate biofunctionalised DNA primers for use in polymerase chain reaction and electrochemical detection of PCR product

Ahmed M. Debela[a], Mayreli Ortiz[a], Valerio Beni[a∫], Serge Thorimbert [c], Denis Lesage[c], Cole Richared [c], Bernold Hasenknopf[c] Ciara K. O´Sullivan[a,b*]*

[a]Departament d'Enginyería Química, Universitat Rovira i Virgili, Avinguda Països Catalans, 26, 43007 Tarragona, Spain,

[b]ICREA, Passeig Lluis Companys 23, 08010 Barcelona, Spain

[c]UPMC Univ Paris 06, Institut de Chimie Moléculaire UMR CNRS 7071, 4 place Jussieu, 75252 Paris Cedex 05, France.

Abstract The synthesis, characterisation and application of polyoxometalate biofunctionalised oligonucleotide primers for use in thermal cycling mediated DNA amplification (POM-primer) are described. Copper mediated Husgen 1, 3 cycloaddition click chemistry was compared with generic amidino coupling for both Keggin and Dawson POMs, in either acetonitrile or DMSO. The POM-primer conjugates were characterised using ESI-MS and Raman spectroscopies, gel electrophoresis and AFM, and successful coupling demonstrated. The functionality of the primer-POM was demonstrated via electrochemical detection of hybridisation to a complementary surface immobilised probe. The primer-POM was then used as a forward primer in combination with a biotinylated reverse primer for the PCR amplification of a *Francisella tularensis* related sequence. The amplicon was evaluated using gel electrophoresis and efficient DNA amplification observed. Streptavidin coated beads were used to generate single stranded DNA from the duplex PCR product via heat denaturation and the POM-labelled strand was liberated for subsequent detection. Gold electrodes were functionalised with 3'-thiol or 5'-thiol terminated probes and electrochemical detection of the POM-5'-labelled single stranded DNA generated from the PCR product demonstrated. As expected, in both cases a better limit of detection and sensitivity was achieved with the 3'thiol probe that resulted in the POM-label being in closer proximity to the electrode surface, and this effect was notably better in the case of the Dawson POM, which can be attributed to the size and charge of the Dawson POM that facilitates an improved steric access. The report details the first use of POMs as an electrochemical label in a

---

∫ †Current affiliation: Department of Physics, Chemistry and Biology (IFM), Linkoping University, S-58183, Linkoping, Sweden

bioanalytical assay, the first report of a DNA primer being chemically linked to a DNA primer and the first report of the successful incorporation of a POM-primer in the polymerase chain reaction. The combination of these facilitates sensitive, direct and substrate-free electrochemical detection of PCR products. Future work will look at labelling the dNTPs with POMS and using them in PCR for an enhanced response and decreased detection limit.

Keywords: Polyoxometalates (POMs), primers, PCR, single stranded DNA (ssDNA), electrochemical, detection

Introduction

DNA sensors are attractive tools for genetic analysis of infections, inherited diseases as well as cancer. There is increasing need for rapid and low cost DNA analysis, primarily driven by applications in personalised pharmacogenomics, clinical diagnostics, rapid pathogen detection, food traceability and forensics. Detection approaches include detection of changes in long-range charge transport though the π-stack of DNA duplex,[1] or the use of exogenous redox-active reporters with preferential affinity for duplex DNA[2] or sandwich assays based on redox-labelled DNA probes that bind to a target DNA sequence.[3] Numerous attempts have been demonstrated via electrochemical probing of enzyme labels,[4] binary probes,[5] nanoparticle tags[6] and redox labels[6-8].

Polyoxometalates (POMs) are nanometer sized transitional metal oxide clusters with a spectrum of potential applications in catalysis,[9-13] material science,[10,11,13] medicine,[14] photo and electrochromism[10] as well as magnetism.[9,11] Among the many interesting properties POMs possess, is their rich redox chemistry, with stable redox states, and multiple electron-transfer steps.[15] Furthermore these properties can be controlled and fine-tuned through organic functionalisations and variation of either the heteroions and/or addenda ions to make them attractive candidates for selective, long-lived, stable, and tuneable redox-active devices.[15] Interestingly their dimensions are on the same scale as biomolecules, but denser and more regular in size, unveiling exciting possibilities for their interaction with biological species. The aforementioned properties together with the high surface area, the improved surface reactivity, and rapid heterogeneous electron transfer make these materials invaluable potential candidates for bioelectroanalytical applications.

Although there are various types of POMs, Keggin $(XW_{12}O_{40})^{n-}$ and Dawson $(X_2W_{18}O_{62})^{n-}$ [9-13] are the most widely studied. Keggin type POMs are spherical with diameter 1.2 nm while plenary Dawson POM is 1.2 nm in length and 0.6 nm in width. Organic functionalisation not only broaden their applications but also improve long-term stability, solubility, redox behavior, spectroscopic response and biological activities of the clusters as well as facilitating the construction of novel POM based functional materials.[10,12,16,17] Organic functionalisation of POMs has been carried out via either placement of oxo ligands with different organic groups such as imido[18] or diazenido[19] or the coupling of lacunary POMs with organosilyl/germyl[20-22] organo-phosphoryl/phosphonates[23] and organotin derivatives.[24-26] Among the various functionalisation strategies the route utilising organotin incorporation into hetropolytungstates is known to provide[25,26] robust and hydrolytically stable oxide clusters which will be functional under physiological conditions.

There are numerous reports detailing the chemical modification of PCR primers either to improve PCR efficiency [27] or to introduce labels for direct detection of the amplified products.[28] Most of the reports utilises either radioactive or, more recently, fluorescently labelled primers, as the use of fluorescently labelled primers has eliminated most of the drawbacks of radioactive species labelled primers like hazardous radioactivity, lengthy exposure for detection of signals of products, and limited sensitivity.[29] In the early works of Koch *et al.*[30] anthraquinone labelled primers were efficiently used for solid phase PCR, whilst Kuhr and co-workers[31, 32] utilised four different ferrocene derivatives to functionalise amine terminated primers, which were subsequently used in PCR and the PCR products were separated using capillary electrophoresis coupled to a sinusoidal–voltammetric detector. A related work was also reported for primer extension reaction for electrochemical SNP detection using ferrocene labelled primers. Various reports have demonstrated that the size of the labels attached to the primer has minimal negative effect on the amplification efficiency of Taq polymerase.[53]

In the work reported here, we use activated mono-oxo acylated polyoxotungstates $[SiW_{11}O_{39}\{Sn(CH_2)_2CO)\}]^{8-}$ (SiW_{11}Sn-Keggin) and $[P_2W_{17}O_{61}\{Sn(CH_2)_2CO)\}]^{6-}$ (P_2W_{17}Sn-Dawson) to link with a 5′-NH_2 terminated DNA forward primer using either click chemistry with an alkyne terminated DNA primer or carbodiimide coupling chemistry

with an amine-terminated DNA primer. The functionalised primer was characterised using a battery of techniques, including electrophoresis, mass spectroscopy, and AFM as well as Raman spectroscopy. The functionality of the POM-labelled primers was demonstrated through hybridisation with a surface-immobilised probe. The labelled primers were successfully used in the polymerase chain reaction and the PCR product characterised using electrophoresis. Single stranded DNA was generated from the PCR product via exonuclease digestion and detected and the performance of the Dawson and Keggin labelled DNA compared.

Materials and methods

All chemicals and reagents used were of analytical grade. Potassium dihydrogen phosphate (KH_2PO_4), potassium chloride (KCl) and mercaptohexanol (MCH) were purchased from Fluka. Sodium chloride (NaCl) was received from Probus and hydrochloric acid (HCl, (35%)) from Panreac, and sodium perchlorate ($NaClO_4$) from Acros Organics. Sodium hydroxide, sulfuric acid (95-97%), trizma base and boric acid were purchased from Scharlau (Barcelona, Spain). Calcium hydride (CaH_2),copper(I) bromide (CuBr), phosphate-buffered saline (PBS), triethyl ammonium acetate, trisodium citrate, acetone, dimethyl sulfoxide (DMSO), acetonitrile (MeCN), perchloric acid (70%), triethyl amine, glacial acetic acid, *tert*-butanol, ethylenediaminetetraacetic acid disodium salt dihydrate 99% (EDTA) and tris[(1-benzyl-1*H*-1,2,3-triazol-4-yl)methyl]amine (TBTA), were all acquired from Sigma Aldrich.

Unfunctionalised Dawson[34] and Keggin[35] POMs and functionalised and activated Dawson ($TBA_6[\alpha_2\text{-}P_2W_{17}O_{61}\{SnCH_2CH_2C(=O)\}]$)[36] and Keggin ($TBA_4[SiW_{11}O_{39}\{SnC_2H_4C(=O)\}]$)[37] POMs and their corresponding azide bearing derivatives $TBA_7[P_2W_{17}O_{61}SnR]$ and $TBA_4[SiW_{11}O_{39}SnR]$ were prepared as previously reported.[38] Unless otherwise noted, all reactions were carried out under argon atmosphere with magnetic stirring. Acetonitrile was dried over CaH_2 and distilled before use.

DNA Sequences

HPLC purified synthetic oligonucleotide sequences were purchased from Biomers (Germany).

The sequences used in this study are the following:

For preparation of POM-labelled primer:

Francisella tularensis: 5′NH_2 forward primer (5′-NH_2-$(CH_2)_6PO_3$-ATTACAATGGCA GGCTCCAGA-3′)

Francisella tularensis 5′alkyne forward primer (5′-HC≡$C(CH_2)_3CONHC_6H_{10}PO_3$-ATT ACA ATG GCA GGC TCC AGA-3′)

For PCR amplification:

Francisella tularensis target amplicon

5′AAGGAAGTGTAAGATTACAATGGCAGGCTCCAGAAGGTTCTAAGTGCCATGATACA AGCTTCCCAATTACTAAGTATGCTGAGAAGAACGATAAAACTTGGGCAACTGTAACAG TT3'

Francisella tularensis reverse primer: 5′-biotin-CGCTACAGAAGTTATTACCTT GCTTAACTGTTA-3'

KOD XL DNA polymerase was purchased from Merck Millipore (Barcelona) and unmodified nucleotide triphosphates (dATP, dCTP, dGTP and dTTP) were provided by Invitrogen.

Complementary sequences for electrochemical detection

Probe 1 (Sequence Complementary with forward primer): 3'-thiol-$(CH_2)_6PO_3$-TTTTTTTAATGTTACCGTCCGAGGTCT -5'

Partially complementary sequence with DNA amplicon:

Probe 2: 5′-thiol-$(CH_2)_6PO_3$–TTTTTTGGGAAGCTTGTATCATGGCAC-3'

Probe 3 : 3′-thiol-$(CH_2)_6PO_3$-TTTTTTCACGGTACTATGTTCGAAGGG-5'

Conjugation of forward primer to Keggin and Dawson polyoxometalates

POM-DNA conjugation: (I) *Cycloaddition via click reaction with alkyne modified oligonucleotides:* 100 µl of 100 µM of alkyne terminated oligonucleotide (dissolved in water) and 50 µl of 1 mM azide bearing POM (dissolved in DMSO) were lyophilised, and 5 µl of a 10 mM solution of CuBr:TBTA (1:1) in DMSO:tert-butanol (3:1) was added to the lyophilisate. This was followed by addition of DMSO: tert butanol (3:1) and 8 µl of distilled water, before sealing the tube with Teflon to avoid any interference from

moisture with the highly reactive activated POM. The sealed tube was then placed in a thermomixer at 40°C for 3 h and mixed continuously for an additional 5 h at room temperature, followed by addition of 10 µl of triethyl ammonium acetate (2 M) and 400 µl of acetone and an overnight incubation at -20°C. The mixture was then centrifuged at 13000 rpm for 10 min and the supernatant discarded. The pellet was washed with acetone twice to remove the unreacted POM.

(II) *Conjugation of activated POM with amine terminated forward primer:* A tool kit for POM-DNA functionalisation was developed by adopting/modifying an existing protocol for amide formation with POMs to form organic –inorganic hybrids.[36-38] 100 µl of 100 µM oligonucleotide (dissolved in water) was lyophilised and reconstituted in 10 µl distilled water, followed by 5 µl of triethyl amine and subsequent addition of 75 µl of 2.5 mM of the activated POM in anhydrous DMSO. The mixture was maintained under shaking conditions at 40°C for 30 h, followed by the addition of 10 µl of triethyl ammonium acetate and 500 µl of acetone and gentle vortexing for 2 min, and an overnight incubation at -20°C. The solution was centrifuged at 13000 rpm for 10 min and the supernatant was discarded. The whitish pellet was washed in acetone twice to remove the unreacted POM.

PCR amplification and purification: For the amplification of a *Francisella tularensis* associated target, 400 nM each of 5′POM labelled forward primer (5′-POM-ATTACA ATGGCAGGCTCCAGA-3′) and 5′biotinylated reverse primer (5′biot-CGCTAC AGAAGTTATTACCTTGCTTAACTGTTA-3), 10xPCR buffer, 200 mM dNTPs, 1 unit of the KOD polymerase were mixed. Amplification was performed in an iCycler Thermal Cycler (Biorad), with amplification conditions being 2 min at 95°C, followed by 30 cycles of 20 s at 95 °C, 20 s at 60 °C, and 20 s at 72 °C and a final extension step at 72°C for 7 min. At the end of the program, the tubes were held at 4°C and used for further characterisation. The PCR product was purified using a PureLink Quick Gel Extraction and PCR Purification Combo Kit (Invitrogen) to obtain pure dsDNA via the selective binding of dsDNA to a silica membrane-based spin column in the presence of chaotropic salts. Extraction was performed following the manufacturer's procedure and the purified PCR product was eluted with elution buffer (10 mM Tris–HCl)

Mass spectroscopy: A LTQ-Orbitrap XL (Thermo Electron Corporation, Bremen, Germany) mass spectrometer equipped with an ESI source was used to acquire high resolution mass spectra. The experiments were performed in negative ion mode. Nitrogen was used as a sheath gas. The spray voltage was set at 4.5 kV for all experiments. 10 μM POM modified primer was dissolved in a mixture of acetonitrile/water/acetic acid (89%/9%/2%). The solutions were subjected to ESI and infused continuously at a flow rate of 20 μl per min. The mass spectrometer was set for three microscans, an activation time of 30 ms, normalised collision (radial resonant excitation) energies were between 5 and 50%, and isolation window was set at 2.0 Th for LTQ and 1.4 Th for Orbitrap, The resolution was set to 100 000 (FWHM at m/z 400). Mass spectra were acquired between 4000 and 100 *m/z* with a scan speed of 10 s/scan. All acquired data were analysed using Xcalibur 2.0.7 software (Thermo Finnigan) and the results were compared with those simulated by mMass.

Raman spectroscopy: Acquisition of the Raman spectra was achieved using a Renishaw 2003 Spectrometer operating at wavelength of 785 nm with 50x objective lens. The spectra were analysed using Wire 3.2 version software (Renishaw plc, Gloucestershire, GL12 8JR, United Kingdom).

Atomic Force Microscopy Atomic force microscopy (AFM) was carried out using a 5420 Atomic Force Microscope from Agilent Technologies (USA). Diluted POM-DNA solution was slowly dropped onto a mica substrate and dried under nitrogen atmosphere. Images were acquired in tapping mode using an enhanced resolution AFM tip (single diamond-like carbon extra tip at the apex of gold coated silicon etched probe) and a cantilever coated with gold 124 μm in length and 25 μm in width with a force constant of 5 N and resonance frequency of 150 kHz. Areas of 1 μm^2 were scanned at a rate of 0.5 Hz. The images were processed using WSxM 5.0 Develop 3.3.[39]

Generation of Single Stranded DNA: SIMAG-Streptavidin particles (10 mg/ml in PBS) were resuspended and 35 μl of the suspension was taken, and subsequently washed with 1x saline sodium citrate (SSC) buffer. After repeating the washing step twice, 100 μl of the PCR product and 100 μl of 2x buffer were added. The mixture was incubated for 30 min at room temperature, to allow the magnetic beads to interact with the biotinylated PCR product. Following incubation the supernatant was discarded and particles washed twice

with 1 x SSC buffer. POM labelled single stranded DNA (ssDNA) was then liberated by addition of Milli-Q water which was heated to 95°C for 5 min, and following the application of the separator the supernatant was removed.

Gel electrophoresis analysis: 5 µl of each ssDNA sample, with 4 µl of 6x loading buffer (40% glycerol and bromophenol blue), was loaded on a 2.4% agarose gel stained with GelRed nucleic acid stain (Biotium). Synthetic ssDNA of known concentrations was prepared in the same manner as the samples and loaded together. Gels were analysed with ImageJ software. Quantification was facilitated by running the gel of a known concentration of unmodified primers along with the modified primers.

Electrochemical Measurements: All electrochemical measurements were carried out using an Autolab model PGSTAT 12 potentiostat/galvanostat controlled with the General Purpose Electrochemical System (GPES) software (Eco Chemie B.V., The Netherlands). A classic three electrode set up was used with Ag/AgCl as a reference electrode, Pt wire counter electrode and gold working electrode (diameter of 2 mm), which were purchased from CHI Instruments. All the potentials are recorded with respect to the reference electrode.

Electrode/sensor preparation: Gold electrodes were polished with 0.3 and 0.05 µm alumina for ca. 5 min for each size, followed by sonication for 5 min in water. This was followed by electrochemical cleaning in 0.5 M H_2SO_4, sweeping for 40 cycles between 0.2 and 1.6 V vs Ag/AgCl with a scan rate of 250 mV/s. This was followed by immersion of the gold electrodes in a solution of thiolated ssDNA (5 µM in 1.0 M KH_2PO_4). After 3 h of incubation at room temperature the electrodes were rinsed with Tris-HCl buffer and dried with a stream of nitrogen. Backfilling was achieved via immersion in 0.5mM mercaptohexanol for 30 min and the probe-modified electrodes were subsequently washed with Tris-HCl buffer solution and dried with argon.

Electrochemical detection of POM labelled DNA primer *:* The functionality of the POM labelled DNA and the possibility of its' electrochemical detection was demonstrated via hybridisation of the labelled primer (21-mer) with a surface tethered complementary probe (21-mer) and the hybridisation conditions (hybridisation time, temperature and buffers) as well as electrochemical detection conditions (the DPV

parameters, modulation amplitude and modulation time) for the detection of the POM labelled PCR product were optimised.

Detection of ssDNA generated from PCR product: The concentration of PCR product was estimated from the gel electrophoresis using the image-J software. The electrodes modified with a surface tethered complementary probe (21-mer) were exposed to a range of concentrations of the single stranded DNA generated from the PCR product (6.25 - 100 nM in Tris-HCl, pH 6.0, containing 0.5 M NaCl), as well as a blank that served as a control. Following exposure (at 37°C for 1 h), the electrode was washed with Tris-HCl buffer and dried with a stream of nitrogen. Electrochemical measurements were performed at room temperature in a 10 mL electrochemical cell using a three-electrode configuration. Differential pulse voltammetry (DPV) measurements was recorded at potentials between -0.9 and 0V (vs Ag/AgCl), pulse amplitude of 0.1 V, step potential, 10 mV, pulse width 100 ms and pulse period of 5 ms.

Results and discussion

POM-DNA conjugation

A variety of approaches and different reaction conditions were attempted to conjugate the Keggin and Dawson POMs to the 21-mer forward primer. The difference in solubility of POM and DNA is one of the key problems to be solved for maximising the yield and to this end, all reactions were performed in the presence of a slight amount of water to facilitate the dissolution of the oligonucleotide, despite the fact that the nucleophilic water results in deactivation of the activated POM. To counteract this loss a large excess of POM was used. The Hugsen 1, 3 cycloaddition click-chemistry approach (Scheme 1a) was first probed, as this method has been previously reported for the conjugation of POM with organic molecules.[37,38] As previously detailed for click reaction involving DNA molecules,[40] CuBr:TBTA (tris[(1-benzyl-1*H*-1,2,3-triazol-4-yl)methyl]amine) was used to stabilise the Cu(I), increasing its catalytic effect and the solubility of Cu(I) in organic solvents. However, the yield of the conjugate obtained was very low and this method was not further pursued.

A second approach (Figure 4.1 b) using generic amidino coupling was thus explored. The forward primer was lyophilised and then re-dissolved in a slight amount of water in the presence of a catalytic amount of triethyl amine and a 20 X molar excess of Keggin/Dawson POM. As mentioned previously, this large excess is to compensate for any deactivation of the cyclic ester POM. The use of DMSO and acetonitrile as a reaction solvent were compared, and whilst acetonitrile resulted in a milky suspension, DMSO allowed complete dissolution, and both solvents resulted in a very good coupling efficiency, achieving yield of 87 % for P_2W_{17} and 84 % for SiW_{11} using DMSO and around 80 % using acetonitrile as reaction solvent. The POM-primer conjugates were then characterised via Raman and ESI-MS.

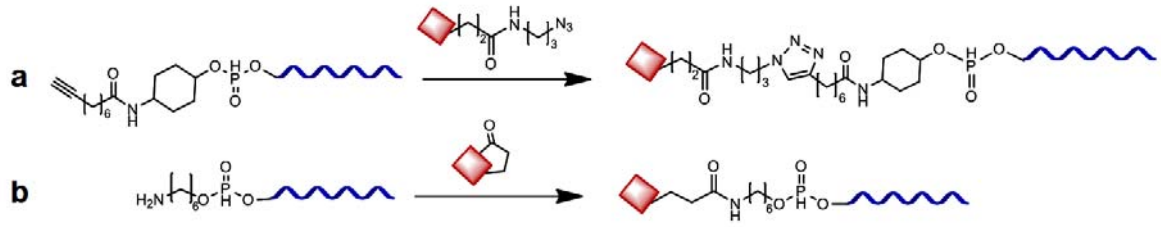

Scheme 4. 1. Schematic depiction of the POM post functionalisation strategies a) 1,3 cycloaddition reaction (click reaction) for coupling of azide bearing POM with alkyne terminated 21-mer forward primer. b) The reaction between aminated 21-mer forward primer and carboxylate activated POM.

ESI-MS Characterisation of Keggin and Dawson POM-modified forward primers

POMs have isotopic sets of signals arising from stable isotopes of the core transition metals (W, Mo), which can be fitted to determine the exact formula[41] and are thus highly suited to characterisation using electrospray ionisation-mass spectroscopy (ESI MS). Various peaks corresponding to the functionalised POMs with charge states -4, -5 and -6 , with tetra butyl ammonium (TBA) were observed. Figure 1 and 2 show signals obtained for Keggin (SiW_{11})-primer with a m/z ratio ranging from 1500-2000 with charge states -5 and -6, whilst for the Dawson (P_2W_{17})-primer a m/z ratio ranging from 1800-3000 corresponding to charge states -4 and -6 was observed. Furthermore, the average mass from the deconvoluted spectra for the (SiW_{11})-primer and (P_2W_{17})-primer (Figure S1 supporting information) was 9684.29 and 11186.88, respectively. These average mass values fit well with the sum of the mass of the DNA (6722) and the SiW_{11} POM 2851 and

the P_2W_{17} POM 4338 along with the counter cations TBA (nx242), with n being 2-6. These MS values unambiguously confirm the successful conjugation of the POMs to the DNA primer. The ESI MS spectra also show some unreacted POM as a result of deactivation of the cyclic ester.

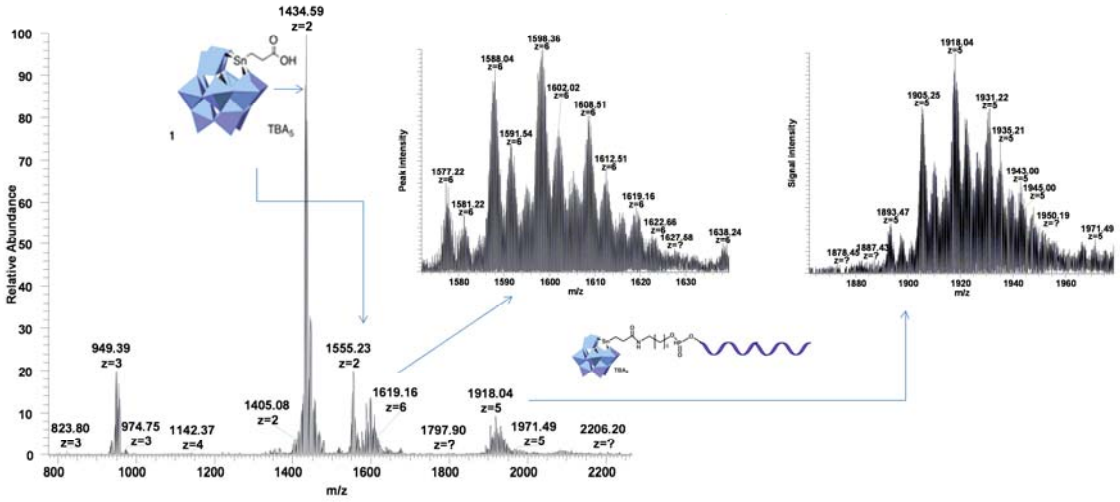

Figure 4. 1. ESI MS spectra of Keggin POM (SiW11) modified 21-mer forward primer.

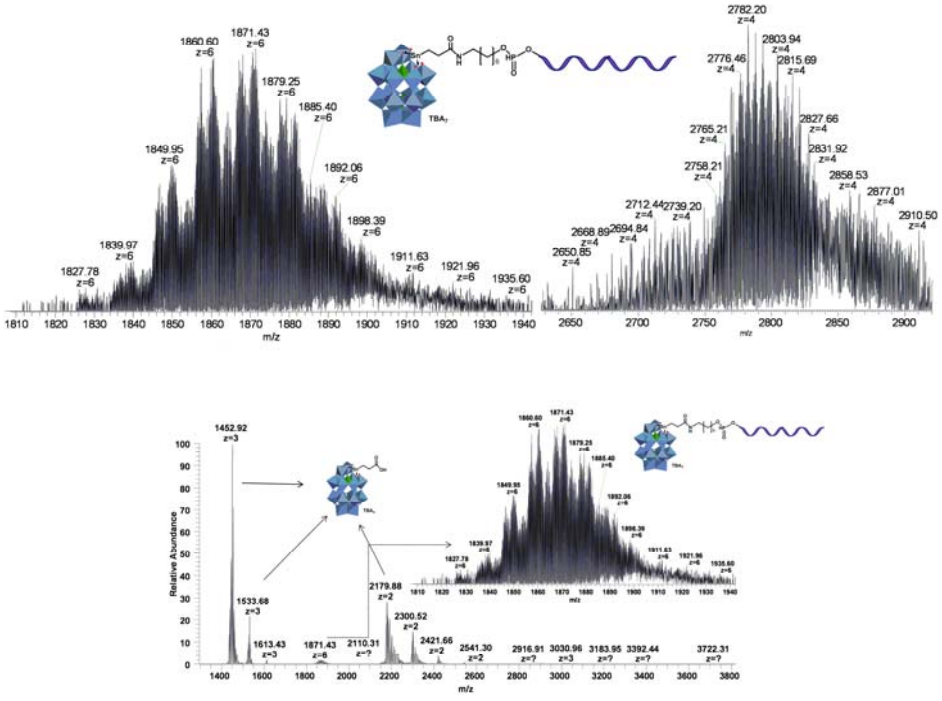

Figure 4. 2. ESI MS spectra of Dawson POM (P2O17) 21-mer forward primer.

Raman characterisation of POM-modified primer

Figure 4.3 shows (from bottom to top) the Raman spectra of both Dawson and Keggin POMs (Table 1 Supporting information) at the consecutive steps of their modification for conjugating to the DNA primer. The first important feature to be highlighted is the presence of the fingerprint bands of POMs such as $\nu_{\sigma}P\text{-}O_{a}$, $\nu_{\sigma}W{=}O_{d}$, $\nu_{\alpha\sigma}W\text{-}O_{b}\text{-}W$, $\nu_{\alpha\sigma}W\text{-}O_{c}\text{-}W$, attributed to bond stretchings within the POM cluster, confirming intact POM framework from the beginning to the end of synthesis.[42,43] The previous results obtained in ESI-MS and FTIR for the modified POM-COOH compensate the non-visualisation of the band of carbonylic group which is difficult to observe in Raman spectra. Following modification of the POM via the introduction of SnC_2H_4COOH moiety and precipitation with TBA as counter ion, the bands corresponding to the Csp_3-H are observed. In the final POM modified primers (Figure 4.3 and Table 4. 1), additional bands corresponding to the phosphodiester bonds and the DNA bases are also present. Finally, the band of carbonylic group observed in the POM-DNA conjugates corroborates the conjugation of POM to the DNA via amide bond formation.[45]

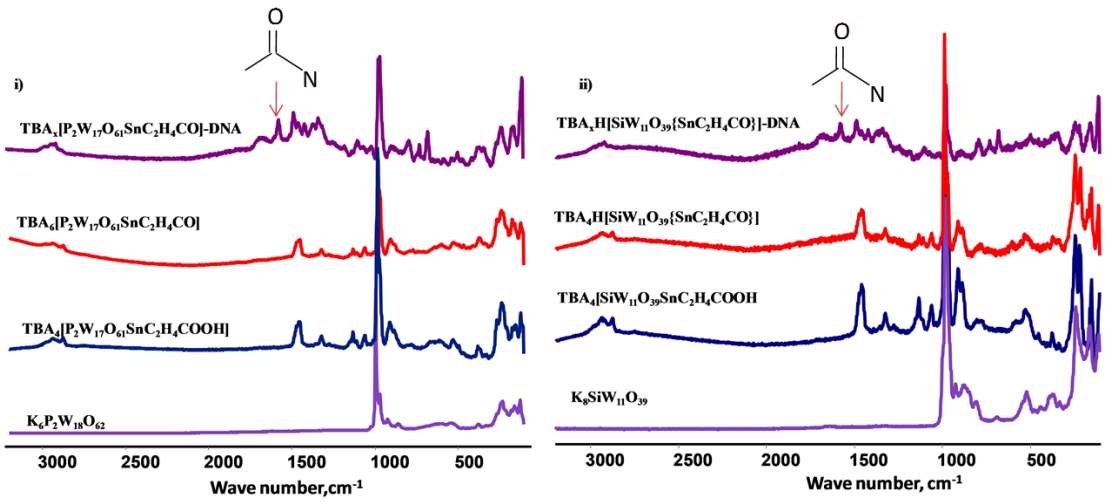

Figure 4. 3. Raman spectra showing the steps followed for POM, (i) P2W17and (ii) SiW11 functionalisation of DNA.

Ta-ble 4. 1. Raman shift assignments for POM functionalised primer

Peak Positions			
SiW_{11}-DNA	P_2W_{17}-DNA	Literature[44,45]	Assignments
679	677	678	G
725	726	729	A
785	792	785	T, C
1102	1092	1098	PO_2^-
1334	1335	1336	A
1487	1481	1485	A,T,C
1574	1578	1576	A(ring st)
1677	1685	1674	Amide I
1647	1643	1636	Amide I
1487	1487	1490	Amide II

Electrochemical detection of POM labelled DNA primers

Differential pulse voltammetry (DPV) was used to further evaluate the functionality of the POM primer conjugates in the potential ranges 0 and -0.9 vs Ag/AgCl in pre-stirred buffer solution. Unlike other reported POMs functionalised with organic groups, which show two characteristic reduction waves,[15] Keggin POM–primer and Dawson POM-primer showed a either single wave or two very close redox potentials in the range -0.2 and -0.5 V (vs Ag/AgCl), following the hybridisation assay with capture probe on gold electrodes (Figure 4. 4).

Figure 4. 4 shows, as expected, that the DPV responses increased as the concentration of POM-primer was increased. The hybridisation conditions including buffer, pH, temperature and the DPV detection parameters were optimised to be 1 h hybridisation at 37^{o}C in Tris-HCl containing 500 mM NaCl at pH 6. The optimum DPV conditions were pulse amplitude of 0.1 V, step potential of 10 mV, pulse width 100 ms and pulse period of 5 ms.

The calibration curves show a slightly better sensitivity for the Dawson POM labelled primer, with similar limits of detection of 10.8 and 14.5 nM, for the Keggin and Dawson labelled primers, respectively. The successful conjugation of the POMs to DNA primers was thus again proven, and furthermore the functionality of the conjugate and the ability to sensitively electrochemically detect the POM labels demonstrated.

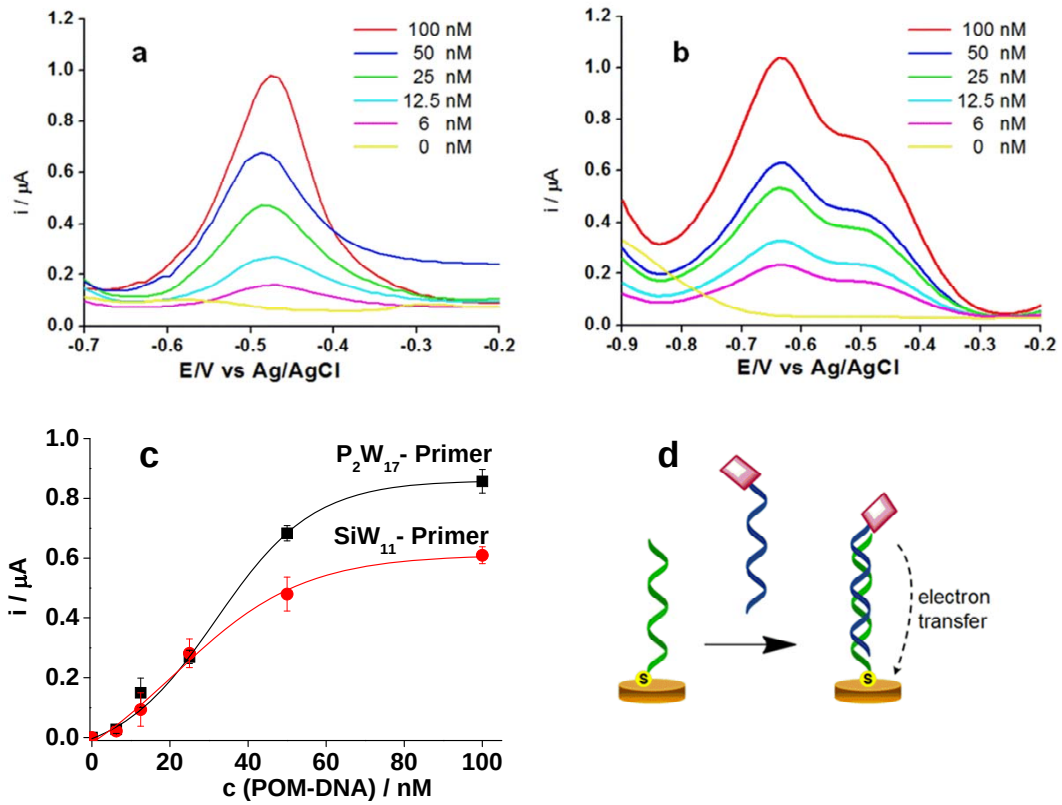

Figure 4. 4. DPV responses obtained for the serial dilutions of POM a) Keggin (SiW11-Primer) and b) Dawson (P2W17-DNA) modified primers hybridised to 21-mer capture probe (probe 1) on gold electrodes. c) The calibration plots for detection of POM modified primers over a 0 nM -100 nM concentration range with correlation coefficient of R^2 = 0.996, for Keggin and 0.998 for Dawson POM modified primers after 1 h hybridisation at 37°C, d) Schematic representation of the system.

PCR Amplification of DNA target using POM-functionalised forward primer

Following the confirmation of the successful conjugation of the POMs to the DNA primer using ESI MS and Raman spectroscopies the conjugates were characterised using gel electrophoresis. Gel electrophoresis of the modified primers was carried out in 2% w/v agarose gel in acetate buffer, pH 6. These conditions were specifically chosen to avoid any detachment of the SnC_2H_4COOH of the POM due to the higher pH of the more commonly used Tris-Borate-EDTA (TBE) buffer (pH=8.3). As can be seen in Figure 5a, the migration of the POM labelled primers is slightly retarded as compared to the unlabelled primer, again proving the successful labelling of the primers. The gel bands were used to semi-quantify the POM labelled primers and calculate the yield of the reaction products using the ImageJ analysis software.

The labelled forward primers were then successfully used for the PCR amplification of the DNA target, and thus inherently the POM labels were observed not to affect the activity of the polymerase. The polymerase mixture, KOD Xl, used the polymerase in both its' mutant and native form and is known to be capable of amplifying long and complex targets with robust yield and high accuracy.[46] As can be seen in Figure 5, there is a notable difference in migration between POM bearing and non POM bearing PCR products (Figure 4. 5b).

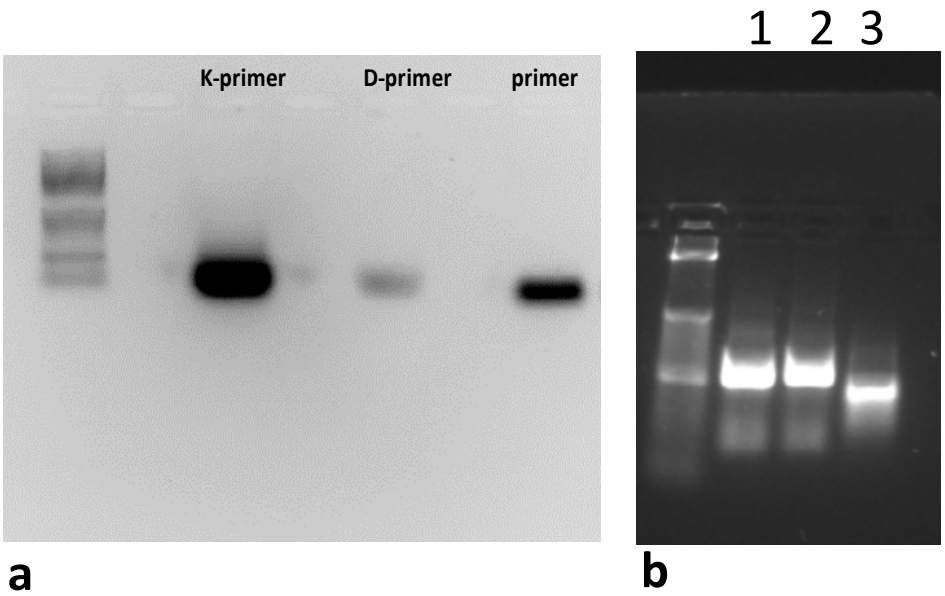

Figure 4. 5 a) Gel electrophoresis of POM functionalised (Keggin SiW11, (K-primer), and Dawson, P2W17, (D-primer) and un-functionalised forward primer (primer). b) gel electrophoresis of PCR products amplified using POM functionalised primers ((1 for Keggin-DNA and 2 for Dawson-DNA) and 3 for PCR product with un-functionalised primer.

AFM visualisation of POM-labelled PCR product

AFM was carried out to image the POM-labelled PCR product. A diluted solution of Keggin POM-labelled PCR product was deposited on mica and carefully dried under vacuum. AFM was recorded in tapping mode using an ultra-sharp tip. Figure 4.6 shows the 2D and 3D AFM topographic pictures of the Keggin POM-labelled PCR product. The appearance of the free POM is clearly different from the conjugate (Supporting information, Figure S2.) and to the best of our knowledge; this is the first report of the AFM imaging of a POM-DNA conjugate.

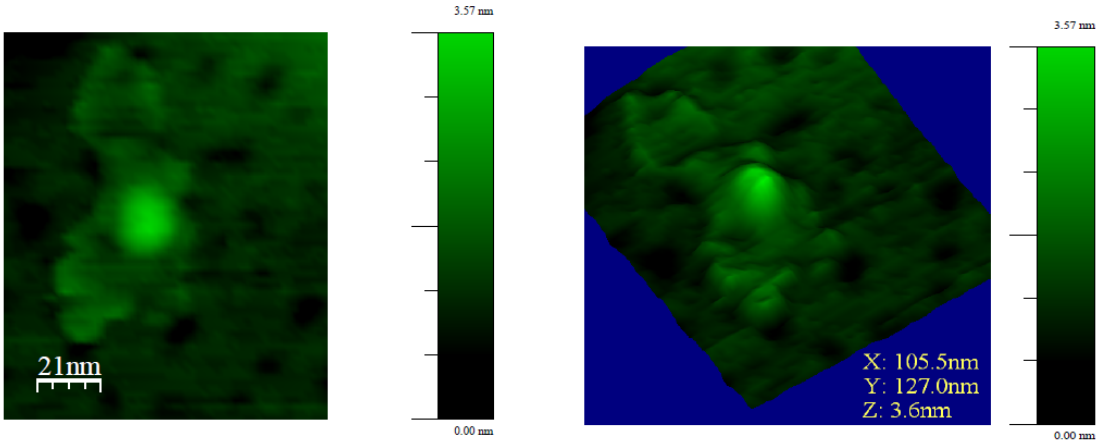

Figure 4. 6. 2D (left) and 3D (right) AFM pictures of Keggin POM (SiW11) bearing PCR product.

Electrochemical detection of PCR product

Biotinylated reverse primers were employed with the intention of generating the ssDNA by exploiting the strong biotin streptavidine interaction. This was preferred as the enzymatic methods for ssDNA generation require higher pH (>8.5) which would be detrimental to the POM DNA coupling resulting demetalation. After thorough mixing the PCR product with suspension of the streptavidine coated beads (see methods section) the ssDNA is generated by heating for 5min at temperature of 95°C and employing a magnet.

Figure 4. 7 shows two strategies for electrochemical detection of POM bearing ssDNA by previous hybridisation to 21-mer 5'- (probe 2, strategy 1) and a 21-mer 3'-(probe 3, strategy 2) surface tethered probes. It was accomplished for evaluating the better detection attending to the compromise between steric hindrance during hybridisation with the capture probe and electron transfer for electrochemical detection. To facilitate the accessibility of POM-ssDNA for binding, both immobilised primers (probe 2 and 3) incorporated a 6T spacer. Table 4. 2 shows similar limits of detection for all system in the nanomolar range, which is slightly better for Dawson POM-ssDNA. For Keggin POM-ssDNA, the sensitivity was also similar for both strategies, while for the bulkier non-spherical Dawson-POM-ssDNA the difference is almost 4 times higher for strategy 2 with respect to strategy 1. It is likely that once the steric hindrance is minimised by the 6T tail, the closer position to the surface in strategy 2, facilitates the electron transfer.

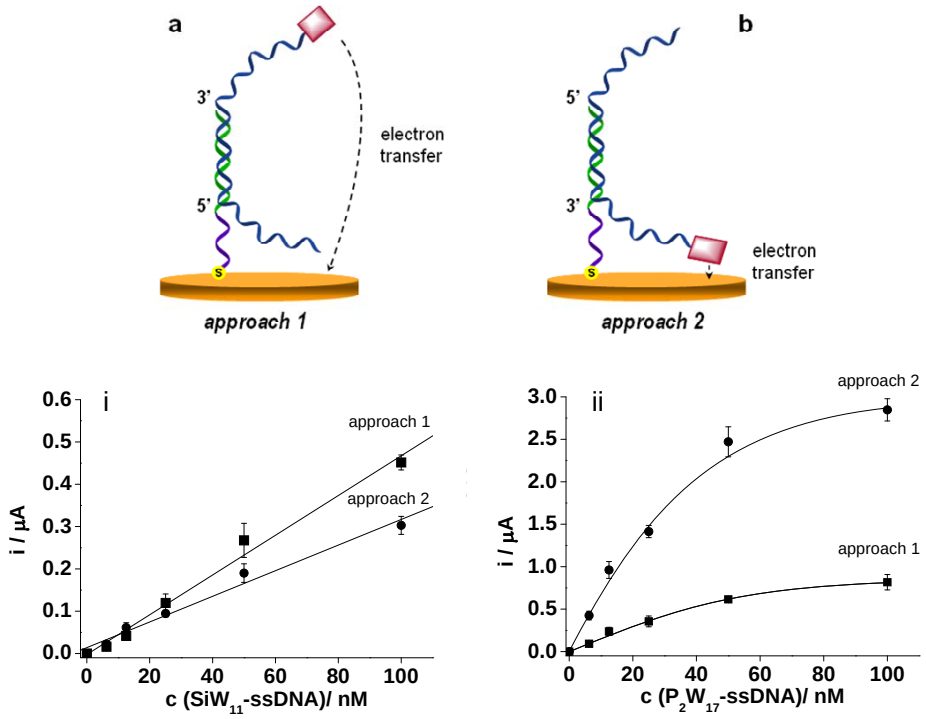

Figure 4. 7. The two formats used for testing the hybridiszation assay for detection of POM bearing ssDNA a) Surface tethered 21-mer probe immobilised via 5' -terminal and b) Surface tethered 21-mer probe immobilised via 3'-terminal i) and ii) are calibration plots for the hybridisation assay with POM bearing ssDNA for each of the detection strategies.

Table 4. 2. Data extracted from the calibration plots in **Figure 4. 7** c and d

	Strategy 1		**Strategy 2**	
Parameters	**SiW_{11}**	**P_2W_{17}***	**SiW_{11}**	**P_2W_{17}***
LOD (nM)	9.6	6.4	7.6	5.6
R	0.99418	0.98901	0.99074	0.98926
Sensitivity (nA/nM)	4.7	12.0	3.0	47.8

* The calculations were carried out taking the linear range from 0 to 50 nM.

In addition a difference in sensitivity in one order of magnitude for Dawson POM-ssDNA in comparison with Keggin POM-ssDNA systems was also observed (Figure 4.7 i and ii

and Table 4. 2). Considering only the charge density of Keggin and Dawson anions, it is known that it is easier to reduce the Keggin POM due to better electron transfer.[47] However, in aqueous conditions it is not only the charge density that plays a major role in the redox reaction but various factors[48] can be attributed to electron transfer. In the work reported here, the interaction of the POMs with the DNA as well as their orientation following hybridisation could have an effect on the electron transfer, and consequently show an effect on sensitivity and the detection limit. In addition, the effect of demetalation in case of Keggin could contribute to the lower current response, and the lower sensitivity observed for the Keggin POM bearing DNA.

Conclusions

In summary, we have demonstrated the functionalisation, characterisation and application of polyoxometalate labelled oligonucleotides in PCR and direct electrochemical detection of PCR products. The synthesised POM-primer conjugates were characterised using various techniques, including ESI MS, Raman spectroscopy and gel electrophoresis. Having confirmed the synthesis, the functionality of the primers was demonstrated via an electrochemical hybridisation assay with capture probes tethered on the surface of gold electrodes. Different strategies were tested to evaluate platforms to achieve improved detection limits and sensitivity with POM bearing ssDNA generated from PCR products. This report is only the second report of a DNA primer linked to an electrochemically active redox molecule and demonstrates the huge potential of the use of polyoxometalate as electrochemical labelss in bioanalytical applications.

Acknowledgement

AMD acknowledges Generalitat de Catalunya for mobility grant awarded for the stay at IPCM, UPMC, Paris, France. 2012 BE100872 (BE-DGR).

References

1. E. L. S. Wong, J. J. Gooding, Charge Transfer through DNA: A Selective Electrochemical DNA Biosensor, *Anal. Chem.* **2006**, 78, 2138–2144
2. J. Wakai, A. Takagi, M. Nakayama, T. Miya, T. Miyahara, T. Iwanaga, S. Takenaka, Y. Ikeda, M. Amano, A novel method of identifying genetic mutations using an electrochemical DNA array, *Nucleic Acids Res.* **2004**, 32, e141.
3. Y. Xiao, A. A. Lubin, B. R. Baker, K. W. Plaxco, A. J. Heeger, Single-step electronic detection of femtomolar DNA by target-induced strand displacement in an electrode-bound duplex, *Proc. Natl. Acad. Sci. U.S.A.* **2006**, 103, 16677–16680.
4. G. D. Liu, T. M. H. Lee, J. Wang, Nanocrystal-Based Bioelectronic Coding of Single Nucleotide Polymorphisms, *J. Am. Chem. Soc.* **2005**, 127, 38–39
5. D. M. Kolpashchikov, Binary probes for nucleic acid analysis, *Chem. Rev.* **2010**, 110, 4709–4723.
6. Z. Wu, J.-H. Jiang, G. L. Shen, R. Q. Yu, Highly sensitive DNA detection and point mutation identification: an electrochemical approach based on the combined use of ligase and reverse molecular beacon, *Hum. Mutat.* **2007**, 28, 630–637.
7. C. H. Fan, K. W. Plaxco, A. L. Heeger, Electrochemical interrogation of conformational changes as a reagentless method for the sequence-specific detection of DNA, *Proc. Natl. Acad. Sci. U.S.A.* **2003**, 100, 9134–9137
8. D. M. Jenkins, B. Chani, M. Kreuzer, G. Presting, A. M. Alvarez, B. Y. Liaw, Hybridization probe for femtomolar quantification of selected nucleic acid sequences on a disposable electrode. *Anal. Chem.* **2006**, 78, 2314–2318.
9. C. L. Hill, Special issue on polyoxometalates, *Chem. Rev.* **1998**, 98,1-390.
10. L. Cronin and A. Müller, Special issue on polyoxometalates, *Chem. Soc. Rev.*, **2012**, 41, 7325-7648.
11. K. Hindson, U. Kortz and T. Liu, Special issue on polyoxometalates, *Eur. J. Inorg. Chem*, **2013**,1556–1967.
12. Dolbecq, E. Dumas, C. R. Mayer, P. Mialane, Hybrid Organic–Inorganic Polyoxometalate Compounds: From Structural Diversity to Applications, *Chem. Rev.* **2010,**110, 6009-6048.

13. D.L. Long, E. Burkholder, L. Cronin, Polyoxometalate clusters, nanostructures and materials: From self assembly to designer materials and devices, *Chem. Soc. Rev.* **2007,** 36, 105-112.
14. Hasenknopf, *Front. Biosci.* Polyoxometalates: introduction to a class of inorganic compounds and their biomedical applications, *Front. Biosci.,* **2005**, 10, 275-287.
15. M. Sadakane, E. Steckhan, Electrochemical Properties of Polyoxometalates as Electrocatalysts, *Chem. Rev.* **1998,** 98, 219.
16. A. Proust, B. Matt, R. Villanneau, G. Guillemot, P. Gouzerh , G. Izzet, Functionalization and post-functionalization: a step towards polyoxometalate-based materials, Chem. Soc. Rev**. 2012**, 41, 7605-7622.
17. S. Thorimbert, B. Hasenknopf, E. Lacôte, Cross-Linking Organic and Polyoxometalate Chemistries, *Isr. J. Chem*. **2011**, 51, 275-280.
18. J. Zhang, F. Xiao, J. Hao, Y. Wei, The chemistry of organoimido derivatives of polyoxometalates, *Dalton Trans.* **2012**, 41, 3599-3615.
19. Bustos, D. Mac-Leod Carey, K. Boubekeur, R. Thouvenot, A. Proust, P. Gouzerh, Aryldiazenido derivatives: A new entry to the functionalization of Keggin polyoxometalates, *Inorg. Chim. Acta* **2010**, 363, 4262-4268.
20. B. Matt; S. Renaudineau; LM. Chamoreau; C. Afonso; G. Izzet, A. Proust, Hybrid Polyoxometalates : K
21. eggin and Dawson Silyl Derivatives as Versatile Platforms*, J. Org. Chem.* **2011**,76, 3107-3112.
22. K. Nomiya, Y. Togashi, Y. Kasahara, S. Aoki, H. Seki, M. Noguchi, S. Yoshida, Synthesis and Structure of Dawson Polyoxometalate-Based, Multifunctional, Inorganic–Organic Hybrid Compounds: Organogermyl Complexes with One Terminal Functional Group and Organosilyl Analogues with Two Terminal Functional Groups, *Inorg. Chem.* **2011**, 50, 9606-9619.
23. N. Joo, S. Renaudineau, G. Delapierre, G. Bidan, L.-M. Chamoreau, R. Thouvenot, P. Gouzerh, A. Proust, Organosilyl/germyl polyoxotungstate hybrids for covalent grafting onto silicon surfaces : towards molecular memories,*Chem. Eur. J.* **2010**,16, 5043-5051.
24. R. Villanneau, D. Racimor, E. Messner-Henning, H. Rousselière, S. Picart, R. Thouvenot, A. Proust, Insights into the Coordination Chemistry of Phosphonate Derivatives of Heteropolyoxotungstates, *Inorg. Chem.* **2011**, 50,1164-1166.

25. L. F. Piedra-Garza, S. Reinoso, M. H. Dickman, M. M. Sanguineti, U. Kortz, The first 3-dimensional assemblies of organotin-functionalized polyanions *Dalton Trans.* **2009**, 38, 6231-6234.
26. G. Sazani, M. T. Pope, Organotin and organogermanium linkers for simple, direct functionalization of polyoxotungstates, *Dalton Trans.* **2004,**1989-1994.
27. F. Zonnevijlle, M. T. Pope, Attachment of organic groups to heteropoly oxometalate anions, *J. Am. Chem. Soc.* **1979**, 101, 2731– 2732.
28. J. Shum, N. Paul, Chemically modified primers for improved multiplex PCR, *Anal Biochem.* **2009**, 388, 266-272.
29. J. Pandey, K. Ganesa, R. K. Jain, Variations in T-RFLP profiles with differing chemistries of fluorescent dyes used for labeling the PCR primers, *J. Microbiol. Meth.* **2007**, 68, 633-638.
30. R. A. Fekete, M. J. Miller, D. K. Chattoraj, Fluorescently labeled oligonucleotide extension: a rapid and quantitative protocol for primer extension, *BioTechniques* **2003,** 35, 90 – 94.
31. T. Koch , N. Jacobsen , J. Fensholdt, U. Boas, M. Fenger, H. M. Jakobsen, Photochemical Immobilization of Anthraquinone Conjugated Oligonucleotides and PCR Amplicons on Solid Surfaces, *Bioconjugate. Chem.* **2000**, 11, 474.
32. S. A. Brazill, P. H. Kim, W. G. Kuhr, Capillary Gel Electrophoresis with Sinusoidal Voltammetric Detection: A Strategy To Allow Four-"Color" DNA Sequencing, *Anal. Chem.* **2001**, 73**,** 4882.
33. S. A. Brazill, W. G. Kuhr, A Single Base Extension Technique for the Analysis of Known Mutations Utilizing Capillary Gel Electrophoreisis with Electrochemical Detection, Anal. *Chem*. **2002**, *74*, 3421.
34. H. B. Shen, M. Hu, Y. B. Wang, H. Q. Zhou, Polymerase chain reaction of nanoparticle-bound primers, *Biophys. Chem.* **2005**, 115, 63-66.
35. R. Contant *Inorg. Synth*. **1990**, **27**, 107.
36. Tézé, G. Hervé, R. G. Finke, D. K. Lyon, *Inorg. Synth*. **1990,** 27, 85-96.
37. Boglio, K. Micoine, E. Derat, R. Thouvenot, B. Hasenknopf, S. Thorimbert, E. Lacote, M. Malacria, Regioselective Activation of Oxo Ligands in Functionalized Dawson Polyoxotungstates, *J. Am. Chem. Soc.* **2008**, 130, 4553-4561.
38. A. M. Debela, M. Ortiz, C. K. O´Sullivan, S. Thorimbert, B. Hasenknopf, Postfunctionalization of Keggin silicotungstates by general coupling procedures *Polyhedron,* **2014**, 68, 131-137.

39. K. Micoine, B. Hasenknopf, S. Thorimbert, E. Lacôte, M. Malacria, A General Strategy for Ligation of Organic and Biological Molecules to Dawson and Keggin Polyoxotungstates, *Org. Lett.* **2007**, 9, 3981-3984.
40. The images were processed using Nanotec Electronica WSxM freeware: I. Horcas, R. Fernández, J. M. Gómez-Rodriguez, J. Colchero, J. Gómez-Herrero and A. M. Baro, *Rev. Sci. Instrum.,* **2007**, **78**, 013705.
41. P. Kele, X. Li, M. Link, K. Nagy, A. Herner, K. Lőrincz, S. Béni, O. S. Wolfbeis , Clickable fluorophores for biological labeling--with or without copper, *Org. Biomol. Chem*. **2009**, **7**, 3486-3490.
42. F.Wilson, H. N. Miras, M. H. Rosnes, L. Cronin, Real-Time Observation of the Self-Assembly of Hybrid Polyoxometalates Using Mass Spectrometry, *Angew. Chem. Int. Ed.* **2011**, 50, 3720 – 3724.
43. Rocchiccioli-Deltcheff, M. Fournier, R. Franck, R. Thouvenot, Vibrational Investigations of Polyoxometalates. 2. Evidence for Anion-Anion Interactions in Molybdenum (V1) and Tungsten (V1) Compounds Related to the Keggin Structure, *Inorg. Chem*. **1983**, 22, 207–216
44. M. Granadeiro, R. A. S. Ferreira, P. C. R. Soares-Santos, L. D. Carlos, H. I. S. Nogueira, Lanthanopolyoxometalates as Building Blocks for Multiwavelength Photoluminescent Organic–Inorganic Hybrid Materials, *Eur. J. Inorg. Chem.*, **2009**, 5088–5095.
45. A. Barhoumi, D. Zhang, F. Tam, N. J. Halas, Surface-Enhanced Raman Spectroscopy of DNA, *J. Am. Chem. Soc.* **2008**, 130, 5523–5529.
46. N.E. Triggs, J. J. Valentin, An investigation of hydrogen bonding in amides using Raman spectroscopy, *J. Phys. Chem*. **1992**, 96, 6922-6931.
47. H. Sawai, A. Ozaki-Nakamura, M. Mino, H. Ozaki, Synthesis of New Modified DNAs by Hyperthermophilic DNA Polymerase: Substrate and Template Specificity of Functionalized Thymidine Analogues Bearing an sp^3-Hybridized Carbon at the C5 α-Position for Several DNA Polymerases, *Bioconjugate Chem*. **2002**, 13, 309–316.
48. B. Matt, X. Xiang, L. A. Kaledin, N. Han, J. Moussa, H. Amouri, S. Alves, C. L. Hill, T. Lian, G. D. Musaev, G. Izzet, A. Proust, Long lived charge separation in iridium(III)-photosensitized polyoxometalates: synthesis, photophysical and computational studies of organometallic–redox tunable oxide assemblies, *Chem. Sci.,* **2013**, 4, 1737–1745.

49. B. Keita, F. Girard, L. Nadjo, R. Contant, J. Canny, M. Richet, Metal ion complexes derived from the α_1 isomer of $(P_2W_{17}O_{61})^{10-}$: comparison with the corresponding α_2 species, *J. Electroanal. Chem.* **1999**, 478, 76-82.

Supporting information

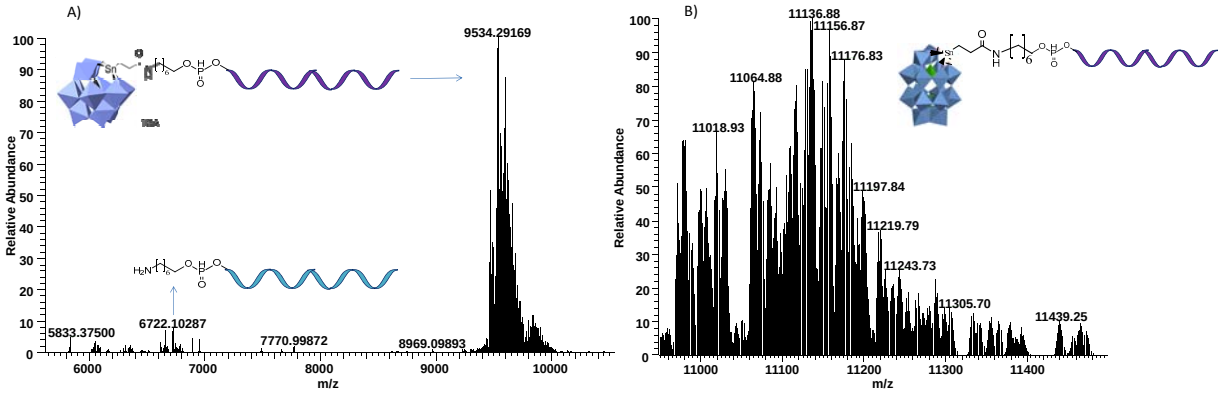

Figure S1. ESI MS of POM modified primers the spectra are after deconvolution of the peaks obtained for the various charged species. The results show clearly the POM modification of the primers where the base peaks belongs to the POM + DNA masses.

Table S1. Raman shift assignments for functionalised Dawson POMs

Compound	P-O	W=O	W-O_b-W	W-O_c-W
$K_8P_2W_{18}O_{62}$	1025	994 968	921 858	-
$K_{10}P_2W_{17}O_{61}$	1023	974 963	885	802
$(TBA)_4P_2W_{17}O_{61}SnC2H4COOH$	1059	984 969	919 882	797
$(TBA)_5P_2W_{17}O_{61}SnC_2H_4CO$	1058	985 965	902 885	767
$(TBA)_6P_2W_{17}O_{61}SnC2H4CO$-DNA	1057	981 967	910 865	792

Table S2. Raman shift values for functionalised Keggin POMs.

Compound	W=O	W-O_b-W	W-O_c-W	W-$O_{b/c}$-W
$K_8SiW_{11}O_{39}$	979 923	878	805	524
$(TBA)_4SiW_{11}O_{39}SnC_2H_4COOH$	986 965	909 885	801	524
$(TBA)_5SiW_{11}O_{39}SnC_2H_4CO$	985 965	913 888	785	527
$(TBA)_6SiW_{11}O_{39}SnC_2H_4CO$-DNA	923 978	865	805	522

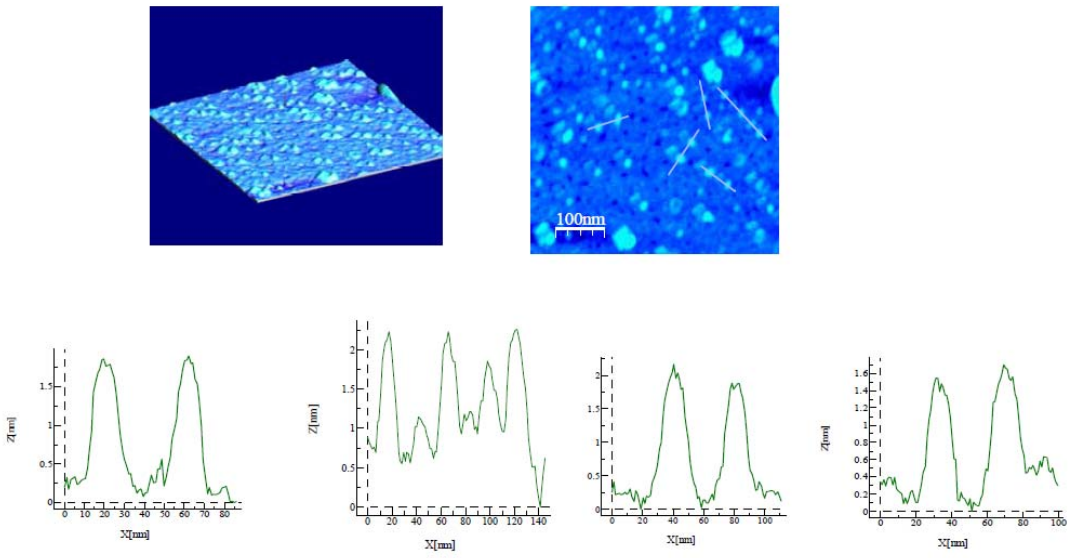

Figure S2 . 2D (left) and 3D (right) AFM pictures of Keggin POM. Bottom part: profiles of POM.

Chapter 5.

Design Synthesis characterisation and PCR incorporation polyoxometalate labeled nucleotides

Ahmed M. Debela[a], *Mayreli Ortiz*[a], Marketa Svobodova, *Serge Thorimbert* [c], *Bernold Hasenknopf* [c] *Ciara K. O´Sullivan,*[a,b]

[a]*Departament d'Enginyería Química, Universitat Rovira i Virgili, Avinguda Països Catalans, 26, 43007 Tarragona, Spain,*

[b]*ICREA, Passeig Lluis Companys 23, 08010 Barcelona, Spain*

[c]*UPMC Univ Paris 06, Institut de Chimie Moléculaire UMR CNRS 7071, 4 place Jussieu, 75252 Paris Cedex 05, France.*

Design Synthesis characterisation and PCR incorporation polyoxometalate labeled nucleotides

Ahmed M. Debela[a], *Mayreli Ortiz*[a], Marketa Svobodova, *Serge Thorimbert* [c], *Bernold Hasenknopf* [c] *Ciara K. O´Sullivan,*[a,b]

[a]*Departament d'Enginyería Química, Universitat Rovira i Virgili, Avinguda Països Catalans, 26, 43007 Tarragona, Spain,*

[b]*ICREA, Passeig Lluis Companys 23, 08010 Barcelona, Spain*

[c]*UPMC Univ Paris 06, Institut de Chimie Moléculaire UMR CNRS 7071, 4 place Jussieu, 75252 Paris Cedex 05, France.*

Abstract

The design, synthesis, characterisation and use in PCR for polyoxometalate modified nucleotides described. POMs were linked at 7 deaza modified of purines and 5 deaza modified pyrimidines by adopting a method developed for linking activated carboxy POMs with amine terminated molecules. The synthesised POM –nucleotide conjugates were characterised high resolution ESI MS. The conjugates were subsequently used in PCR along with unmodified dNTPs. The gel electrophoresis analysis showed amplification until 60% substitution of the natural dNTP for Keggin (SiW_{11}) POM modified dNTPs. The hindrance of amplification is pronounced for Dawson POM (P_2W_{17}) dNTPs, amplification only observed for substitution less than 20% of the modified dNTPs. The electrochemical characterisation of the amplified amplicons showed redox potentials corresponding to the POMs a redox potential suitable for electrochemical APEX.

Introduction

Electrochemical DNA sensors are one of the most attractive tools for genetic analysis of infections, inherited diseases as well as cancer. Varieties of redox active species are used to conjugate with DNA to increase sensitivity of detection. These species are selected for use in DNA sensing based their redox potential (with in -0.9V to 0.9V potential window vs Ag/AgCl) in such a way no damage occurs to the probe on the surface as a result of the redox reaction. There are three groups of labels used for DNA labeling, the first group of

labels are the so called groove binders which preferentially bind to DNA duplex, the second class of labels make use of the electrostatic interaction with DNA sugar phosphate back bone, and the third class of labels are the result of the progress in synthetic methodologies to functionalise DNA. The latter class has received enourmous arttention due to the improved stability and reliability of the covalent bond formed. This class was also employed to functionalise DNA nucleotides for enzymatic incorporation. A number redox labels such as ferrocene[1], [Ru/Os(bpy)$_3$] complexes (bpy=2,2'-bipyridine)[2] , amino and nitrophenyl groups[3]. The interesting feature of this class of labels is the enzymatic incorporation can be further utilised in a similar fashion as the 'four colour' genothyping method by electrochemicaly monitoring the incorporation of the redox potential of the incorporated.Despite their interesting characteristics the above mentioned labels are far from being used for diagnostic application due to limited stability in air or in moisture[4]. So the search for highly stable, low cost and easy to functionalise lables is highly desirable.

Polyoxometalates (POMs) are nanometer sized transitional metal oxide clusters with a spectrum of potential applications in catalysis[5-9], medicine[11], material science[6, 7, 9, 10] photo and electrochromism[6] as well as magnetism[7,12]. Among the many interesting properties POMs possess, is their rich redox chemistry, with stable redox states, and multiple electron-transfer steps[13]. Furthermore these properties can be controlled and fine-tuned through organic functionalisations and variations of either the heteroions and/or addenda ions to make them attractive candidates for selective, long-lived, stable, and tunable redox-active devices[14]. Interestingly their dimensions are on the same scale as biomolecules, but denser and more regular in size, unveiling exciting possibilities for their interaction with biological species. The aforementioned properties together with the high surface area, the improved surface reactivity, and rapid heterogeneous electron transfer make these materials invaluable potential candidates for bioelectroanalytical applications. Functionalisation of POMs do not only broaden their applications but also improve long-term stability, solubility, redox behavior, spectroscopic response and biological activities of the clusters as well as facilitating the construction of novel POM based functional materials[15-19]. Organic functionalisation of POMs has been carried out via either placement of oxo ligands with different organic groups such as imido[20] or diazenido[21] or the coupling of lacunary POMs with organosilyl/germyl[22] organo-phosphoryl/phosphonates[23] and organotin derivatives[24-26]. Among the various

functionalisation strategies the route utilising organotin incorporation into hetropolytungstates known to provide[25, 26] robust and hydrolytically stable oxide clusters which will be functional under physiological conditions.

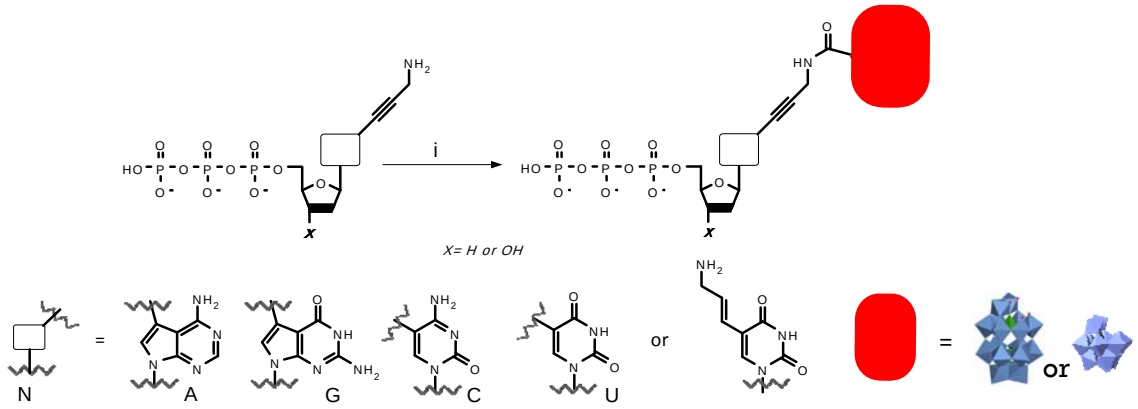

Scheme 5. 1. Showing the method followed for the synthesis of the POM modified (di)deoxynucleotides [d(d)NTPs] (the reaction is carried out in freshly distilled acetonitrile with catalytic amount of triethyl amine] at 37oC for 24hrs.)

In this work we are attempting to use POMs (Keggin and Dawson) for functionalisation of nucleotides with intention of enzymatic labeling of DNA using KOD XL polymerase. Activated mono-oxo acylated polyoxotungstates $[SiW_{11}O_{39}\{Sn(CH_2)_2CO)\}]^{8-}$ (SiW_{11}Sn-Keggin) and$[P_2W_{17}O_{61}\{Sn(CH_2)_2CO)\}]^{6-}$ (P_2W_{17}Sn-Dawson) POMs were used to couple with propargyl amino derivatised nucleotides. (See the schematic of functionalisation). The synthesised nucleotides were characterised by high resolution ESI MS spectroscopy. The POM functionalised dNTPs were used in PCR along with other natural dNTPs.and agarose gel was used to characterise the amplified products. Furthermeore electrochemical techniques were utilised to characterise both the modified dntps and the amplified products.

Materials and methods

All chemicals and reagents used were of analytical grade. Sodium chloride (NaCl, Probus), potassium chloride (KCl, Fluka), sodium perchlorate ($NaClO_4$, Acros Organics), mercaptohexanol (MCH, Fluka), sodium hydroxide, Sulfuric acid (95-97%), trizma base, and boric acid were purchased from Scharlau (Barcelona, Spain). Hydrochloric acid(35%, Panreac), Phosphate-buffered saline (PBS), trisodium citrate, acetone, dimethyl sulfoxide

(DMSO), perchloric acid(70%), triethyl amine, glacial acetic acid, Ethylenediaminetetraacetic acid disodium salt dihydrate 99% (EDTA), were all purchased from Sigma Aldrich. Unfunctionalised Dawson[27a] and Keggin[27b] POMs and functionalised and activated Dawson POMs $TBA_6[\alpha_2\text{-}P_2W_{17}O_{61}\{SnCH_2CH_2C(=O)\}]$[28] and Keggin POMs $TBA_4[SiW_{11}O_{39}\{SnC_2H_4C(=O)\}]$[29] Unless otherwise noted, all reactions were carried out under argon atmosphere with magnetic stirring. Acetonitrile was dried and distilled over CaH_2.

DNA Sequences

HPLC purified synthetic oligonucleotide sequences were purchased from Biomers (Germany). The sequences were used for PCR reaction to study the incorpotration of the modified dNTPs.

Francisella Tularensis target amplicon: 5′AAG GAA GTG TAA GAT TAC AAT GGC AGG CTC CAG AAG GTT CTA AGT GCC ATG ATA CAA GCT TCC CAA TTA CTA AGT ATG CTG AGA AGA ACG ATA AAA CTT GGG CAA CTG TAA CAG TT3′

Francisella Tularensis reverse primer: 5′- biotin CGC TAC AGA AGT TAT TAC CTT GCT TAA CTG TTA-3’

Francisella Tularensis forward primer: 5′-NH_2-$(CH_2)_6PO_3$--ATT ACA ATG GCA GGC TCC AGA-3′)

KOD XL DNA polymerase was purchased from Merck Millipore (Barcelona), unmodified nucleotide triphosphates (dATP, dCTP, dGTP and dTTP) are from Invitrogen.

Propargyl amino derivatised dATP, ddATP, dCTP, ddCTP, dGTP ddGTP, ddUTP and amino allyl dUTP were obtained from genabioscience (Germany).

Procedure for coupling activated POMs with propargyl amino d (d)NTPs: To a freeze dried samples of the propargyl amino bearing d(d)NTPs (100nmol) was added 5µls of triethyl amine followed by addition of 80µl of 1.25mM solution of the activated POMs in freshly distilled acetonitrile. The reaction kept stirring at 37°C for 24hrs. The ESI MS was taken in acetonitrile.

PCR amplification and purification: For the amplification of a Francisella Tularensis associated 128-base target, 400 nM of forward primer (5′-ATT ACA ATG GCA GGC TCC

AGA-3′) and 5′biotinylated reverse primer (5′Biot-CGC TAC AGA AGT TAT TAC CTT GCT TAA CTG TTA-3), 10xPCR buffer, 200mM dNTPs, 1unit of the KOD polymerase were mixed. Amplification was performed in a iCycler Thermal Cycler. (Biorad), with amplification conditions being 2 min at 95°C, followed by 30 cycles of 20 s at 95 °C, 20 s at 60 °C, and 20 s at 72 °C and a final extension step at 72°C for 7 min. At the end of the program, the tubes were held at 4°C.

Mass spectroscopy: A LTQ-Orbitrap XL (Thermo Electron Corporation, Bremen, Germany) mass spectrometer equipped with an ESI source was used to acquire high resolution mass spectra. The experiments were performed in negative ion mode. Nitrogen was used as a sheath gas. Spray voltage was set at 4.5 kV for all experiments. 10μM POM modified primer were dissolved in a mixture of acetonitrile/water/methanol (80%/10%/10%). The solutions were subjected to ESI and infused continuously at a flow rate of 20 μl per min. The mass spectrometer was set for three microscans, an activation time of 30 ms, normalised collision (radial resonant excitation) energies were between 5 and 50%, and isolation window was set at 2.0 Th for LTQ and 1.4 Th for Orbitrap, The resolution was set to 100 000 (FWHM at m/z 400). Mass spectra were acquired between 4000 and 100 *m/z* with a scan speed of 1os/scan. All acquired data were analysed using Xcalibur 2.0.7 software (Thermo Finnigan) and the results were compared with those simulated by mMass.

***Gel electrophoresis analysis*:** □□l of each ssDNA sample, with □□l of 6x loading buffer (40% glycerol and bromophenol blue), was loaded on a 2.4% agarose gel stained with GelRed nucleic acid stain (Biotium). Synthetic ssDNA of known concentrations was prepared in the same manner as the samples and loaded together. Gels were analysed with ImageJ software.

Electrochemical Measurements*:* All electrochemical measurements were carried out using an Autolab model PGSTAT 12 potentiostat/galvanostat controlled with the General Purpose Electrochemical System (GPES) software (Eco Chemie B.V., The Netherlands). A classic three electrode set up was used with a Ag/AgCl reference electrode, Pt wire counter electrode and gold working electrode (diameter of 2mm), which were purchased from CHI Instruments. All the potentials are recorded with respect to the reference electrode.

Electrode preparation: drop sense gold electrodes were used for echecking the electrochemical property of the PCR products. The activation of the GCEs was performed in saturated sodium carbonate solution for 2 min at a potential of 1.2 V vs Ag/AgCl to eliminate any hydrocarbon adsorbed from the environment, followed by sweeping the potential for 10 cycles between 0 and 1.0 V vs Ag/AgCl at 250 mV/s in 0.1 M sodium perchlorate.

Result and discussion

Design and synthesis of POM labeled nucleotides: various deoxy and dideoxy triphosphates analogues of all the four natural nucleotides bearing Dawson POM ($P2W_{17}Sn$-) or Keggin POM ($SiW_{11}Sn$) were synthesised. Plethora of literatures shows that modification at position 5 of pyrimidine and position 7 of purine nucleotides are tolerable for enzymatic incorporation and without the destabilisation of the helical structure[30]. It is also known that the introduction of acetylene linker between the nucleobase and a bulky substituent will make the modified dNTPs better substrates for incorporation in to a growing DNA strand. Commercially available nucleotide triphosphates with modification at position 5 of pyrimidines (C ,U) and position 7 of purines (A,G) were utilised to functionalise with activated POMs following the method developed for linking POMs with amine terminated oligonucleotides [see chapter 4] and other small molecules [28,29] with slight modification such as the use of freshly distilled acetonitril solution with slight amount of triethyl amine to avoid the possible degradation of the phosphate groups as well as loss of POM activeity as a result of ring opening. High resolution electron spray mass spectroscopy (ESI MS) was utilised to characterise the products.

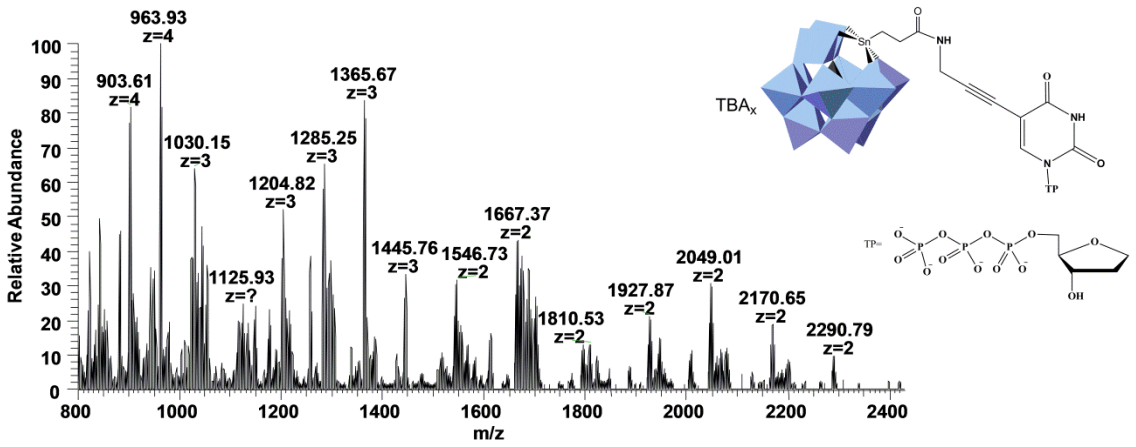

Figure 5. 1. ESI MS spectra of (Keggin) SiW11 POM modified dUTP

Table 5. 1. Data extracted from the ESI MS spectra of the Keggin (SiW_{11}) Modified dUTP

Entry	Charge	Simulated(m/z)	Observed(m/z)	Composition(Keggin-dUTP)
1	2	1686.5882	1686.88916	(TBA)2(K-COC12H19N3O14P3)
2	2	1807.7306	1807.52722	(TBA)3(KCOC12H19N3O14P3)
3	3	1124.3923	1124.25647	(TBA)3(KCOC12H19N3O14P3)
4	2	1928.873	1928.87268	(TBA)4(KCOC12H19N3O14P3)
5	3	1205.1539	1205.4873	(TBA)4(KCOC12H19N3O14P3)
6	4	843.2944	843.2948	(TBA)4(KCOC12H19N3O14P3)
7	2	2050.0153	2050.0127	(TBA)5(KCOC12H19N3O14P3)
8	3	1285.9155	1285.24512	(TBA)5(KCOC12H19N3O14P3)
9	4	903.8656	903.61346	(TBA)5(KCOC12H19N3O14P3)
10	5	674.6356	674.83459	(TBA)5(KCOC12H19N3O14P3)
11	6	562.1964	562.02753	(TBA)6(KCOC12H19N3O14P3)
12	5	723.0926	723.80505	(TBA)6(KCOC12H19N3O14P3)
13	4	964.4367	964.43298	(TBA)6(KCOC12H19N3O14P3)
14	3	1366.6771	1366.67151	(TBA)6(KCOC12H19N3O14P3)
15	2	2171.1577	2171.65381	(TBA)6(KCOC12H19N3O14P3)
16	2	2292.3001	2292.29004	(TBA)7(KCOC12H19N3O14P3)
17	3	1447.4387	1448.0979	(TBA)7(KCOC12H19N3O14P3)
18	4	1025.0079	1025.50269	(TBA)7(KCOC12H19N3O14P3)
19	2	1616.006	1616.4375	(TBA)(TEA)(KCOC12H19N3O14P3)
20	3	1238.8607	1236.64014	(TBA)4(TEA)(KCOC12H19N3O14P3)
21	5	646.4027	647.31769	(TBA)4(TEA)(KCOC12H19N3O14P3)

ESIMS characterisation of the modified nucleotides: POMs have isotopic sets of signals arising from stable isotopes of the core transition metals (W, Mo), which can be fitted to

determine the exact formula[31] and are thus POMs are highly suited to characterisation using ESI MS. Various peaks corresponding to the functionalised POMs with charge states 2-, 3- 4^-, 5^- with counter ions tetra butyl ammonium (TBA [$C_{16}H_{36}N$]) and triethyl amine (TEA [$C_6H_{15}N$]) were observed. Figure 5. 1 and table 5. 1 show signals obtained for SiW_{11}-dNTPs with m/z ranging from 800-2400. Similar analysis was performed for P_2W_{17} modified dUTP and various charge states -4, 3-, 2- and of the clusters were observed in the m/z range from 1200-2700. The tables 1 and 2 show the peaks corresponding to the various species representing the POM –dNTP linkage. Similar analysis was performed for the other 3 dNTPs modified with Keggin (SiW_{11}) or Dawson (P_2W_{17}) POMs showing the successful synthesis of the four dNTPs. (See supporting information).

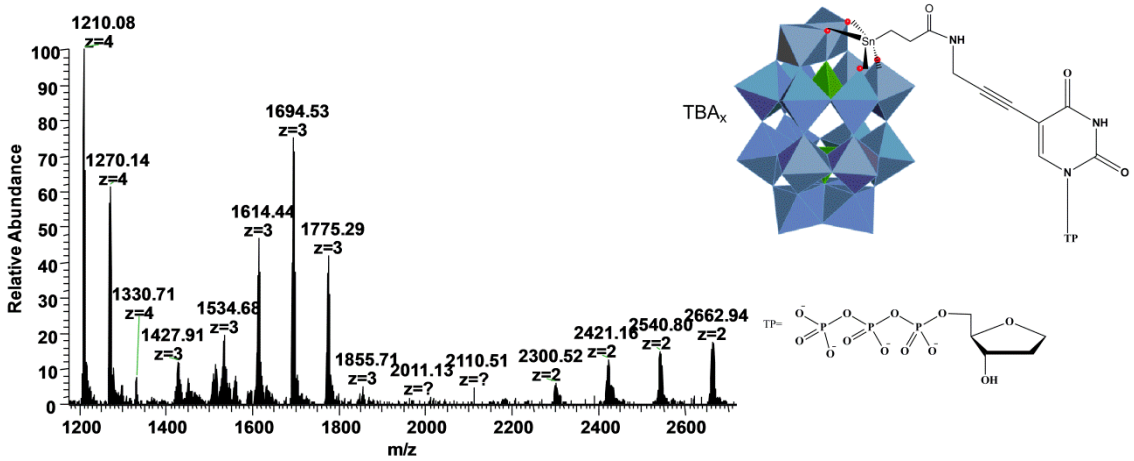

Figure 5. 2. ESI MS sppectra of Dawson (P2W17) POM modified dUTP

Table 5. 2. Data extracted from the ESI MS of Dawson (P2W17) dUTP

Entry	Charge	Simulated(m/z)	Observed(m/z)	Composition(Dawson-dUTP)
1	2	2431.3703	2430..34	(TBA)2(DCOC12H19N3O14P3)
2	3	1620.9137	1620.22	(TBA)3(D-COC12H19N3O14P3)
3	3	2552.5127	2552.97	(TBA)3(DCOC12H19N3O14P3)
4	4	1215.6854	1215.84	(TBA)4(DCOC12H19N3O14P3)
5	3	1701.6753	1701.54	(TBA)4(DCOC12H19N3O14P3)
6	2	2673.6551	2674.97	(TBA)4(DCOC12H19N3O14P3)
7	4	1276.2566	1277.15637	(TBA)5(DCOC12H19N3O14P3)
8	3	1782.4369	1783.63623	(TBA)5(DCOC12H19N3O14P3)
9	2	2794.7975	2797.59766	(TBA)5(DCOC12H19N3O14P3)
10	3	1863.1985	1859.05029	(TBA)6(DCOC12H19N3O14P3)
11	4	1336.8278	1337.07703	(TBA)6(DCOC12H19N3O14P3)
12	4	1397.399	1396.26025	(TBA)7(DCOC12H19N3O14P3)
13	5	1069.4624	1067.00513	(TBA)7(DCOC12H19N3O14P3)
14	3	1573.859	1571.77271	(TBA)2(TEA)(DCOC12H19N3O14P3)
15	4	1180.3944	1179.57593	(TBA)3(TEA)(DCOC12H19N3O14P3)
16	3	1654.6206	1654.52673	(TBA)3(TEA)(DCOC12H19N3O14P3)
17	4	1240.9656	1239.146	(TBA)4(TEA)(DCOC12H19N3O14P3)

Enzymatic incorporation of the different modified dNTPs: The enzymatic incorporation of POM modified dNTPs in PCR was studied by substituting portion of the the natural dNTPs with the modified using KOD XL polymerase. Optimisation of the POM –dNTP concentration was performed by substitution various percentages (12.5%, 25%, 50% 60%, 70%, 80%, 90% anddd100%) of the unmodified for its natural counterpart (the percentage is relative to the normal concentration dNTPs). As shown in figure 1, for Keggin POM modified dUTP, Close to 100% amplicon formation was observed until 60% of the modified dNTP increasing the percentage became deleterious resulting in reduced amplicon yield for 70% of the modified dUTP with amplicon yield of 49% relative the control. Amplicon formation was not detectable beyond 80% substitution of the modified dNTP. Difficult amplicon formation was observed for Dawson POM modified dUTP, where no amplicon formation was detected beyond 25% substitution of the POM modified dUTP (Figure 5.2). The plausible explanations for this would be a) bigger size of

the Dawson POM which would be difficult as the concentration increases. The POM mayhave inhibited the polymerase as concentration increased.

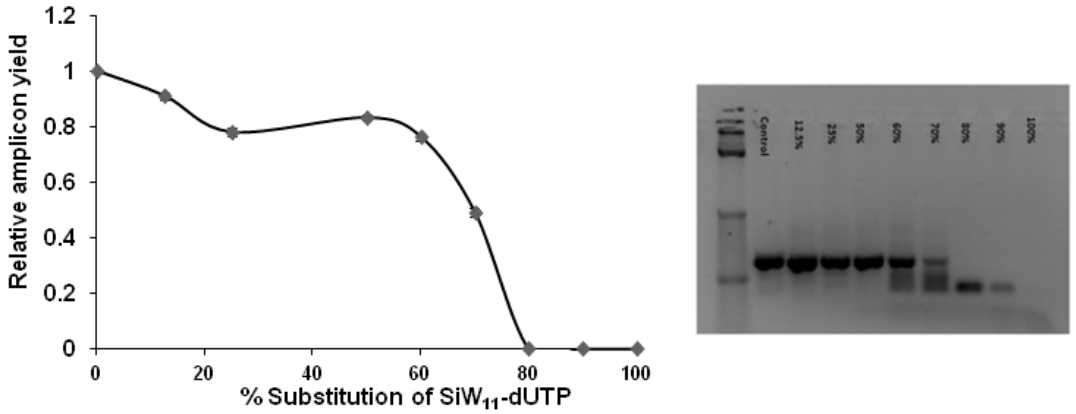

Figure 5. 3. PCR amplicon yields for SiW11-dUTP incorporation studies.and agarose gel analysis of the PCR conditionswith various percentage of the modified dUTP titrated between 0% and 100 %.(percentage is the percentage of biotinylated nucleotide substitution for its natural counterpart)

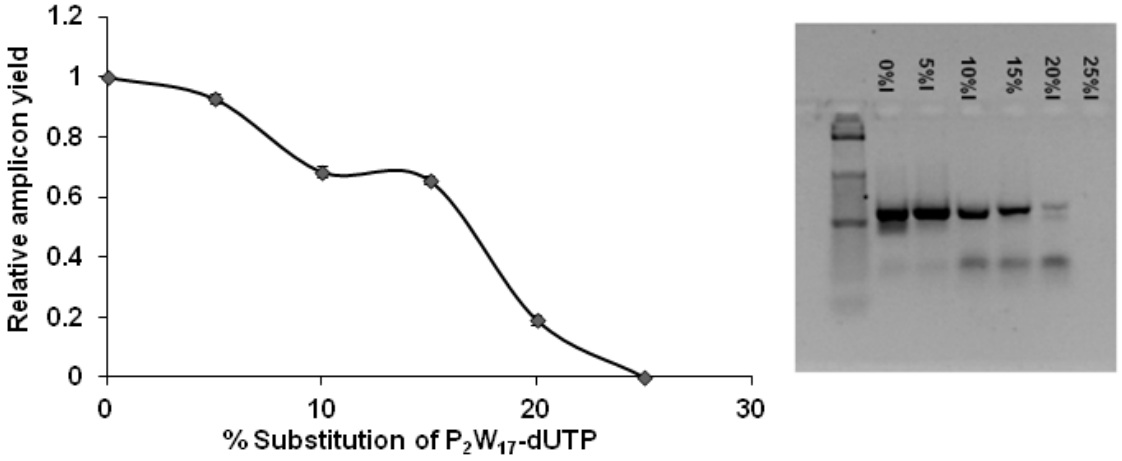

Figure 5. 4. PCR amplicon yields for P2W17-dUTP incorporation studies. And agarose gel analysis of the PCR conditions with various percentage of the modified dUTP titrated between 0% and 25%.

Similar trend was observed with POM modified dCTP. The optimisation work was utilised to amplify with 15-20% substitution of the Dawson POM modified dCTPs, dATP, dGTP and dUTP and a separate PCR reaction tube with 5% of the modified each of the four dNTPs (making 20%V/V relative to the final volume) in one PCR mix [see Figure 5. 5].

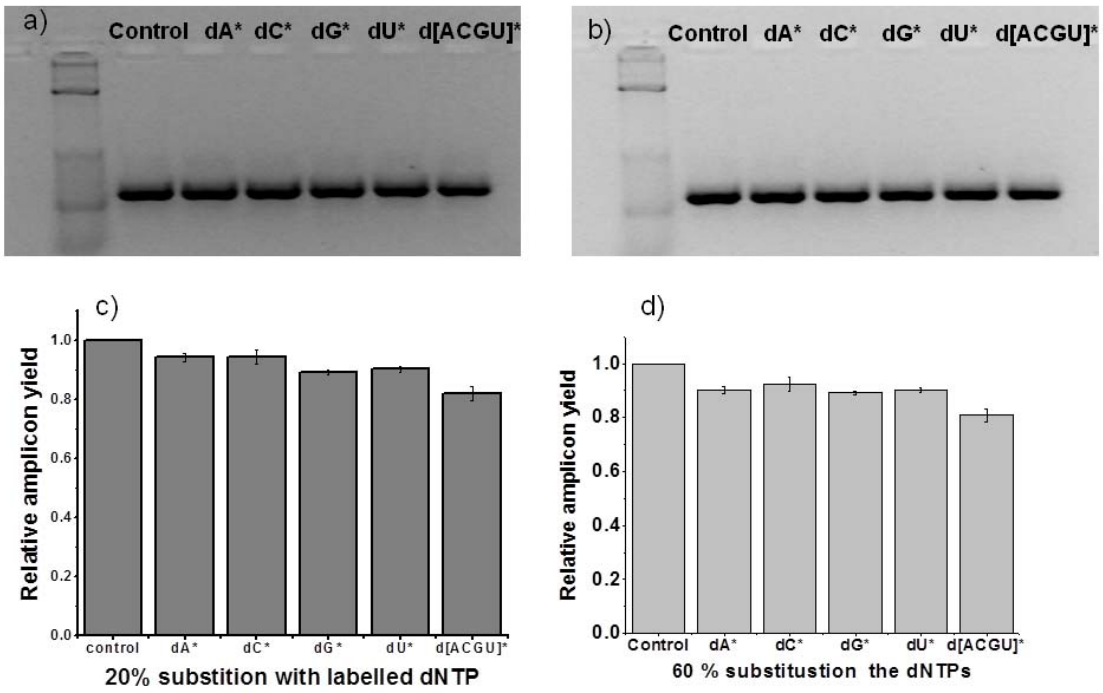

Figure 5. 5. PCR amplicon yields after substitution of 20% of P2W17 modified dNTPs (for each of the four) with their natural counterparts. And a final set of PCR reaction was run for PCR mix containing all the four modified dNTPs (figures a and c). (After substitution of 5% of their natural counter parts). And the corresponding results for 60% substitustion of SiW11 Modified dNTPs for their natural counter parts (figures b and d). The agarose gel analysis of the PCR products was run for 25mn at 110mV potentials.

Electrochemical characterisations: Electrochemical properties of POM labeled nucleotides, dNTPs and POM bearing amplicons were studied by differential pulse voltametry (DPV) on dropsense electrodes. Compared to the free POMs (see supporting

for carboxy bearing P_2W_{17} and chapter 3 for Keggin POM) with 2 or 3 redox wave, POM bearing dNTPs or PCR amplicons happened to give only a single broad peak in the region -0.4 till -0.15 showing with anodic shift by more than 100mV. This suggests easier reduction (facile reduction) compared to the free POM.

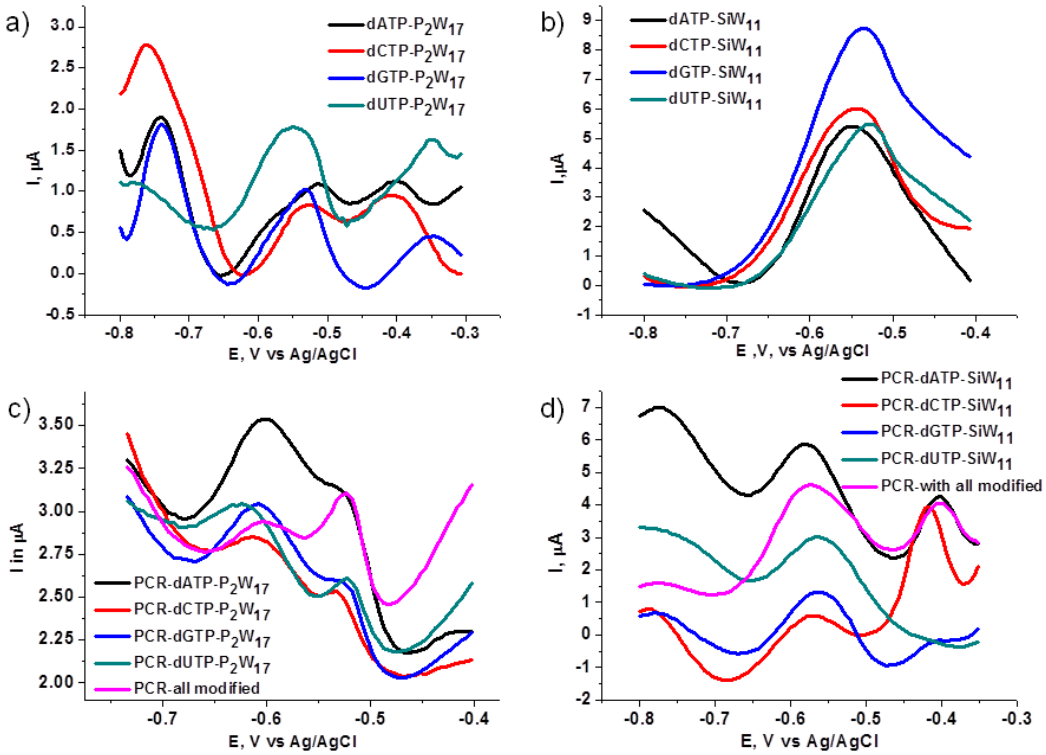

Figure 5. 6. DPV response obtained for POM-modified dNTPs (a and b) and the PCR products (POMs bearing amplicons) obtained after substitution with the natural counterparts (c and d). The DPVs were made on screen printed gold electrodes in 0.1 M $NaClO_4$ solution

Conclusions

Design, synthesis, characterisation and use in PCR for POM modified dNTPs were described. POMs were linked at 7 deaza modified of purines and 5 deaza modified pyrimidines by adopting a method developed for linking activated carboxy POMs with amine terminated molecules. The synthesised POM –nucleotide conjugates were characterised high resolution ESI MS. The conjugates were subsequently used in PCR along with unmodified dNTPs. The gel electrophoresis analysis showed amplification

until 60% substitution of the natural dNTP for Keggin (SiW_{11}) POM modified dNTPs. The hindrance of amplification is pronounced for Dawson POM (P_2W_{17}) dNTPs, amplification only observed for substitution less than 20% of the modified dNTPs. These labeled dNTPS will be exploited for the highly sensitive direct electrochemical detection of PCR products.

References

1. (a)N. E. Heberta, S. A Brazill., Microchip capillary gel electrophoresis with electrochemical detection for the analysis of known SNPs, *Lab Chip,* **2003**, 3, 241–247 (b) P. Brázdilová, M. Vrábel, R. Pohl, H. Pivoňková, L. Havran, M.Hocek, M. Fojta, Ferrocenylethynyl Derivatives of Nucleoside Triphosphates: Synthesis, Incorporation, Electrochemistry, and Bioanalytical Applications, *Chem. Eur. J.* **2007**, 13, 9527 – 9533
2. M.Vrábel, P. Horáková, H. Pivoňková, L. Kalachova, H. Černocká, H. Cahová, R. Pohl, P. Šebest, L. Havran, M. Hocek, M. Fojta, Base-Modified DNA Labeled by [Ru(bpy)3]2+ and [Os(bpy)3]2+ Complexes: Construction by Polymerase Incorporation of Modified Nucleoside Triphosphates, Electrochemical and Luminescent Properties, and Applications, *Chem. Eur. J.* **2009**, 15, 1144-1154
3. H. Cahova, L. Havran, P. Brazdilova, H. Pivonˇkova, R. Pohl, M. Fojta, M. Hocek, Aminophenyl- and Nitrophenyl-Labeled Nucleoside Triphosphates: Synthesis, Enzymatic Incorporation, and Electrochemical Detection, *Angew chem*. **2008,** 47, 2059-2062
4. Elschenbroich,A. Salzer, Organometallics, VCH, Newyork**, 1992**
5. L. Hill, special issue on polyoxometalates, *Chem. Rev*. 98,**1998**, 1–390,
6. L. Cronin and A. Müller, special issues, *Chem. Soc. Rev.* **2012**, 41, 7325-7648,
7. K. Hindson, U. Kortz and T. Liu, special issue on polyoxometalates, *Euro. J. Inorg Chem.,* **2013**, 1556–1967
8. Dolbecq, E. Dumas, C. R. Mayer, and P. Mialane, Hybrid Organic–Inorganic Polyoxometalate Compounds: From Structural Diversity to Applications, *Chem. Rev*. **2010,** 110, 6009–6048
9. D.L. Long, E. Burkholder, L. Cronin, *Chem. Soc. Rev*. **2007**, 36, 105–121
10. R. Neumann, Activation of Molecular Oxygen, Polyoxometalates, and Liquid-Phase Catalytic Oxidation, *Inorg. Chem.*, **2010,** 49, 3594–3601

11. (a) B. Hasenknopf, Polyoxometalates: introduction to a class of inorganic compounds and their biomedical applications, *Front. Biosci.* **2005,** 10, 275–287 (b) H.-K. Yang, Y.-X. Cheng, M.-M. Su, Y. Xiao, M.-B. Hu, W. Wanga, Q. Wang, Polyoxometalate–biomolecule conjugates: A new approach to create hybrid drugs for cancer therapeutics, *Bioorg. & Med. Chem. Lett*. **2013**, 23,1462–1466
12. U. Kortz, A. Müller, v. S. Joris, S. Juergen, D. Naresh and D. Martin, Polyoxometalates: Fascinating Structures, Unique Magnetic Properties, *Coord. Chem. Rev.*, **2009**, 253, 2315–2327.
13. M. T. Pope, In Mixed Valence Compounds; Brown, D. B., Ed.; D.Reidel: Dordrecht, **1980**; p 365. (b) M. Sadakane, E. Steckhan, Electrochemical Properties of Polyoxometalates as Electrocatalysts, *Chem. Rev.* **1998**, 98, 219-238
14. L. Shaoqin, V. Dirk, G. K. Dirk, Smart Polyoxometalate-Based Nitrogen Monoxide Sensors, *Anal. Chem.,* **2004**, 76, 4579-4582
15. P. Pradeep, M. F. Misdrahi, F.-Y. Li, J. Zhang, L. Xu, D. L. Long, T. Liu, L. Cronin, Synthesis of Modular "Inorganic–Organic–Inorganic" Polyoxometalates and Their Assembly into Vesicles, *Angew. Chem. Int. Ed*. **2009**, 48, 8309-8313.
16. A. Proust, B. Matt, R. Villanneau, G. Guillemot, P. Gouzerh , G. Izzet, Functionalization and post-functionalization: a step towards polyoxometalate-based materials, *Chem. Soc. Rev.* **2012**, 41, 7605-7622.
17. D. Li, P. Yin, T. Liu, Supramolecular architectures assembled from amphiphilic hybrid polyoxometalates, *Dalton Trans,* **2012**, 41, 2853-2861.
18. S. Thorimbert, B. Hasenknopf, E. Lacôte, Cross-Linking Organic and Polyoxometalate Chemistries, *Isr. J. Chem*. **2011**, 51, 275-280.
19. Y. Zhu, LS. Wang, J. Hao, ZC. Xiao, YG. Wei, Y. Wang, Synthetic, Structural, Spectroscopic, Electrochemical Studies and Self-assembly of Nanoscale Polyoxometalate–Organic Hybrid Molecular Dumbbells, *Cryst. Growth Des.,* **2009**, 9, 3509-3518.
20. J. Zhang, F. Xiao, J. Hao, Y. Wei, The chemistry of organoimido derivatives of polyoxometalates, *Dalton Trans.* **2012**, 41, 3599-3615
21. C. Bustos, D. Mac-Leod Carey, K. Boubekeur, R. Thouvenot, A. Proust, P. Gouzerh, Aryldiazenido derivatives: A new entry to the functionalization of Keggin polyoxometalates, *Inorg. Chim. Acta ,* **2010**, 363, 4262-4268.

22. B. Matt, S. Renaudineau,; LM. Chamoreau,; C. Afonso; G. Izzet, A. Proust, Hybrid Polyoxometalates : Keggin and Dawson Silyl Derivatives as Versatile Platforms, *J. Org. Chem.* **2011**, 76, 3107-3112
23. R. Villanneau, D. Racimor, E. Messner-Henning, H. Rousselière, S. Picart, R. Thouvenot, A. Proust, Insights into the Coordination Chemistry of Phosphonate Derivatives of Heteropolyoxotungstates, *Inorg. Chem.* **2011**, 50, 1164-1166.
24. S. Reinoso, M. H. Dickman, A. Praetorius, L. F. Piedra-Garza, U. Kortz, Phenyltin-Substituted 9-Tungstogermanate and Comparison with its Tungstosilicate Analogue *Inorg. Chem*. **2008**, 47, 8798-8806 (b) L. F. Piedra-Garza, S. Reinoso, M. H. Dickman, M. M. Sanguineti, U. Kortz, The first 3-dimensional assemblies of organotin-functionalized polyanions, *Dalton Trans.* **2009,** 38, 6231-6234
25. G. Sazani, M. T. Pope, Organotin and organogermanium linkers for simple, direct functionalization of polyoxotungstates, *Dalton Trans.* **2004,** 1989-1994
26. F. Zonnevijlle ; M. T. Pope, Attachment of organic groups to heteropoly oxometalate anions, *J. Am. Chem. Soc.* **1979,** 101, 2731– 2732
27. a) R. Contant, Inorg. Synth. 27, **1990,** 107 b) A. Teze and G. Harve, Inorg. Synth. **1990**, 27,89
28. C. Boglio, K. Micoine, E. Derat, R. Thouvenot, B. Hasenknopf, S. Thorimbert, E. Lacote, M. Malacria, Regioselective Activation of Oxo Ligands in Functionalized Dawson Polyoxotungstates, *J. Am. Chem. Soc*. **2008**,130, 4553.
29. A. M. Debela, M. Ortiz, C. K. ÓSullivan, S. Thorimbert, B.Hasenknopf, post functionalization of Keggin Silicotungtates by general coupling procedures, *Polyhedron*, **2014,** 131-137
30. Hocek M., Fojta M. , Cross-coupling reactions of nucleoside triphosphates followed by polymerase incorporation. Construction and applications of base-functionalized nucleic acids, *Org. Biomol. Chem.*, **2008**, 6, 2233-2241(b) Čapek P., Cahová H., Pohl R., Hocek M. , Gloeckner C., Marx A., An Efficient Method for the Construction of Functionalized DNA Bearing Amino Acid Groups through Cross-Coupling Reactions of Nucleoside Triphosphates Followed by Primer Extension or PCR, *Chem. Eur. J.* **2007**, 13, 6196 – 6203
31. C.A. Ohlin, Reaction Dynamics and Solution Chemistry of Polyoxometalates by Electrospray Ionization Mass Spectrometry, *Chem. Asian J.* **2012**, 7 262–270. (b) Michelle T. M, Tom W, Karin B., Rosemary P., Peter J. S. R., Richard A. J. O'H., Anthony G. W., Gas-Phase Fragmentation of Polyoxotungstate Anions, *Inorg. Chem.*,

2009, 48, 598–606 (c) E. F.Wilson, H. N. Miras, M. H. Rosnes, L. Cronin, Real-Time Observation of the Self-Assembly of Hybrid Polyoxometalates Using Mass Spectrometry, *Angew. Chem. Int. Ed.* **2011**, 50, 3720 – 3724.

Supporting information

This contains ESI MS spectra along with the table for values extracted from the spectra for POM modified
dNTPs.

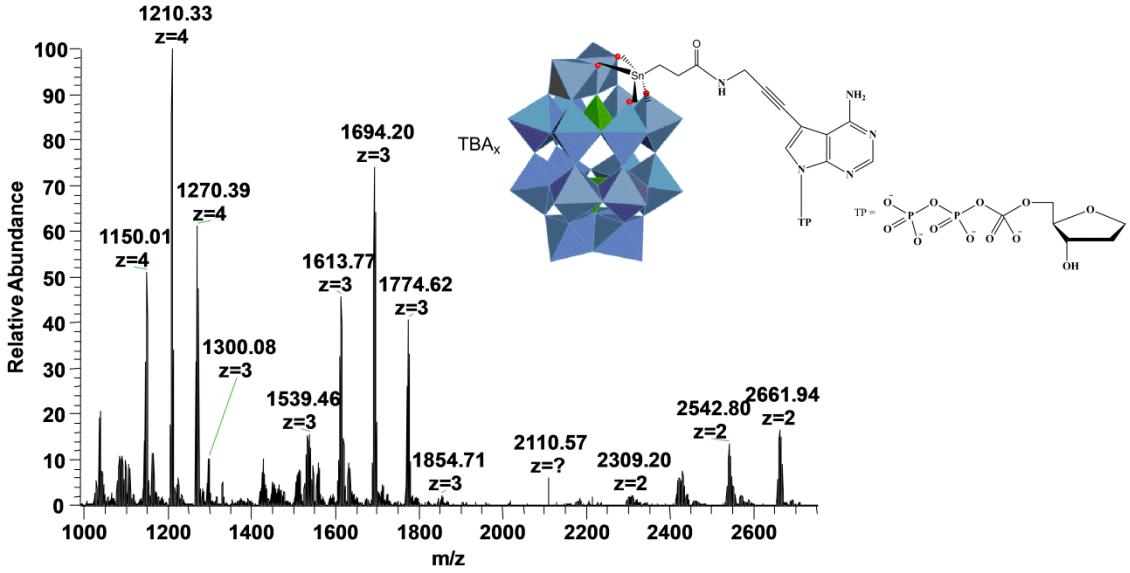

Figure S1. ESI MS spectra of Dawson dATP

Table S1. Data extracted from ESI MS of Dawson dATP

Entry	Charge	Simulated(m/z)	Observed(m/z)	Composition(D-dATP)
1	2	2442.3863	2455.31228	TBA2(DCONHC14H20N4O12P3)
2	3	1628.2577	1632.54822	(TBA)3(DCONHC14H20N4O12P3)
3	2	2563.5287	2569.97241	(TBA)3(DCONHC14H20N4O12P3)
4	4	1221.1934	1232.90344	TBA 4(DCONHC14H20N4O12P3)
5	3	1709.0193	1724.63184	TBA 4(DCONHC14H20N4O12P3)
6	2	2684.6711	2688.59595	TBA 4(DCONHC14H20N4O12P3)
7	4	1281.7646	1284.66528	TBA 5(PDCONHC14H20N4O12P3)
8	3	1789.7809	1788.61414	TBA5(DCONHC14H20N4O12P3)
9	2	2805.8135	2805.8135	TBA5(DCONHC14H20N4O12P3)
10	3	1870.5425	1868.04565	TBA 6DCONHC14H20N4O12P3)
11	4	1342.3358	1330.71326	TBA 6(DCONHC14H20N4O12P3)
12	5	1025.4118	1027.9519	TBA 6(DCONHC14H20N4O12P3)
13	2	2491.7256	2486.18701	TBA)2(TEA)(DCONHC14H20N4O12P3)
14	3	1580.3291	1589.09021	(TBA 2(TEA)(DCONHC14H20N4O12P3)
15	2	2614.0889	2614.0922	(TBA)3(TEA)(DCONHC14H20N4O12P3)
16	3	1661.9645	1655.53394	(TBA 3(TEA)(DCONHC14H20N4O12P3)
17	4	1246.4735	1245.29688	(TBA 4(TEA)(DCONHC14H20N4O12P3)
18	3	1742.7261	1745.16248	(TBA 4(TEA)(DCONHC14H20N4O12P3)
19	3	1823.4877	1822.91992	(TBA)5(TEA)(DCONHC14H20N4O12P3)
20	4	1307.0447	1306.86926	(TBA 5TEA)(DCONHC14H20N4O12P3)
21	3	1890.9014	1903.67456	(TBA 5(TEA)3DCONHC14H20N4O12P3)
22	4	1357.605	1367.93689	TBA 5 TEA3(DCONHC14H20N4O12P3)
23	4	1810.1398	1798.49902	TBA 4 TEA3(DCONHC14H20N4O12P3)
24	3	1297.0308	1297.73987	TBA 4(TEA)3(DCONHC14H20N4O12P3)
25	4	1236.4626	1232.15222	TBA 3(TEA)3(DCONHC14H20N4O12P3)
26	3	1729.3782	1725.30286	TBA 3(TEA)3(DCONHC14H20N4O12P3)
27	2	2594.067	2587.46045	TBA 2(TEA)3(DCONHC14H20N4O12P3)
28	3	1648.6166	1637.87268	TBA 2TEA3(DCONHC14H20N4O12P3)

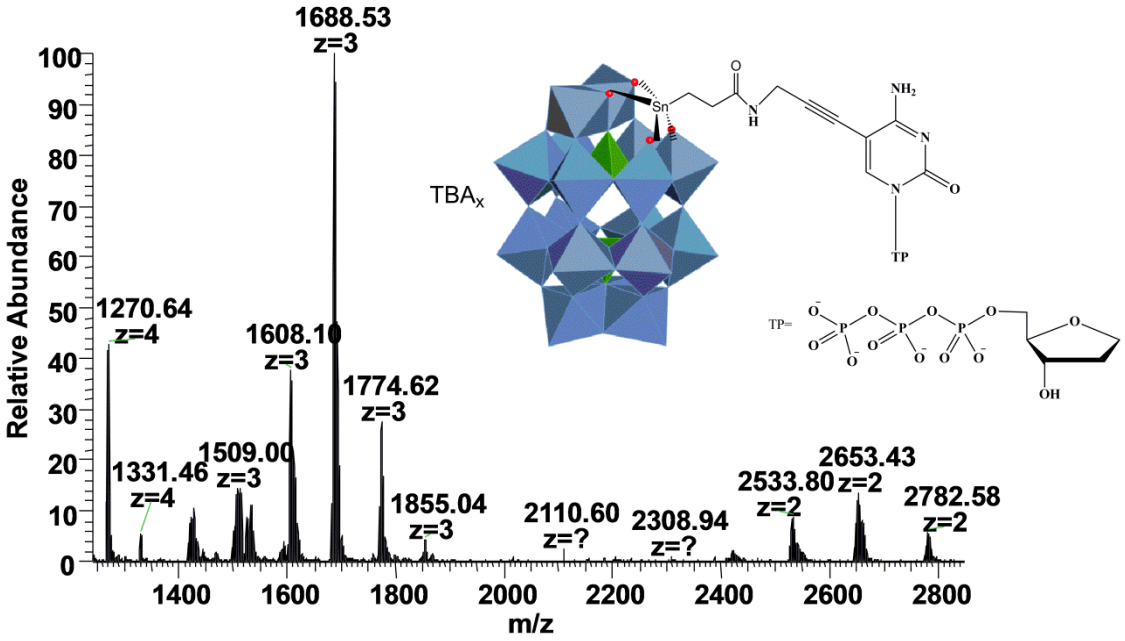

Figure S2. ESI MS spectra of P2W17 (Dawson) dCTP

Table S2. ESI MS spectra data extracted from fig S2

Entry	Charge	Simulated(m/z)	Observed(m/z)	Composition(Dawson-dCTP)
1	2	2430.3744	2429.65039	(TBA)2(DCOC12H19N4O13P3)
2	3	1620.2498	1620.42908	(TBA)3(DCOC12H19N4O13P3)
3	2	2551.5168	2551.29102	(TBA)3(DCOC12H19N4O13P3)
4	4	1215.1875	1215.06763	(TBA)4(DCOC12H19N4O13P3)
5	3	1701.0114	1701.52026	(TBA)4(DCOC12H19N4O13P3)
6	2	2672.6592	2672.43823	(TBA)4(DCOC12H19N4O13P3)
7	2	2793.8016	2793.06738	(TBA)5(DCOC12H19N4O13P3)
8	3	1781.773	1781.28137	(TBA)5(DCOC12H19N4O13P3)
9	4	1275.7587	1275.38708	(TBA)5(DCOC12H19N4O13P3)
10	5	972.1501	972.65625	(TBA)5(DCOC12H19N4O13P3)
11	3	1862.5346	1866.0415	(TBA)6(DCOC12H19N4O13P3)
12	4	1336.3299	1336.91736	(TBA)6(DCOC12H19N4O13P3)
13	3	1815.4798	1815.58557	(TBA)5(TEA)(DCOC12H19N4O13P3)
14	4	1301.0385	1301.36096	(TBA)5(TEA)(DCOC12H19N4O13P3)

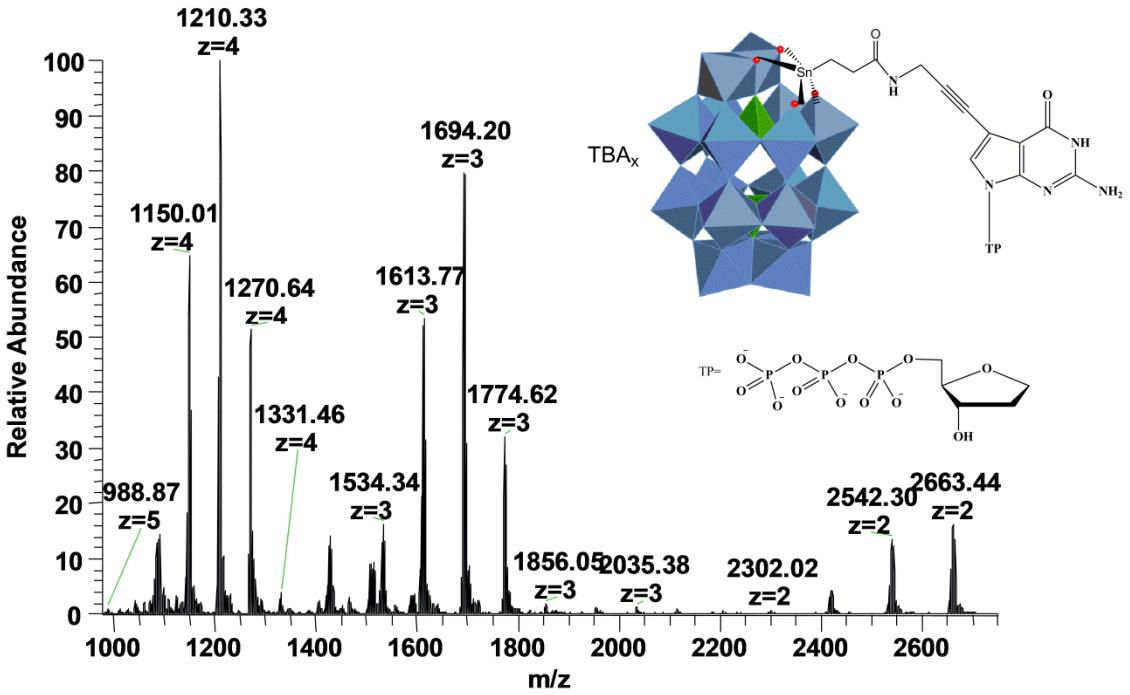

Figure S3. ESI MS spectra of Dawson (P_2W_{17}) modified dGTP

Table S3. Data extracted from ESI MS spectra of Dawson modified dGTP

Entry	Charge	Simulated(m/z)	Observed(m/z)	Composition(Dawson-dGTP)
1	2	2449.8799	2448.20044	(TBA)2(DCOC14H20N5O13P3)
2	3	1633.2534	1634.1322	(TBA)3(DCOC14H20N5O13P3)
3	2	2571.0222	2569.83008	(TBA)3(DCOC14H20N5O13P3)
4	4	1224.9402	1224.34509	(TBA)4(DCOC14H20N5O13P3)
5	3	1714.015	1714.89319	(TBA)4(DCOC14H20N5O13P3)
6	2	2692.1646	2694.47437	(TBA)4(DCOC14H20N5O13P3)
7	5	979.9523	978.86127	(TBA)5(DCOC14H20N5O13P3)
8	4	1285.5114	1285.91663	(TBA)5(DCOC14H20N5O13P3)
9	3	1794.7766	1793.65137	(TBA)5(DCOC14H20N5O13P3)
10	3	1875.5382	1874.8689	(TBA)6(DCOC14H20N5O13P3)
11	4	1346.0826	1346.58032	(TBA)6(DCOC14H20N5O13P3)
12	5	1028.4092	1028.20544	(TBA)6(DCOC14H20N5O13P3)
13	4	1406.6538	1405.64807	(TBA)7(DCOC14H20N5O13P3)
14	3	1956.2998	1956.62903	(TBA)7(DCOC14H20N5O13P3)
15	3	1586.1986	1586.08691	(TBA)2(TEA)(DCOC14H20N5O13P3)
16	5	951.7194	951.42664	(TBA)4(TEA)(DCOC14H20N5O13P3)
17	4	1250.2203	1250.83899	(TBA)4(TEA)(DCOC14H20N5O13P3)
18	3	1747.7218	1747.87976	(TBA)4(TEA)(DCOC14H20N5O13P3)
19	4	1310.7915	1309.11829	(TBA 5(TEA)(DCOC14H20N5O13P3)
20	3	1828.4834	1826.59558	(TBA)5(TEA)(DCOC14H20N5O13P3)

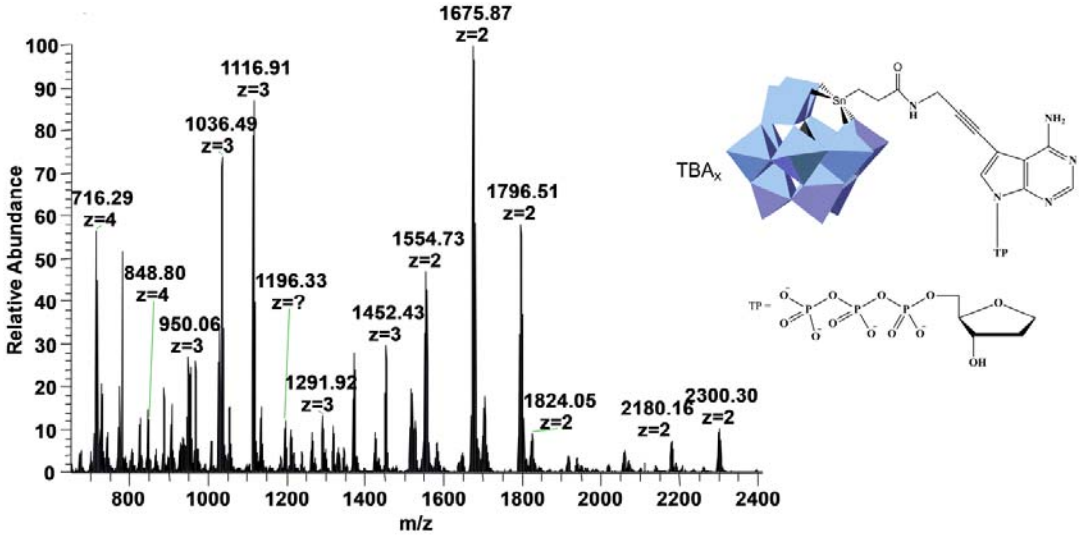

Figure S4.ESI MS spectra of Keggin (SiW11) modified dATP

Table S4. Data extracted from the ESI MS spectra of Keggin (SiW11) modified dATP

Entry	Charge	Simulated(m/z)	Observed(m/z)	Composition(Keggin-dATP)
1	2	1697.6042	1696.9021	(TBA)2(KCONHC14H20N4O12P3)
2	3	1131.7363	1130.24182	(TBA)3(KCONHC14H20N4O12P3)
3	2	1818.7465	1818.54761	(TBA)3(KCONHC14H20N4O12P3)
4	4	848.8024	848.04822	(TBA)4(KCONHC14H20N4O12P3)
5	3	1212.4979	1212.49634	(TBA)4(KCONHC14H20N4O12P3)
6	2	1939.8889	1939.88416	(TBA)4(KCONHC14H20N4O12P3)
7	2	2061.0313	2061.02271	(TBA)5(KCONHC14H20N4O12P3)
8	3	1293.2595	1293.25195	(TBA)5(KCONHC14H20N4O12P3)
9	4	909.3735	909.36816	(TBA)5(KCONHC14H20N4O12P3)
10	5	679.042	679.43835	(TBA)5(KCONHC14H20N4O12P3)
11	2	2182.1737	2181.66064	(TBA)6(KCONHC14H20N4O12P3)
12	3	1374.0211	1374.67883	(TBA)6(KCONHC14H20N4O12P3)
13	4	969.9447	969.93811	(TBA)6(KCONHC14H20N4O12P3)
14	5	727.4989	727.49384	(TBA)6(KCONHC14H20N4O12P3)
15	2	2303.3161	2302.80005	(TBA)7(KCONHC14H20N4O12P3)
16	3	1454.7827	1454.77087	(TBA)7(KCONHC14H20N4O12P3)
17	4	1030.5159	1030.25732	(TBA)7(KCONHC14H20N4O12P3)
18	5	775.9559	775.94977	(TBA)7(KCONHC14H20N4O12P3)
19	3	1165.4431	1165.5072	(TBA)3(TEA)(KCONHC14H20N4O12P3)
20	4	813.5113	813.56067	(TBA)3(TEA)(KCONHC14H20N4O12P3)
21	2	1869.3068	1870.45728	(TBA)3(TEA)(KCONHC14H20N4O12P3)
22	4	874.0825	874.13062	(TBA)4(TEA)(KCONHC14H20N4O12P3)
23	3	1246.2047	1246.60498	(TBA)4(TEA)(KCONHC14H20N4O12P3)
24	2	1990.4492	1990.59851	(TBA)4(TEA)(KCONHC14H20N4O12P3)

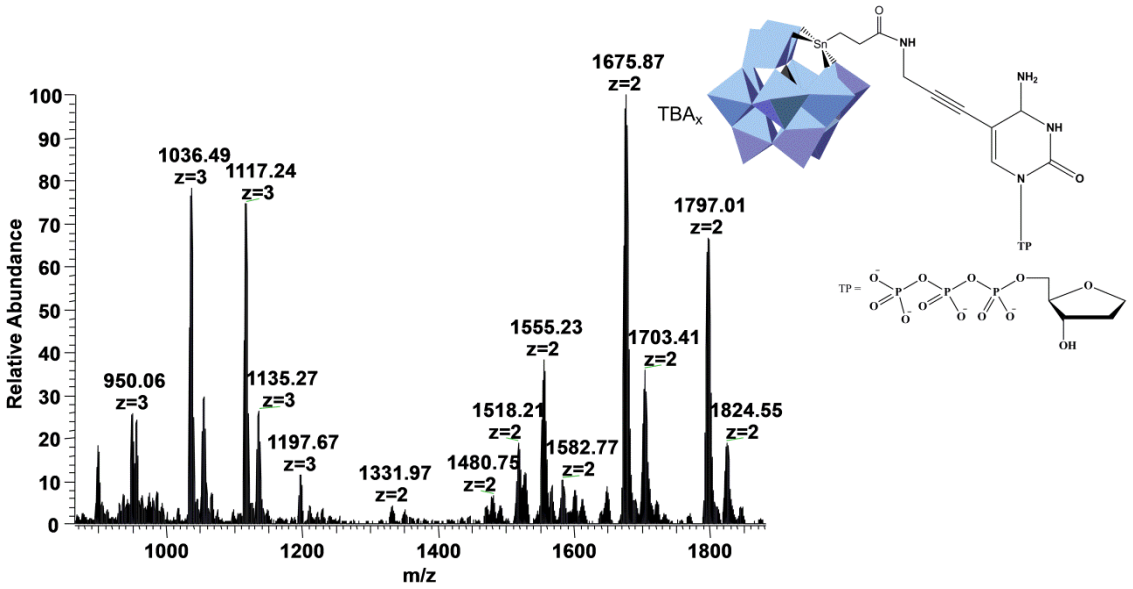

Figure S5. ESI MS spectra of Keggin (SiW11) modified dCTP

Table S5. Data extracted from the ESI MS spectra of Keggin (SiW11) modified dCTP

Entry	Charge	Simulated(m/z)	Observed(m/z)	Composition(Keggin-dCTP)
1	2	1685.5923	1685.89294	(TBA)2(KCOC12H19N4O13P3)
2	2	1806.7346	1804.51807	(TBA)3(KCOC12H19N4O13P3)
3	3	1123.7284	1121.91722	(TBA)3(KCOC12H19N4O13P3)
4	2	1927.877	1926.24268	(TBA)4(KCOC12H19N4O13P3)
5	3	1204.4899	1204.57214	(TBA)4(KCOC12H19N4O13P3)
6	4	842.7964	842.2998	(TBA)4(KCOC12H19N4O13P3)
7	4	903.3576	903.3676	(TBA)5(KCOC12H19N4O13P3)
8	3	1366.0131	1365.45947	(TBA)6(KCOC12H19N4O13P3)
9	4	963.9388	964.7226	(TBA)6(KCOC12H19N4O13P3)
10	2	1615.0101	1615.38306	(TBA)(TEA)(KCOC12H19N4O13P3)
11	2	1736.1525	1736.51965	(TBA)2(TEA)(KCOC12H19N4O13P3)
12	3	1076.6736	1075.91333	(TBA)2(TEA)(KCOC12H19N4O13P3)
13	4	807.5053	807.22089	(TBA)3(TEA)(KCOC12H19N4O13P3)
14	3	1157.4352	1157.53345	(TBA)3(TEA)(KCOC12H19N4O13P3)
15	2	1978.4373	1972.67981	(TBA)4(TEA)(KCOC12H19N4O13P3)
16	3	1238.1968	1238.81287	(TBA)4(TEA)(KCOC12H19N4O13P3)

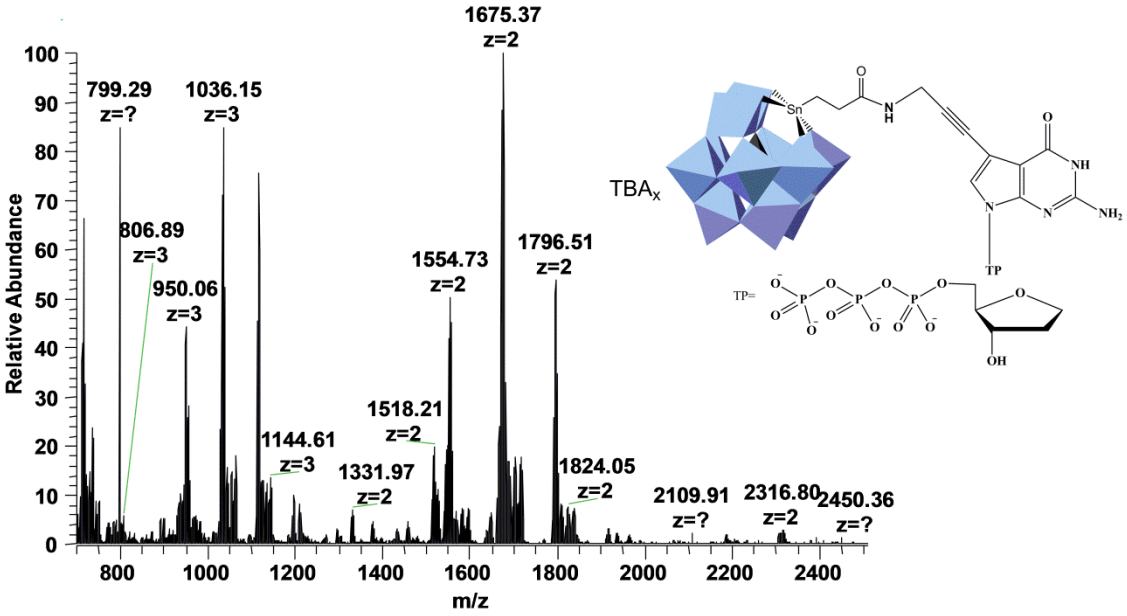

Figure S6. ESI MS spectrs of Keggin (SiW11) modified dGTP

Table S6. Data extracted from ESI MS spectra of Keggin (SiW_{11}) dGTP

Entry	Charge	Simulated(m/z)	Observed(m/z)	Composition(dGTP)
1	2	1705.0977	1705.41296	(TBA)2(KCOC14H20N5O13P3
2	2	1826.2401	1825.04956	(TBA)3(KCOC14H20N5O13P3)
3	3	1136.732	1136.93933	(TBA)3(KCOC14H20N5O13P3)
4	2	1947.3825	1946.38049	(TBA)4(KCOC14H20N5O13P3)
5	3	1217.4936	1219.34253	(TBA)4(KCOC14H20N5O13P3)
6	4	852.5491	853.04926	(TBA)4(KCOC14H20N5O13P3)
7	2	2068.5249	2068.52075	(TBA)5(KCOC14H20N5O13P3)
8	3	1298.2552	1298.91785	(TBA)5(KCOC14H20N5O13P3)
9	4	913.1203	913.3678	(TBA)5(KCOC14H20N5O13P3)
10	5	682.0394	682.23834	(TBA)5(KCOC14H20N5O13P3)
11	2	2189.6673	2189.66113	(TBA)6(KCOC14H20N5O13P3)
12	3	1379.0168	1380.01086	(TBA)6(KCOC14H20N5O13P3)
13	4	973.6915	972.18396	(TBA)6(KCOC14H20N5O13P3)
14	5	730.4964	730.31219	(TBA)6(KCOC14H20N5O13P3)
15	2	2310.8096	2311.79663	(TBA)7(KCOC14H20N5O13P3)
16	3	1459.7784	1458.76843	(TBA)7(KCOC14H20N5O13P3)
17	4	1034.2627	1034.8175	(TBA)7(KCOC14H20N5O13P3)
18	5	778.9533	777.7664	(TBA)7(KCOC14H20N5O13P3)
19	2	1634.5155	1634.84949	(TBA)(TEA)(KCOC14H20N5O13P3)
21	3	1089.6772	1085.83167	(TBA)2(TEA)(KCOC14H20N5O13P3)
22	4	817.258	816.55872	(TBA)3(TEA)(KCOC14H20N5O13P3)
23	3	1170.4388	1170.29333	(TBA)3(TEA)(KCOC14H20N5O13P3)
24	2	1876.8003	1871.95947	(TBA)3(TEA)(KCOC14H20N5O13P3)
25	2	1997.9427	1997.98694	(TBA)4(TEA)(KCOC14H20N5O13P3)
26	3	1251.2004	1251.59802	(TBA)4(TEA)(KCOC14H20N5O13P3)
27	4	877.8292	877.62982	(TBA)4(TEA)(KCOC14H20N5O13P3)
28	3	1331.962	1331.97192	(TBA)5(TEA)(KCOC14H20N5O13P3)
29	4	938.4004	938.38672	(TBA)5(TEA)(KCOC14H20N5O13P3)
30	5	702.2635	702.53772	(TBA)5(TEA)(KCOC14H20N5O13P3)

Chapter 6

Electrochemical APEX for genotyping MYH7 gene; a low cost strategy for detection of disease causing mutations

Ahmed M. Debela[a], Mayreli Ortiz[a], Serge Thorimbert [c], Bernold Hasenknopf [c] Ciara K. O´Sullivan,[a,b]

[a]Departament d'Enginyería Química, Universitat Rovira i Virgili, Avinguda Països Catalans, 26, 43007 Tarragona, Spain,

[b]ICREA, Passeig Lluis Companys 23, 08010 Barcelona, Spain

[c]UPMC Univ Paris 06, Institut de Chimie Moléculaire UMR CNRS 7071, 4 place Jussieu, 75252 Paris Cedex 05, France.

Electrochemical APEX for genotyping MYH7 gene; a low cost strategy for detection of disease causing mutations

Ahmed M. Debela[a], Mayreli Ortiz[a], Serge Thorimbert [c], Bernold Hasenknopf [c]
Ciara K. O´Sullivan,[a,b]

[a]*Departament d'Enginyería Química, Universitat Rovira i Virgili, Avinguda Països Catalans, 26, 43007 Tarragona, Spain,*

[b]*ICREA, Passeig Lluis Companys 23, 08010 Barcelona, Spain*

[c]*UPMC Univ Paris 06, Institut de Chimie Moléculaire UMR CNRS 7071, 4 place Jussieu, 75252 Paris Cedex 05, France.*

Abstract

We report the use of four different organic molecules for the covalent labeling of ddNTPs for use in electrochemical APEX. The labels were chosen based on their distinguishable redox potentials. Two strategies were developed to test on surface nucleotide incorporation and detect SNPs known to occur in MYH7 gene.A proof-of-concept was demonstrated by incorporating a labelled ddNTP to hybridise to the first base of the immobilised probes, and was then demonstrated using the real-life scenario of having the ddNTPs incorporated through the 3'OH at the other end of the probe immobilised through the 5' terminus. The results obtained confirm the electrochemical detection of SNPs, representing a huge stride in the development of electrochemical APEX.

Introduction

The completion of the human genome Project (HGP) has paved the way for mapping the diversity in the overall genome sequence thus helping to understand the genetic causes of inherited diseases and susceptibility to drugs or environmental toxins. Over the past decade the development of new strategies for genotyping has attracted increasing interest, driven by the need for cost effective and efficient strategies to take advantage of the knowledge acquired during HGP and of the large variety of molecular methods developed to assess a broad range of biological phenomena (e.g., genetic variation, RNA

expression, protein-DNA interactions and chromosome conformation). Finally, the advance of technology across diverse fields, including microscopy, surface chemistry, nucleotide biochemistry, polymerase engineering, computation, data storage and others, have made alternative strategies for genotyping increasingly practical to realise[1].

In the genome sequence there exists individual variations which include: single nucleotide polymorphisms (SNPs), insertions and deletions (indels), microsatellites (MSs), and differences in the methylation status of important regions (e.g. CpG islands). However, the majority of the variations are attributable to SNPs. SNPs are point mutations which are DNA sequence variations that occur when a single base pair in a genome among individuals is altered where the less common variant occurs in at least 1% of the total population[2]. SNPs are attributable for 90% of the genetic variations[3] and the rest is attributable to insertions or deletions of one or more bases, repeat length polymorphisms and rearrangements[4]. The decoding of the human genome has revealed the presence of around 10 million SNPs (roughly 1 every 300-1000 bases) [3]. Depending on their locations in the genome, SNPs may have different consequences at the phenotypic level. SNPs present in regulatory sites of a gene will perturb the transcriptional rate, affecting the expression level of encoded protein. In the coding region, SNPs may alter the structure and, hence, function of encoded protein. These SNPs are often recognised as molecular markers of genetic disorders and disease predisposition. Among the genetic diseases known many are associated with genetic variations to mention some Tay Sachs[5] , cysticfibrosis [6], thalassaemia[7] sickle cell anaemia[8] etc. Hence SNP genotyping is of fundamental importance for the early identification as well as diagnosis of genetic disorders and disease predisposition which may potentially allow for a more personalised approach to medicine.

The majority of the genotyping methods in use involve one or more of the fundamental molecular biology process which includes hybridisation and enzyme assisted methods such as nucleotide incorporation, primer ligation and nucleolysis. These in turn are clubbed with different transduction methods such as mass spectroscopy[9], fluorescence/optical[10], or chemiluminescence[11], electrochemical[12] etc to make the overall genotyping possible. Electrochemical transduction approaches are attractive due to the possibility of performing analysis in miniaturised, compact, simple to operate and low cost instrumentations. Moreover, electrochemical measurements are rapid and very low

limits of detections can be achieved, making electrochemical transduction very versatile and suitable for on-site analysis. Many electrochemical DNA detection platforms for SNP analysis rely on analysis of the difference hybridisation related events (eg. Charge transport) for the mismatchs relative to the complementary targets[13]. Other approaches involve post hybridisation application of redox active reporters with preferential affinity for duplex DNA[14] or sandwich assay based on redox labeled DNA probes that hybridise with the target DNA[15]. There are several reports that employ enzyme conjugates[16], nanoparticles tags[12] and redox labels[17-19] for SNP detection. A relatively small number of reports has been documented utilising the enzymatic discrimination of alleles along with electrochemical transduction methodologies for SNP detection. This could be in part attributed to the tedious and cumbersome steps involved in the synthesis of redox labels. The level of maturity in electrode surface functiolisation and synthetic conjugation of redox labels with nucleotides have opened up great opportunity to linkup the high specificity of enzymatic incorporation with very high sensitivity of electrochemical approaches.

Arrayed primer extension (APEX) is a high throughput genotyping method that exploits dideoxy nucleotides for scanning unknown mutations over large regions of a DNA sequence[20]. Typically, the APEX procedure involves locus specific PCR amplification which will subsequenctly fragmented using uracil N-glycosylase. The fragmented PCR products will then be denatured and hybridised to complementary capture probes on a glass array in a reaction mixture. Once hybridised, they serve as primers for template-dependent DNA polymerase extension reactions by using four fluorescently labeled dideoxynucleotides. Imaging is followed by data analysis to convert the fluorescence information into sequence data[21]. APEX can interrogate hundreds to thousands of SNPs in a single multiplexed reaction simultaneously. As the genotype information is obtained by single base extension performed by a specific DNA polymerase, this approach has a higher discrimination power but a lower throughput per run when compared to methods based on allele-specific oligonucleotide hybridisation (microarrays)[20d]. Recently, this concept has been extended to a second generation APEX device that allows multiplex (640-plex) DNA amplification and detection of SNPs and mutations[22].

Motivated by the high accuracy and specificity of the fluorescent APEX, we demonstrated electrochemical solid phase single base extension for SNP detection. The

ddNTPs used were covalently linked with four different redox active compounds (ferrocene, methylene blue, anthraquinone and phenothiazine) at positions favourable for enzymatic incorporation. The redox labels are known to have four distinctive redox potentials and used for SNP typing of known mutations to occur in MYH7 gene. Electrochemical techniques CV and DPV were used to interrogate the incorporations.

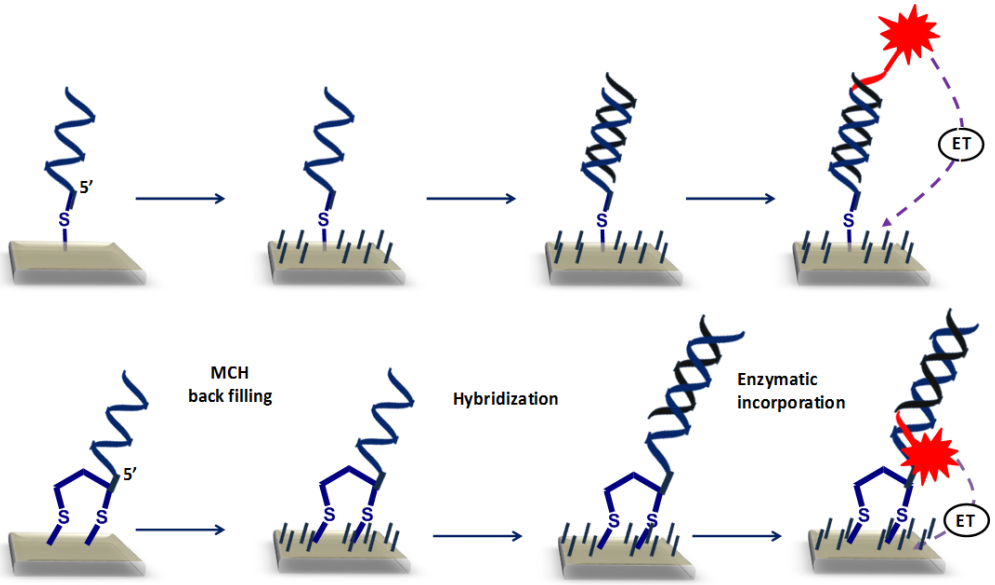

Scheme 6. 1. Showing the platforms evaluated for electrochemical SNP detection. Thiolated DNA probes (strategy I) or thioctic acid end labeled DNA probes (Strategy II) were immobilised on polished and electrochemically cleaned electrodes. This was followed by backfilling with MCH. The modified electrodes were incubated at 37 oC for hybridisation with complementary target hybridising up until the SNP site which eventually used for enzymatic incorporation of the corresponding labeled ddNTPs for electrochemical interrogation.

Materials and methods

All chemicals and reagents used were of analytical grade and purchased from various companies. Potasium dihydrogen phosphate (KH_2PO_4, fluka), sodium chloride (NaCl, Probus), potassium chloride (KCl, Fluka), sodium perchlorate ($NaClO_4$, Acros Organics), mercaptohexanol (MCH, Fluka), sodium hydroxide, Sulfuric acid (95-97%), trizma base, and boric acid were from Scharlau (Barcelona, Spain). Hydrochloric acid (35%,

Panreac),Phosphate-buffered saline (PBS), trisodium citrate, acetone, dimethyl sulfoxide (DMSO), perchloric acid (70%), triethyl amine, glacial acetic acid, phenothiazine, anthraquinone carboxylic acid, ferrocene carboxylic acid, N-(3-dimethylaminopropyl) N′-ethylcarbodiimide hydrochloride and N-hydroxy succinimide were all purchased from Sigma Aldrich. Mono carboxylic methylene blue is obtained from emp Biotech GmbH, the propargyl amino modified ddNTPs perchased from genabioscience. Unless otherwise noted, all reactions were carried out under argon atmosphere with magnetic stirring. The organic solvents were redistilled before use. Thermosequanase polymerase was purchased from GE health care.

Table 6. 1. MYH7 Sequences used in the study

labeled ddNTP	Sequences
MB-ddU	thiol-5'-GGG ACT AGG GGA CTG AAG AA3'
	3'-CCC TGA TCC CCT GAC TTC TTA AAT-5'
Fc-ddG	thiol-5'-GGG ACT AGG GGA CTG AAG AA3'
	3'-CCC TGA TCC CCT GAC TTC TTC AAT GTG AGG GCA TTT CTT GGT-5'
PTZ-ddC	thiol-5'-GTG GTG GGA CTA GTT CAC A -3'
	5'-AC CGG GGA CAA AAC CGA AGT GTG AAC TAG TCC CAC CAC-3'
Anth-ddA	thiol-5'-TAC AAG TGT TAA CAC ACA GTG AA-3'
	5' -TAA CGA GGA GGT ATT TTG TGT TAA TTT CAC TGT GTG TTA ACA CTT GTA-3'
MB-ddU	thioctic-5'-A GTG GTG GCC GCC TAC CGG-3'
	5'-CCG GTA GGC GGC CAC CAC-3'
PTZ-ddC	thioctic-5'-GAA GAA GTC AGG GGA TCA GGG-3'
	5'-CCC TGA TCC CCT GAC TTC TT-3'
Anth-ddA	thioctic-5'-T AA GTG ACA CAC AAT TGT GAA CAT-3'
	5' ATG TTC ACA ATT GTG TGT CAC TT-3'
Fc-ddG	thioctic-5'-CAC CTG CAT AAT GTG TGT ATC TGT-3'
	5' ACA GAT ACA CAC ATT ATG CAG GT-3'

DNA sequences: The DNA sequences were designed following previous report[23] on a group of patients (Safor region, Valencia) with a mutated MYH7 gene and known to suffer from laing cardiomayopathy. Among the 8 SNPs reported to occur around the mutated gene sequence, only 5 (rs2277474, rs743567, rs8005199, rs11621360, rs875908) of the SNPs were used to design the sequences for electrochemical APEX. The sequences were selected using specific oligonucleotide selection and design programs

(http://bioinfo.ebc.ee/apex2/). The sequences were designed in such a way to detect the SNPs using four different labeles corresponding to the four bases. HPLC purified synthetic oligonucleotide sequences were purchased from Biomers.net (Germany).

Analytical details

FT-IR spectra were recorded from a Bruker Tensor 27 ATR diamond PIKE spectrophotometer. The ^{1}H, ^{31}P and ^{13}C NMR spectra were respectively recorded at 400, 162 and 100 MHz with a Bruker AVANCE 400 equipped with a sensor. Chemical shifts are reported in ppm using ^{1}H and ^{13}C for the residual solvent peak as internal reference (d = 7.26 and 77.2 ppm, respectively, for $CDCl_3$, d = 2.50 and 39.5 ppm for (DMSO d_6), d = 1.94 and 118.26 ppm for CD_3CN). 85% H_3PO_4 in water was used as an external reference for ^{31}P. Mass spectrometry was carried out using an ion trap type Bruker Esquire (R=3000) coupled to an electrospray source (ESI-MS) at the Paris Institute of Molecular Chemistry (IPCM). 10 µM of the compounds solutions in CH_3CN were injected using a syringe pump with flow rate 160 µL.min-1. The detector was used in negative ion mode at a voltage of 3500V. The voltage difference between the orifice and the skimmer is set at 45 V to avoid decomposition of the POMs. The LMCO (low-mass cutoff) of the ion trap was set at 80 in order to preferentially trap ions above m/z ratio.

Electrochemistry: All electrochemical measurements were carried out using an Autolab model PGSTAT 12 potentiostat/galvanostat controlled with the General Purpose Electrochemical System (GPES) software (Eco Chemie B.V., The Netherlands). A classical three electrode set up was used with a Ag/AgCl reference electrode, Pt wire counter electrode and gold electrodes (with inner diameter of 2mm), which were purchased from CHI Instruments, Inc. All the potentials are recorded with respect to the reference electrodes.

Electrode preparation: Gold electrodes were polished with 0.3 and 0.05 µm alumina for ca. 5 mins for each size; followed by sonication for 5min in water. Then electrochemical cleaning with 0.5M H_2SO_4, sweeping for 40 cycles between 0.2 and 1.6 V. The real surface area (Ar) of the electrochemically activated gold electrode could be calculated by integrating the current beneath the cathodic wave of the cyclic voltammgrams of H_2SO_4 solution on the basis of the quantity of consumed charge 482 µC cm-2 . According to the

ratio of the real surface area (Ar) to the geometrical area (Ag), the high roughness factor (rf= Ar / Ag) of 2.54 in average was obtained, which implied the adequate activation of the bare gold electrode [24,] this step was performed to check the similarity of the electrodes used for functionalisation and analysis.

The cleaned gold electrodes were immersed in a solution of thiol/thioctic acid modified ssDNA (5 µM in 1.0 M KH_2PO_4 buffer solutions) for immobilisation following reported methods[25]. After 3 hrs of incubation at room temperature the electrodes were rinsed with tris buffer and dried with stream of nitrogen. Mercaptohexanol backfilling was made with 0.5mM solution for 30min the probe modified electrodes were subsequently washed with trisbuffer solution and died with copious amount of argon.

DNA Hybridisation of target DNA was performed by incubation of the so prepared electrodes in a buffer solution [10mM trisma HCl with 0.5M NaCl solution (pH7) containing the respective target DNA corresponding to the four bases] for 1 hr at 37°C this results in complementary strand formation up until SNP region. The electrodes were washed with the hybridisation buffer and dried and made ready for primer extention [PEX] reaction.

PEX reaction: this nucleotide incorporation reaction was performed with thermosequanase (GE health care), the prepared electrodes were incubated with a solution containing 1µM of the redox labeled ddNTP (four separate reaction for each base), 20mM tris HCl, pH8.5, 50% glycerol, 0.1mM EDTA, 0.5% Tween, 0.5%nonidet-P40, 1mM DTT, 100mM KCl, 65mM MgCl, 0.5units of thermosequanase DNA polymerase,1,5units thermoplasma acidophilum inorganic pyrophosphatase. The electrodes were sealed with parafilm inculbated at 42°C for additional 30min, the electrodes subsequently washed with hybridisation buffer kept read for electrochemical assay.

Electrochemical interrogation: DPV was used to detect the incorporation. The measurements were performed at room temperature in 10ml electrochemical cell with the normal three electrode configuration (see details in the text) the electrodes were transferred to 10mM trisma hydrochloride buffer containing 0.5M NaCl, pH 7, DPV were recorded at various potential windows depending on the redox potential of the labels (vs

Ag/AgCl), pulse amplitude of 0.1 V, step potential, 10mV, pulse width 100msec and pulse period 5msec.

Synthesis and characterisation of redox labeled ddNTPs

Labeled ddNTPs were synthesised utilising the NHS esters of the redox labels and subsequent reaction with alkyl amine arm of the ddNTPs. To the NHS ester (2.4µmol, 3equiv) in DMSO was added 100µl of Na_2CO_3-$NaHCO_3$ buffer (0.1M, pH=8.7) followed by addition of 800nmols of the propargyl amino ddNTPs. After sonication for 10min the reaction kept in thermomixer shaking for 6hrs. After the reaction time TLC confirmed the complete consumption of the triphosphate. The reaction mixture was kept in the freezer overnight followed by freez drying. Preparative TLC ($CHCl_3$/CH_3OH, 85/15) and ESI MS shows the synthesis of the products. The products were directly used for electrochemical primer extention reaction.

*β-(10-phenthiazinyl) propionitril***:** this compound was synthesised following previously reported method[26] . Briefly, to an ice cooled stirring mixture of phenothiazine (4g) and acrylonitrile (10ml) was added tetra butyl ammonium hydroxide (1ml, 40% in water), the exotermic reaction was allowed to warm to room temprature. After the reaction subsided freshly distilled dioxane (25ml) was added. The reaction mixture was kept under reflux for 3hrs. The mixture was poured to vigourosly stirring distilled water. Solid residue was recrystalised from cold acetone. An off white solid was obtained with yield of 75%. ESI MS obtained 275 for sadium salt $C_{15}H_{12}N_2SNa$ in methanol.

β-(10-phenthiazinyl) propionic acid: This compound was also synthesised following literature report[26] with yield of 90%.1H, NMR ((250 MHz, DMSO) 2.63 (t, 2H, CH_2CO), 4.12 (t, 2H, NCH_2), 6.92-7.06 (m,4H) 7.14-7.25(m,4H) and 9.92(1H, COOH)The ESI MS was obtained as sodium salt: $C_{15}H_{13}NSO_2Na$= 294.05.

*2,5-dioxopyrrolidin-1-yl 3-(10H-phenothiazin-10-yl) propanoate NHS ester(PTZ-ETCOONHS):*To a stirring solution of β-(10-phenthiazinyl) propionic acid in a freshly distilled dichloromethane (DCM) (408mg, 1.5mmol) was added N-(3-dimethylaminopropyl) N′-ethylcarbodiimide hydrochloride (288mg, 1.5mmol) and N-hydroxy succinimide (180mg,1.5mmol) the mixture was left stirring at room temprature for 18hrs. Column chromatography in dichloromethane gave a white product (60%

yield). 1H, NMR ((250 MHz, DMSO) 2.81 (s, 4H, $COCH_2CH_2CO$), 3.14 (t,2H,CH_2CO),4.27(t,2H,NCH_2),6.96-7.09(m,4H) 7.18-7.27 (m,4H) 13C 25.9($COCH_2CH_2CO$), 29.45(CH_2CO), 42.01(NCH_2) 116.03, 123.45, 124.42, 127.73, 128.16, 144.51, 167.88 (COO),170.39 ($COCH_2CH_2CO$) The ESI MS was obtained as sodium salt: $C_{19}H_{16}N_2SO_4Na$= 391.07.

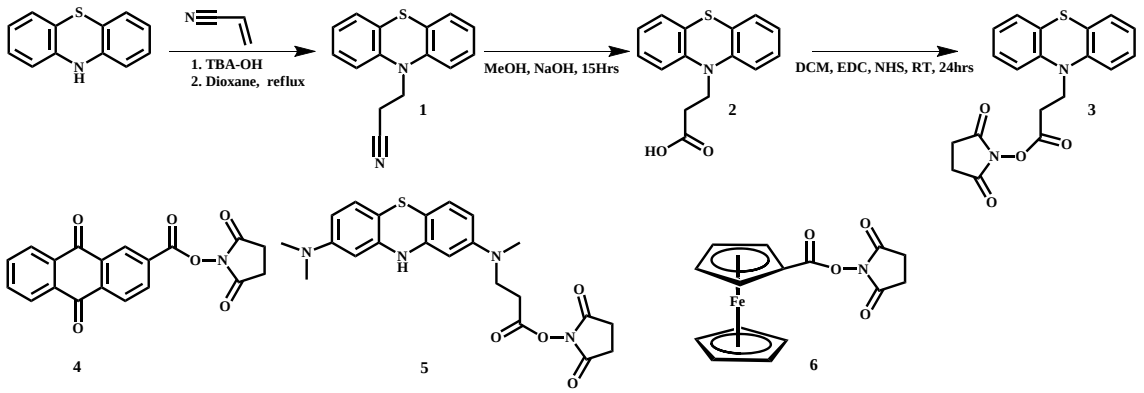

Scheme 6. 2. The functionalisation strategy followed to get the activated ester of phenothiazine (4) and activated esters of anthraquinone (5), methylene blue (6) and ferrocene (7)

*Preparation Phenothiazine-ddCTP (phenothiazin-10(10aH)-yl-propanamido)prop-1-yn-1-yl)-4-amino-2-ddCTP:*These were prepared following the general procedure described earlier, HR ESI MS was taken due to limited amount of sample we have for other analysis. For phenothiazine ddCTP the observed masses are 757 for M , 758 for (M+H), 780 for (M+Na) and 401 for $(M+2Na)^{2+}$ confirming the successful synthesis of the labeled ddCTP.

2,5-dioxopyrrolidin-1-yl 9,10-dioxo-4a,9,9a,10-tetrahydroanthracene-2-carboxylate(Anthraquinone carboxylic acid NHS): To a stirring solution of anthraquinone-2-carboxylic acid (381mg,1.5mmol) in a freshly distilled DCM was added N-(3-dimethylaminopropyl) N′-ethylcarbodiimide hydrochloride (288mg,1.5mmol) and N-hydroxy succinimide (180mg, 1.5mmol) the mixture was left stirring at room temprature for 18hrs. column chromatography in dichloromethane gave a white product (60% yield).1H, NMR (250 MHz, DMSO) 2.95 (s, 4H, $COCH_2CH_2CO$), 7.96-8.03 (m, 2H), 8.24-8.30 (m,2H), 8.42-8.45 (1H,dd), 8.54-8.58 (1H,dd),8.76(1H,d,) 13C 26.09

($COCH_2CH_2CO$), 128.55, 129.5, 133.58, 134.23, 135.4, 161.29 (COO), 170.61(CH_2COCH_2),181.91(CCOC) The ESI MS was obtained as sodium salt: $C_{19}H_{11}NO_6Na$= 372.04.

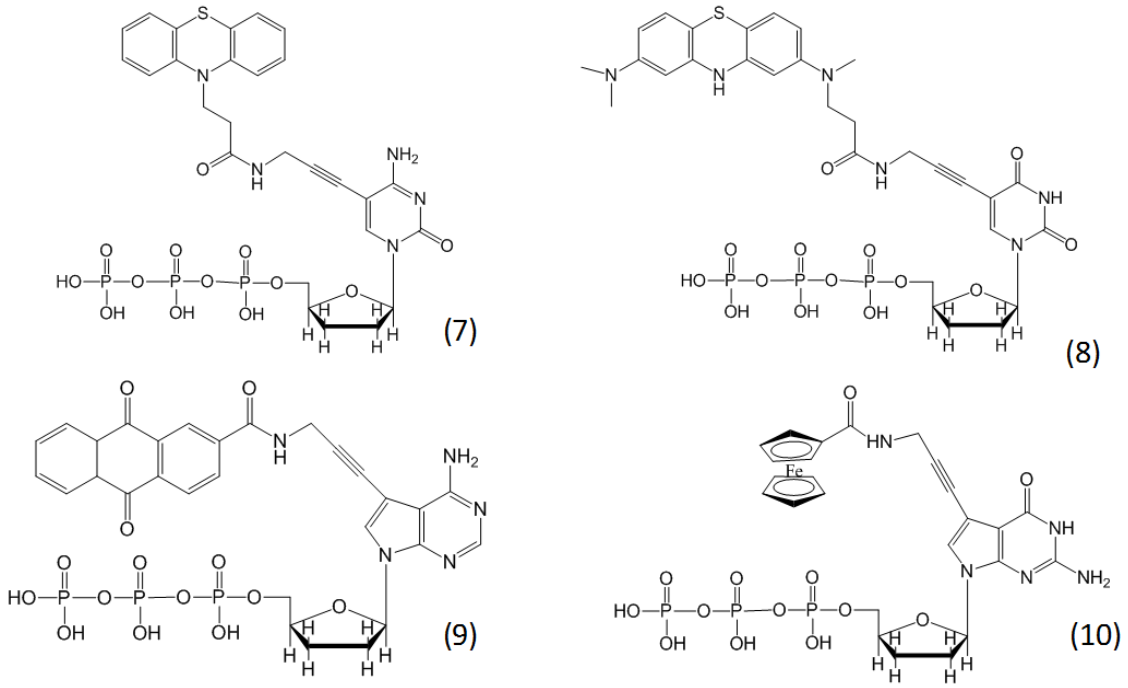

Figure 6. 1. Structure of phenothiazine ddCTP (7), Methylene blue ddUTP (8), anthraquinone ddATP (9) and ferrocene ddGTP (10)

Preparation of anthraquinone labeled ddATP: These were also prepared following the method described the text. HRESI MS was taken due to limited amount of sample we have for PEX reaction. For anthraquinone ddATP the observed mass is for the molecule with loss of 1H and 2H 762 and 761.

Ferrocene carboxylic N-hydroxysuccinimide ester: To a stirring solution of *ferrocene carboxylic* acid (345mg, 1.5mmol) in a freshly distilled DCM was added N-(3-dimethylaminopropyl) N′-ethylcarbodiimide hydrochloride (288mg,1.5mmol) and N-hydroxy succinimide (180mg, 1.5mmol) the mixture was left stirring at room temprature for 18hrs. Column chromatography in DCM gave a white product (60% yields). 1H, NMR ((250 MHz, DMSO), 2.9 (s,4H,$COCH_2CH_2CO$),4.43 (s,5H,Fc), 4.58 (t,2H,Fc) 13C 25.67 ($COCH_2CH_2CO$), 64.3, 70.79,70.74,72.80,167.37,169.52 (CH_2COCH_2), The ESI MS was obtained as sodium salt: $C_{15}H_{13}NO_3FeNa$= 351.02. the activated ester is used for

preparation of ferrocene – ddGTP following the procedure described earlier. Signals from HRESIMS representing the compounds confirm the successful synthesis of the compounds.

Monocarboxy methylene blue NHS ester: similar methodology was followed to synthesis the NHS ester and NMR was taken in DMSO. 1H, NMR ((250 MHz, DMSO) 2.83 (s, 4H, $COCH_2CH_2CO$), 3.2 (t,2H,CH_2CO),4.1(t,2H,NCH_2),7.57 (m,4H) 7.9 (m,4H)13C 19.9 ($COCH_2CH_2CO$), 25.93(CH_2CO), 53.11(NCH_2),63.93, 107.21,121, 138.63, 168 (COO),170 ($COCH_2CH_2CO$) The ESI MS was obtained as sodium salt: $C_{22}H_{23}N_4SO_3Na$= 446.16. This was used for synthesis of methylene blue ddUTP following similar protocol as described earlier. HRESIMS is shown Figure 2.

Results and discussion

The four different redox labeles were chosen based on their distinctive redox potentials in various literatures. Phenothiazine was functionalised with ankyl arm bearing carboxyl end following the step wise reaction oprotocol described in Scheme 3. While the carboxyl group derivatives of ferrocene, anthraquinone and methylene blue are commercially available. The carboxy group bearing derivatives were activated following the EDC-NHS protocol. The activated forms were used to functionalise propargyl amino bearing ddNTPs (ddATP, ddCTP, ddGTP, ddUTP) to achieve compounds to be used in solid phase primer extention (SPEX) reaction. All the synthesised labels were characterised by NMR, ESI MS, and ATR FT-IR (see experimental section).

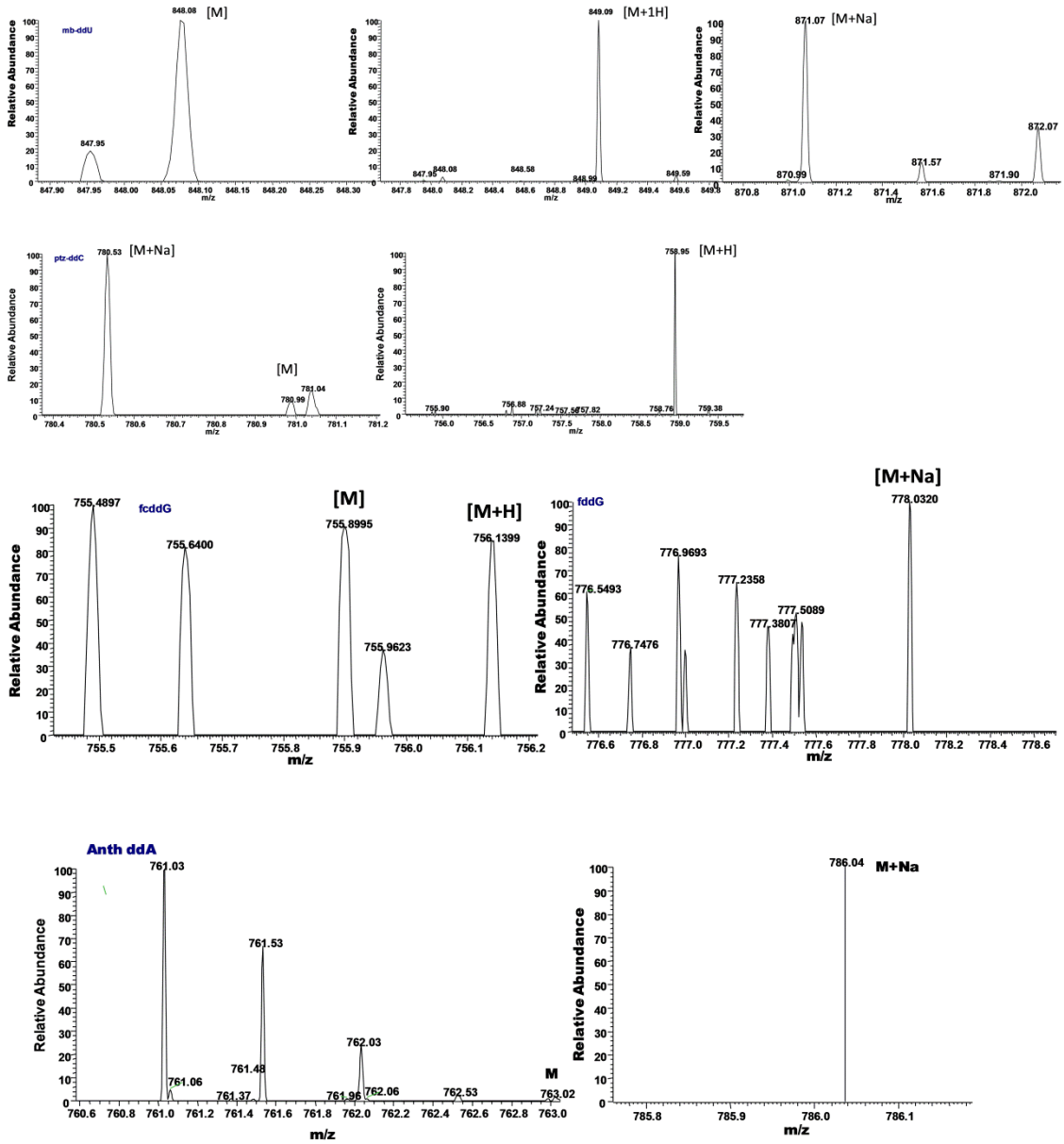

Figure 6. 2. The HR ESI MS data for the labeled ddNTPs

Design of the electrochemical APEX protocol

Various contradicting reports appear on the ease of electron transfer for redox labeles anchored to surface tethered DNA duplex. Plaxco and coworkers [27] and other groups[28] demonestrated a strong electrochemical response for ferrocene labeles placed close to electrode surface while Di Guisto et al[29] reported weaker response when labeles are closer to the electrode surface. However later work by A. Anne[30] and Ikeda[31] demonstrated in detail the charge transfer using ferrocene to give plausible explanation for the charge transport in DNA. They concluded charge transport in DNA duplex to be

dependent not only in the position of the label in the duplex but also on the dynamic properties of the DNA. In our work we tempted to compare two strategies where the label will be enzymatically incorporated either at the end of surface tethered duplex i.e. far from the electrode surface (strategy I) or the label incorporation reaction occurring close to the electrode (strategy II) both strategies are shown in Scheme 6. 1.

Comparison of the two strategies

As shown in the scheme 1 'APEX reactions' were performed after hybridisation of the template followed by enzymatic incorporation of the label modified ddNTP which eventually terminates the reaction. The electrochemical interrogation of the incorporated labeles was performed by monitoring the redox reaction by employing the differential pulse voltmetery (DPV) in potentials windows corresponding to the labels. The normalised peak current was used to compare the two strategies where higher peak current was observed for the second strategy than the first (Figure 3). This could be attributed to the closeness of the redox label to the electrode surface.

Even though one of the mechanism by which methylene blue (MB) is thought to interact with free guanines in a DNA and used for electrochemical hybridisation assay, in the present work the sequences for detection of the SNPs using MB modified ddUTP were designed to avoid any interaction with free G after formation of the duplex preceding the solid phase primer extension reaction.

In addition to the improved signal obtained from the second strategy a bipodal cyclic thioctic acid disulfide anchoring unit for the immobilisation of the capture probes was used. This was observed to improve the stability of the surface tethered probes, which prevents the detachemnt/displacement by other thiols in the enzymes buffers. This also improves the stability at elevated temperature during the SPEX reaction.

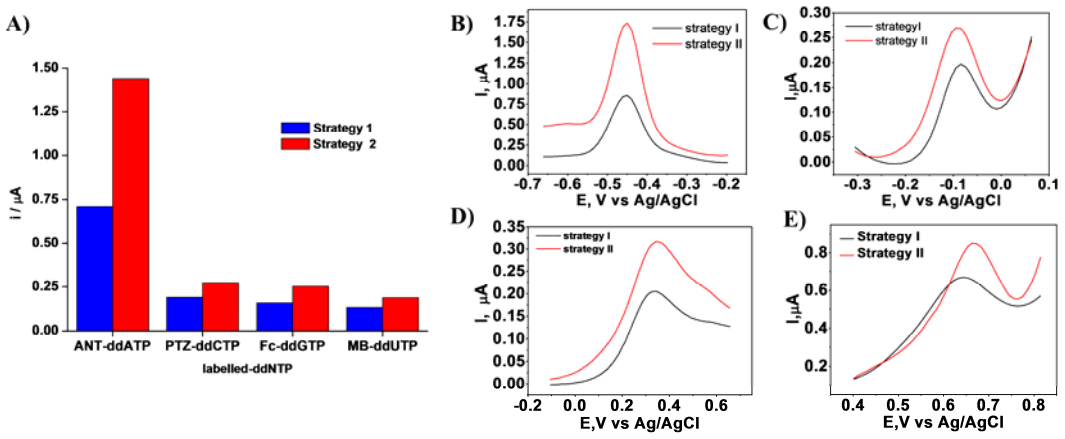

Figure 6.3. DPVs showing the comparison of the two approaches utilising the incorporation of the various labeled ddNTPs. (Methylene blue modified ddUTP, anthraquinone modifed ddATP, ferrocene modified ddGTP and phenothiazine modified ddCTP).

Demonstration of labelled ddNTP incorporation

Modified polymerases have been shown highly tolerant to nucleotide to nucleotide modifications with various groups at 5 positions of pyrimidine bases (C and U) and 7 position of purine bases (A and G). Various reports indicate the incorporation of ferrocene [29, 32, 33], anthraquinone[29b,34], phenothiazine [35] and others. For surface tethered probes and primer extention reactions the only way to proof the incorporation of the modified ddNTP after termination of the reaction is the use of indirect methods like electrochemical methods. In this study cyclic voltametries were investigated/analysed following different formalisms. The first of which is the investigation of the surface confinement of the redox labels by taking taking the CVs at different scan rates. The peak current is proportional to the scan rate[36] (i.e the solid lines are linear fits based on the methods of least squares) in contrast to $\upsilon^{1/2}$ dependence which could arise from diffusing species following the Nernestian behavior. The results obtained thus confirm the surface confinement of the incorporated labeled ddNTPs.

$$i_p = \frac{n^2F^2}{4RT}\vartheta A\tau_O^* \qquad (1)$$

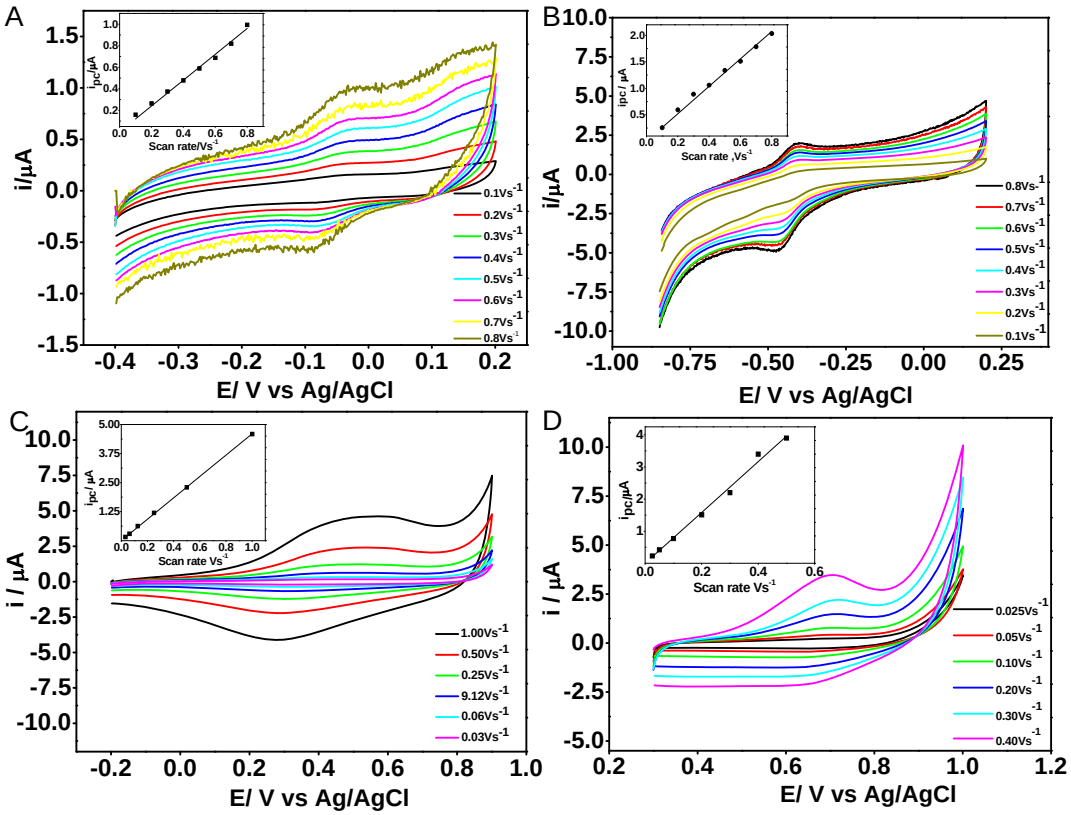

Figure 6. 4. Cyclic voltametries at different scan rates for surface tethered DNA duplexes incorporated with four different labels. Insets are the corresponding plots of peak current, Ipc, [A] versus the scan rate, υ [Vs^{-1}].

Specificity of label incorporation

Having demonstarated the incorporation of the labels, the specificity of the enzymatic incorporation of the labeled ddNTPs was checked in the presence all the four labeled ddNTPs. The results in fugure 6.5 show the specific incorporation of the labeled ddNTPs which conforms to the literature reports on the specificity of enzymatic incorporation. However, methylene blue labeled ddUTP signals interfered with the signals due to electrostatic interactions of methylene blue.

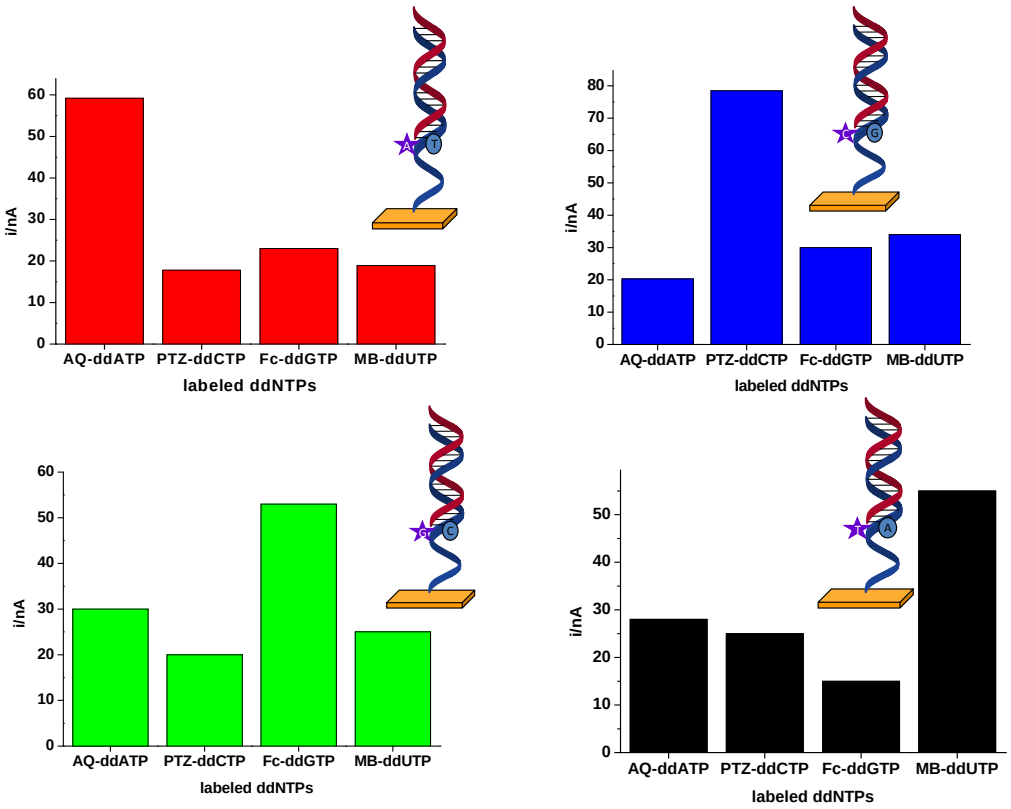

Figure 6.5. Results obtained for testing the specificity of the enzymatic incorporations.

To overcome the background signals arising from electrostatic interations from MB/AQ labelled ddNTPs, we investigated the incorporability of polyoxometalste labeled ddUTP or ddATP. In addition to the incorporability of the POM labeled ddUTP the signals happened to be less affected by background signals unlike MB-ddUTP or anth-ddATP. Due to the higher stability of the Dawson POM compared to Keggin labeled POM the signals after incorporation are slightly higher than those observed for Keggin labeled ddUTP. Inspite of this both Keggin and Dawson POMs incorporations happened to have their redox signal in the same region (≈-0.5).

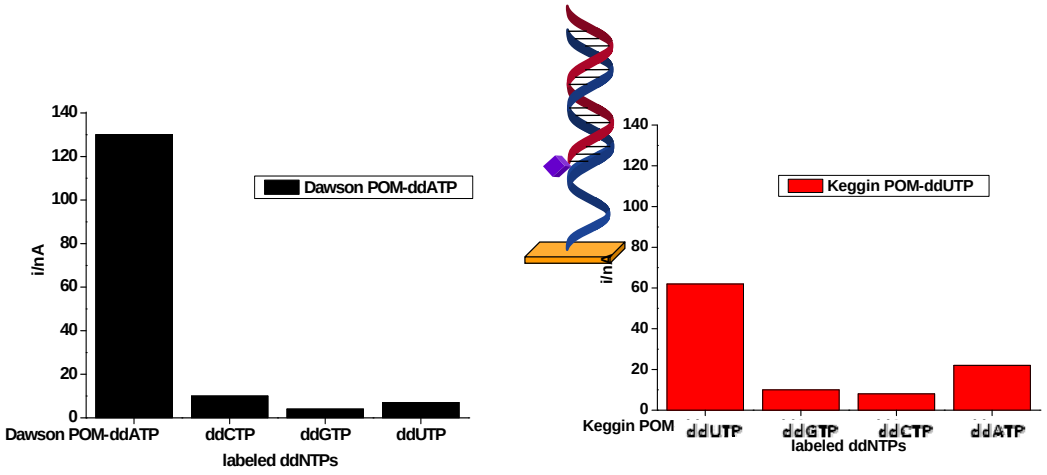

Figure 6.6 Bar graphs showing the incorporation as well as the nonspecific tests for POM (Keggin and Dawson type) labeled ddNTPs.

Conclusions

We have demonstrated the design, synthesis and characterisation of electroactive molecules having distinctive redox potentials. The compounds synthesised have been conjugated with propargyl amine derivatised ddNTPs for use in electrochemical primer extension termination assays. The assays developed can be adopted for the development of electrochemical APEX using arrays of electrodes for the detection of multiple mutations /SNPs in a genome. Coupling the high specificity of this method with the high sensitivity, low cost and compatibility with miniaturisation of electrochemical techniques would offer an excellent platform for the detection of mutation as well as sequencing of DNA templates. The use of POM labeled ddNTPs seem to have solved problems related back ground signals and future work will focus of the synthesis of four different POMs with distinguishable redox potentials.

References

1. J.Shendure, J. Hanlee, Next-generation DNA sequencing, *Nat. Biotechn*. **2008**, 26, 1135 – 1145
2. J. Brookes, The essence of SNPs. *Gene,* **1999**, 234,177–86
3. J.C. Venter, M.D Adams, E.W. Myers, P.W. Li, R.J. Mural, G.G. Sutton, H.O. Smith, M. Yandell,C.A. Evans,R.A. Holt, *et al.* The sequence of the human genome. *Science*, **2001,** 291, 1304–1351.
4. R. Sachidanandam, D. Weissman, S.C. Schmidt, et al. A map of human genome sequence variation containing 1.42 million single nucleotide polymorphisms. *Nature,* **2001**; 409, 928–33
5. F. A. Gravel, J. T. R. Clarke, M. M. Kaback, D. Mahuran, K. Sandhoff, K. Suzuki, In The metabolic and molecular basis of inherited disease;C.R. Scriver, A.L. Beauder, W.S. Sly, D. Valle, Eds.; McGraw-Hill: New York,**1995**; 2, 2839-2879
6. H. Levy, A. Murphy, F. Zou, C. Gerard, B. Klanderman, B. Schuemann, R. Lazarus, C. K. García, C. J. Celedón, M. Drumm, M. Dahmer, M. Quasney, K. Schneck, M. Reske, R. M. Knowles, B. G. Pier, C. Lange, T.S. Weiss, IL1B polymorphisms modulate cysticfibrosis lung disease, *Pediatr. Pulmonol,* **2009**, 44, 580–593.
7. Muniz, G. Martinez, J. Lavinha, P. Pacheco, β-Thalassaemia in Cubans: Novel Allele Increases the Genetic Diversity at the HBB Locus in the Caribean, *Am. J. Hemathology*, **2000,** 64, 7-14
8. Y. D. Wu, L. Ugozzoli, K. B. Bal, B. R. Wallace, Allele-specific enzymatic amplification of beta-globin genomic DNA for diagnosis of sickle cell anemia, *Proc. Natl Acad. Sci.* USA, **1989**, 86, 2757–2760
9. K. Meyer, P. M. Ueland, Use of Matrix assisted laser desorption ionization time of flight mass spectrometry for multiplex genotyping, *Adv. Clinic. Chem.* **2011**, 53, 1-29
10. X. Duan, L. Liu; S. Wang, Homogeneous and one-step fluorescent allele-specific PCR for SNP genotyping assays using conjugated polyelectrolytes, *Biosens. Bioelectro.*, **2009**, 24, 2095–2099.
11. Ding, Z. Wang, H.Zhong, S. Zhang, Ultrasensitive chemiluminescence quantification of single-nucleotide polymorphisms by using monobase-modified Au and CuS nanoparticles, *Biosens. Bioelectro*, **2010**, 25,1082
12. G. Liu, Y. Lin, Electrochemical Quantification of Single-Nucleotide Polymorphisms Using Nanoparticle Probes, *J. Am. Chem. Soc.* **2007**, 129, 10394–10401. b) G. Liu; T. M.

H. Lee; J. Wang Nanocrystal-Based Bioelectronic Coding of Single Nucleotide Polymorphisms *J. Am. Chem. Soc.* **2005**, 127, 38–39.

13. E. L. S. Wong; J. J. Gooding Charge Transfer through DNA: A Selective Electrochemical DNA Biosensor*, Anal. Chem.* **2006**, *78*, 2138–2144.
14. J. Wakai; A. Takagi; M. Nakayama; T. Miya; T. Miyahara;T. Iwanaga; S. Takenaka; Y. Ikeda; M. Amano, A novel method of identifying genetic mutations using an electrochemical DNA array. *Nucleic Acids Res.* **2004**, *32*, e141.
15. C. J. Yu; Y. J. Wan; H. Yowanto; J. Li; C. L. Tao; M. D. James; C. L. Tan; G. F. Blackburn;, T. J. Meade, Electronic Detection of Single-Base Mismatches in DNA with Ferrocene-Modified Probes *J. Am. Chem. Soc.***2001**, *123*, 11155–11161. (b) Y. Xiao; A. A. Lubin; B. R. Baker; K. W. Plaxco; A. J. Heeger Single-step electronic detection of femtomolar DNA by target-induced strand displacement in an electrode-bound duplex**,** *Proc. Natl. Acad. Sci. U.S.A,.* **2006**, *103*, 16677–16680.
16. G. C King, D. A. De Giusto, W. A. Wlassoff, S. Giesebrecht, E. Flening, G. D. Tyrelle, Proofreading genotyping assays and electrochemical detection of SNPs, *Hum. Mutat.* **2004**, *23*, 420–425.
17. H. Fan, K. W. Plaxco, A. L. Heeger, Electrochemical interrogation of conformational changes as a reagentless method for the sequence-specific detection of DNA, *Proc. Natl. Acad. Sci. U.S.A.* **2003**, *100*, 9134–9137
18. M. Jenkins, B. Chani, M. Kreuzer, G. Presting, A. M. Alvarez, B. Y. Liaw, Hybridization Probe for Femtomolar Quantification of Selected Nucleic Acid Sequences on a Disposable Electrode*, Anal. Chem.* **2006**, *78*, 2314–2318
19. A. Lubin, R. Y. Lai, B. R. Baker, A. J. Heeger, K. W. Plaxco, Sequence-Specific, Electronic Detection of Oligonucleotides in Blood, Soil, and Foodstuffs with the Reagentless, Reusable E-DNA Sensor, *Anal. Chem.* **2006**, *78*, 5671–5677.
20. J. M. Shumaker, A. Metspalu, C. T. Caskey, mutation detection by solid phase primer extention, *human mutat* **1996**, 7, 346-54 (b) A. Kurg, N. Tõnisson, I. Georgiou, J.Shumaker, J.Tollett, A. Metspalu arrayed primer extension:solid phase four colour, DNA resequencing and DNA mutation detection technology, *Genet test* , **2000**, 4, 1-7 (c) N. Tõnisson, J. Zernant, A. Kurg, H. Pavel, G.Slavin, H.Roomere, A.Meiel, P.Hainaut,A Metspalu; evaluating the arrayed primer extension resquencing assay of TP53 tumour suppressor gene *Proc. Natl acad sci (USA),* **2002,** 99, 5503-5508 (d) T. Pastinen, A. Kurg, A. Metspalu, L. Peltonen, A. C. Syvanen. Minisequencing: a

specific tool for DNA analysis and diagnostics on oligonucleotide arrays, *Genome Res.* **1997**, 7, 606–14

21. A.C. Syvanen, Accessing genetic variation: genotyping single nucleotide polymorphisms, *Nat Rev Genet*. **2001**, 2, 930-42.
22. K. Krjutškov, R. Andreson, R. Mägi, T. Nikopensius, A. Khrunin, E. Mihailov, V. Tammekivi, H. Sork, M. Remm,A. Metspalu, Development of a single tube 640-plex genotyping method for detection of nucleic acid variations on microarrays, *Nucleic Acids Res.,* **2008**, 36, e75
23. N. Muelas, P. Hackman, H. Luque, T. Suominen, C. Espinós, M. Garcés-Sánchez, T. Sevilla, I. Azorín, J. M. Millán, B. Udd, J. J. Vílchez, Spanish MYH7 founder mutation of Italian ancestry causing a large cluster of Laing myopathy patients. *Clin Genet*. **2012,** 81,491-4.
24. J. C. Hoogvliet, M. Dijksma, B. Kamp, W. P van Bennekom, Electrochemical Pretreatment of Polycrystalline Gold Electrodes To Produce a Reproducible Surface Roughness for Self-Assembly: A Study in Phosphate Buffer pH 7.4, *Anal. Chem.* **2000,** 72, 2016-2021
25. M. T. Herne, J. M. Tarlov, Characterization of DNA Probes Immobilized on Gold Surfaces., *J. Am. Chem. Soc.,***1997**, 119, 8916-8920
26. E.F. Godefroi, E. L. Whittle, The Preparation of Some Derivatives of β-(10-Phenothiazinyl)propionic Acid and β-(2-Chloro-10-phenothiazinyl)propionic Acid, *J.Org. Chem*, **1956,** 21,1163-1168
27. Fan, K. W. Plaxco, A. J. Heeger, Electrochemical interrogation of conformational changes as a reagentless method for the sequence-specific detection of DNA, *Pro. Natl. Acc. Sci.(USA)* **2003**, 100, 9134-9137
28. Y. Huang, Y.-L. Zhang, X. Xu, J.-H. Jiang, G.-L. Shen, R.-Q. Yu , Highly Specific and Sensitive Electrochemical Genotyping via Gap Ligation Reaction and Surface Hybridization Detection, *J. Am. Chem. Soc.* **2009**,131, 2478-2480
29. (a) D. A. Di Giusto , W. A. Wlassoff, S. Giesebrecht, J. J. Gooding , G. C. King , Multipotential Electrochemical Detection of Primer Extension Reactions on DNA Self-Assembled Monolayers, . *J. Am. Chem. Soc*. **2004**, 126, 4120-4121 (b) D. A. Di Giusto, W. A. Wlassoff; S. Giesebrecht; J. J. Gooding;, G. C. King, Enzymatic synthesis of redox-labeled RNA and dual-potential detection at DNA-modified electrodes, *Angew. Chem., Int. Ed*. **2004**, 43, 2809-2812.

30. Anne C. Demaille, Electron Transport by Molecular Motion of redox-DNA Strands: Unexpectedly Slow Rotational Dynamics of 20-mer ds-DNA Chains End-Grafted onto Surfaces via C6 Linkers, *J. Am. Chem. Soc.* **2008**,130, 9812-9823
31. M. Inouye, R. Ikeda, M. Takase, T. Tsuri, J. Chiba, Single-nucleotide polymorphism detection with "wire-like" DNA probes that display quasi "on–off" digital action, *Pro. Natl. Acc. Scie. (USA),* **2005,** 102, 11606-11610
32. N. E. Heberta, S. A. Brazill, Microchip capillary gel electrophoresis with electrochemical detection for the analysis of known SNPs, *Lab Chip*, **2003**, 3, 241–247
33. P. Brázdilová, , M. Vrábel, R. Pohl, H. Pivoňková, L. Havran, M. Hocek, M. Fojta, Ferrocenylethynyl Derivatives of Nucleoside Triphosphates: Synthesis, Incorporation, Electrochemistry, and Bioanalytical Applications, *Chem. Eur. J.* **2007**, 13, 9527 – 9533
34. J. Balintova, R. Pohl, H. Petra, P. Vidlkov, L. Havran, M. Fojta, M. Hocek, Anthraquinone as a Redox Label for DNA: Synthesis, Enzymatic Incorporation, and Electrochemistry of Anthraquinone-Modified Nucleosides, Nucleotides, and DNA, *Chem. Eur. J.* **2011**, 17, 14063 – 14073
35. T. M. Tierney, W. M. Grinstaff, Synthesis and Stability of Oligodeoxynucleotides Containing C8-Labeled 2'-Deoxyadenosine: Novel Redox Nucleobase Probes for DNA-Mediated Charge-Transfer Studies, Org. let. **2000**, 2, 3413
36. J. A. Bard, R. L. Faulkner Electrochemical Methods: Fundamentals and Applications p591

Chapter 7.
Conclusions and future work

This PhD project had an overall goal of developing an electrochemical tool genotyping of disease causing mutations.

In chapter 2, a two-step process for the electrochemical hydrogenation and subsequent electrochemical chlorination to form a highly reactive surface with wide potential application was described. Electrochemical chlorination was extremely rapid and does not require elevated temperatures or noxious reagents, making it very attractive for industrial application. Furthermore, the surface obtained following electrochemical chlorination was compared to that obtained after chemical chlorination and observed to be markedly less damaged and probably consequently, notably more organised. The highly reactive surface obtained could be used for anchoring of a plethora of moecules ranging from olefins to thiols), but due to the huge range of easily available diverse thiolated molecules, we decided to use this as a model system. In the first instance, a ferrocene labelled alkylthiol was used as a model to optimise the immobilisation process in terms of hydrogenation and chlorination times, applied potential and duration of immobilisation. The developed methodology was then used in an example of an "application" of the formed reactive surface for anchoring of a thiolated DNA probe and the functionality of the DNA probe following immobilisation was demonstrated. The thermal stability and functionality of the immobilised DNA was evaluated and compared to the stability of self-assembled monolayers on gold. The modified surfaces were characterised using AFM, Raman, ATR-FTIR, XPS and SEM. all of which concurred on the superior surface obtained using electrochemical chlorination as well as confirming the presence of a C-S bond. The developed methodology is extremely robust, cost-effective and applicable to scale-up with a simple two-step electrochemical process to produce a highly reactive carbon surface that can subsequently be functionalised with a plethora of different molecules.

In Chapter 3, we presented the design, synthesis and characterisation of functionalised Keggin type POMs. The functionalisation of the POMs had two goals: the first is to introduce an organic arm which will be utilised to introduce various groups including biomolecules. The second is to optimise the conditions for coupling DNA with

functionalised POMs. Two post functionalisation strategies were successfully utilised and optimised for Keggin (SiW_{11}) type POMs for the fist time and the fuctionalised POMs along with Dawson type (P_2W_{17}) POMs functionalised similarly were utilised for coupling with DNA primers and dNTPs and ddNTPs. As a result, silico- and phosphotungstates together represent now a family of POMs with different electrochemical properties, but a common coupling methodology, making them potentially suitable for use as specific redox labels in bioanalytical applications.

In Chapter 4, we demonstrated the functionalisation, characterisation and applicability of polyoxometalate labelled oligonucleotides in PCR and the subsequent direct electrochemical detection of PCR products. The synthesised POM-primer conjugates were characterised using various techniques including ESI MS and Raman spectroscopies and gel electrophoresis, amongst others. Having confirmed a successful conjugation, the functionality of the primers was checked by electrochemical hybridisation assay with capture probes tethered on the surface of gold electrodes. Different strategies were tested to achieve improved sensitivity and detection limits with POM bearing ssDNA generated from PCR products. The use of polyoxometalates in bioanalytical applications has huge potential and the he redox potentials obtained with POM labeled dNTPs and POM labeled primers are close to zero. It is plausible to tune the redox potentials of the diverse POM clusters to achieve four distinct potential bearing labels for use in electrochemical genotyping or for in electrochemical labeling of biomolecules in general. In Chapter 5, the design, synthesis, characterisation and use in PCR for POM modified dNTPs were described. POMs were linked at 7 deaza modified of purines and 5 position modified pyrimidines by adopting a method developed for linking activated carboxy POMs with amine terminated molecules. The synthesised POM –nucleotide conjugates were characterised high resolution ESI MS. The conjugates were subsequently used in PCR along with unmodified dNTPs. The gel electrophoresis analysis showed amplification until 60% substitution of the natural dNTP for Keggin (SiW_{11}) POM modified dNTPs. The hindrance of amplification is pronounced for Dawson POM (P_2W_{17}) dNTPs, where amplification was only observed for substitution levels of less than 20% of the modified dNTPs. The development of electrochemically distinguishable nucleotides via the use of POMs may pave the way for novel labels for use in DNA sensing or genotyping.

Finally, in Chapter 6, we synthesised and characterised four reactive label bearing ddNTPs and use them for 'four colour' type SNP genotyping and showed the possibility of electrochemical detecting SNPs in a known mutation. The use of four different labels for each base allows the identification of the nucleotides incorporated. The results reported in this study can be utilised in the development of electrochemical APEX platforms for detection of SNPs.

Future work

Future work will utilise the developed robust surface functionalisation strategy to fabricate low cost arrays of carbon electrode for the detection of SNPs using APEX. In addition to this we will search for POMs with distinguishable redox potentials for labeling DNA for real time montoring of PCR amplification as well as in multiplex PCR in addition to use for genotyping. In addition, we will integrate solid phase isothermal amplification formats developed in our group to develop a microfluidic chip capable of extracting DNA, amplifying DNA and generating ssDNA fragments and finally the detection of SNPs in the genome samples analysed.